

**ASSESSMENT OF ENERGY CONSERVATION IN INDIAN CEMENT
INDUSTRY AND FORECASTING OF CO₂ EMISSIONS**

*Thesis submitted to
Cochin University of Science and Technology
in partial fulfillment of the requirement
for the award of the Degree of
Doctor of Philosophy in Engineering
Under the Faculty of Engineering*

By

A. RAMESH
(Reg. No. 3191)

Under the guidance of
Prof. (Dr.) G. MADHU



**DIVISION OF SAFETY AND FIRE ENGINEERING
SCHOOL OF ENGINEERING
COCHIN UNIVERSITY OF SCIENCE AND TECHNOLOGY
KOCHI – 682 022, KERALA, INDIA.**

October 2012

Assessment of Energy Conservation in Indian Cement Industry and Forecasting of CO₂ Emissions

Ph.D. Thesis under the Faculty of Engineering

Author

A. Ramesh

Research Scholar
School of Engineering
Cochin University of Science and Technology
Kochi - 682022
Email: rameshgec71@gmail.com

Supervising Guide

Prof. (Dr.) G. Madhu

School of Engineering
Cochin University of Science and Technology
Kochi - 682022
Email: profmadhu@rediffmail.com

Division Safety and Fire Engineering
School of Engineering
Cochin University of Science and Technology
Kochi - 682022

October 2012



**DIVISION OF SAFETY AND FIRE ENGINEERING
SCHOOL OF ENGINEERING
COCHIN UNIVERSITY OF SCIENCE AND TECHNOLOGY
Kochi – 682022, KERALA, INDIA.**

Dr. G. Madhu
Professor and Head

Ph: 0484-2862180
Fax: 91-484-2550952
e-mail: Profmadhu@cusat.ac.in

Certificate

This is to certify that the thesis entitled “**Assessment of Energy Conservation in Indian Cement Industry and Forecasting of CO₂ Emissions**” submitted by Mr. A Ramesh to the Cochin University of Science and Technology, Kochi for the award of the degree of Doctor of Philosophy is a bonafide record of research work carried out by him under my supervision. The contents of this thesis, is full or in parts, have not been submitted to any other institute or university for the award of any degree or diploma.

Place: Kochi - 22
Date:

Prof. (Dr.) G. Madhu
Supervising Guide

Declaration

I hereby declare that the thesis entitled “**Assessment of Energy Conservation in Indian Cement Industry and Forecasting of CO₂ Emissions**” is based on the original work done by me under the supervision of Prof.(Dr).G.Madhu, Head, Division of safety and Fire Engineering, School of Engineering, Cochin University of Science and Technology, Kochi. No part of this thesis has been presented for any other degree from any other university or Institution.

Place: Kochi -22

A.Ramesh

Date:

Dedicated to
the ever loving memories of
my beloved father, Mr. Appu

Acknowledgements

This thesis is the result of five years of part time work whereby I have been accompanied and supported by many people. It is a pleasant aspect that I have now the opportunity to express my gratitude to all of them

I wish to thank and express my deep sense of gratitude to my guide Prof G Madhu for his invaluable guidance. I have been associating with him since 2006 when I started my thesis work. Throughout the course he has provided the inspiration and kept the interest burning in me. I thank him for his keen interest at every stage of my PhD programme. He is one of the kindest human being I have seen among the teaching community. In every sense he has been a true teacher, and a great philosopher to me.

I express my sincere gratitude to Dr. V.N.Narayanan Namboothiri, Member, Doctor committee, for his valuable and timely help.

I am extremely thankful to Dr. P.A. Soloman Associate Proffessor in chemical Engineering, Govt.Engineering College Thrissur, my colleague, for his support and help throughout my research work. He kept a constant vigil on the progress of my work and was always accessible whenever I was in need of an advice.

I would like to thank Mr.Sreekanth Paniker and Mr.Deepak .B, my favourite old PG students, those who helped me in understanding the fundamentals of software and also for data collection.

I wish to thank my mother Radha P P, my wife Rekhia A, children Gouri and Goutham for the affectionate support and encouragement they have rendered during the course of my research work.

I thank God almighty for giving me the opportunity to do this work.

A. Ramesh

Abstract

Cement industry ranks 2nd in energy consumption among the industries in India. It is one of the major emitter of CO₂, due to combustion of fossil fuel and calcination process. As the huge amount of CO₂ emissions cause severe environment problems, the efficient and effective utilization of energy is a major concern in Indian cement industry. The main objective of the research work is to assess the energy consumption and energy conservation of the Indian cement industry and to predict future trends in cement production and reduction of CO₂ emissions. In order to achieve this objective, a detailed energy and exergy analysis of a typical cement plant in Kerala was carried out. The data on fuel usage, electricity consumption, amount of clinker and cement production were also collected from a few selected cement industries in India for the period 2001 - 2010 and the CO₂ emissions were estimated. A complete decomposition method was used for the analysis of change in CO₂ emissions during the period 2001 - 2010 by categorising the cement industries according to the specific thermal energy consumption. A basic forecasting model for the cement production trend was developed by using the system dynamic approach and the model was validated with the data collected from the selected cement industries. The cement production and CO₂ emissions from the industries were also predicted with the base year as 2010. The sensitivity analysis of the forecasting model was conducted and found satisfactory. The model was then modified for the total cement production in India to predict the cement production and CO₂ emissions for the next 21 years under three different scenarios. The parameters that influence CO₂ emissions like population and GDP growth rate, demand of cement and its production, clinker consumption and energy utilization are incorporated in these scenarios. The existing growth rate of the population and cement production in the year 2010 were used in the baseline scenario. In the scenario-1 (S1) the growth rate of population was assumed to be gradually decreasing and finally reach zero by the year 2030, while in scenario-2 (S2) a faster decline in the growth rate was assumed such that zero growth rate is achieved in the year 2020. The mitigation strategies

for the reduction of CO₂ emissions from the cement production were identified and analyzed in the energy management scenario.

The energy and exergy analysis of the raw mill of the cement plant revealed that the exergy utilization was worse than energy utilization. The energy analysis of the kiln system showed that around 38% of heat energy is wasted through exhaust gases of the preheater and cooler of the kiln system. This could be recovered by the waste heat recovery system. A secondary insulation shell was also recommended for the kiln in the plant in order to prevent heat loss and enhance the efficiency of the plant. The decomposition analysis of the change in CO₂ emissions during 2001- 2010 showed that the activity effect was the main factor for CO₂ emissions for the cement industries since it is directly dependent on economic growth of the country. The forecasting model showed that 15.22% and 29.44% of CO₂ emissions reduction can be achieved by the year 2030 in scenario-1 (S1) and scenario-2 (S2) respectively. In analysing the energy management scenario, it was assumed that 25% of electrical energy supply to the cement plants is replaced by renewable energy. The analysis revealed that the recovery of waste heat and the use of renewable energy could lead to decline in CO₂ emissions 7.1% for baseline scenario, 10.9 % in scenario-1 (S1) and 11.16% in scenario-2 (S2) in 2030. The combined scenario considering population stabilization by the year 2020, 25% of contribution from renewable energy sources of the cement industry and 38% thermal energy from the waste heat streams shows that CO₂ emissions from Indian cement industry could be reduced by nearly 37% in the year 2030. This would reduce a substantial level of greenhouse gas load to the environment.

The cement industry will remain one of the critical sectors for India to meet its CO₂ emissions reduction target. India's cement production will continue to grow in the near future due to its GDP growth. The control of population, improvement in plant efficiency and use of renewable energy are the important options for the mitigation of CO₂ emissions from Indian cement industries.

Keywords: Cement industry, energy and exergy analysis, waste heat recovery system, complete decomposition analysis, system dynamic model, CO₂ emissions

Contents

Chapter -1

INTRODUCTION.....	01 - 08
1.1 Background -----	01
1.2 Research Problem-----	04
1.3 Objectives -----	05
1.4 Outline of the Thesis -----	07

Chapter -2

LITERATURE REVIEW	09 - 48
2.1 Introduction-----	09
2.2 Energy and Exergy Analysis -----	10
2.3 Decomposition Analysis -----	27
2.4 Forecasting Models -----	37
2.5 Conclusion -----	48

Chapter -3

ENERGY AND EXERGY ANALYSIS OF THE RAW MILL OF THE CEMENT PLANT	49 - 102
3.1 Introduction-----	49
3.2 About the Plant-----	51
3.3 Cement Manufacturing Processes -----	52
3.3.1 Mining -----	53
3.3.2 Raw meal preparation -----	53
3.3.3 Clinkerisation and Coal grinding -----	55
3.3.4 Cement grinding and packing -----	57
3.4 Theoretical Analysis-----	59
3.4.1 Mass balance -----	59
3.4.2 Energy balance. -----	60
3.4.3 Exergy balance -----	60
3.4.4 Physical exergy -----	61
3.4.5 Chemical exergy -----	62
3.4.6 Exergy efficiencies -----	63
3.5 Raw mill -----	65
3.6 Raw mill analysis -----	67
3.7 Results and Discussion -----	70
3.7.1 Mass balance of the Raw Mill (Production rate of 117 tonnes per hour)-----	71

3.7.2	Heat losses from raw mill (Production rate of 117 tonnes per hour)-----	73
3.7.2.1	Determination of mixture room temperature (Production rate of 117 tonnes per hour)-----	73
3.7.2.2	Drying room heat loss (Production rate of 117 tonnes per hour)-----	77
3.7.2.3	Grinding room heat loss (Production rate of 117 tonnes per hour)-----	77
3.7.3	Energy analyses of the raw mill (Production rate of 117 tonnes per hour)-----	77
3.7.3.1	Efficiency of the raw mill (Production rate of 117 tonnes per hour)-----	81
3.7.4	Exergy analysis of the raw mill (Production rate of 117 tonnes per hour)-----	82
3.7.4.1	Exergy efficiency of the raw mill (Production rate of 117 tonnes per hour)-----	87
3.7.5	Mass balance of the Raw Mill (Production rate of 121 tonnes per hour)-----	88
3.7.6	Determination of mixture room temperature and heat loss (Production rate of 121 tonnes per hour)-----	90
3.7.7	Exergy analysis of the raw mill (Production rate of 121 tonnes per hour)-----	95
3.8	Conclusion-----	101

Chapter -4

ENERGY AND EXERGY ANALYSIS OF THE KILN SYSTEM IN THE CEMENT PLANT 103 - 151

4.1	Introduction-----	103
4.2	Kiln System-----	104
4.3	Kiln System Analysis-----	107
4.4	Results and Discussion-----	112
4.4.1	Mass balance of the Kiln System (Production rate of 1400 tonnes per day)-----	112
4.4.2	Energy balance of the Kiln System (Production rate of 1400 tonnes per day)-----	114
4.4.3	CO ₂ emissions-----	121
4.4.4	Energy conservation opportunities-----	121
4.4.5	Waste heat recovery steam generation (WHRSG) – Production rate of 1400 tonnes per day-----	122
4.4.6	Heat recovery from the kiln surface (Production rate of 1400 tonnes per day).-----	126
4.4.7	CO ₂ reduction methods in cement plants.-----	128
4.4.8	Exergy balance of the kiln system (Production rate of 1400 tonnes per day).-----	132

4.4.9	Mass balance of the Kiln System (Production rate of 1369 tonnes per day)-----	137
4.4.10	Energy balance of the Kiln System (Production rate of 1369 tonnes per day)-----	140
4.4.11	Exergy balance of the kiln system (Production rate of 1369 tonnes per day)-----	145
4.5	Conclusion -----	150

Chapter -5

**DECOMPOSITION ANALYSIS OF CO₂ EMISSIONS
CHANGES IN THE INDIAN CEMENT INDUSTRIES.....153- 175**

5.1	Introduction -----	153
5.2	Decomposition Analysis -----	155
5.3	Methodology-----	156
5.4	Data Integration and Classification-----	157
5.5	Complete Decomposition Approach -----	163
5.6	Carbon dioxide emissions from the cement production process -----	166
5.7	Carbon dioxide emissions from calcination (process emissions) -----	167
5.8	Carbon dioxide emissions from fuel use-----	167
5.9	Calculation of CO ₂ emissions -----	167
5.10	Results and discussion-----	170
5.11	Conclusion -----	174

Chapter -6

FORECASTING MODEL FOR CO₂ EMISSIONS..... 177 - 215

6.1	Introduction-----	177
6.2	Overview of Cement Industries in India -----	178
6.3	History of Cement Production in India -----	180
6.4	System Dynamics -----	181
6.5	System Dynamic Model Based on Data Collected from the Selected Cement Industries-----	182
6.5.1	Model Validation -----	184
6.5.2	Sensitivity Test-----	186
6.6	Modified model -----	191
6.6.1	Cement demand and production -----	191
6.6.2	Energy consumption -----	192
6.6.3	CO ₂ emissions -----	192
6.7	Scenario generation-----	195
6.7.1	Baseline scenario -----	195

6.7.2	Modified scenerios -----	196
6.7.3	Energy management scenario -----	196
6.8	Results and Discussion -----	197
6.8.1	Baseline scenario -----	197
6.8.2	Modified scenario -----	198
6.8.3	Energy management scenario -----	211
6.9	Conclusion -----	215

Chapter -7

SUMMARY AND CONCLUSIONS217 -224

7.1	Introduction-----	217
7.2	Conclusions-----	219
7.3	Scope for Future Work-----	224

REFERENCES 225 - 240

ANNEXURES

PUBLICATIONS

CURRICULUM VITAE

List of Tables

Table 3.1	Equipment details-----	52
Table 3.2	Operation data of Raw Mill for the production rate of 117 tonnes per hour -----	67
Table 3.3	Operation data of Raw Mill with production rate of 121 tonnes per hour -----	69
Table 3.4	Mass balance in raw mill (Production rate of 117 tonnes per hour)-----	71
Table 3.5	Determination of mixture room temperature (Production rate of 117 tonnes per hour)-----	74
Table 3.6	Energy balance (Production rate of 117 tonnes per hour)-----	79
Table 3.7	Enthalpy balance (Production rate of 117 tonnes per hour) -----	84
Table 3.8	Entropy balance (Production rate of 117 tonnes per hour)-----	85
Table 3.9	Exergy balance (Production rate of 117 tonnes per hour)-----	86
Table 3.10	Mass balance in the raw mill (Production rate of 121 tonnes per hour) -----	88
Table 3.11	Determination of mixture room temperature (Production rate of 121 tonnes per hour)-----	91
Table 3.12	Energy balance of raw mill (Production rate of 121 tonnes per hour) -----	93
Table 3.13	Enthalpy balance of the raw mill (Production rate of 121 tonnes per hour)-----	97
Table 3.14	Entropy balance of the raw mill (Production rate of 121 tonnes per hour)-----	98
Table 3.15	Exergy Balance of the raw mill (Production rate of 121 tonnes per hour)-----	99
Table 4.1	Chemical reactions process in kiln system-----	105
Table 4.2	Operation data of kiln system for the production rate of 1400 tonnes per day -----	107
Table 4.3	Operation data of kiln system for the production rate of 1369 tonnes per day -----	110
Table 4.4	Entropy balance for kiln system (Production rate of 1400 tonnes per day -----	116
Table 4.5	Enthalpy balance for kiln system (Production rate of 1400 tonnes per day)-----	133
Table 4.6	Entropy balance for kiln system (Production rate of 1400 tones per day)-----	134

Table 4.7	Exergy balance for the kiln system (Production rate of 1400 tonnes per day)-----	135
Table 4.8	Entropy balance for kiln system (Production rate of 1369 tonnes per day -----	141
Table 4.9	Enthalpy balance for kiln system (Production rate of 1369 tonnes per day)-----	146
Table 4.10	Entropy balance for kiln system (Production rate of 1369 tonnes per day)-----	147
Table 4.11	Exergy balance for kiln system (Production rate of 1369 tonnes per day)-----	149
Table 5.1	Classification of industries according to specific thermal energy consumption-----	158
Table 5.2	Cement production from the selected cement industries in India -----	159
Table 5.3	Clinker production from the selected cement industries in India -----	160
Table 5.4	Specific thermal energy consumption of the selected cement industries in India -----	161
Table 5.5	Specific power consumption of the selected cement industries in India-----	162
Table 5.6	Carbon emission factor and fraction of carbon oxidized -----	169
Table 5.7	Carbon dioxide emission per kWh generation of electricity for different fuels -----	170
Table 6.1	Electrical and thermal specific energy consumption-----	179
Table 6.2	Comparison of the quantity of cement production with model projection -----	185
Table 6.3	Sensitivity of model tested with cement production growth multiplier is changed from 0.092 to 0.101 for the year 2021 onwards -----	187
Table 6.4	Projection of cement production and CO ₂ emissions -----	189
Table 6.5	Projection of thermal energy, electrical energy and clinker consumptions -----	190
Table 6.6	Projection of population of India under the baseline scenario (BS), scenario-1 (S1) and scenario-(S2)-----	201
Table 6.7	Projection of cement production for the baseline scenario (BS), scenario-1 (S1) and scenario-2 (S2)-----	202
Table 6.8	Projection of cement demand for the baseline scenario (BS), scenario-1 (S1) and scenario-2 (S2)-----	204
Table 6.9	Projection of thermal energy consumption for the baseline scenario (BS), scenario-1 (S1) and scenario-2 (S2) -----	205

Table 6.10	Projection of electrical energy consumption for the baseline scenario (BS), scenario-1 (S1) and scenario-2 (S2) -----	207
Table 6.11	Projection of clinker consumption for the baseline scenario (BS), scenario-1 (S1) and scenario-2 (S2) -----	208
Table 6.12	Projection of CO ₂ emissions for the baseline scenario (BS), scenario-1 (S1) and scenario-2 (S2)-----	210
Table 6.13	Projection of CO ₂ emissions for energy management scenario -----	213

List of Figures

Fig. 3.1	Flow sheet of raw meal preparation-----	54
Fig. 3.2	Flow sheet of clinkerisation and coal grinding-----	56
Fig. 3.3	Flow sheet of cement grinding and packing -----	58
Fig.3.4	Schematic diagram of raw mill -----	66
Fig.3.5	Mass balance in the raw mill (Production rate of 117 tonnes per hour) -----	72
Fig. 3.6	Distribution of Temperature in the raw mill (Production rate-----	75
Fig.3.7	Energy flow diagram of raw mill (Production rate of 117 tonnes per hour) -----	80
Fig 3.8	Sankey diagram of raw mill (Production rate of 117 tonnes per hour)-----	82
Fig. 3.9	Grassmann (exergy band diagram) diagram of raw mill (Production rate of 117 tonnes per hour) -----	87
Fig.3.10	Mass balance diagram of raw mill (Production rate of 121tonnes per hour) -----	89
Fig.3.11	Temperature distribution of raw mill (Production rate of 121 tonnes per hour) -----	92
Fig.3.12	Energy flow diagram of raw mill (Production rate of 121 tonnes per hour)-----	94
Fig. 3.13	Sankey diagram of raw mill (Production rate of 121 tonnes per hour)-----	95
Fig.3.14	Grassmann (exergy band diagram) diagram of raw mill (Production rate of 121 tonnes per hour) -----	100
Fig. 4.1	Kiln system -----	106
Fig.4.2	Schematic diagram of the kiln system (Production rate of 1400 tonnes per day)-----	108
Fig. 4.3	Schematic diagram of the kiln system (Production rate of 1369 tonnes per day) -----	111
Fig. 4.4	Mass balance in the kiln system (Production rate of 1400 tonnes per day)-----	114
Fig.4.5	Energy flow diagram (Sankey diagram) of kiln system (Production rate of 1400 tonnes per day) -----	120
Fig. 4.6	Waste heat recovery steam generation application-----	122
Fig. 4.7	Waste heat recovery steam generation unit with steam flash cycle-----	126

Fig.4.8	Exergy flow diagram (Sankey diagram) of the kiln system (Production rate of 1400 tonnes per day) -----	136
Fig. 4.9	Mass balance in the kiln system (Production rate 1369 tonnes per day)--	140
Fig.4.10	Energy flow diagram of the kiln system (Production rate of 1369 tonnes per day)-----	144
Fig.4.11	Exergy flow diagram of the kiln system (Production rate of 1369 tonnes per day)-----	149
Fig. 5.1	Cement production and CO ₂ emissions from the selected cement industries in India -----	155
Fig. 5.2	Decompositions of CO ₂ emissions changes in group A Industries -----	172
Fig. 5.3	Decompositions of CO ₂ emissions changes in group B Industries -----	172
Fig. 5.4	Decompositions of CO ₂ emissions changes in group C Industries -----	173
Fig. 6.1	Cement production and capacity in India for the period 1971-2010 -----	181
Fig. 6.2	Flow diagram of the system dynamic model -----	183
Fig. 6.3	Comparison of the quantity of cement production with model projection -----	185
Fig. 6.4	Sensitivity of the model tested with cement production growth multiplier is changed from 0.092 to 0.101 for the year 2021 onwards -----	187
Fig. 6.5	Projections of Cement production and CO ₂ emissions -----	188
Fig. 6.6	Projection of thermal energy consumption-----	188
Fig. 6.7	Projection of electrical energy consumption-----	189
Fig. 6.8	Projection of clinker consumption-----	190
Fig. 6.9	Flow diagram of the system dynamic model baseline scenario, scenario-1(S1) and scenario- 2(S2)-----	195
Fig. 6.10	Projections of population of India under the baseline scenario (BS), scenario-1 (S1) and scenario-2 (S2).-----	200
Fig. 6.11	Projections of cement production for the baseline scenario (BS), scenario-1 (S1) and scenario-2 (S2).-----	200
Fig. 6.12	Projections of cement demand for the baseline scenario (BS), scenario-1 (S1) and scenario-2 (S2). -----	203
Fig. 6.13	Projections of thermal energy consumption for the baseline scenario (BS), scenario-1 (S1) and scenario-2 (S2). -----	203

Fig. 6.14 Projections of electrical energy consumption for the baseline scenario (BS), scenario-1 (S1) and scenario-2 (S2). -----	206
Fig. 6.15 Projections of clinker consumption for the baseline scenario (BS), scenario-1 (S1) and scenario-2 (S2) -----	206
Fig. 6.16 Projections of CO ₂ emissions for the baseline scenario (BS), scenario-1 (S1) and scenario-2 (S2)-----	209
Fig. 6.17 Annual projections of CO ₂ emissions from the cement industry for energy management scenario; the combined effect of 38% of thermal energy recovery from waste heat streams (WHRS) and 25% contribution of electrical energy from the renewable source of energy are taken into account -----	211
Fig. 6.18 Percent reduction in CO ₂ emissions from the cement industry for energy management scenario; the combined effect of 38% of thermal energy recovery from waste heat streams(WHRS) and 25% contribution of electrical energy from the renewable source of energy are taken into account. The baseline scenario (BS), scenario-1 (S1) and scenario-2 (S2) are shown seperately-----	212
Fig.6.19 Flow diagram of the system dynamic model for cement sector under energy management scenario -----	214

Abbreviations

CMA	Cement Manufactures Association
EA	Environment Agency
IEA	International Energy Agency
INR	Indian Rupees
IPCC	Intergovernmental Panel on Climate Change
OPC	Ordinary Portland Cement
PPC	Portland Pozzalana Cement
PSC	Portland Slag Cement
RM	Raw mill
WBCSD	World Business Council for Sustainable Development
WEC	World Energy Council
WEO	World Energy Outlook
WHRSG	Waste Heat Recovery Steam Generation
TPH	Tonnes per hour
ESP	Electro static precipitator
TPD	Tonnes per day
GCT	Gas condition tower
CCS	Carbon capture and storage

Greek Symbols

ϵ	Exergy efficiency	(%)
α_i	Activity coefficient of the component 'i'	
ψ	Specific exergy	kJ/kg
η	Energy efficiency	(%)
ϵ	Emissivity	
η_{td}	Transmission and distribution efficiency(%)	
σ	Stefan Boltzmann constant	W/m ² K ⁴
μ	Dynamic viscosity Ns/m ²	
ρ	Density of air kg/m ³	

English Symbols

A	Area.	m ²
A _{effect}	Activity (production) effect	
CE	CO ₂ emissions per kWh electricity generation	grams/ kWh
c _p	Specific heat	kJ/kg-K
C _t	Yearly CO ₂ emissions of the particular group of the cement industries	
D	Diameter	m
E	Energy transfer	kJ/sec
EC	Electricity consumption	kWh
E _k	Energy transfer rate in the kiln system	kJ/kg- clinker

Ex	Exergy flow rate in the raw mill	kJ/h
(Ex) _k	Exergy flow per kg of clinker in the kiln system	kJ/kg- clinker
G _r	Grashof number	
F	Consumption of fuel at a time	Terajoules
h	Specific enthalpy	kJ/kg
h _a	Convection heat transfer coefficient	W/m ² °C
H	Calorific value	kJ/kg
I _{effect}	Energy intensity effect	
k	Thermal conductivity	W/m °C
L	Length	m
M	Molecular weight ratio of carbon dioxide to carbon	
m	Mass flow rate in the raw mill	kg/h
m _{cli}	Mass flow rate of clinker	kg-clinker/sec
m _k	Mass flow of material through the kiln system per kilogram of clinker production	kg/kg- clinker \
N	Fraction of carbon oxidised in the fuel	
O	Carbon emission factor of the fuel	Tonnes/ Terajoules
P	Pressure	kPa
P _o	Reference pressure	kPa
P _{effect}	Pollution coefficient effect	
Pr	Prandtl number	
Q	Heat flow rate in the raw mill	kJ/h
Q _k	Heat flow per kg of clinker in the kiln system	kJ/kg- clinker
R	Gas constant	kJ/kg-K
Re	Reynolds number	
R _t	Thermal resistance	K/W
r	radius	m
s	Specific entropy	kJ/kg-K
S _{effect}	Structural effect	
T	Temperature	°C/K
t	Thickness	mm
$\frac{W}{m^3}$	Specific volume	m ³ /kg
V ₀	Velocity relative to the earth surface	m/sec
W	Work transfer rate	kJ/Sec
x	Molar fraction of component	
Z ₀	Altitude above sea level	m
ΔT _{ave}	Average grinding room Temperature	°C
ΔH	Enthalpy change of material in raw mill	kJ/h
ΔS	Entropy change material in raw mill	kJ/h
ΔH _k	Enthalpy change of material in kiln system	kJ/kg-clinker
ΔS _k	Enthalpy change of material in kiln system	kJ/kg-clinker K

Subscripts

<i>air</i>	Air
<i>b</i>	Bulk mean
<i>c</i>	Coal
<i>ca</i>	Cooler inlet air
<i>cd</i>	Conduction
<i>cs</i>	Cooler
<i>cm</i>	Coal mill gas
<i>co</i>	Cooler hot air
<i>cli</i>	Clinker
<i>cv</i>	Convection
<i>ca</i>	Cooler inlet air
<i>d</i>	Dust
<i>dest</i>	Destruction
<i>e</i>	Electricity
<i>eg</i>	Exhaust gas
<i>f</i>	Film
<i>g</i>	Gas
<i>in</i>	In
<i>ins</i>	Insulation
<i>ia</i>	Infiltrated air
<i>kiln</i>	Kiln
<i>L</i>	Loss
<i>l</i>	Limestone
<i>lt</i>	Laterite
<i>lm</i>	Moisture in laterite
<i>m</i>	Moisture
<i>ml</i>	Moisture in limestone
<i>out</i>	Out
<i>o</i>	Outer
<i>ph</i>	Preheater
<i>pa</i>	Primary air
∞	Ambient
<i>ra</i>	Radiation
<i>rm</i>	Raw meal
<i>rs</i>	Return from separator
<i>s</i>	Surface
<i>sh</i>	Shaft
<i>sl</i>	Sweetener limestone
<i>sm</i>	Moisture in sweetener limestone
<i>st</i>	Steam
0	reference state (dead state condion)

.....SC.....

INTRODUCTION

<i>Contents</i>	1.1	<i>Background</i>
	1.2	<i>Research Problem</i>
	1.3	<i>Objectives</i>
	1.4	<i>Outline of the Thesis</i>

1.1 Background

Cement is produced worldwide in virtually all countries (Worrell et al., 2001) as an important building material. With the Government of India giving boost to various infrastructure projects, housing facilities and road networks, the cement industry in India is currently growing at an enviable pace. The Indian cement industry is the second largest producer of cement in the world just behind China, but ahead of the United States and Japan. In 1971, India produced 14.40 million tonnes (MT) of cement and it increased to 201.16 million tonnes in 2010 (CMA, 2010). India's per capita annual cement consumption increased from 26 kilograms (kg) in 1971 to 156 kg in 2010 (CMA, 2010). In other words, India's cement output and annual cement consumption per capita increased by factors of 17 and 6 from 1971 to 2010 respectively. Parallel to the rapid growth of cement production, the energy consumption of India's cement industry also increased significantly. The production of cement clinker from limestone and chalk is the main energy consuming process in this industry. The most widely used cement

type is Portland cement, which contains 95% cement clinker. Clinker is produced by heating limestone to temperatures above 950° Celsius. Cement production is an energy-intensive process in which energy represents 20 to 40% of total production costs. Most of the energy used is in the form of fuel for the production of cement clinker and electricity for grinding the raw materials and finished cement. Since cement production consumes an average between 4 to 5 GJ per tonne of cement, this industry uses 8 to 10 EJ of energy annually. Coal is the main fossil fuel used in India's cement industry, accounting for nearly 94% of the total final energy consumption of India's cement industry. The higher energy consumption in India is partially due to the harder raw material and poor quality of fuel. Waste heat recovery from the hot gases in the system has been recognized as a potential option to improve the energy efficiency (Khurana, 2002). The cement industry produces 5% of global man-made carbon dioxide, a major gas contributing to climate change (WBCSD, 2005). In short, the main environmental challenges facing the cement manufacturing industry are (Environment Agency, 2005) releases to air of oxides of nitrogen, sulphur dioxide, particulates and carbon dioxide, use of resources, especially primary raw materials and fossil fuel and generation of waste.

The cement production is a major source of carbon dioxide (CO₂) emissions from fossil fuel combustion, as well as the consumption of large amount of electricity, which is mainly produced by India's coal dominated power industry. Besides energy-related CO₂ emissions, cement production also emits large amount of CO₂ from the clinker calcinations process (Worrell et al., 1995).

In light of the cement industry's role as a main energy consumer and CO₂ emitter in India, this industry deserves analysis and assessment of future production estimates as well as possible energy savings and CO₂ emissions reduction policies and option. This research aims to assess the current status of energy consumption and CO₂ emissions and quantitatively project future production trends and estimate the potential for energy savings and CO₂ emissions reduction of India's cement industry.

At the outset, the previous literature in the areas of energy analysis exergy analysis, decomposition and forecasting models have been reviewed. The review indicated the inadequacy of sufficient research on prediction of CO₂ emissions in Indian Cement Industries. During the second phase, a case study has been conducted in a typical cement industry in Kerala. The objective of the study was to estimate the various recoverable forms of energy losses during the production processes. As continuation to this, data such as cement production, clinker production, thermal and electrical energy consumption of 13 selected cement industries in India for the period 2001-2010 have been collected in order to estimate CO₂ emissions. After this, according to the energy consumption, the above industries are grouped into A, B and C and a complete decomposition model were developed to analyze the changes in CO₂ emissions from the base year 2001. The details of the work are presented in this research work. Followed by this, a dynamic model was developed to predict CO₂ emissions of the above industries for the next 21 years. The model was validated with the historical data and also the sensitive test of the model was conducted. Finally the above model was modified and used to forecast the cement production, energy consumption and related CO₂ emissions under three different scenarios for the cement production in India.

1.2 Research Problem

Problem definition

Among the entire energy intensive sector, cement industry is a major emitter of carbon dioxide (CO₂). This is due to dominant use of carbon intensive fuel, mainly coal. According to Hendriks et al. (1999), this industry is responsible for 5% of the Global emissions of CO₂ whereby such emissions are from calcinations and fuel combustion. Cement production accounts to nearly 2% of the world's total energy demand (WEC, 1995). The high intensity of CO₂ reduces the reflectivity of the surface and allows greater absorption of solar radiation, thus cause global warming. The possibility of such significant changes demonstrates the need to study the effect of cement production due to its large amount of CO₂ emissions. It is obvious that the increasing demand of cement in the construction industry worldwide has contributed to the green house effect and scarcity of material and energy sources. Continuation to this, the efficient and effective utilization of energy has started to gain a vital significance. In such a situation, the collection and evaluation of periodical data concerning cement industry have become the primary targets for studies on energy saving and to protect the environment.

The above results indicate the huge necessity of a continuous assessment of energy conservation study for the mitigation of CO₂. Numerous studies have been conducted in energy conservation and CO₂ mitigation actions are reported in many countries. The forecasting of CO₂ emissions from this sector becomes essential because of the production growth rate due to higher demand. There have been reported a number of projection in this area in different countries. Hayashi and Krey (2005) used regression of GDP growth and cement production for their projection. The

pure economic-driver based projections usually did not take into consideration resource constraints and did not incorporate important non-linear effects, such as saturation effects. As a result, these projections were often quite high compared to other physical driver based projections. In 2002, Soule et al. (2002) projected the future trends and opportunities in China's cement industry, but in retrospect, their projections were much lower than the actual situation. Now, recently some researchers have done forecasting models in Indian scenario, but none of them with real time plant data and result validation. This research concept of forecasting of CO₂ emissions and with mitigation options from the cement industries on system dynamic approach will be outstanding support as a reference for upcoming research since the analysis have been carried on with dynamic condition.

1.3 Objectives

- 1) To conduct energy and exergy analysis of the cement industry.
- 2) To identify the area in which energy conservation opportunities are in the cement industry.
- 3) To collect data on fuel usage, electricity consumption and amount of clinker and cement production from the major cement industries in India.
- 4) To estimate CO₂ emissions of the selected cement industries in India.
- 5) To perform decomposition analysis of the change in CO₂ emissions in the cement industries.
- 6) To develop a basic dynamic model for forecasting CO₂ emissions with the data of selected cement industries.

- 7) To develop the modified model to forecast the cement production and CO₂ emissions in Indian cement industries under various scenarios.

The forecasting model was developed based on the data collected from the important cement industries in India. The prominent findings of the work were in obtaining the model to predict the CO₂ emissions from the cement production in India. So a modified model was also developed to forecast the cement production and corresponding CO₂ emissions from 2010 to the next 21 years for the cement production in India. Energy conservation management scenario was also discussed. The projection of this scenario states that recovery of waste heat and also using renewable energy in the cement industries will help to reduce CO₂ emissions.

The research also investigated a detailed energy analysis of a typical cement plant in important areas like kiln system and raw mill section. It was found that a huge amount of heat energy carried by the waste heat steams from the kiln system of the cement plant. So a waste heat recovery steam generation system (WHRSG) was proposed for the plant which could generate a power from the waste heat streams. A secondary insulation shell was also recommended for the kiln system of the plant. It will prevent the heat loss from the plant at the same time enhance the efficiency of the kiln system. It was found that a large amount of heat was lost due to conduction, convection and radiation from the surface of the raw mill of the plant. The second low efficiencies of the raw mill and kiln system were also estimated. It was found that the exergy utilization in the raw mill was worse than energy utilization. The exergy analysis accounts for the operation, indicating the location of energy degradation in the process. The main

cause of irreversibility in the kiln system was due to conversion of chemical energy of the fuel to thermal energy.

In this research a detailed analysis has been conducted to find the nature of factors affecting the change in energy related CO₂ emissions among the important cement industries in India. The factors that lead to CO₂ emissions are pollution coefficient effect, energy intensity effect, structural effect and activity effect. A specific detailed technique known as complete decomposition is used to evaluate the relative contribution of components that accounts for changes in energy induced CO₂ emissions. It was revealed that the activity effect of Indian cement industries is the most important component of carbon dioxide emissions.

1.4 Outline of the Thesis

The thesis mainly emphasises on the development of forecasting model for CO₂ emissions from the cement industries in India. The introduction of the thesis is given in the chapter 1. The literature survey reporting previous works are delineated in the chapter 2. The energy and exergy analysis of the raw mill in a typical cement industry are illustrated in Chapter 3. The theory of energy and exergy is also discussed in this chapter. The energy and exergy analysis of the kiln system of the cement industry is narrated in Chapter 4. The various thermal energy conservation opportunities are also discussed in this chapter. The project attempts in complete decomposition analysis of CO₂ emissions of the selected and grouped cement industries in India are discussed in Chapter 5. In chapter 6, a model is developed for forecasting CO₂ emissions from the data of the selected cement industries in India. The model is validated with historical data and the sensitivity test is also conducted. This model is used to

forecast CO₂ emissions and cement production. Again this model has been modified for prediction of CO₂ emissions due to the cement production in India under different scenario. Energy management scenario was also applied in the model in order to view the reduction in CO₂ emissions. The results and discussion were addressed at the end of the each relevant chapter. Finally, Chapter 7 summarises the research work, clearly pointing out the conclusions drawn from the energy and exergy analysis, decomposition analysis, forecasting models and bringing out the scope for future research work in this area. A list of references cited follows this chapter.

Thus the thesis is organized in a methodical way.

.....❧.....

LITERATURE REVIEW

Contents	2.1 <i>Introduction</i>
	2.2 <i>Energy and Exergy Analysis</i>
	2.3 <i>Decomposition Analysis</i>
	2.4 <i>Forecasting Models</i>
	2.5 <i>Conclusion</i>

2.1 Introduction

India emits more than 5% of global CO₂ emissions, and emissions continue to grow. CO₂ emissions have almost tripled between 1990 (600 million tonnes) and 2009 (1600 Million tonnes). The WEO (World Energy Outlook), 2010 New Policies Scenario projects that CO₂ emissions in India will increase by almost 2.5 times between 2008 and 2035. A large share of these emissions is produced by the industrial sector, which represents 54% of CO₂ in 2009, up from 40% in 1990 (IEA, 2011). In this situation, the efficient and effective utilization of energy has started to gain a vital significance in Indian Industrial sectors. This research work is focused on energy conservation and CO₂ emissions in Indian Cement Industrial scenario. To identify the problem an extensive literature survey was conducted. The studies in this chapter are divided mainly into three groups as follows:

- 1) Literature on energy and exergy analysis and emissions mitigation options.

- 2) Energy consumption, CO₂ emissions and decomposition analysis
- 3) Studies on forecasting models.

Literatures on energy analysis were collected to understand energy saving opportunities in the industry and reducing emissions. The literature on exergy also has been collected to understand location energy degradation areas. Previous works on decomposition modeling were collected to understand the influence factors that affect energy consumption and emissions in the industrial sectors. Forecasting models on energy consumption and emissions were collected to understand how the model could be developed from the results of the present study.

2.2 Energy and Exergy Analysis

The energy sources have been exhausted rapidly at the moment in addition, raising the energy costs (Utlu and Hepbasli, 2008). Several studies are currently going on controlling the mechanisms responsible for the energy degradation to minimize the system losses and to reduce the costs (Bejan, 1996) As energy analysis fails to indicate both the energy transformation and the location of energy degradation, in recent years, emerged a growing interest in the principle of special ability to measure different types of energy to work popularly known as exergy (Niksiar and Rahimi, 2009). Extensive application of exergy analysis can lead to reduction in the natural resources use and, thus, decrease the environmental pollution. The main purpose of exergy analysis is to detect and assess quantitatively the thermodynamic imperfections causes of thermal and chemical processes. The exergy method of thermodynamic analysis is based upon both the first and the second laws of thermodynamics together, while the energy analysis is based upon the first law only. It is a feature of the exergy concept to allow quantitative assessment of energy degradation

(Morris and Szargut, 1996). Recently, there is a growing interest in the use of both the energy analysis and the exergy analysis assessments for energy utilization to save energy and thereby achieve financial savings. Dincer et al. (2003) applied the energy and exergy analyses in the industrial sector of Saudi Arabia, Utlu and Hepbasli (2008) studied these analyses in the Turkish industrial sector, Al-Gandoor et al. (2010) presented the energy and exergy utilization of the USA manufacturing sector.

Dincer and Rosen (2009) studied the concepts of exergy analysis and the linkages between exergy and environmental impact. Several issues regarding the exergies of waste emissions are being addressed. Exergy is a measure of the degree of disequilibrium between a substance and its environment. The relation between several measures of environmental impact potential and exergy are being investigated by comparing current methods used to assess the environmental impact potential of waste emissions and the exergy associated with those emissions.

Khurana et al. (2002) conducted a research on energy balance in a cement industry. They used the data from an existing plant in India with a production capacity of 1MT per annum. They found that about 35% of the input energy was lost with the waste heat streams.

Koroneos et al. (2003) studied the exergy analysis of solar energy, wind power and geothermal energy. The actual use of energy from the existing available energy is discussed. In addition, renewable energy sources are compared to the non-renewable energy sources on the basis of efficiency.

Engin and Ari (2005) performed an energy audit analysis of a dry type rotary kiln system with a capacity of 600 tonnes of clinker per day

working in a cement plant in Turkey. For the heat loss through hot flue gas and cooler exhaust, a waste heat recovery steam generation system was proposed which could be recovered at 1 MW energy.

Koroneos et al. (2005) used exergy analysis methodology in cement production in Greece. The analysis involved assessment of energy and exergy input at each stage of the cement production process. The chemical exergy of the reaction is also calculated and taken into consideration. It is found that 50% of the exergy is lost even though a big amount of waste heat is being recovered.

Rasul et al. (2005) conducted a research base data from the Indonesian Portland cement plant. They presented a simple model to evaluate the thermal performance of the cement industry. They developed a model based on the mass, energy as well as exergy balance. The results obtained were that burning efficiency is 52.7%, cooler efficiency is 45%, and the heat recovery efficiency is 51.2%. There was high heat loss at the cooler of 19% and it was mostly due to convection and radiation

Ishikawa (2005) presented a study to assess the environmental impact. He has shown the importance of using several ways together: Life Cycle Assessment (LCA), Exergy-Mass Analysis (ExMA), and Total Material Requirement (TMR), in addition to the evaluation of the production of cement and eco-cement processes. The results reveal that exergy of wasted materials of the cement production process are larger than eco-cement production in both types of system boundaries. There is a lower exergy emissions due to exergy mass analysis in an eco-cement process by using Life Cycle Assessment and the Total Material Requirement method showed the same tendency of exergy mass analysis.

Zafer et al. (2006) performed energy and exergy study in a raw mill of capacity 82.9 tonnes per hour in a cement plant in Turkey. The energy and exergy efficiencies of the raw mill are determined to be 84.3% and 25.2% respectively. This study is based on fixed dead state temperature.

Al-Hinti et al. (2008) proposed a system for the utilization of dissipated heat from the surfaces of cement processing kilns at the Jordan Cement Factories in heating heavy fuel oil used in the burning process of these kilns. They found that for 1000 m² effective kiln surface area, a total of 5 MW heat can be recovered. The proposed system consists of a closed loop of coil-shaped, 50 mm-diameter, high conductivity steel tube in which the thermal oil is circulated. The coil is arranged to pass around the kiln's shell to absorb the available heat and then through a counter flow heat exchanger to transfer the absorbed heat to the heavy fuel oil. The resulting annual savings are around \$0.54 million for the Jordan Cement Factory. The payback period of the system is 200 days.

Ziya et al. (2009) investigated the effects of varying dead-state temperatures on the energy and exergy analyses of a Raw Mill of a cement plant. The sensitivity of the energy and exergy are examined and calculated according to the varying dead-state temperatures. The exergy efficiency value ranges from 44.5% to 18.4% at varying dead-state temperature values between -18°C and 41°C. The sensitivity analysis result indicates that varying dead-state temperatures have an effect on the exergy efficiency.

Ziya and Zuhail (2009) performed energy and exergy analysis to evaluate energy and exergy efficiency in each process at the cement factory. Efficiencies (energy/exergetic) of the processes for the raw mill,

the rotary kiln, the trass mill and the coal mill on the production line have been found to be 84%/25%, 61%/49%, 74%/13% and 74%/18% respectively.

Sogut et al. (2009) examined heat recovery from the rotary kiln for a cement plant in Turkey. It is determined that 5% of the waste heat could be utilized with the heat recovery exchanger. The useful heat obtained is expected to partially satisfy the thermal loads of 678 dwellings in the vicinity through a new district heating system. This system is expected to decrease domestic-coal and natural gas consumption by 51.55% and 62.62% respectively.

Sogut et al. (2009) conducted a performance study on trass mill in a cement plant based on the actual operational data using energy and exergy analysis method. The operation of the trass mill spends a lot of energy. The primary efficiency of the process was found to be 74% and 26% of the remaining energy lost with heat losses. In this system, energy recovery may be realized from hot flue gasses and heat losses. They stated that if the energy recovery rate of heat losses would be 40%, this rate could be increased to about 14% for the whole trass mill process. Thus, energy efficiency of the system is to be risen from 74% to 84%. The exergy efficiency is found to be 10.67% for the trass mill. In the trass mill, exergy losses have been calculated to be about 89% and the exergy losses are exhausted due to the irreversibility. The exergy losses could be decreased to 33% using the energy recovery system established before the mill unit. The usable exergy rate of the hot gasses and steam going up the flue gas were estimated to be 4%. They concluded that if this improvement could be made, exergy efficiency of the system would go up to about 48%.

Kamate and Gangavati (2009) studied exergy analysis of a heat-matched bagasse -based cogeneration plant of a typical 2500 tonnes per day sugar factory, using backpressure and the extraction of condensing steam turbine. In the analysis, exergy methods, in addition to the more conventional energy analyses were employed to evaluate overall and component efficiencies and to identify and assess the thermodynamic losses. They noticed that, the boiler was the least efficient component and turbine, the most efficient component of the plant. The results showed that, at optimal steam inlet conditions of 61 bar and 475°C, the backpressure steam turbine cogeneration plant perform with energy and exergy efficiency of 86.3% and 30.7% and condensing steam turbine plant perform with energy and exergy efficiency of 68.2% and 26%

Ganapathy et al. (2009) studied exergy analysis performed on an operating 50 MW unit of lignite fired steam power plant at Thermal Power Station-I, Neyveli Lignite Corporation Limited, Neyveli, Tamil Nadu, India. The distribution of the exergy losses in several plant components during the real time plant running conditions has been assessed to locate the process irreversibility. The comparison between the energy losses and the exergy losses of the individual components of the plant showed that the maximum energy losses of 39% occur in the condenser, whereas the maximum exergy losses of 42.73% occur in the combustor

Wang et al. (2009) examined the exergy analysis of four cogeneration systems such as single flash steam cycle, dual-pressure steam cycle, Organic Rankine Cycle and the Kalina cycle of the cement industries and a parameter optimization for each of the cogeneration system was achieved by means of Genetic Algorithm (GA) to reach maximum exergy efficiency. The optimum performance for different cogeneration systems were

compared under same working condition. It was found that Kalima Cycle can achieve the highest exergy efficiency (44.9%) and the Organic Rankine Cycle shows the lowest exergy efficiency (36.6%). The single pressure steam cycle (42.3%) and dual pressure steam cycle (40.9%) has a better performance in recovering waste heat of the cement plants. They noted that the Organic Rankine Cycle, which is superior in recovering low grade waste heat, was not be suitable for waste heat recovery in the cement plant due to relatively high temperature of the waste heat sources.

Khaliq (2009) proposed conceptual trigeneration system based on the conventional gas turbine cycle for the high temperature heat addition while adopting the heat recovery steam generator for process heat and vapour absorption refrigeration for the cold production. Combination of first and second law approach was applied and computational analysis was performed to investigate the effects of overall pressure ratio, turbine inlet temperature, pressure drop in the combustor, heat recovery steam generator and evaporator temperature on the exergy destruction in each component, first law efficiency, electrical to thermal energy ratio, and second law efficiency of the system. It was found that maximum exergy is destroyed during the combustion and steam generation process; which represents over 80% of the total exergy destruction in the overall system.

Aljundi (2009) conducted a study on energy and exergy analysis of Al-Hussein power plant in Jordan. His primary objectives were to analyze the system components separately and to identify and quantify the sites having largest energy and exergy losses. In addition, the effect of varying the reference environment state on this analysis was also performed. Energy losses mainly occurred in the condenser where 134 MW is lost to the environment while only 13 MW was lost from the boiler system. The

percentage ratio of the exergy destruction to the total exergy destruction was found to be maximum in the boiler system (77%) followed by the turbine (13%), and then the forced draft fan condenser (9%). In addition, the calculated thermal efficiency based on the lower heating value of fuel was 26% while the exergy efficiency of the power cycle was 25%. For a moderate change in the reference environment state temperature, no drastic change was noticed in the performance of major components.

Ziya et al. (2010) conducted a study on rotary kiln of Turkey Cement Plant and a mathematical model was developed for a new heat recovery heat exchanger. From the energy and exergy analysis of the plant, it was found that highest energy loss occurs in the rotary kiln process compared to trass, farine and coal mills. Around 73% of waste heat from the rotary kiln has been transferred to the fluid through the modelled heat exchanger. For 120 m² gross floor areas, around 78 residences could be heated with this recovered waste heat.

Ahmet (2010) presented an alternative method to investigate the irreversibility in a cement plant. Energy and exergy balances were calculated for the whole system and its sub-units, which consist of clinker cooling, rotary kiln, calciner and preheater cyclone units. In the analyses, irreversibility sources were identified as combustion, chemical reaction, and heat transfer to raw material during mixing in the system, and heat transfer between the system and its environment. Irreversibilities in the system were classified as recoverable and unrecoverable. Recoverable ones were exergy destruction via waste heat caused by stack gas, stack dust, clinker and unused coolant outlet air. Recoverable exergy destruction was found to be 18.5% of the total irreversibility. It was concluded that the heat transfer irreversibility can be easily recovered compared to the others by

minimizing the heat loss from rotary kiln. By reducing the heat losses in rotary kiln, calciner and cyclone groups, energy consumption could be decreased to 360.81 kJ per kilogram of clinker. Energy saving could be increased to 1036 kJ per kilogram of clinker when the exergy destruction of hot gases leaving the cyclone group and clinker cooler are recovered. When all systems are considered, left hot air disposed from clinker cooler in cement plant is usable for drying of coal and raw materials. Heat loss from the outer surface of rotary kiln could be decreased by applying appropriate isolation or coating. Hot stack gases disposed from first cyclone could also be used for drying of coal and raw materials or could be used in generating electricity using steam recuperation system.

Vedat (2011) conducted the energy and exergy assessments of an existing dry-type rotary kiln system, which was composed of a pre-heater cyclone group, kiln and clinker cooler. The results showed that, the energy efficiency of the present system is 54.9%. The major heat loss sources have been determined as kiln exhaust (20%), cooler exhaust (12.80%), combined radiative and convective heat transfer from kiln surfaces (2.91%), and sensible heat loss by the clinker discharge (2.2%). For the first two losses, a conventional WHRSG system, and a pre-heater system were proposed and corresponding calculations showed that 28966 kW (10.78%) for WHRSG and 30877 kW (11.5%) for the preheater system of the input energy were recovered. Overall, 22.28% of the input energy was saved with the use of the proposed systems. The exergy efficiency of the kiln was determined to be 28.9%. The exergy efficiencies of the WHRSG and pre-heater were 70.6% and 81.5%, respectively. These indicate relatively remarkable improvement over the existing system. The author concluded that waste energy recovery systems must also be incorporated in the design of new

industries to minimize energy consumption, manufacturing costs and to improve the product quality.

Adem and Kanoglu (2012) conducted a study on energy and exergy analysis of a raw mill. The first and second law efficiencies of the raw mill are determined to be 61.5% and 16.4%, respectively. The effects of ambient air temperature and moisture content of raw materials on the performance of the raw mill were also investigated. The data collected over a 12-month period indicates that first and second law efficiencies of the raw mill increases, as the ambient temperature increases and the moisture content of the raw materials decreases. The specific energy consumption for farine production was determined to be 24.75 kWh/tonne of farine. It was found that by using external hot gas supply, a reduction of 6.7% energy consumption happens in the farine production

Madloola et al. (2012) reviewed exergy analysis, exergy balance, and exergetic efficiencies for the cement industry. It was found that the exergy efficiency for cement production unit ranges from 18% to 49% and the exergy loss due to the irreversibility from kiln was higher than the other units in cement production plant. The raw feed pre-heating causes the lowest irreversibility within the cement plant. The highest energy efficiency was found in raw mill but the exergy efficiency remains lower than 26%. The lowest exergy efficiency was found in trass mill of the cement plant. In the cogeneration systems, the biggest exergy loss occurred in the turbine expansion process and next to that was the condensation process.

The following studies concentrated on performance analysis as well as mitigation action to reduce emissions from cement industries.

Claudia and Leticia (1998) studied Energy use and CO₂ emissions in Mexican cement industry analyzed for the period 1982-1994. From 1982-1994 energy use in Mexican cement industry increased by 10.8% and CO₂ emissions related to both energy use and the industrial process increased by 40%. During this period, it was found that the energy intensity dropped significantly. This was due to modernization of existing plant, increased production of blended cement and the use of alternative fuels. It was also found that preheating system and automatic control at several process results in more efficient energy use. They noted that the operation of modern kiln with long residence time and high temperature ensured low emissions also.

Worrell et al. (2000) performed an in-depth analysis of the US cement industry, identifying carbon dioxide savings, cost-effective energy efficiency measures and potential between 1970 and 1997. They gave the energy efficiency improvement and carbon dioxide emissions reductions in the production of cement in the US cement industry. Such large amounts of energy saving need to improve the energy efficiency of combination process. Any success in this direction, improving machine design and choosing optimal operating and environmental conditions could possibly lead to the development of new approaches toward energy saving in cement production.

Rehan and Nehdi (2005) discussed climate change, the current and proposed actions for mitigating its effects, and the implications of such actions for the cement industries. They examined emerging policy instruments such as environmental taxes and financial incentives in the form of grants, subsidies, and/or tax credits for taking action to protect the environment. They also discussed the traditional methods like CO₂

captured and CO₂ sink in order to reduce greenhouse gas emissions. They suggested that the Government needs to increase R&D investments in commercializing new kiln types, development of economic and effective complementary products for concrete made with blended cements, and improvements in construction practices. Such measures are likely to prove valuable in reducing GHG emissions of the cement industry.

Shammakh et al. (2008) discussed the effective control strategies to mitigate emissions in cement plant. They developed a mathematical programming model to determine the best cost effective strategy to minimize CO₂ emissions from cement plant. Efficiency improvement measures were found to be effective options to meet emissions reduction targets up to 10%. The model recommended that fuel switching and carbon capture needed to be implemented to achieve more than 10% emissions reduction

Dennis and Van (2009) studied an overview of the emissions from Australian cement sector including both the emissions from the chemical process itself, as well as the associated emissions from energy use within those processes. He mentioned two benefits of CO₂ capture and storage in the cement industries over power generation. Firstly, cement kilns produce much more concentrated stream of CO₂ (up to 31%) compared to power stations (12 to 14%), hence lower cost is required to achieve the desired volume of CO₂ for storage. Secondly, cement kilns have exhaust gas temperatures of approximately 200°C or above and this heat can be used to recover the solvent used in the capture process. The use of this heat from a cement plant does not impact the production of cement. But in power generation station, low pressure steam needs to be diverted from the turbines resulting in less electricity being produced.

Huntzinger and Eatmon (2009) employed LCA method to evaluate and compare the environmental impact and carbon emissions of four cement manufacturing processes as: (1) the production of traditional Portland cement, (2) blended cement (natural pozzolans), (3) cement where 100% of waste cement kiln dust is recycled into the kiln process, and (4) Portland cement produced when cement kiln dust was used to sequester a portion of the process related CO₂ emissions. Analysis using Sima Pro 6.0 software proved that blended cements led to the greatest environmental and carbon emissions savings. The utilization of cement kiln dust for sequestration showed acceptable mitigation of carbon emissions as well as 5% reduction in environmental impact over the traditional Portland cement. The recycling of cement kiln dust was found to have little environmental savings over the traditional process.

Rodriguez et al. (2009) proposed a new process to produce carbon dioxide in pure form. In this process, combustion and calcination reactions take place in different chambers. As a result, flue gases produced due to fuel combustion and carbon dioxide generated from decomposition of limestone were not mixed. In the new design, required energy for calcination was supplied by a hot stream of CaO. It was claimed that by implementing the proposed changes, 50% carbon dioxide emissions reduction can be achieved compared to the conventional process. Although it was a great effort to reduce CO₂ emissions in cement plant the following draw backs were observed such as difficulty and impracticality of carrying and recycling a very hot solid stream (CaO stream) as heat carrier, extra cost due to the installation of an extra combustion chamber to reheat CaO stream and low rate of CaO fed to the kiln (only 2% of total produced CaO).

Bundela and Vivek (2010) conducted a study Kymore Cement Works and proposed to install a power plant of 9 MW which would be operated with the recovered waste heat from the clinker coolers and kilns from its both clinker units, so expected reduction in CO₂ emissions would be 48000 tonnes per year. They reported that the hot air from cooler and kiln passing through the electrostatic preceptor (ESP) is taken to the waste heat recovery exchangers. The hot flue gases will pass through a Heat Exchanger by which the temperature of the waste gas is transferred to the internal elements of the heat exchangers which is used for heating of the thermo oil. In turn, this thermal oil vaporizes the organic fluid in close loop cycle. Multi level pressure turbine system will be installed which increases usable heat content resulting in higher power output.

Kabir et al. (2010) studied a detailed thermal energy audit of a pyroprocessing unit for a dry process kiln systems. The results revealed that fuel combustion provides 95.48% (4164.02 kJ/ kg of clinker) of the total energy input to the unit. The kiln exist gases and kiln shell were the major sources of thermal energy losses, amounting to 27.9% (1216.75 kg/kg of clinker) and 10.84% (472.56 kg/kg of clinker) respectively. The thermal efficiency of the unit was 41%, low enough to consider implementing thermal energy conservations measures. Conservation techniques for improving specific energy utilisation efficiency and reducing Green House Gas emissions were proposed. WHRSG and secondary shell energy conservation measures were studied. The WHRSG could generate up to 4.4 MW of electricity, which could lead to an annual power saving of 42.88 MWh/year. They found that the secondary shell concept can save up to 5.30 MW of thermal energy, which was equivalent to 10.4% of the total input energy. Fuel consumption was reduced by an equivalent percentage margin

and energy efficiency of the unit increased by 5%. Total cost saved for the use of WHRSG and secondary shell concept was 2318.18 USD/year, and 14.10% reduction in Green House Gas emissions was achieved.

Jan et al. (2010) conducted a study on the evolution of the cement industry in Poland over the period 1998–2008 and the resulting changes in CO₂ emissions. They presented sources of CO₂ emissions in cement industry and also discussed the potential ways to reduce emissions. These actions were introduction on a large-scale (98%) of less energy-consuming ‘dry method’, modernization of installations, introduction of alternative fuels, and the use of waste as raw materials and additives to cement. It was found that the Polish cement industry reduced significantly the emissions factor per tonne of cement in the period 1988–2008 by 28%. In 1988, the factor amounted to 0.879 tonnes CO₂/tonnes of cement and 1.1 tonnes CO₂/tonnes of clinker, while in 2008, 0.631 tonnes CO₂/tonnes of cement and 0.865 tonnes CO₂/tonnes respectively of clinker. It was also noted that the introduction of Emissions Trading Scheme forces cement industry to take actions, so as to limit the emissions of CO₂.

Moya et al. (2011) carried out the cost effectiveness analysis of some of the best available technologies (BAT) that could result in energy consumption and CO₂ emissions reduction in the European Union’s (EU27) cement industry. The results indicated that the possible thermal energy improvement in the clinker production, if all BATs were implemented, was 10%. It was also found that some of the technologies considered in the study were not cost effective at the moment.

Ali et al. (2011) presented different techniques to reduce CO₂ emissions from the cement manufacturing industries in their study. They

mentioned that the CO₂ capture from the flue gases store it away into the soil or ocean is a cost effective way and this can reduce carbon emissions by as much as 65–70%. By reducing the clinker to cement ratio with the addition of various additives, CO₂ emissions can be reduced substantially. It was found that the substituting fossil fuels with alternative fuels may play a major role in the reduction of carbon dioxide emissions. They noted that the greatest opportunities to reduce energy consumption and lowering emissions associated with cement manufacturing process will be obtained with improvements in pyroprocessing. Raw material drying at the raw mills, waste heat recovery from kilns exit gases using steam generator and Kiln shell heat loss reductions can be considered for the pyroprocessing improvements.

Ziya and Zuhail (2011) modelled a rotary kiln process of a cement plant in Turkey and analysed using annual operation data in order to study the global effects caused by exergetic inefficiency. Annual averages of the exergy efficiency of the kiln and its exergetic improvement potential were found to be 48.5% and 110.58 GJ/h, respectively. For that system, CO₂ emissions caused by exergetic losses were calculated for the coal mixture and the natural gas as an average of 38,004 kg/h and 12,668 kg/h, respectively.

Ziya (2012) examined exergetic efficiency of Turkish cement production and CO₂ emissions caused by the sector due to exergetic losses and environmental effects by considering the clinker production between 1999 and 2007. The exergy analysis was based on dead state temperature. The CO₂ emissions of the clinker production according to exergy losses, improvement and energy potentials were determined. Exergy efficiency of the kiln and exergetic improvement potential were found to be 43.04% and

123.29×10^6 GJ/h respectively on average. In that system, CO₂ emissions caused by exergetic losses were calculated as 75.18×10^6 kg/h, 25.06×10^6 kg/h and 81.45×10^6 kg/h respectively on average for the coal mixture, natural gas and fuel-oil. He concluded that the present technique is suggested as a useful tool developing energy policies and providing energy conservation measures.

Emad et al. (2012) conducted a simulation study on existing pyro-processing unit in Dashtestan cement plant using Aspen HYSYS software. In order to optimize the case study process, reduce fuel consumption as well as emissions mitigation, a novel unit was designed and simulated with the same operating condition. The main difference between base case and new process was the design of calciner stage where 90% of CaCO₃ and MgCO₃ were decomposed to CaO, MgO and CO₂ without consuming any fuel. In that stage, required energy for decomposition reactions and maintaining calciner temperature at 890 °C was supplied by a very hot stream of CO₂. The extra amount of CO₂ should be fed to the calciner at 1200 °C in startup step. After operation, the amount of pure CO₂ leaves calciner at 890 °C and was heated up by the kiln exhaust stream and then recycled to the calciner. The results of new process were then compared to the base case process. It was found that the novel process could reduce 2.3% of process fuel consumption, mitigating 66% of CO₂ emissions as well as reduction in NO₂ and SO₂. They concluded that in the new process the capture could be eliminated since the pure CO₂ produced by separating decomposition and combustion reaction.

Shuangzhen and Xiaochun (2012) studied the current strategies of energy efficiency improvement, CO₂ captured in cement production and fly ash blended cement in China. They noted the following points in this study.

New Suspension Preheater, which introduces direct contact between high temperature kiln exhaust and the calcination zone, makes the high quality heat exchange more efficient and saves almost 1/3 energy in cement production. Waste Heat Recovery in cement production, such as Organic Rankine or Kalina Cycle, will take advantage of low grade heat (for example, from the preheating exhaust and clinker cooling) in the range of 300°C - 500°C for cogeneration, and significantly improve energy efficiency in cement production. CO₂ capture is more efficient and technologically feasible in cement production than fossil fuel fired power plants: lime looping seems to be a good fit because of its technical reliability and inexpensive/convenient raw material limestone in cement production. Fly ash either from coal or from alternative fuels should be studied further for recycle in cement/concrete to reduce the energy input and the CO₂ emissions for cement production.

2.3 Decomposition Analysis

Reitler et al. (1987) proposed a method to decompose change in industrial energy consumption into three factors, namely production quantity, production structure and specific consumption. Li (1990) used the Divisia index approach to examine the structural change and energy intensity of 17 manufacturing sectors in Taiwan during 1971 to 1985. Their study found that changes in sectoral energy intensities played a major role in affecting Taiwan's manufacturing aggregate fuel and electricity intensities during that period, while the structural effect was relatively insignificant. Howarth et al. (1991) decomposed the manufacturing energy use change in eight OECD countries from 1973 to 1987 by the Laspeyres index method and compared the results to those obtained by using the Divisia index method. They discussed the output, industry structure and energy intensity effects and found minor differences between the Laspeyres index and the Divisia index calculations.

Another study for nine OECD countries was conducted by Torvanger (1991). He used the Divisia approach to decompose the change of CO₂ emissions related to energy use. His study found that the major contribution to reduced CO₂ intensity in the studied countries was a reduction in energy intensity and a reduced production share of energy intensive sectors. Park (1992) selected three factors, including structural change, energy intensity and output level, to decompose the industrial energy consumption in Korea for 1973-89. Liu et al. (1992) proposed two parametric Divisia index methods that transformed the integral path problem in the Divisia index into a parametric estimation. Also, an adaptive weighting Divisia method was introduced with detailed mathematical analysis to estimate the parameter values for the case of Singapore industry. Ang and Lee (1994) extended the work of Liu et al. (1992) and compared five specific decomposition methods by using data from Singapore and Taiwan. They concluded that the decomposition results were method dependent. Ang (1995) also extended the methods to deal with the decomposition of industrial energy consumption at multiple levels of sector disaggregation, which allowed more adequate use of the decomposition method if the energy and output data were available. Greening et al. (1997) proposed comparison of six decomposition methods for manufacturing in 10 OECD countries. Sun (1998, 1999) presented a complete decomposition model to solve residual terms.

The pioneering work by Grossman and Krueger (1991) adapted the decomposition method to the context of environmental studies. They decomposed CO₂ emissions change into economy scale, economy composition and technology factors, for the members of the North American Free Trade Agreement. They concluded that economic growth tends to alleviate pollution problems.

Huang (1993) used multiplicative arithmetic mean Divisia indices, to decompose energy intensity changes in Chinese secondary industry and the six sectors into which he divided it in the period 1980–1988 based on the effects of structural change and improvements in energy intensities. The six sectors were: paper, chemicals, building, metal, mechanical–electric–electronic (MEE), and other secondary industry. He found that the main contribution to declining intensity in each industry was from the improvements in subsector intensity during the period.

Claudia and Leticia (1998) analyzed the factors that influenced energy use and CO₂ emissions in the Mexican cement industry from 1982 to 1994 using the Laspeyres index method. They observed relative importance of fuel intensity, clinker activity, the cement to clinker ratio, and the use of waste tires as an alternative fuel in the changes of clinker fuel use. The changes in CO₂ emissions were divided into energy intensity, cement activity, the cement to clinker ratio, and primary and final fuel-mix effects. During this period, energy intensity for this industry decreased by 28%. The intensity of CO₂ emissions related to energy use declined by 17%, and the intensity of CO₂ emissions associated with the cement industrial process dropped by 1.7%. Although energy-related CO₂ intensities decreased, overall CO₂ emissions increased by 40%, due to growth of Mexican cement production. The analysis shows that although important efforts were directed at modernization and material change, development pressures (the building of infrastructure in the case of cement) and the growth of cement exports drove CO₂ emissions up.

Paul and Bhattacharya (2004) used complete decomposition approach to analyze the change in CO₂ emissions at major economic sectors like agriculture, industry and transport in India for the period 1980-1996. The

observed changes in the energy-related CO₂ emissions were divided into four factors: pollution coefficient, energy intensity, structural changes and economic activity. It was found that economic growth has the largest positive effect on CO₂ emission changes in all the major economic sectors.

Syed et al. (2007) conducted decomposition analysis energy consumption in to the scale of economic activity, structural technological effect and economic structure in Pakistan for the period 1960-1998. The economy in the country was divided into two groups such as low energy intensity structure and high energy intensity structure. The results showed that the increased energy strength was due to both the activity effect and structural effect. The inefficient use of energy was due to the change in economic strength and economic activity in the country. The results further indicated that improved efficiency of energy use was due to efficient use of energy by relatively high energy intensive group in the country.

Fisher et al. (2003) examined the absolute decline in energy consumption as well as intensity decline during 1997–1999 in China. They applied the multiplicative arithmetic mean Divisia methods to a unique set of enterprise-level data. They decomposed both total energy intensity as well as intensities computed for each of the individual fuels and electricity. They found that the proportion of change in energy intensity explained by structural change rises as the level of disaggregation becomes finer.

Rehan and Nehdi (2005) discussed climate change, the current and proposed actions for mitigating its effects, and the implications of such actions for the cement industries. The paper examined emerging policy instruments such as Environmental taxes and financial incentives in the form of grants, subsidies, and/or tax credits for taking action to protect the

environment. They also discussed the traditional methods like CO₂ captured and CO₂ sink in order to reduce greenhouse gas emissions. The author also suggested that the Government need to increase R&D investments in commercializing new kiln types, development of economic and effective complimentary products for concrete made with blended cements, and improvements in construction practices. Such measures are likely to prove valuable in reducing GHG emissions of the cement industry.

Lise (2006) conducted the four factor decomposition for Turkey for the period 1980-2003. The study identified a structural (composition) effect for the changing shares of sectors in GDP. The GDP effect, structure effect, and carbon intensity effect were all associated with substantial increases in emissions, while the energy intensity effect led to a small reduction in emissions.

Lee and Oh (2006) produced the five factor decomposition for 15 APEC countries between 1980 and 1998. This group includes high, middle and lower income countries. They reported that although GDP and population were strong factors associated with an increase in emissions in all cases, the high income countries falls in energy intensity and the share of fossil fuels, as well as a change in the fossil fuel mix all contributed to partially offsetting the impacts of growth in the economies. The group of lower income countries was dominated by China which, in the period, experienced a large fall in energy intensity, offsetting nearly half the impact of the increase in income and population.

Wachsmann et al. (2009) assessed the structural decomposition of energy use in the industrial and household sectors in Brazil from 1970 to 1996. They observed that energy usages by households were small

compared to the changes in total energy consumed in Brazil, while industry sector was the main contributor to growth in energy use. They concluded that the affluence effects of economic activity and population were the main determinants of energy use growth in Brazil, while the improvement in energy intensity and change in household energy usage were pointed to as factors contributing to decreased energy use. They also showed that in Brazil, structural arrangements favouring exporting-oriented industries or infrastructure-related investments, among other sectorial compositions, were potentially associated with higher energy demand, which had an associated impact on emissions.

Ipek et al. (2009) conducted a study to identify the factors that contribute to changes in CO₂ emissions for the Turkish economy by utilizing Log Mean Divisia Index (LMDI) method during the period 1970–2006. In the study, Turkish economy was divided into three aggregated sectors, namely agriculture, industry and services, and energy sources used by these sectors were aggregated into four groups: solid fuels, petroleum, natural gas and electricity. The result showed that the main component that determines the changes in CO₂ emissions of the Turkish economy was the economic activity. It was also found that structural effect and energy intensity effect were not a significant factor in changes in CO₂ emissions.

Sudhakara and Binay (2010) used decomposition analysis for the selected thirteen manufacturing industries such as (1) chemical (2) beverages and tobacco, (3) food products, (4) machinery, (5) aluminum and aluminum products, (6) copper and copper products, (7) iron and steel, (8) mining, (9) cement, (10) other nonmetallic and mineral products, (11) paper and paper products, (12) textiles, and (13) transport equipment. The period of analysis was from 1992 to 2005. The study helped in identifying the

industry in terms of where the potential exists for efficiency improvement and pollution abatement. Unlike most of the sub-sectors, the textile industry increased energy use and CO₂ in the study period because of mechanization. In the paper industry, there was a decline in the intensity since 2000 and it is evident that improvement is ongoing. Decomposition of the energy intensity effects observed in the fuel substitution in the sector indicated that the structural effect was the main contributor to the changes in energy intensity. It had 2.3 times higher influence in reducing energy consumption and 3.1 times in reducing CO₂ emissions than intensity effect.

Nicola and Smeeta (2011) conducted a decomposition analysis study for a sample of 20 developing countries to discriminate shifts of energy intensity depending on the change of the structural economies composition from those depending on energy efficiency. They found that energy intensity component depending on energy efficiency shows a negative trend for 14 out of 20 countries and the structural component was more than one for 14 out of 20 countries. They concluded that during the growth path, developing countries tend to grow in “dirty” sectors by worsening the structural component of energy intensity; on the other hand, growth improves technical efficiency. But in countries like Latvia, both structural and the energy efficiency effect worsen over time. The fact that a majority of countries give a negative trend of energy intensity over time suggests that the energy efficiency effect in many cases dominates the structural effect.

Jiang (2011) used Logarithmic Mean Divisia Index Model (LMDI), for the analysis of changes in CO₂ emissions and percentages of contributors for China during the period 1995-2007. Four effects resulted in changes in CO₂ emissions, including economic scale, industrial structure, energy

intensity or energy efficiency, and carbon intensity. The most significant factor contributes to an increase in CO₂ emissions during the study period was due to economic development, followed by a change in the industrial structure and energy structure or carbon intensity. The decrease in energy intensity would lead to carbon emissions reductions, but the increase in CO₂ emissions during the decade was definitely caused by economic growth, and the change in economic structure and energy structure. Improvement in energy intensity had a positive effect on carbon emissions. The results also show that the four effects were not the same for different periods of time. The energy intensity decrease and economic development were the major reasons for increases in CO₂ emissions during the period 1995-2000. However, the economic development could take up as large as 85.8% of all increases in CO₂ emissions during the period 2002-2007.

Luciano and Shinji (2011) evaluated the changes in CO₂ emissions from energy consumption in Brazil for the period 1970–2009. The results demonstrated that economic activity and demographic pressure were the leading forces explaining emissions increase. On the other hand, carbon intensity reductions and diversification of energy mix towards cleaner sources were the main factors contributing to emissions mitigation, which were also the driving factors responsible for the observed decoupling between CO₂ emissions and economic growth after 2004. This study assessed the changes in CO₂ emissions from energy consumption in Brazil. The results showed that emissions change has been predominantly influenced by economic activity and population growth. It was observed that fuel diversification toward lower emissions sources and carbon intensity was amongst the factors that contributed to the deceleration of emissions growth for the period 1970–2009.

Li and Yang (2011) used a structural decomposition analysis model to measure the effects of CO₂ emissions intensity reduction of four factors, involving energy efficiency, energy structure, industry structure, and economy growth mode for the period 1997-2007. The changes in energy efficiency and energy structure were the major drivers for promoting decrease in CO₂ emissions intensity. On the other hand, the industry structure and economy growth mode were the major drivers for increasing CO₂ emissions intensity. They suggested that continued efforts need to be made to adjust industry structure and change economy growth modes so as to achieve the goal of cutting CO₂ emissions per unit of GDP by 40 to 45% in 2020 from 2005. They concluded that decrease in CO₂ emissions intensity depends largely on economy growth and energy consumption. Moreover, economy growth depends on industry structure and growth mode. Energy consumption depends on energy efficiency and energy structure. So, adjusting industry structure, transforming economy development mode, and advancing energy efficiency would be greatly helpful for China to substantially reduce the CO₂ emissions intensity in the future.

Simone et al. (2011) conducted a study on fossil-fuel related CO₂ emissions in Austria and Czechoslovakia for 1830–2000. The drivers of CO₂ emissions were discussed by investigating the variables of the standard Kaya identity for 1920–2000 and conducting a comparative Index Decomposition Analysis. Proxy data on industrial production and household consumption were analysed to understand the role of the economic structure. CO₂ emissions increased in both countries in the long run. Czechoslovakia was a stronger emitter of CO₂ throughout the time period, but per-capita emissions significantly differed only after World War I,

when Czechoslovakia and Austria became independent. The difference in CO₂ emissions increased until the mid-1980s, explained by the energy intensity and the composition effects, and higher industrial production in Czechoslovakia. Counter balancing factors were the income effect and house hold consumption. After the Velvet revolution in 1990, Czechoslovakia CO₂ emissions decreased, and the energy composition effect lost importance. Despite their different political and economic development, Austria and Czechoslovakia reached similar levels of per-capita CO₂ emissions in the late 20th century. They concluded that neither Austrian “eco-efficiency” nor Czechoslovakia structuring have been effective in reducing CO₂ emissions to a sustainable level. Thus a fundamentally new economic structure with different ways of production and consumption is needed for a future shift towards sustainability. This will also require radically new policy measures.

Vladimír (2012) conducted a complete decomposition analysis in order find the changes in energy consumption in the countries of EU-27 in the period 1990-2008. The method decomposes the change in energy use into three different effects: a change in energy consumption due to an increase in economic activity (the activity effect), a change in energy consumption due to a relative increase of significance of a country in the group (the structure effect) and a change in energy consumption due to a change of energy efficiency measured as energy intensity (the intensity effect). The results showed that there was a difference in the development of these effects between the old (EU-15) and the new member countries. As the activity effect was on average 1.13 times higher in the old member countries, it showed that the economic growth in the examined period was more pronounced in the old member countries. The structure effect was highly diversified within each group. The change in energy use explained

by this effect shows a relative increase in significance of the structure. The intensity effect was almost universally negative in all countries and it was the main diversifying factor between the two groups. Compared to the old member countries, the new member countries did show almost twice as big reduction in their energy intensity. This was due to stricter energy efficiency and energy saving policies in the new member countries. Finally, he concluded that there was a difference in magnitudes of the activity effect and the intensity effect, which were big enough to affect the overall change. The only observable difference in the variability was for the activity effect, which was higher for the old member countries.

2.4 Forecasting Models

Sanjib and Sahu (1992) developed a system dynamics model to study the long-term dynamic behaviour of the Indian oil and gas exploration/exploitation industry for the period 1965-2005. The dynamics of finite and non-renewable fossil fuel resources were portrayed in the model and were linked with the financial sector. The credibility of the model has been enhanced through model validation. Model-generated projections were compared to the projections made by the industry and the Indian government and thereby found satisfactory in both trend and values. The effect of important variables on the model has been studied in order to choose alternative policies. The expected behaviour of the model has been analyzed under a standard run and under changed conditions. Perhaps the most striking revelation of the study was that oil production will start declining after attaining a peak of 39.5 million tonnes during 1994-96. Similarly, gas production will start falling after reaching a peak of 25.1 billion cubic meters during 1997-99. They concluded that in order to face the difficult situation in India, alternate policies must be adopted. This will

mitigate the oil crisis to some extent in the short term, but will be unable to contain growing demand and the consequent imports in the long run.

Choucri et al. (1990) conducted a detailed simulation analysis to study Egypt's oil industry as a near-typical, non-OPEC, oil-producing developing country. This model was used to explore implications of alternative scenarios for government policies (which affect Egypt's domestic consumptions directly), world oil prices (which influence earnings from export), and geological parameters (which affect the condition of resources and reserves) on patterns of production, exports, and earnings. The model effectively distinguished foreign oil companies and government agents as well as oil-producing regions which disaggregated geologically, to represent the characteristics of oil production; moreover, it made a distinction between domestic consumptions and exports as well as the domestic and international prices. The model had three exogenous variables including export and subsidized domestic prices, discovery and development prices, and initial levels of reserves and undiscovered oil.

Anand et al. (2005) used system dynamic approach for estimating the methane emissions from rice fields in India till the year 2020. Mitigation options studied for curtailing the methane emissions include rice production management, use of low methane emitting varieties of rice, water management and fertilizer amendment. They concluded that improved high yielding rice varieties together with efficient cultivation techniques will certainly contribute to the curtailment of the methane emission fluxes.

Brian and Chang (2005) used System dynamic modelling for the prediction of solid waste generation in a fast-growing urban area based on a set

of limited samples. The analysis gave various trends of solid waste generation associated with five different solid waste generation models using a system dynamics simulation tool – Stella. Research findings indicated that such a new forecasting approach may cover a variety of possible causative models and track inevitable uncertainties down when traditional statistical least-squares regression methods were unable to handle such issues.

Laszlo et al. (2006) developed a global model simulation (CEMSIM) to quantitatively analyze the future development of cement sector. The model has been used to study the most important trends in the world cement market concerning production, technology development, energy consumption and carbon emissions in the 2000-2030 periods. The main focus was on CO₂ reduction potential of the sector, examining the energy efficiency improvement option. In the reference scenario, it was assumed that there was no carbon tax on the carbon emissions and therefore the carbon value is set to zero. The 1550 MT of cement production in 1997 was projected to reach 2800MT by 2030. They stated that the reason behind this was due to intensive growth of cement consumption in developing regions, mainly China, South East Asia and India. It was observed that the global CO₂ emissions from the cement industry increases to more than 50% in the reference scenario and would reach 2100 MT by 2030. In the emissions trading scenario, the carbon value (tax) was introduced so the reduction of CO₂emissions observed in EU15, EU 27 and Annex B countries compared to the BAU2010 (reference scenario).

Carlos et al. (2008) developed a system dynamics model for the global energy supply and demand. It combines the peak oil theories with some economic feedback. The model included the depletion dynamics of conventional and non conventional oil, coal, gas and nuclear energy. A

strong rhythm of substitution of these energies by renewable and fusion energy was also modelled and simulated. The prediction was presented in two scenarios called “optimistic” scenario, and “pessimistic” scenario. In the “optimistic scenario” the capital available for technological advance did not depend on GDP, and therefore, when the GDP declines, the technological advance was not affected. The renewable hypothesis, which is a very optimistic one, was applied in this model. The growth of renewable energies will approach technical potential quickly, and the investments required to increase production did not decrease GDP. The results of CO₂ emissions in the optimistic scenario were very similar to the bottom of IPCC scenarios. In the pessimistic scenario, the renewable hypothesis and the technology were modified. This means that the renewable energies are not developed quickly enough to prevent being directed by the economic crisis (like the rest of non renewable energies), then their contribution to the total energetic mix will be marginal. They observed that there was a peak in the global energy before 2015 and a catastrophic decline afterward. The peak was directly related to the stagnation of the world economy.

Yarnal and Puranik (2009) used system dynamic approach for simulation of cogeneration system by system dynamics software to get different data used for the determination of energy management policy. The results of the model showed that energy management activities can be improved through system dynamics modelling. The various applications pointed the advantages of "system dynamics," particularly in energy management, and assists decision making procedures in the management level.

Stefano Armenia et al. (2010) proposed a System Dynamics model in order to forecast the demand of road fuels in UE countries up to 2020. The

model was validated on available historical data. The main driver on fuel consumption was represented by the transportation demand in terms of passengers per kilometre in each year. Historical data has shown that many countries in Eastern Europe are having an important economic growth, which thus influences the transportation demand. Simulation results showed that the cumulated CO₂ emissions from the eleven non-big five countries were substantially equivalent to the production of only one country among the big five. It was found that emissions due to diesel consumption strongly grow, while at the same time, emissions due to gasoline consumption fall. This was due to “dieselization” trend.

Li and Yang (2010) developed an SD model in order to analyse the causal relationships among various elements in the complex system of energy consumption in Shanxi Province, China. The model consists of four subsystems subsequently, i.e., energy consumption, economic growth, demographic changes, and environmental protection. By using five different development modes, a series of key factors in the model, such as energy-saving technology, coal washing rate, and SO₂ emissions, were reasonably controlled so as to realize the medium and long term forecasting of GDP growth rate, unit GDP energy consumption, and gross emissions of SO₂ from year 2010 to 2020. Comparing trends in energy consumption among different development modes, and fully accounting for the realistic situation in Shanxi Province, the fifth mode (i.e., consistently making efforts in technology development, sticking to cleaning and environmental conservation and strict control of contaminant emissions) has proved to be the optimal mode to realize the coordinated relationship between economic development and energy consumption. According to the fifth mode, they gave the policy recommendations for the sustainable energy consumption

such as improving the current equipment, closing down a variety of enterprises with outdated production capacity, enhancing reuse and circulation of resources, reducing contaminant emissions and promoting the development of new energies such as solar energy and marsh gas.

Monica and Mukherjee (2010) used MARKAL modelling technique for the projection energy consumption in large scale industries like steel, aluminium and cement in India under two alternative scenarios: Business as Usual (BAU) and Efficient (EFF) scenario. The Business as Usual (BAU) , which assumes the continuation of ongoing practice and Efficient (EFF) scenario assumes that best practice, would be adopted gradually to reach energy efficiency. The results observed that in the BAU practice in 2031, the energy consumption is likely to go up to 226.9 MTOE in steel sector. But if energy efficiency measures were adopted fully, there is a reduction potential of about 8% in 2031. This shows the scope of energy efficiency improvement. The result of aluminium sector shows that 17 percent reduction potential was observed in 2031 in EFF scenario. This established that there is a scope for significant energy efficiency improvement in aluminium industry also. Technology transfers and consolidations have also pushed up the industry efficiency. When they applied the MARKAL model for the cement industry, energy reduction potential between BAU and EFF scenarios in 2031 was found to be about 6%. For the cement demand projections, it follows that if economy grows at a rate of 8 percent; demand for cement will grow to 387 MT in 2031 from 48 MT in 2006.

Junchen et al. (2011) used a system dynamics model to predict the natural gas consumption in China. He stated that natural gas would become an important substitution for coal in some parts of the Chinese primary energy consumption. The model predicted that the gas consumption in

China would continue to increase fast to 89.5 billion cubic meters in 2010; 198.2 billion cubic meters in 2020, before finally reaching 340.7 billion cubic meters in 2030. It was also found that the consumption structure would change and scenario analysis is used to assess this closely. Parameters like GDP, total population, urbanization rate and investment proportions of different industries were chosen to reflect the storylines of the three scenarios such as high level, reference level and low level. Gas consumption in the low case scenario was the largest, while consumption of high level was the smallest. This was explained by the fact that high case was mainly relying on tertiary industry. However, all results showed that the Chinese natural gas consumption would increase quickly. Finally, he gave some policy suggestions on natural gas exploration and development, infrastructure constructions and technical innovations to promote sustainable development of China's natural gas industry.

Oggioni et al. (2011) investigated the eco-efficiency measure for 21 prototypes of cement industries operating in many countries by applying a data envelopment analysis (DEA). They reported that with the model, the eco-efficiency of cement DMUs (decision making units) can be measured either as a contraction of CO₂ emissions or as an increased utilization of alternative fuels and raw materials. The analysis showed that the units' efficiency levels were affected by the tendency of different DMUs. It was found that the emerging countries, such as India and China, which are the largest cement producers in the world, appear efficient. They stated that it was due to the recent economic booms and the energy efficiency targets imposed by their authorities have forced their cement companies to invest in the most advanced technologies.

Hsiao and Chung (2011) examined the dynamic relationships between pollutant emissions, energy consumption, and the output for Brazil during 1980-2007. They observed inverted U-shaped relationships of both emissions-income and energy consumption-income implies that both environmental damage and energy consumption firstly increases with income, then stabilize, and eventually decline. The causality results indicated that there was a bidirectional strong causality running between income, energy consumption and emissions. They suggested that in order to reduce emissions and to avoid a negative effect on the economic growth, Brazil should adopt the dual strategy of increasing investment in energy infrastructure and stepping up energy conservation policies to increase energy efficiency and reduce wastage of energy. The Grey prediction model (GM) was applied to predict emissions, energy consumption and real output for the period between 2008 and 2013. The forecasting ability of the GM model was compared with the autoregressive integrated moving average model over the out-of sample period between 2002 and 2007. The results were very close to each other. They suggested that government of Brazil can apply these results for their dynamic adjustment of energy and environmental policies to achieve optimal economic development.

Nastaran and Abbas (2012) presented a system dynamics model in order to analyze energy consumption in Iran's iron and steel industry. Gas, oil and electricity consumed in the steel industry have been projected under various steel production and export scenarios while taking into account new energy price regime. The results show that in short term, the subsidy reform could lead to 15% and 7% reductions in gas and electricity consumption, respectively, due to a mild improvement in energy efficiency. In the long run, potential reductions were 33% in gas and 23% in electricity consumption

resulting from deploying a full suite of energy saving plan and industry renovation. The simulation result also showed that in the production scenario, 34 million tonnes of crude steel plus 45 million tonnes of final steel would be produced compared to the base year production of 12 and 15 million tonnes, respectively. Consequently, total direct and indirect gas consumption in the steel industry would reach 18.3 billion cubic meters per year by 2030.

Maa et al. (2012) constructed a system dynamic model for wetland management in order to analyze the interactions between the ecological, social and economic factors related to wetlands in Tianjin. The statistical data in Tianjin from 1990 to 2008 have been used to verify the model. The author selected six typical models for scenario simulation in 2010, 2030 and 2050. The study found that wetland management system dynamics model is a multi-feedback, multi-interface and nonlinear complex system. Seven scenario analyses with seven different management policies runs were conducted. The scenario analysis found that: the current management mode has obvious defects for the future development. The ecological and environmental condition of wetlands will become worse, environment pollution will increase, and the environment will be significantly deteriorated. Therefore, it does not meet wetland sustainable development requirement under current management, and need to be improved. Promoting technological development, and slowing down urbanization process will be helpful for certain aspects of wetland development, but they are not essential ways for solving the sustainable related problems. Environmental control methods such as enhancing sewage treatment technology could be assistant policy for wetland sustainable management as some indicators need to be improved. As for the alternative policies

tested, ‘controlling population’, ‘improving wetland restoration technology’, and ‘improving industry structure’ are sustainable policies that lead to better conditions. Thus, the author suggested that ecological protection, population control and industrial structure adjustment are sustainable approaches to achieve wetland wise utilization and protection in this area. Hence these methods could be applied in wetland sustainable management in the future.

Jing et al. (2012) conducted a study to analyze current energy and carbon dioxide (CO₂) emissions trends in China’s cement industry as the basis for modeling different levels of cement production and rates of efficiency improvement and carbon reduction in 2011-2030. Three cement output projections were developed based on analyses of historical production and physical and macroeconomic drivers. For each of these, three production projections, energy savings and CO₂ emissions reduction potentials were estimated in a best practice scenario and two continuous improvement scenarios relative to a frozen scenario. The results revealed that the potential for cumulative final energy savings of 27.1 to 37.5 exajoules and energy-related direct emissions reductions of 3.2 to 4.4 gigatonnes in 2011–2030 under the best practice scenarios. The continuous improvement scenario produces cumulative final energy savings of 6.0 to 18.9 exajoules and reduced CO₂ emissions from 1.0 to 2.4 gigatonnes. This analysis highlighted that increasing energy efficiency was the most important policy measure for reducing the cement industry’s energy and emissions intensity. In addition, policies to reduce total cement production offer the most direct way of reducing total energy consumption and CO₂ emissions.

Guangyong et al. (2012) used grey prediction model to forecast carbon emissions, energy consumption and real GDP for Shanghai, China

during 2011-2020. Based on the data from 1978-2010, they analyzed the causal relationships between carbon emissions, energy consumption, and economic growth in Shanghai, adopting the co-integration and vector error correction methods. The empirical results showed, in the long-run equilibrium, that there was a positive relationship of a long-term equilibrium between carbon emissions and energy consumption in Shanghai. However, between carbon emissions and real GDP, there was a negative correlation. Besides, in the short-run equilibrium, energy consumption was the important impact on carbon emissions. The causality results show that there was a bidirectional causality relationship between carbon emissions, real GDP and energy consumption. For the purpose of reducing carbon emissions and not adversely affecting economic growth, Shanghai should optimize the structure of energy consumption and develop new energy. So the developed optimal forecasting models of real GDP, energy consumption and carbon emissions had good prediction precision with MAPEs of less than 3%. They concluded that the results can be applied to adjust the energy and environmental policies dynamically to achieve the best economic development.

Yuren et al. (2012) proposed a carbon emissions reduction potential model based on technology diffusion and structural adjustment to the cement industry in Chongqing. The model predicted that the unit carbon emissions of Chongqing's cement industry will be 0.5779 ton in 2020, and decreased by 31% compared to 0.8332 ton in 2005. The author found that under technical condition of 2005, carbon emissions from raw material decomposition, fuel combustion and power consumption were 44.4%, 36.1%, 12.4% respectively, this proportion changed to 54.5%, 26.3% and 12.3% in 2020. The author concluded that there are dramatic technology

developments in fuel combustion and power consumption in 2020. That is, new dry process will be adopted in all cement industry; ball mill will be completely replaced with vertical mill in 2020.

2.5 Conclusion

After a pervasive literature survey conducted on energy analysis, CO₂ emissions and forecasting models, it is concluded that research work in this area is very limited in number in Indian Cement Industry scenario. However, as mentioned in chapter 1, cement industries in India are growing at a faster momentum in their production due to rapid developments in the infrastructure. About 94% of the thermal energy requirement is met by coal in the Indian cement industries. The higher energy consumption in India is partially due to the harder raw material and poor quality of fuel. So the cement industries in India deserve energy analysis, continuous monitoring of CO₂ emissions and assessment of future production and emissions. Under these circumstances, the energy and exergy analysis study is attempted in this work paying attention to energy saving opportunities and energy degradation areas in a typical cement industry in India. The decomposition analysis of CO₂ emissions from the cement industries help to monitor its variation for the past 10 years. The forecasting model is used to predict the future cement production and CO₂ emissions in Indian cement sector under different scenarios.



ENERGY AND EXERGY ANALYSIS OF THE RAW MILL IN THE CEMENT PLANT

<i>Contents</i>	3.1 <i>Introduction</i>
	3.2 <i>About the Plant</i>
	3.3 <i>Cement Manufacturing Processes</i>
	3.4 <i>Theoretical Analysis</i>
	3.5 <i>Raw Mill</i>
	3.6 <i>Raw Mill Analysis</i>
	3.7 <i>Results and Discussion</i>
	3.8 <i>Conclusion</i>

3.1 Introduction

Traditional methods of thermal system analysis are based on the first law of thermodynamics. These methods use an energy balance of the system to determine heat transfer between the system and its environment. The first law of thermodynamics introduces the concept of energy conservation, which states that energy entering a thermal system with fuel, electricity, flowing streams of matter, and so on, is conserved and cannot be destroyed. In general, energy balance provides no information on the quality or grades of energy crossing the thermal system boundary and no information about internal losses. By contrast, the second law of thermodynamics introduces the useful concept of exergy in the analysis of thermal systems. Exergy is a measure of the quality or grade of energy and it can be destroyed in the thermal system (Dincer et al., 2004). The second law states that part of the exergy entering a thermal system with fuel,

electricity, flowing streams of matter, and so on is destroyed within the system due to irreversibility. The second law of thermodynamics uses an exergy balance for the analysis and the design of thermal systems. The main purpose of exergy analysis is to discover the causes and quantitatively estimate the magnitude of imperfection of a thermal or chemical process. Exergy analysis leads to a better understanding of the influence of thermodynamic phenomena on the process effectiveness, comparison of the importance of different thermodynamic factors, and determination of the most effective ways of improving the process under consideration (Szargut et al.,1998). Rosen and Dincer (2004) have reported that examining the relation among exergy and energy and the environment makes it clear that exergy is directly related to sustainable development.

The ratio of exergy to energy in a substance is called energy quality. Forms of energy such as macroscopic kinetic energy, electrical energy, and chemical Gibbs free energy are 100% recoverable as work, and therefore have an exergy equal to their energy. However, forms of energy such as radiation and thermal energy can not be transformed completely to work, and have exergy content less than their energy content. The exact proportion of exergy in a substance depends on the amount of entropy relative to the surrounding. Entropy production is equivalent to exergy loss which is equivalent to lost work. So exergy is an indication of energy quality. The energy transformation processes in a system can only proceed from a higher quality form to a lower quality form unless there is some net input of energy quality (such as for example work) from the surroundings.

One of the cement industry situated in Kerala, India, is considered for the present investigation. In this study, energy and exergy analysis of the

raw mill unit of the plant is conducted by using the actual plant operational data.

3.2 About the Plant

The typical plant selected for the case study is located in Palakad district, Kerala. It is a public sector company fully owned by the Govt of Kerala. The plant has an installed capacity of 4.2 lakh tonnes per annum. The plant was commissioned in April, 1984. The plant has adopted dry process with four stage suspension pre-heater for cement manufacturing. Limestone, the principle raw material is mined mechanically from the captive mine about 9 kms away from the plant. The material is then crushed in two stage crushing at the mines and is conveyed to the plant site by a 6.2 km mono cable aerial rope way. In the plant, the material is blended in the stacker re-claimer system for pre-homogenization. The limestone and other additives (sweetener grade limestone and laterite) are ground in closed circuit raw mill. The raw meal thus prepared is blended in huge blending silos and stored in storage silos. The raw meal is then fed to a four stage suspension pre-heater. The preheated raw meal is then fed to coal fired rotary kiln. In the kiln, the material is then burned at 1280 °C and clinker is formed. It is then cooled down in grate cooler and stored in clinker stockpile. The clinker along with the required quantity of additives (gypsum, slag and fly ash) is ground in the closed circuit cement mill and thus different grade cement is produced as per the requirement. In the ordinary portland cement (OPC) the clinker and gypsum ratio is 95:05, for portland pozzalana cement (PPC) the mixture consists of clinker, dry fly ash and gypsum in the ratio of 65:25:05 and portland slag cement (PSC) the clinker, slag and gypsum are mixed in the ratio of 65:25:05. The grounded OPC, PPC, PSC are stored in separate silos. From the silos, it is

fed into the packing house and the packing is done by electronic packing machines. After packing the products as per requirement, they are dispatched through rail or road. The details of major equipments for the manufacturing of cement in the plant are given in the Table 3.1.

Table 3.1 Equipment details

Sl. No	Section	Equipment	Size/Capacity
1	Crusher	Primary Crusher Secondary Crusher	400 TPH 250 TPH
2	Raw material Grinding	Raw Mill	4.2 m dia & length 12.5 m, 120 TPH
3	Clinkerisation	Rotary kiln with four stage suspension preheater	4.4m dia & Length 65m, 1215 TPD
4	Coal Grinding	Coal Mill	3.2 m dia & length 6.5 m, 14 TPH
5	Cement Grinding	Cement Mill	3.8 m dia & length 15.5m, 80 TPH
6	Packing	Electronic Packer and Rotary Packer	1 No – 600 TPH 1 No – 60 TPH

3.3 Cement Manufacturing Processes

The different stages of cement production in the plant are given as follows.

- 1) Mining.
- 2) Raw meal preparation.
- 3) Clinkerisation and coal grinding.
- 4) Cement grinding and packing.

The material and gas flow during cement manufacturing process in the cement plant are described as follows.

3.3.1 Mining

The mines are located at about 9 kms from the factory, inside the forest. The main raw material, limestone is in the form of hard rocks. These rocks are drilled and blasted. The boulders of limestone are reduced in size to 25 mm using two crushers namely primary crusher and secondary crusher. This limestone of 25 mm size is transported to the factory through a ropeway system. Limestone received in the plant is stacked in the stockpile.

3.3.2 Raw meal preparation

The flow sheet of the raw mill system is shown in the Fig. 3.1. The raw materials such as limestone, sweetener limestone and laterite are extracted from their respective hoppers through weigh feeders in correct proportion. The material thus extracted moves through a common belt conveyor into the raw mill. A part of the kiln exhaust gas is used for drying the raw meal. In raw mill the raw materials are ground to the required fineness. The ground raw meal is then transported to turbo air separator for separating the raw meal into fine and coarse particles. The fine particles are then transported to blending silo through an air slide and bucket elevator while coarse particles are returned to the mill through a screw conveyor for further grinding.

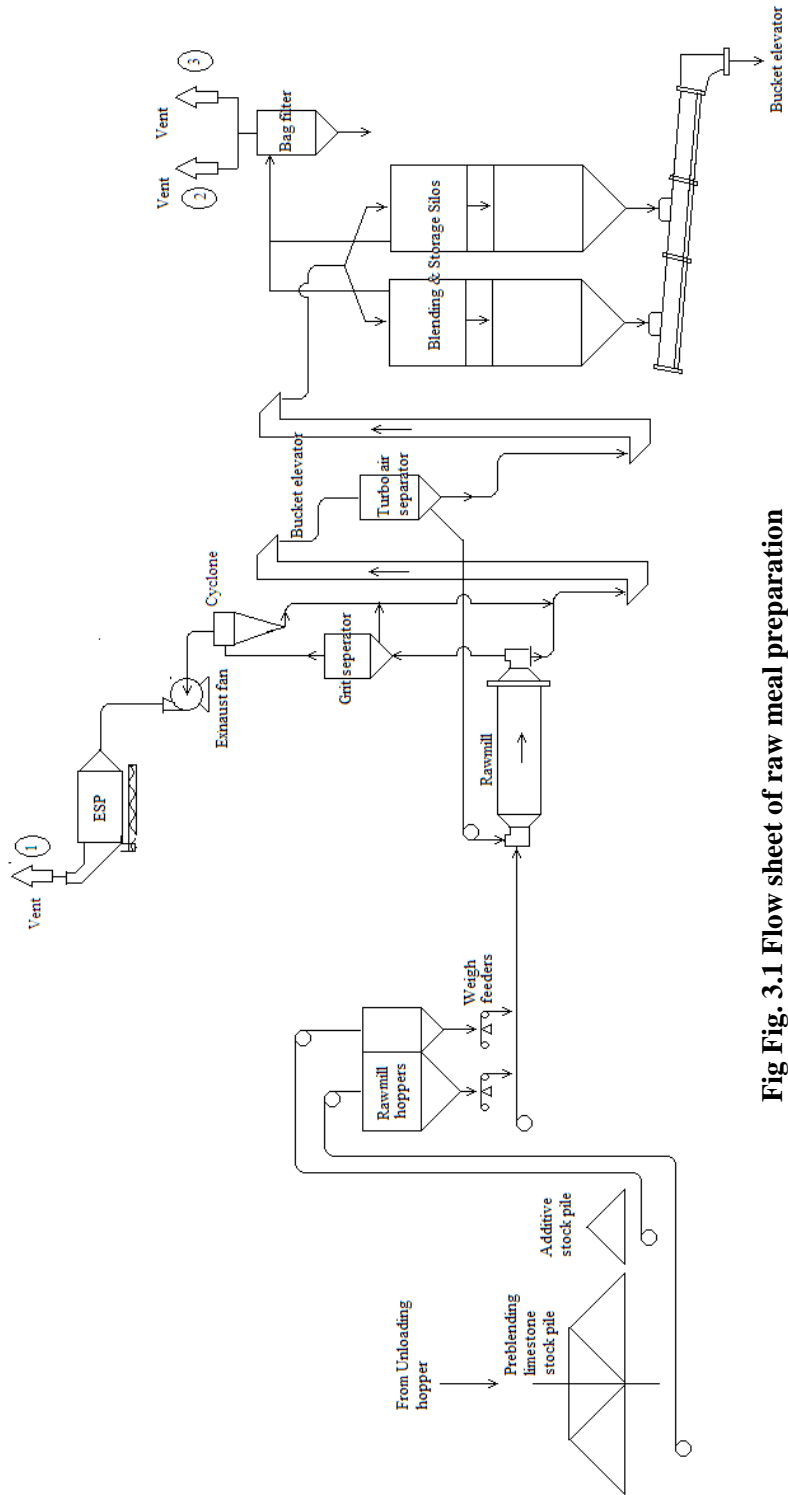


Fig Fig. 3.1 Flow sheet of raw meal preparation

The raw meal transported to the blending silo is blended using compressed air. The blended raw meal is stored in the storage silos. The raw meal then extracted through air slides and is transported through a bucket elevator. The quantity of raw meal going to the rotary kiln is controlled by the weigh feeder installed below the load cell. From the load cell hopper the material is transported to bucket elevator. The belt bucket elevator then lifts the raw meal to the top of the preheater.

A part of the hot gas from the kiln is used for drying the raw meal in the raw mill. The gas moves through the raw mill to a grid separator. In the grid separator, the fine and coarse particles of raw meal carried with the gas are separated. The gas then flows to a cyclone and dust is collected. Final dust separation take place in the electro static precipitator and the clean gas is vented to the atmosphere through stack no.1. The dust collected in the cyclone is transported to the bucket elevator and dust collected in electro static precipitator is recycled to load cell hopper. To dedust, the dust-laden air from filling silo, bag dust collectors are used and the clean gas is vented through stack no. 2 & 3.

3.3.3 Clinkerisation and Coal grinding

Flow sheet of the kiln and coal mill shown in Fig. 3.2. The raw meal, from raw mill is lifted to the top of the preheater by bucket elevator. The material thus moves through the preheater cyclone down to the rotary kiln. Hot gas from the kiln moves upwards as a result of which heat transfer takes place between raw meal and hot gas and raw meal gets partly calcined. The partly calcined raw meal then moves to the rotary kiln. Kiln is fired from the other end using pulverized coal. Due to rotation of the kiln the raw materials exposed to hot gases and in its course, it gets fully calcined.

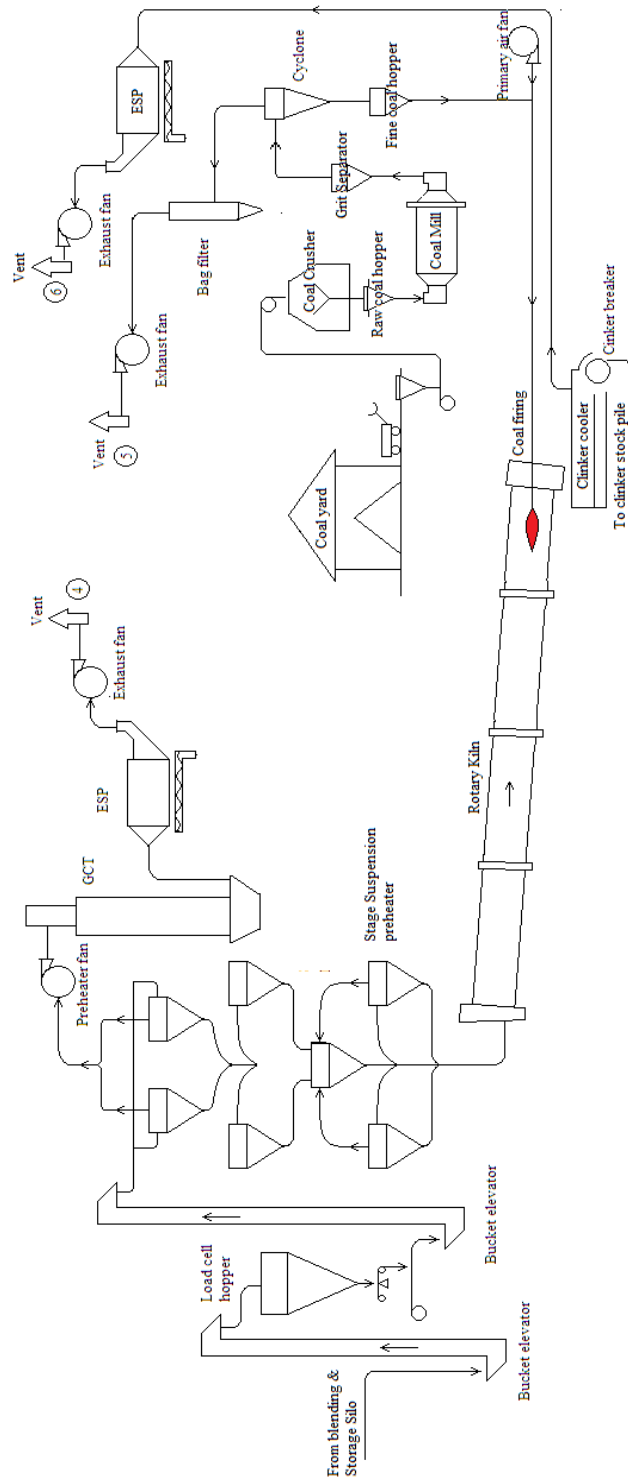


Fig. 3.2 Flow sheet of clinkerisation and coal grinding

The calcined material then enters to the burning zone of the kiln and the entire chemical reactions takes place there and clinker is formed. The clinker then passes through a clinker cooler for cooling.

The primary air from the primary air fan and secondary air drawn from the cooler moves through the kiln and preheater to electro static precipitator via. gas condition tower (GCT). The suction is created by the preheater fan. The dust collected in electro static precipitator and gas condition tower is returned to load cell hopper in kiln feed section and clean gas is vented to atmosphere through stack no 4.

Coal is the fuel used to fire the kiln. Coal is pulverized in the coal mill before feeding into the kiln along with the primary air. The hot air required for drying the coal inside the mill is drawn from the grate cooler. For de-dusting the gas from coal mill, a bag filter is used. The collected dust is fed back to fine coal hopper. The clean gas from the bag filter is vented through stack no. 5.

The dust-laden air from the grate clinker cooler is passed through an electro static precipitator of high efficiency that can handle hot gas; by a high efficiency induced draft fan and chimney arrangement (stack no.6). The electro static precipitator separates fine dust from the gas stream, which gets collected in pyramidal hoppers. The dust thus collected is transported to the exiting deep bucket conveyor using stream of rotary airlocks and a screw conveyor.

3.3.4 Cement grinding and packing

Flow sheet of the cement mill and packer de-dusting is shown in Fig.3.3 Clinker from the clinker stockpile is extracted through belt conveyor to clinker hopper. Gypsum is also extracted through the same belt conveyor to gypsum hopper from gypsum shed. From these hoppers clinker and gypsum is extracted according to preset conditions to cement mill for grinding.

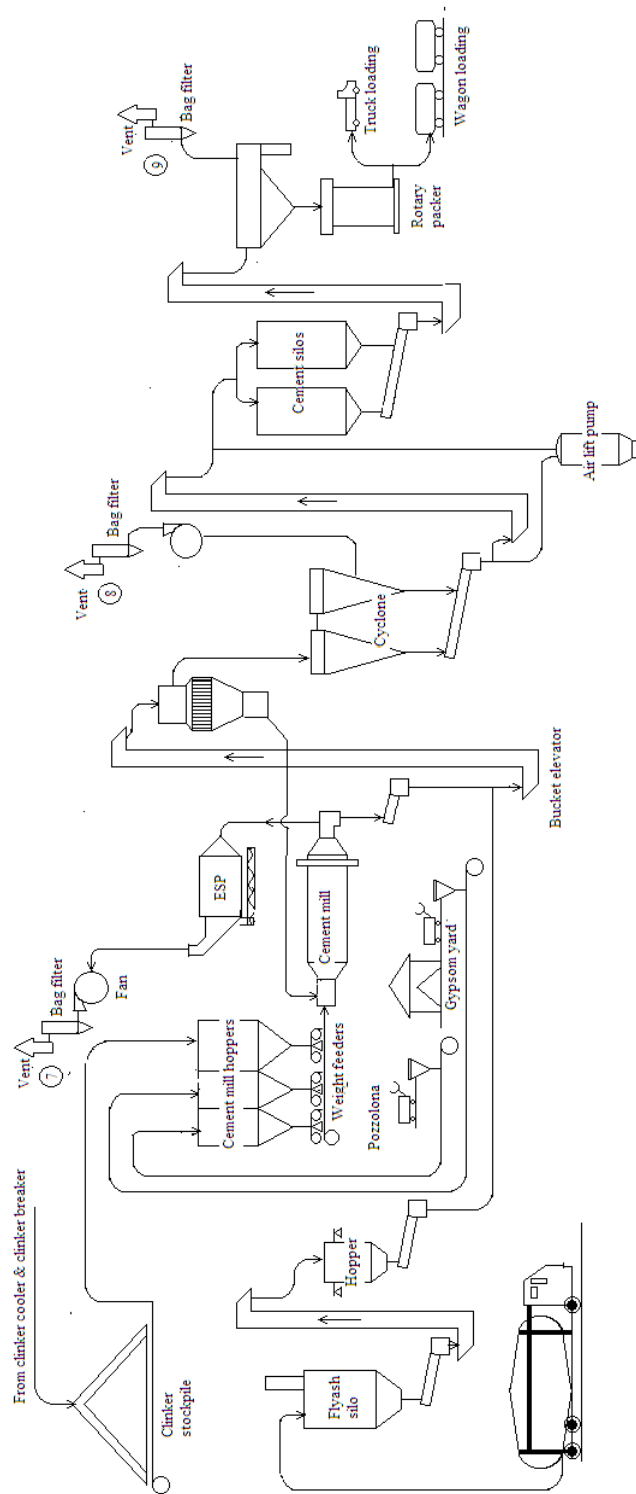


Fig. 3.3 Flow sheet of cement grinding and packing

The output from the mill along with dry fly ash stored in fly ash silo is fed to a high efficiency separator using a belt elevator where material is separated to fine and coarse. The coarse material is fed to the mill inlet through a solid flow meter for regrinding. Fine material, separated using cyclones and bag filters, is fed to the cement silo through air slide stream and bucket elevator system. From the silo it is fed to the packing house. In the packing house, electronic rotary packers are used for packing; conveyors for transport and loading machines for load the filled bags from packer to truck/wagon.

The dust-laden gas from the cement mill is passed through an electro static precipitator (ESP) and bag filter system for removing dust. After that the clean gas is vented out through stack number.7. Bag dust collectors are provided in the separator circuit and the clean gas is venting through stack no.8. During operation of the packer machine and connected accessories, dust-laden air is produced. This is de-dusted through bag filter and clean gas is vented out through stack no.9.

3.4 Theoretical Analysis

For a general steady state, steady-flow process, the following balance equations are applied to find the work and heat interactions.

3.4.1 Mass balance

The mass balance equation can be expressed in the rate form as

$$\sum m_{in} = \sum m_{out} \text{ -----(3.1)}$$

where m is the mass flow rate, and the subscript ‘in’ stands for inlet and ‘out’ for outlet (Bejan, 1988).

3.4.2 Energy balance.

The general energy balance can be expressed as

$$\sum E_{in} = \sum E_{out} \text{ ----- (3.2)}$$

$$Q_{net,in} + \sum m_{in} h_{in} = W_{net,out} + \sum m_{out} h_{out} \text{ ----- (3.3)}$$

where E_{in} is the rate of energy transfer in, E_{out} is the rate of energy transfer out

$Q_{net,in} = Q_{in} - Q_{out}$ is the rate of net heat input,

$W_{net,out} = W_{out} - W_{in}$ is the rate of net work output, and h is the specific enthalpy (Balkan et al., 2005).

Assuming no change in kinetic and potential energies with any heat or work transfer, the energy balance given in Eq. (3.3) can be simplified to flow enthalpies only:

$$\sum m_{in} h_{in} = \sum m_{out} h_{out} \text{ ----- (3.4)}$$

3.4.3 Exergy balance

The exergy balance is stated around a control region delimited by specific boundaries.

$$Ex_{in} + Ex_Q = Ex_{out} + W_{sh} + \sum Ex_{dest} \text{ ----- (3.5)}$$

where Ex is the rate of exergy transfer in, Ex_{out} is the rate of exergy transfer out, Ex_Q is the rate of exergy transfer due to heat, W_{sh} is the rate of exergy transfer due to work and Ex_{dest} is the exergy destroyed.

The above equation can also be written in the following form

$$\Sigma \left(1 - \frac{T_0}{T_t} \right) Q_t - W_{sh} + \sum m_{in} \psi_{in} - \sum m_{out} \psi_{out} = \sum Ex_{dest} \text{ ----- (3.6)}$$

where Q_t is the heat transfer rate through the boundary at temperature T at location t , Ψ is the specific exergy (Bejan, 1988).

The expression for specific exergy is written as

$$\psi = (h - h_0) - T_0 (s - s_0) + \psi_{ch} + \frac{V_0^2}{2} + gZ_0 \quad \text{-----(3.7)}$$

where h is the specific enthalpy, s is the specific entropy subscript zero indicates properties at the reference environment of P_0 and T_0 , ψ_{ch} is the chemical exergy, V_0 is Velocity relative to the earth surface and Z_0 is the altitude above sea level.

The exergy flow to the control region is always greater than that from the control region. The difference between the two, the rate of loss of exergy, is called the irreversibility rate. The irreversibility rate is calculated from the Gouy-Stodola relation, which states that the irreversibility rate of a process is the product of the entropy generation rate for all systems participating in the process and the temperature of the environment.

$$\text{Irreversibility} = \sum Ex_{dest} = T_0 S_{gen} \quad \text{-----(3.8)}$$

where S_{gen} is the rate of entropy generation and T is the temperature, while the subscript zero denotes conditions of the reference environment (Bejan, 1988).

3.4.4 Physical exergy

Physical exergy, known also as thermo-mechanical exergy, is the work obtainable by taking the substance through reversible process from its initial state (T, P) to the state of the environment (T_0, P_0) (Rosen et al., 2005).

The specific physical exergy is written as:

$$\Psi_{ph} = (h-h_0) - T_0 (s-s_0) \text{ -----(3.9)}$$

where h is the specific enthalpy, s is the specific entropy
subscript zero indicates properties at the reference environment

For a perfect gas with a constant c_p

$$\psi_{ph} = c_p (T - T_0) - T_0 (c_p \ln \frac{T}{T_0} - R \ln \frac{P}{P_0}) \text{ ----- (3.10)}$$

For solids and liquids when assuming a constant specific heat c :

$$\psi_{ph} = c[(T - T_0) - T_0 \ln(\frac{T}{T_0})] - v_m(P - P_0) \text{ -----(3.11)}$$

where v_m is the specific volume, determined at temperature T_0 .

3.4.5 Chemical exergy

Chemical exergy is equal to the maximum amount of work obtainable when the substance under consideration is brought from the environmental state (T_0, P_0) to the dead state (T_0, P_0, μ_{0i}) by processes involving heat transfer and exchange of substances only with the environment. The specific chemical exergy at P_0 can be calculated by bringing the pure component in chemical equilibrium with the environment. For pure reference components, which also exist in the environment, the chemical exergy consist of the exergy, which can be obtained by diffusing the components to their reference concentration P_{00} . The specific molar chemical exergy of a reference component 'i' present in the environment at partial pressure $P_{00,i}$ is:

$$\psi_{0i} = RT_0 \ln \frac{P_0}{P_{00,i}} \text{ -----(3.12)}$$

The chemical exergy of a gaseous mixture or a mixture of ideal liquids is given by:

$$\psi_{ch} = \sum_i x_i [\psi_{0i} + RT_0 \ln (x_i)] \text{ -----(3.13)}$$

where x represents the molar fraction of component i and ψ_{oi} its standard chemical exergy (Masanori and Abdelaziz, 2002).

The chemical exergy of real solutions can be computed from:

$$\psi_{ch} = \sum_i x_i [\psi_{oi} + RT_0 \ln (\gamma_i x_i)] \quad \text{-----} (3.14)$$

where γ_i is the activity coefficient of the component i , and R is the gas constant (Masanori and Abdelaziz, 2002).

The chemical exergies of gaseous fuels are computed from the stoichiometric combustion chemical reactions. The standard chemical exergies of various fuels are published in the literature (Kotas, 1985; Bejan, 1988).

For many fuels, the chemical exergy can be estimated on the basis of the Net Combustion Value (NCV). The relation between the NCV and the chemical exergy is:

$$\psi_{ch} = \Phi \times \text{NCV} \quad \text{-----} (3.15)$$

where Φ can be calculated with formulae based on the atomic composition. For different fuels Φ ranges between 1.04 and 1.08.

3.4.6 Exergy efficiencies

Different ways of formulating exergy efficiency proposed in the literature have been given in details (Cornelissen, 1997). Three definitions of exergetic efficiencies for steady state processes are found in the literature.

The traditional exergetic efficiency is the ratio of the total outgoing exergy flow to the total incoming exergy flow:

$$\epsilon_1 = \frac{Ex_{out}}{Ex_{in}} \quad \text{-----} (3.16)$$

This is an unambiguous definition and can be used for all process plants and units.

Often there is a part of the output exergy that is unused, i.e. an exergy wasted ($E_{x_{waste}}$) to the environment. In this case, exergy efficiency may be written as follows

$$\epsilon_2 = \frac{\text{Exergy out} - \text{Exergy waste}}{\text{Exergy in}} \quad \text{-----} (3.17)$$

When all the components of the incoming exergy flows are not transformed to other component, the untransformed components give a false impression of the performance of the process plant or unit. Then exergetic efficiency is defined by Kotas (1985) as a ratio of the desired exergy output to the exergy used.

$$\epsilon_3 = \frac{E_{x \text{ desired output}}}{E_{x \text{ used}}} \quad \text{-----} (3.18)$$

where $E_{x \text{ desired output}}$ is all exergy transfer rate from the system, which must be regarded as constituting the desired output, plus any by-product that is produced by the system, while $E_{x \text{ used}}$ is the required exergy input rate for the process to be performed. The exergy efficiency given in Eq. (3.18) may also express as follows (Torres, 1998):

$$\epsilon_3 = \frac{\text{desired exergetic effect}}{\text{exergy used to drive the process}} = \frac{\text{product}}{\text{fuel}} \quad \text{-----} (3.19)$$

To define the exergetic efficiency, both a product and a fuel for the system being analysed are identified. The product represents the desired result of the system. Accordingly, the definition of the product must be consistent with the purpose of purchasing and using the system. The fuel represents the resources

expended to generate the product and is not necessarily restricted to being an actual fuel such as natural gas, oil, or coal. Both the product and the fuel are expressed in terms of exergy (Moran, 1999).

3.5 Raw mill

Specification of raw mill

Type: Ball mill (Ball size 90 mm to 30 mm)

Length = 12.5 m

Diameter = 4.2 m

Drying chamber length=2.5m

Grinding chamber length =10 m

Mill RPM 15.1

Drives 1350 kW × 2

Raw materials feeder capacity.

- (i) Limestone weight feeder = 150 TPH
- (ii) Additive weight feeder I = 50 TPH
- (iii) Additive weight feeder II = 30 TPH

The three main raw materials used for manufacturing cement in the plant are limestone, sweetener lime stone (quality limestone) and laterite (supplements iron oxide & aluminium oxide). The above three materials are separately transported to the mill hoppers through a common belt conveyor system meant for them. From the three hoppers, material is fed in to the raw mill through electronic weigh feeders which maintains the required uniform feed rate and percentages of the three materials fed.

Fig.3.4 shows the schematic diagram of the raw mill. The raw mill is a cylindrical shell consists of two sections which are called drying section and grinding section. Input material after being mixed in the drying section

is taken into the grinding section. Raw materials contain small amount of water. So the raw material must be heated up before it is fed into the grinding section. This is done by taking heat from the exhaust gas of rotary kiln in the drying chamber of the raw mill. After the heat treatment, it is fed into the grinding section, where it is ground into the required size. In the grinding shell, the grinding media balls are charged to 30% by volume. When the cylinder of the raw mill rotates driven by the transmission gear, under the inertial centrifugal force, the grinding media will stick onto the lining board on the internal wall of the cylinder of the grinding mill and rotate together with the cylinder. The grinding media are brought to a certain height, and then fall down under the gravity, and during this process, the grinding media will crush the materials inside the cylinder, and at the same time the grinding media repeatedly move up and down inside the rotating grinding chamber and will have sliding and rolling movement, so that the grinding media, the lining board and the materials to be ground will grind with each other, so that the materials are crushed to a finer granularity.

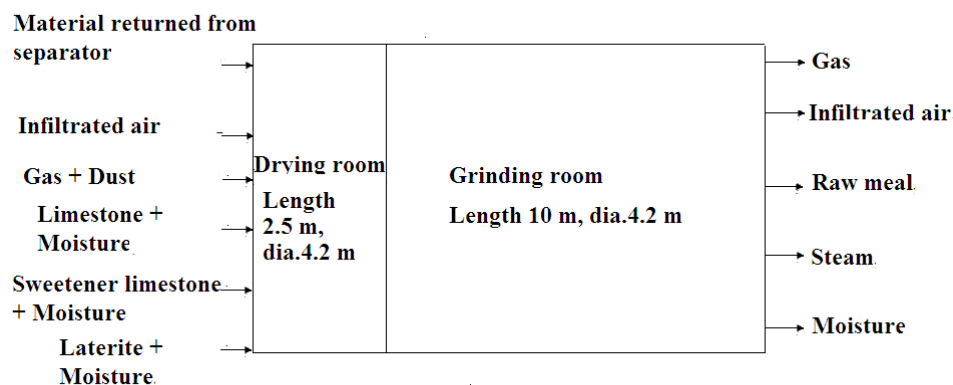


Fig.3.4 Schematic diagram of raw mill

This ground material is taken away by means of bucket elevator into silos for storage purposes. A turbo air separator is provided between the raw mill and bucket elevator. This is used to separate fine and coarse

materials from the grinded mixture. The coarser materials are again fed in to the raw mill and the finer particles are sending to the silos for storage.

3.6 Raw mill analysis

The raw mill is considered as the control volume for energy and exergy analysis in this section. The streams into the system are the raw materials (limestone, sweetener limestone and laterite), returned material from separator, gas, dust and leaking air and streams leaving the system are raw meal with moisture, steam, gas and leaking air.

The energy and exergy modelling technique is applied to the RM for two different operating conditions as follows.

I) Production rate of 117 tonnes per hour

The operation data of the raw mill with production rate of 117 tonnes per hour for the analysis is shown in the Table 3.2.

Table 3.2 Operation data of Raw Mill for the production rate 117 tonnes per hour

Ambient temperature	30 °C
Raw meal production rate	117 TPH
Temperature of raw meal	88°C
Limestone feed	98.36 TPH
Sweetener limestone feed	12.71 TPH
Laterite feed	5.96 TPH
Temperature of feed	30 °C
Temperature of gas at mill inlet	360°C
Temperature of gas at mill outlet	88 °C
Flow rate of gas at mill outlet (mill fan inlet)	100450 Nm ³ /hr
O ₂ present in raw mill outlet gas	9%
O ₂ present in raw mill inlet gas	6%
Recirculation load	67% of material in the separator
Dust concentration in hot gas supplied to the mill	37 g/ Nm ³
Surface temperature of drying room	72°C
Surface temperature of grinding room	82°C

Temperature of hot gas from the kiln system at the inlet of the raw mill and the temperature of hot gas leaving the mill are continuously measured by the probes which are installed on the system. The input and output material temperatures are measured with the help of thermocouple. The input and output gas volume at various locations is measured with pitot tube with manometer assembly. The surface temperatures of the drying and grinding chamber are measured with a non contact digital infrared thermometer.

The raw materials such as limestone, sweetener limestone and laterite in the proportion 84:11:5, having the moisture rate of 1.96%, 10.7% and 4.8% respectively coming from the material silos is dried and then ground in the raw mill in the presence of hot gas (360 °C) coming from the preheater. The oversized material separated in the separator is returned (average 67%) back to the raw mill, having the temperature of 78°C. The undersized material including dust is withdrawn as product (117000 kg/hr) from the separator with moisture content of 0.5%. The raw meal and other streams leave the mill with a temperature of 88°C. Since the whole system runs in vacuum, leaking air enters into the raw mill from environment. The details of various streams entering and leaving the raw mill for this operating condition is shown in Fig. 3.5.

II) Production rate of 121 tonnes per hour

The operation data of the raw mill with production rate of 121 tonnes per hour for the analysis is shown in the Table 3.3.

Table 3.3 Operation data of Raw Mill with production rate 121 tonnes per hour

Ambient temperature	30 °C
Raw meal production rate	121TPH
Temperature of raw meal	88°C
Limestone feed	101.74 TPH
Sweetener limestone feed	13.14 TPH
Laterite feed	6.16 TPH
Temperature of gas at mill inlet	362 °C
Temperature of feed	30 °C
Temperature of gas at mill outlet	88 °C
Flow rate of gas at mill outlet (mill fan inlet)	102800Nm ³ /hr
O ₂ present in raw mill outlet gas	9%
O ₂ present in raw mill inlet gas	6%
Recirculation load	67% of products in the separator
Dust concentration in hot gas supplied to the mill	37 g/ Nm ³
Surface temperature of drying room	72°C
Surface temperature of grinding room	82°C

When the production capacity of the plant is increased there is a chance to decrease the temperature of the product and thereby an increased moisture content in the product (raw meal). In order to prevent this effect the hot gas supplied to the mill with increased temperature compared to lower feed operation. Accordingly in this operating condition the temperature of the gas at inlet is maintained at 362°C in order to keep minimum moisture in the product (0.5%). The raw meal production rate in this operating condition is 121000 kg/hr with a temperature of 88 °C. The

various streams of the raw mill for this operating condition are shown in Fig.3.10

3.7 Results and Discussion

Here the energy and exergy modelling technique is applied to a raw mill with two different operating conditions are discussed. The specific heat capacity (c_p) of the each input and output material for analysis has been calculated by using relation $c_p = a + b \times T + \frac{c}{T^2}$ where a, b and c are the constants for the components of material and T represents temperature in Kelvin (Perry and Green, 1984). The compositions of input and output materials are shown in Annexure A. The constants of each component of the input and output materials are taken from standard hand book (Perry and Green, 1984).

3.7.1 Mass balance of the Raw Mill (Production rate of 117 tonnes per hour)

Table 3.4 shows the various streams inlet and outlet of the raw mill for this operating condition. The mass balance in the RM is conceived on the law of conservation using Eq.(3.1) as follows

$$\sum m_{in} = m_{ia} + m_g + m_l + m_{sl} + m_{lt} + m_{rs} + m_{ml} + m_{sm} + m_{tm} + m_d \text{-----}(3.20)$$

$$\sum m_{out} = m_{ia} + m_g + m_{st} + m_{rm} + m_m \text{-----}(3.21)$$

Table 3.4 Mass balance in raw mill (Production rate of 117 tonnes per hour)

Sl. no	Input	Temp, (°C)	Mass, m (kg/h)	Output	Temp, (°C)	Mass, m (kg/h)
1	Infiltrated air (m_{ia})	30	24114	Infiltrated air (m_{ia})	88	24114
2	Gas (m_g)	360	96458	Gas (m_g)	88	96458
3	Limestone (m_l)	30	96426	Steam (m_{st})	88	2989
4	Sweetener limestone (m_{sl})	30	11344	Raw meal (m_{rm})	88	350415
5	Laterite (m_{lt})	30	5672	Moisture (m_m)	88	585
6	Returned from separator (m_{rs})	78	234000			
7	Moisture in Limestone (m_{ml})	30	1929			
8	Moisture in Sweetener limestone (m_{sm})	30	1361			
9	Moisture in laterite (m_{lm})	30	284			
10	Dust (m_d)	360	2973			
	Total		474561			474561

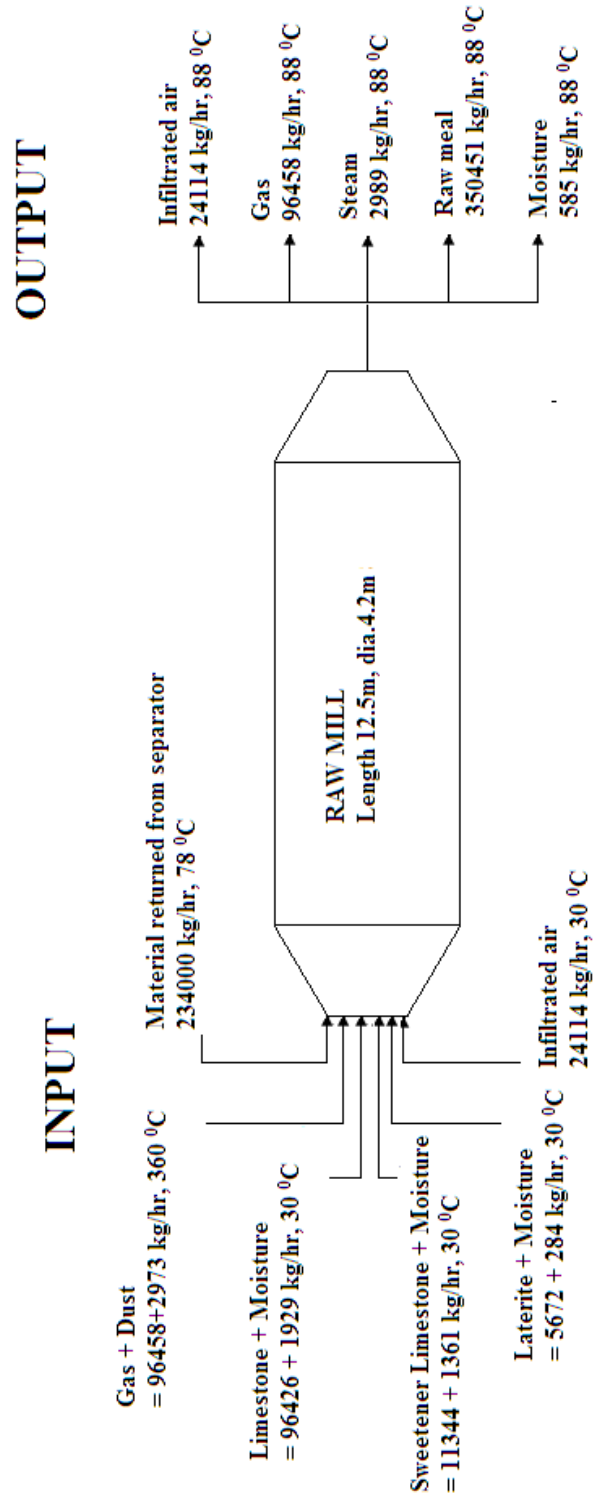


Fig.3.5 Mass balance in the raw mill (Production rate of 117 tonnes per hour)

3.7.2 Heat losses from raw mill (Production rate of 117 tonnes per hour)

Raw mill consists of two sections. Input material after being mixed in the drying room is taken into the grinding section so that the mixture changes into raw meal. The mixture is then, continuously turned with steel winglet until it owns the desired properties and it is sent to the separator with the effect of vacuum pressure from the RM. The heat losses are determined according to the input and output temperature of the raw mill. The heat loss also occurs as it moves towards the exit of the raw mill according to the values of surface temperature. In order to determine the heat loss in the raw mill the detailed temperature distribution of the raw mill is calculated as follows.

3.7.2.1 Determination of mixture room temperature (Production rate of 117 tonnes per hour)

The temperature of the mixture room is determined by balancing the mass and temperatures of the input materials and the mass and temperatures of the collected materials in the mixture room, as given in Eq.(3. 22).

$$\begin{aligned}
 & m_{ia}c_{p_{ia}}T_{ia} + m_gc_{p_g}T_g + m_l c_{p_l}T_l + m_{sl}c_{p_{sl}}T_{sl} + m_{lt}c_{p_{lt}}T_{lt} \\
 & + m_{rs}c_{p_{rs}}T_{rs} + m_{ml}c_{p_{ml}}T_{ml} + m_{sm}c_{p_{sm}}T_{sm} + m_{lm}c_{p_{lm}}T_{lm} + m_d c_{p_d}T_d \\
 & = (m_{ia}c_{p_{ia}} + m_gc_{p_g} + m_l c_{p_l} + m_{sl}c_{p_{sl}} + m_{lt}c_{p_{lt}} + m_{rs}c_{p_{rs}} + m_{ml}c_{p_{ml}} \\
 & + m_{sm}c_{p_{sm}} + m_{lm}c_{p_{lm}} \\
 & + m_d c_{p_d}) T_{mix} \text{-----} (3.22)
 \end{aligned}$$

The temperature of the mixture room is calculated from this equation, while it is given in Table 3.5.

Table 3.5 Determination of mixture room temperature (Production rate of 117 tonnes per hour)

Sl no	Input	c_p (kJ/kg-°C)	Temp, T (°C)	Mass, m (kg/h)	Heat, Q (kJ/h) $m \times c_p \times T$	c_p (kJ/kg-°C)	Mass, m (kg/h)	$m \times c_p$ (kJ/h °C)	T_{mix} (°C)
1	Infiltrated air (m_{ia})	0.9655	30	24114	698431.2	0.9655	24114	23281.04	133.07
2	Gas (m_g)	1.0812	360	96458	37544540.26	1.0812	96458	104290.39	133.07
3	Limestone (m_l)	0.7664	30	96426	2217026.59	0.7664	96426	73900.89	133.07
4	Sweetener limestone (m_{sl})	0.7632	30	11344	259732.22	0.7632	11344	8657.74	133.07
5	Laterite (m_{lt})	0.745	30	5672	126769.2	0.745	5672	4225.64	133.07
6	Returned from separator (m_{rs})	0.8142	78	234000	14860778.4	0.8142	234000	190522.8	133.07
7	Moisture in Limestone (m_{ml})	4.178	30	1929	241780.86	4.178	1929	8059.36	133.07
8	Moisture in sweetener limestone (m_{sm})	4.178	30	1361	170587.74	4.178	1361	5686.26	133.07
9	Moisture in laterite (m_{lm})	4.178	30	284	35596.56	4.178	284	1186.55	133.07
10	Dust (m_d)	0.9971	360	2973	101939.89	0.9971	2973	2964.27	133.07
					56257182.92			422774.94	

Using Eq. (3. 22), the temperature of the mixture room ($T_{\text{mix}}= T_{\text{in}}$) was calculated to be 133.07 °C.

Drying room temperature is accepted as input temperature for the RM. There is a logarithmic relation between drying room temperature and output temperature in order to determine the inner temperature of mill grinding section. This relation is given in the following equation.

$$\Delta T_{\text{ave}} = (T_{\text{in}} - T_{\text{out}}) / \ln(T_{\text{in}}/T_{\text{out}}) \text{-----(3. 23)}$$

$$\Delta T_{\text{ave}} = (133.07 - 88) / \ln(133.07 / 88) = 108.98 \text{ } ^\circ\text{C}.$$

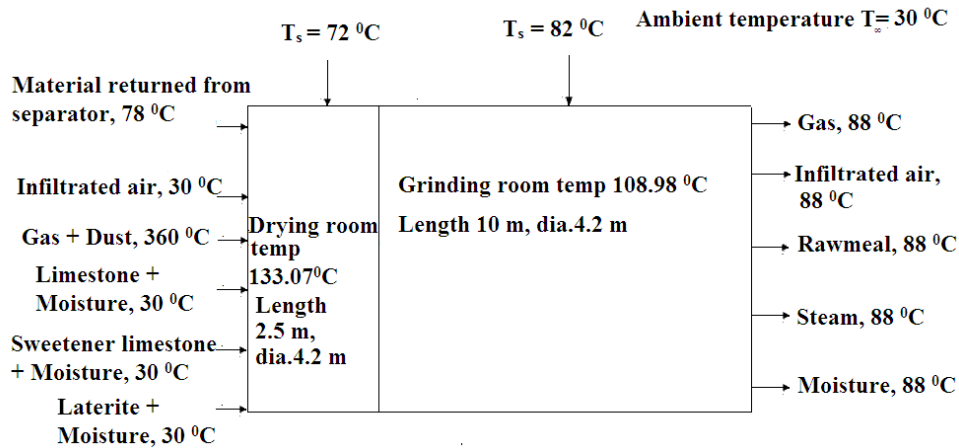


Fig. 3.6 Distribution of Temperature in the raw mill (Production rate of 117 tonnes per hour)

The temperature distribution of the raw mill for this operating condition (Production rate of 117 tonnes per hour) is shown on Fig.3.6. The raw mill consists of two sections such as drying room and grinding room. The inlet gas temperature to the drying room is 360 °C. The temperature of the returned material is 78 °C. The raw materials are entering into the mill with a temperature of 30 °C. The temperature of outlet streams of the mill is 88°C. The surface temperature of the drying room and grinding room for this operating condition was 72 °C and 82 °C respectively. The drying

room and grinding room temperatures for this operating condition was determined as 133.07 °C and 108.98 °C respectively.

Heat losses in the raw mill grinder take place in three various forms. Heat losses within the convection are between the inside temperatures and the surface of the raw mill (Q_{cv1}). The heat loss within the conduction is due to the temperature difference between inner and outer surfaces of the raw mill (Q_{cd}). Heat losses with the convection and radiation occur from the outer surface to the environment (Q_{cv2} and Q_{ra}). The total heat losses are calculated as follows (Frank, 2001).

$$Q_L = Q_{cv1} + Q_{cd} + Q_{cv2} + Q_{ra} \text{ -----(3. 24)}$$

$$Q_{cd} = \frac{(T_{in} - T_s)}{\frac{\ln(\frac{r_o}{r_i})}{2\pi kl}} \text{ -----(3. 25)}$$

$$Q_{cv1} = \pi D_{in} h_a L (T_{in} - T_s) \text{ -----(3. 26)}$$

$$Q_{cv2} = \pi D_o h_a L (T_s - T_\infty) \text{ -----(3. 27)}$$

$$Q_L = \pi D_o \epsilon \sigma (T_s^4 - T_\infty^4) \text{ -----(3. 28)}$$

Heat losses of both rooms are calculated using the following data on the RM. The thermal conductivity material $k = 52 \text{ W/m } ^\circ\text{C}$, heat transfer coefficient of air (h_a) for inner and outer surfaces of the raw mill are 6.83 and 5.8 $\text{ W/m}^2\text{K}$ respectively, emissivity of the raw mill surface $\epsilon = 0.8$. The outer diameter of the raw mill $D_o = 4.28 \text{ m}$ and inner diameter $D_{in} = 4.2 \text{ m}$. The length (L) of drying room and grinding rooms each are 2.5 m and 10 m respectively.

3.7.2.2 Drying room heat loss (Production rate of 117 tonnes per hour)

Using Eq. (3.24)-(3.28) and the data on the raw mill given above along with $T_s = 72^\circ\text{C}$ and $T_{in} = 133.07^\circ\text{C}$ and $T_\infty = 30^\circ\text{C}$, the drying room total heat loss were found to be 2673053.01 Watts.

3.7.2.3 Grinding room heat loss (Production rate of 117 tonnes per hour)

Using Eq. (3.24)-(3.28) and the data on the raw mill given above along with $T_s = 82^\circ\text{C}$ and $T_{in} = 108.98^\circ\text{C}$ and $T_\infty = 30^\circ\text{C}$, the grinding room total heat loss were found to be 4779744.27 Watts.

By taking into account all the losses calculated previously, the total heat losses from the raw mill were obtained to be 26830070.19 kJ/h.

3.7.3 Energy analyses of the raw mill (Production rate of 117 tonnes per hour)

In order to analyse the RM thermodynamically, the following assumptions were made.

- a). The system is assumed as a steady state.
- b). Kinetic and potential energy changes of input and output materials are ignored.
- c). No heat is transferred to the system from the outside.
- d). Electrical energy produces the shaft work in the raw mill.
- e). The change in the ambient temperature is neglected.

Using the above mentioned conditions and using the actual operational data of the plant, an energy balance is applied to the RM. For the calculations the equations can be found in Peray's hand book

(1979). The reference enthalpy is considered to be zero at 0 °C for the calculation.

The energy balance is presented in the Table 3.6 indicates relatively good consistency between heat input and heat output. It is clear from this table that the total energy input to the system is 65225181.37kJ/h. The main heat source is the hot gas from the preheater of the kiln system and the heat is 37544540.26 kJ/hr. The other input consists of energies entering by returned material from separator (14860778.4 kJ/hr), raw materials with moisture (limestone 2458807.45 kJ/hr, sweetener limestone 430319.96 kJ/hr, and laterite 162365.76 kJ/hr), infiltrated air (698431.2 kJ/hr), dust (1067138.33 kJ/hr) and electrical energy consumed by the main driving motors of the mill (8002800 kJ/hr).

Total output comprises of thermal energies contained in raw meal (25383247.68 kJ/hr), hot gas (8271954.85 kJ/hr), infiltrated air (2102514.46 kJ/hr), moisture (215958.6 kJ/hr), steam (516068.78 kJ/hr) heat loss from mill surface (26830070.19 kJ/hr) and unaccounted heat loss (1905366.81 kJ/hr). Fig.3.7 illustrates the energy flow diagram of the raw mill. The detailed calculation of energy analysis is described in Annexure B.

Table 3.6 Energy balance (Production rate of 117 tonnes per hour)

Sl. no	Input	c_p (kJ/kgK)	Temp, T (°C)	Mass, m (kg/h)	Heat, Q $m \times c_p \times T$ kJ/h	Output	c_p (kJ/kgK)	Temp, T (°C)	Mass, m (kg/h)	Heat, Q $m \times c_p \times T$ (kJ/h)
1	Infiltrated air	0.9655	30	24114	698431.2	Infiltrated air	0.9908	88	24114	2102514.46
2	Gas	1.0812	360	96458	37544540.26	Gas	0.9745	88	96458	8271954.85
3	Limestone	0.7664	30	96426	2217026.59	Steam	1.962	88	2989	516068.78
4	Sweetener limestone	0.7632	30	11344	259732.22	Raw meal	0.8232	88	350415	25383247.68
5	Laterite	0.745	30	5672	126769.2	Moisture	4.195	88	585	215958.6
6	Returned from separator	0.8142	78	234000	14860778.4	Heat loss				26830070.19
7	Moisture in Limestone	4.178	30	1929	241780.86	Unaccounted heat loss				1905366.81
8	Moisture in Sweetener limestone	4.178	30	1361	170587.74					
9	Moisture in laterite	4.178	30	284	35596.56					
10	Dust	0.9971	360	2973	1067138.33					
11	Heat from electrical energy				8002800					
					65225181.37					65225181.37

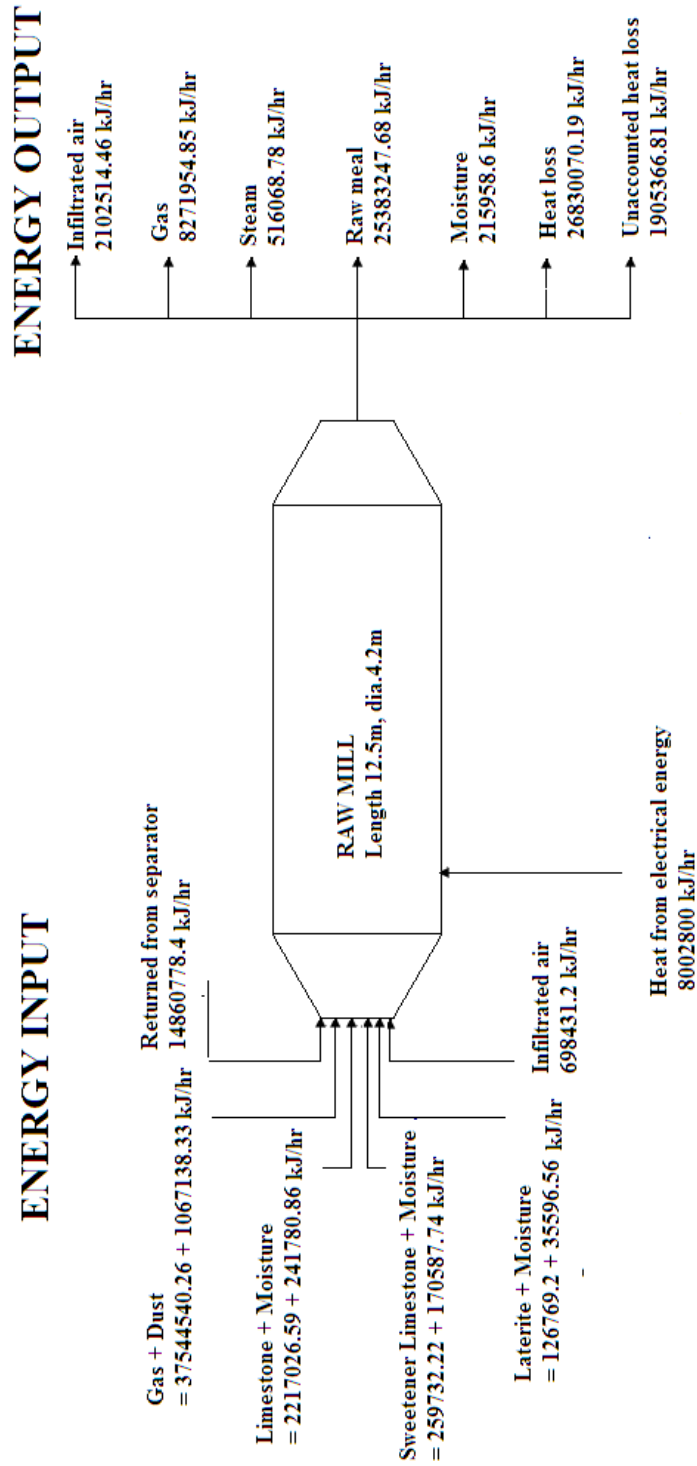


Fig.3.7 Energy flow diagram of raw mill (Production rate of 117 tonnes per hour)

3.7.3.1 Efficiency of the raw mill (Production rate of 117 tonnes per hour)

Energy efficiency of the RM is calculated from the following relation

$$\eta = (\sum m_{out} \times h_{out}) / (\sum m_{in} \times h_{in}) \text{ -----(3.29)}$$

Using energy analysis values and Eq. (3.29), the energy efficiency of the RM is calculated as follows

$$\begin{aligned} \eta &= 36489744.37 / 65225181.37 \\ &= 55.94 \% \end{aligned}$$

Thus the overall thermal efficiency of the RM was found to be 55.94 % and this value is comparable to the raw mill efficiency 61.5% (Adem and Konogle, 2012). The total energy lost (heat loss and unaccounted heat loss) account for 44.06 % of the inlet energy, which is due to friction forces on the bearing unit of the mill and heat loss from the pipes and mill surface. In order to reduce the losses, effective insulation should be applied between the plates arranged circularly at the inner surface of the mill. The piping of hot gas should also be insulated. Moreover, in order to decrease the frictional forces on the bearing unit, an effective lubrication and maintenance is needed.

Fig.3.8 shows the results of energy analysis, helping with the Sankey diagram of raw mill.

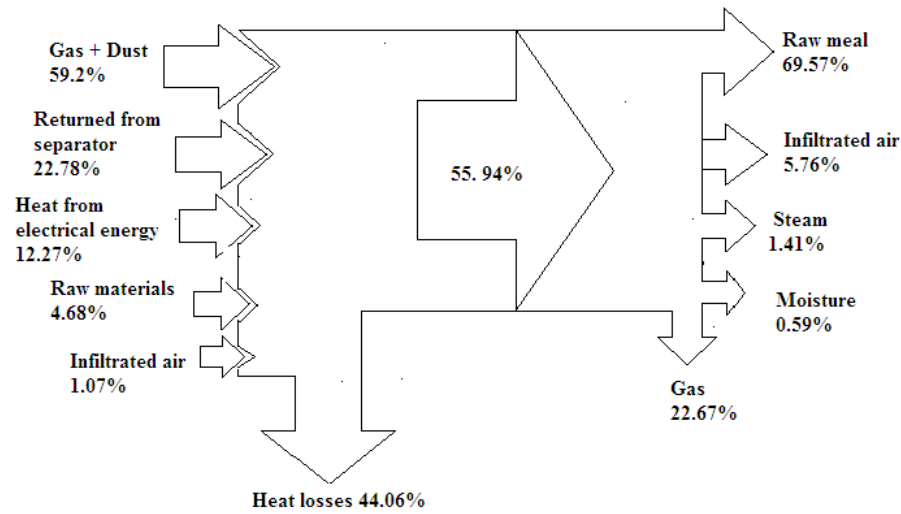


Fig 3.8 Sankey diagram of raw mill (Production rate of 117 tonnes per hour)

For the present operating condition the input energy dominated by hot gas and dust with a contribution 59.2 % while return material from separator accounts for 22.8 % of input energy. The electrical energy accounts for 12.3% of total input energy. The raw material and leaking air are accounts for 4.64 and 1.04 % of input energy respectively. The heat loss from the surface of the mill and unaccounted heat loss jointly were found to be 44.06% of output energy. The heat losses of leaking air and steam account for 4.01% of the output energy. The gas leaving the system account 12.68% of output energy.

3.7.4 Exergy analysis of the raw mill (Production rate of 117 tonnes per hour)

The process for which the exergy analysis performed is assumed to be the raw mill as an open system under the steady state working condition. The reference pressure and temperature for the dead state conditions are assumed to be 101 kPa and 298 K respectively. Equations for the

calculation of exergy of the input and output components are given in the Annexure C. Table 3.7 and 3.8 shows the enthalpy and entropy balance in the raw mill. The exergy analysis for input and output components are shown in Table 3.9. The detailed calculations for the exergy analysis for this operating condition are also described in Annexure C.

The total input exergy consists of exergies of returned material from separator (803923.22 kJ/hr), raw materials with moisture (limestone 3399.95 kJ/hr, sweetener limestone 595.03 kJ/hr, and laterite 224.51 kJ/hr), gas (11523428.22 kJ/hr) infiltrated air (965.77 kJ/hr), dust (327533.43 kJ/hr) and electrical exergy (8002800 kJ/hr). Note that exergy of electricity is equal to itself. The total output includes energies contained in raw meal (1690473.02 kJ/hr), hot gas (550456.90 kJ/hr), infiltrated air (139825.45 kJ/hr), moisture (14351.99 kJ/hr), steam (34296.45) and exergy loss (18233466.33 kJ/hr).

Table 3.7 Enthalpy balance (Production rate of 117 tonnes per hour)

Sl no	Input	c_p (kJ/kg K)	Tem p, (K)	T_o (K)	Mass, m kg/h	Enthalpy, ΔH , (kJ/h)	Output	c_p (kJ/K g K)	Temp, (K)	T_o (K)	Mass, m (kg/h)	Enthalpy, ΔH (kJ/h)
1	Infiltrated air	0.9655	303	298	24114	116405.2	Infiltrated air	0.9915	361	298	24114	1506268.95
2	Gas	1.0812	633	298	96458	34937280.52	Gas	0.9758	361	298	96458	5929794.13
3	Limestone	0.7664	303	298	96426	369504.43	Steam	1.962	361	298	2989	369458.33
4	Sweetener limestone	0.7632	303	298	11344	43288.7	Raw meal	0.8249	361	298	350415	18210612.01
5	Laterite	0.745	303	298	5672	21128.2	Moisture	4.195	361	298	585	154606.73
6	Returned from separator	0.8142	351	298	234000	10097708.4						
7	Moisture in Limestone	4.178	303	298	1929	40296.81						
8	Moisture in Sweetener limestone	4.178	303	298	1361	28431.29						
9	Moisture in laterite	4.178	303	298	284	5932.76						
10	Dust	0.9971	633	298	2973	993031.5						

Table 3.8 Entropy balance (Production rate of 117 tonnes per hour)

Sl no	Input	c_p (kJ/K gK)	Temp, (K)	T_o (K)	Mass, m (kg/h)	Entropy, ΔS (kJ/h K)	Output	c_p (kJ/K gK)	Temp, (K)	T_o (K)	Mass, m (kg/h)	Entropy, ΔS (kJ/h K)
1	Infiltrated air	0.9655	303	298	24114	387.38	Infiltrated air	0.9915	361	298	24114	4585.38
2	Gas	1.0812	633	298	96458	78569.97	Gas	0.9758	361	298	96458	18051.47
3	Limestone	0.7664	303	298	96426	1229.66	Steam	1.962	361	298	2989	1124.7
4	Sweetener limestone	0.7632	303	298	11344	144.06	Raw meal	0.8249	361	298	350415	55436.71
5	Laterite	0.745	303	298	5672	70.31	Moisture	4.195	361	298	585	470.65
6	Returned from separator	0.8142	351	298	234000	31187.2						
7	Moisture in Limestone	4.178	303	298	1929	134.1						
8	Moisture in Sweetener limestone	4.178	303	298	1361	94.62						
9	Moisture in laterite	4.178	303	298	284	19.74						
10	Dust	0.9971	633	298	2973	2233.22						

Table 3.9 Exergy balance (Production rate of 117 tonnes per hour)

Sl no	Input	Enthalpy, ΔH (kJ/h)	T (K)	T_o (K)	Entropy, ΔS (kJ/h)	Exergy, Ex (kJ/h)	Output	Enthalpy, ΔH (kJ/h)	T (K)	T_o (K)	Entropy, ΔS (kJ/h K)	Exergy, Ex (kJ/h)
1	Infiltrated air	116405.2	303	298	387.38	965.77	Infiltrated air	1506268.95	361	298	4585.38	139825.45
2	Gas	34937280.52	633	298	78569.97	11523428.22	Gas	5929794.13	361	298	18051.47	550456.9
3	Limestone	369504.43	303	298	1229.66	3065.63	Steam	369458.33	361	298	1124.7	34296.45
4	Sweetener limestone	43288.7	303	298	144.06	359.15	Raw meal	18210612.01	361	298	55436.71	1690473.02
5	Laterite	21128.2	303	298	70.31	175.29	Moisture	154606.73	361	298	470.65	14351.99
6	Returned from separator	10097708.4	351	298	31187.2	803923.22	Exergy loss					18233466.33
7	Moisture in Limestone	40296.81	303	298	134.1	334.33						
8	Moisture in Sweetener limestone	28431.29	303	298	94.62	235.88						
9	Moisture in laterite	5932.76	303	298	19.74	49.22						
10	Dust	993031.5	633	298	2233.22	327533.43						
11	Exergy due to electrical work					8002800						
						20662870.14						20662870.14

3.7.4.1 Exergy efficiency of the raw mill (Production rate of 117 tonnes per hour)

The exergy efficiency of the RM is calculated from

$$\text{Exergy efficiency}(\epsilon) = \frac{\text{Exergy out} - \text{Exergy waste}}{\text{Exergy in}} \text{-----(3.30)}$$

Using exergy analysis values and Eq. (3.30), the exergy efficiency of the RM is calculated as 11.76%.

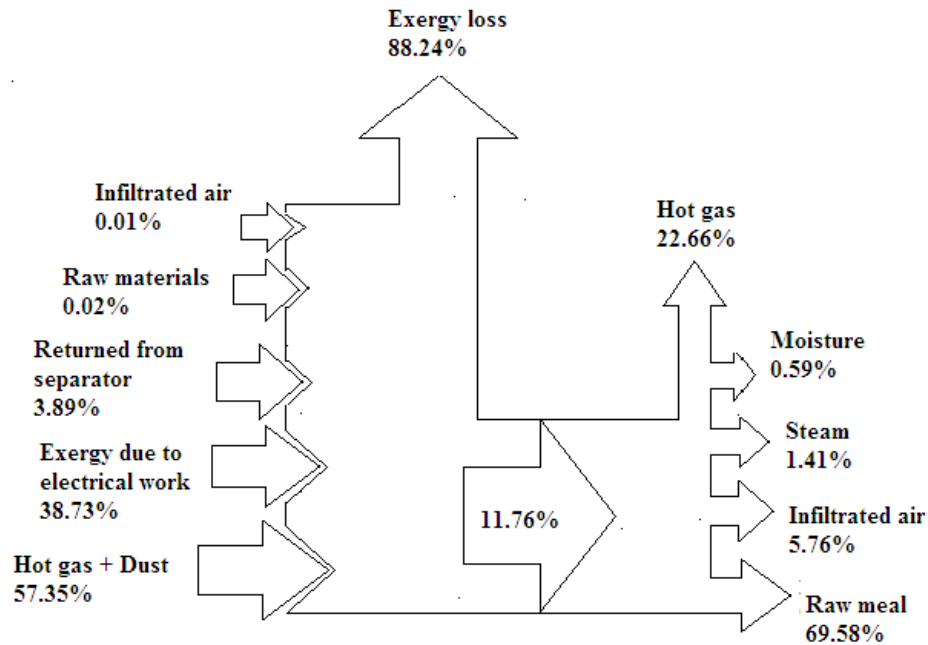


Fig. 3.9 Grassmann (exergy band diagram) diagram of raw mill (Production rate of 117 tonnes per hour)

The exergy band diagram in the Fig.3.9 shows that a great deal of the exergy input to the system is due to gas and dust (57.35 %) followed by exergy of electrical work (38.3 %). The returned material accounts for 3.89 % of input exergies. The contribution of exergies of raw material and leaking air are 0.02 % and 0.01% respectively. An examination of output

exergies shows that exergy loss is responsible 88.24% of the all output exergies.

3.7.5 Mass balance of the Raw Mill (Production rate of 121 tonnes per hour)

The mass balance of the RM for the operating condition with production rate 121 tonnes per hour is given in Table 3.10 and the detailed mass balance is shown in the Fig.3.10

Table 3.10 Mass balance in the raw mill (Production rate of 121 tonnes per hour)

Sl. no	Input	Temp, (°C)	Mass, m (kg/h)	Output	Temp, (°C)	Mass, m (kg/h)
1	Infiltrated air (m_{ia})	30	24679	Infiltrated air (m_{ia})	88	24679
2	Gas (m_g)	362	98714	Gas (m_g)	88	98714
3	Limestone (m_l)	30	99749	Steam (m_{st})	88	3091
4	Sweetener limestone (m_{sl})	30	11735	Raw meal (m_{rm})	88	362395
5	Laterite (m_{lt})	30	5868	Moisture (m_m)	88	605
6	Returned from separator (m_{rs})	78	242000			
7	Moisture in Limestone (m_{ml})	30	1995			
8	Moisture in Sweetener limestone (m_{sm})	30	1408			
9	Moisture in laterite (m_{lm})	30	293			
10	Dust (m_d)	362	3043			
	Total		489484			489484

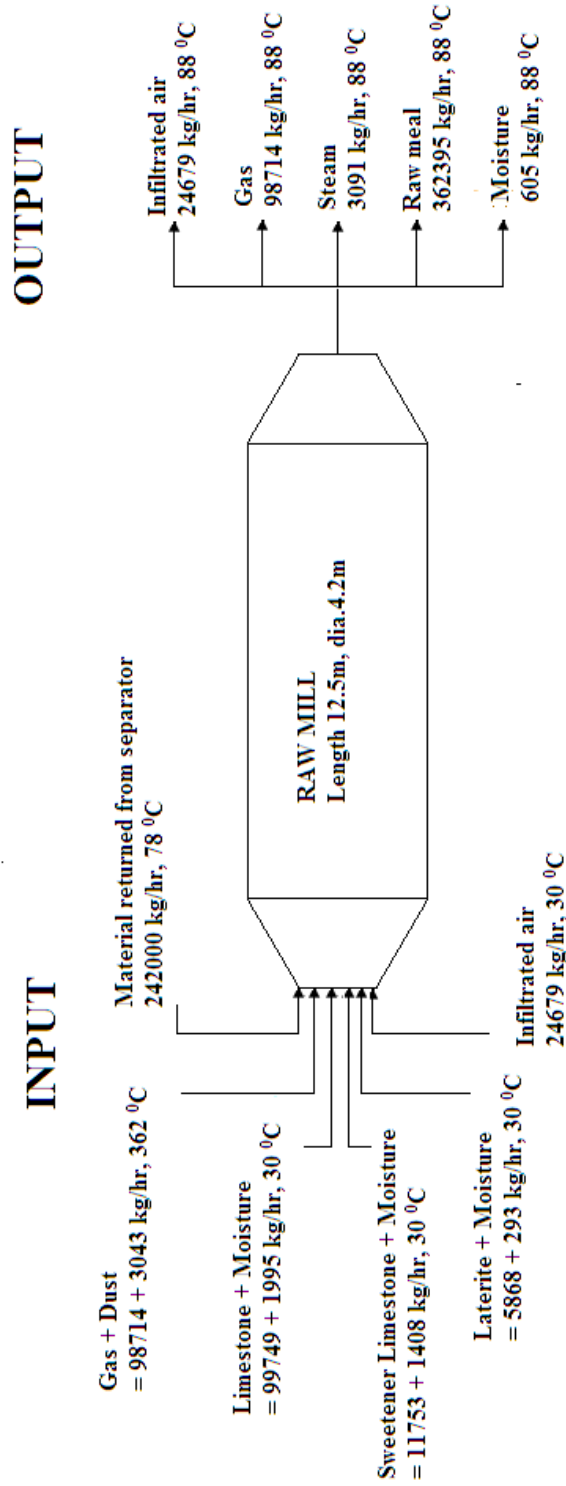


Fig.3.10 Mass balance diagram of raw mill (Production rate of 121tonnes per hour)

3.7.6 Determination of mixture room temperature and heat loss (Production rate of 121 tonnes per hour)

For this operating condition, the temperature of the mixture and grinding rooms are determined to be 131.06°C and 108.98°C respectively. The determination of mixture room temperature is shown in the Table 3.11. The values are almost same as the previous operating condition. The entire streams leave the mill at a temperature of 88°C . Temperature of the product is maintained constant at 88°C by adjusting inlet gas temperature. Therefore the rate of moisture content in the raw meal (0.5%) is same for this operating condition also. The surface temperature of the drying room and grinding room for this operating condition was 72°C and 82°C respectively. In this case the inlet gas temperature was measured as 362°C . The temperature distribution of the raw mill is shown in Fig.3.11. The total heat loss due to conduction and convection and radiation of the drying and grinding rooms were determined to be 26831432 kJ/hr by using the Eq.3.24 to Eq. 3.28. The unaccounted heat loss was found to be $(2815873.98\text{ kJ/hr})$.

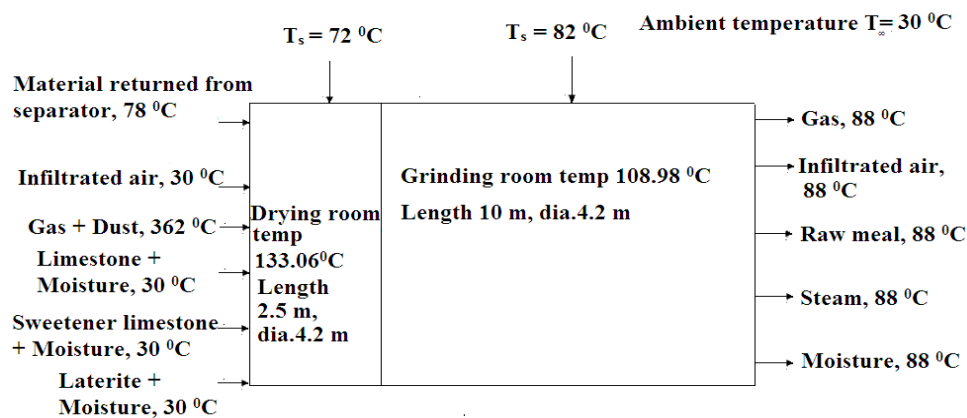


Fig.3.11 Temperature distribution of raw mill (Production rate of 121 tonnes per hour)

Table 3.11 Determination of mixture room temperature (Production rate of 121 tonnes per hour)

Sl no	Input	c_p (kJ/kg °C)	Temp, T (°C)	Mass, m(kg/h)	Heat, Q (kJ/h) $m \times c_p \times T$	c_p (kJ/kg °C)	Mass, m (kg/h)	$m \times c_p$ (kJ/°C)	T_{mix} (°C)
1	Infiltrated air (m_{ia})	0.9655	30	24679	714795.71	0.9655	24679	23827.57	133.06
2	Gas (m_g)	1.0818	362	98714	38656213.56	1.0818	98714	106785.12	133.06
3	Limestone (m_l)	0.7664	30	99749	2293429.01	0.7664	99749	76447.63	133.06
4	Sweetener limestone (m_{sl})	0.7632	30	11735	268684.56	0.7632	11735	8956.15	133.06
5	Laterite (m_{lt})	0.745	30	5868	131149.8	0.745	5868	4371.66	133.06
6	Returned from separator (m_{rs})	0.8142	78	242000	15369186.58	0.8142	242000	197040.85	133.06
7	Moisture in Limestone (m_{ml})	4.178	30	1995	250053.3	4.178	1995	8335.11	133.06
8	Moisture in sweetener limestone (m_{sm})	4.178	30	1408	176478.72	4.178	1408	5882.62	133.06
9	Moisture in laterite (m_{lm})	4.178	30	293	36724.62	4.178	293	1224.15	133.06
10	Dust (m_d)	0.9981	362	3043	105863.47	0.9981	3043	3037.19	133.06
					58002579.32			435908.07	

Energy analyses of the raw mill (Production rate of 121 tonnes per hour)

For this operating condition the energy balance of the Raw Mill (RM) was made and the analysis results of various streams are given in the Table 3.12. In this case total energy input to the system was found to be 67272578.4kJ/h. The input energy to the Raw Mill (RM) consists of energies of gas 38656213.56 kJ/hr, returned material from separator (15369186.58 kJ/hr), raw materials with moisture (limestone 2543482.31 kJ/hr, sweetener limestone 445163.28 kJ/hr, and laterite 167874.42 kJ/hr) infiltrated air (714795.71 kJ/hr), dust (1099462.54 kJ/hr) and electrical energy consumed by the main driving motors of the mill (8276400) kJ/hr. The output energy includes thermal energies of raw meal 26251051.02 kJ/hr, steam 533679.7kJ/hr, gas 8465422.797kJ/hr, infiltrated air 2151777.15 kJ/hr, moisture 223341.80 kJ/hr, heat loss from surface of the mill (26831431.96 kJ/hr) and unaccounted heat loss (2815873.98 kJ/hr). Fig 3.12 demonstrates the energy flow diagram of raw mill for this operating condition. The energy efficiency value was determined by using the Eq.(3.29) and it is found to be 55.93%. This value is very close to previous operating condition.

Table 3.12 Energy balance of raw mill (Production rate of 121 tonnes per hour)

Sl. no	Input	c_p (kJ/kgK)	Temp, T (°C)	Mass, m (kg/h)	Heat, $Q = m \times c_p \times T$ kJ/h	Output	c_p (kJ/kgK)	Temp (°C)	Mass m (kg/h)	Heat, Q $m \times c_p \times T$ (kJ/h)
1	Infiltrated air	0.9655	30	24679	714795.71	Infiltrated air	0.9908	88	24679	2151777.15
2	Gas	1.0818	362	98714	38656213.56	Gas	0.9745	88	98714	8465422.79
3	Limestone	0.7664	30	99749	2293429.01	Steam	1.962	88	3091	533679.7
4	Sweetener limestone	0.7632	30	11735	268684.56	Raw meal	0.8232	88	362395	26251051.02
5	Laterite	0.745	30	5868	131149.8	Moisture	4.195	88	605	223341.8
6	Returned from separator	0.8142	78	242000	15369186.58	Heat loss				26831431.96
7	Moisture in Limestone	4.178	30	1995	250053.3	Unaccounted heat loss				2815873.98
8	Moisture in Sweetener limestone	4.178	30	1408	176478.72					
9	Moisture in laterite	4.178	30	293	36724.62					
10	Dust	0.9981	362	3043	1099462.54					
11	Heat from electrical energy				8276400					
					67272578.4					67272578.4

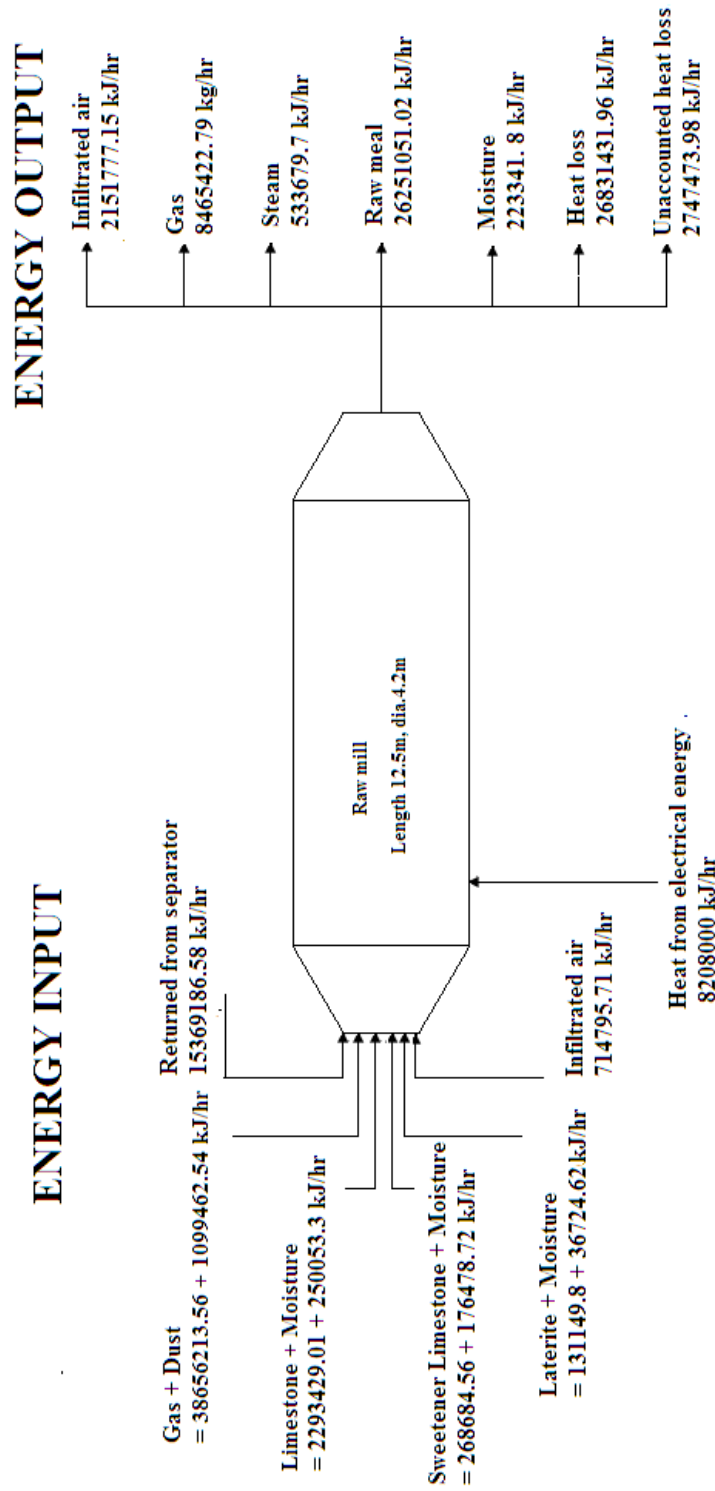


Fig.3.12 Energy flow diagram of raw mill (Production rate of 121 tonnes per hour)

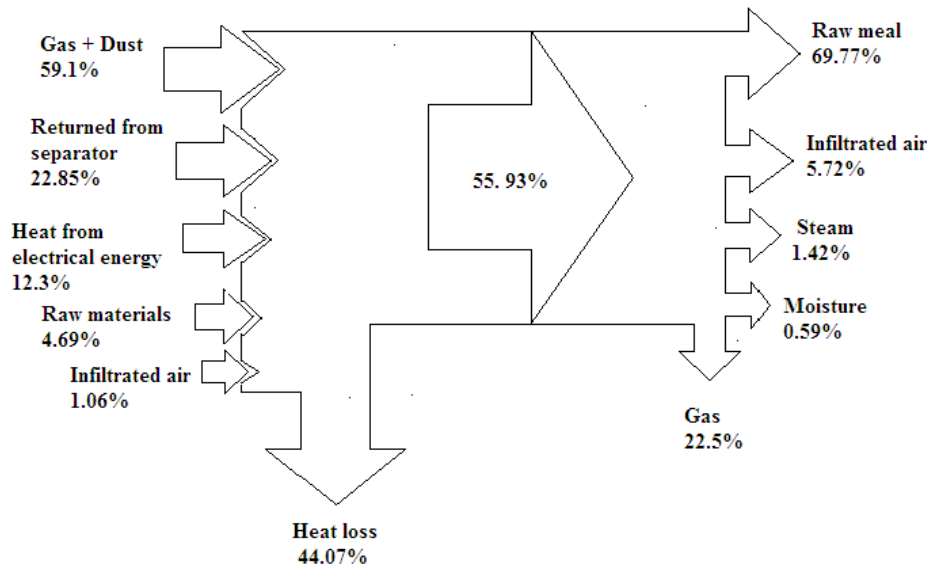


Fig. 3.13 Sankey diagram of raw mill (Production rate of 121 tonnes per hour)

For the changed operating condition (Production rate of 121 tonnes per hour) the results obtained are almost same as the pervious operating condition. Here also the input energy dominated by hot gas and dust with a contribution 59.1% while return material from separator accounts for 22.85% of input. The electrical energy accounts for 12.3% of total input energy. The energies from raw material and leaking air are account for 4.69% and 1.06% of input energy respectively. The total heat loss (heat loss from surface of the mill and unaccounted heat loss) accounts for 44.07% of output energy and leaking air, steam and moisture account for 4.5 % of the output energy. The outlet hot gas accounts for 12.7% of output energy.

3.7.7 Exergy analysis of the raw mill (Production rate of 121 tonnes per hour)

Table 3.13 and 3.14 give the enthalpy and entropy balance in the raw mill respectively. The exergy analysis for the system is shown in Table 3.15. The total input exergy to the Raw Mill (RM) consists of

exergies of gas (11912265.59 kJ/hr) returned material from separator (831426.57kJ/hr), raw materials with moisture (limestone 3517.04kJ/hr, sweetener limestone 615.56kJ/hr, and laterite 232.13 kJ/hr) infiltrated air (988.39kJ/hr), dust (338809.43kJ/hr) and electrical exergy (8208000kJ/hr). The total output exergy includes exergies contained in raw meal (1744569.5 kJ/hr), hot gas (562587.7 kJ/hr), infiltrated air (143000.93 kJ/hr), moisture (14842.65 kJ/hr), and steam (35466.82). The exergy loss for this operating condition was found to be (18863787.11 kJ/hr).

Table 3.13 Enthalpy balance of the raw mill (Production rate of 121 tonnes per hour)

Sl no	Input	c_p (kJ/kg K)	Temp, (K)	T_o (K)	Mass, m kg/h	Enthalpy, ΔH (kJ/h)	Output	c_p (kJ/K gK)	Temp, (K)	T_o (K)	Mass, m (kg/h)	Enthalpy, ΔH (kJ/h)
1	Infiltrated air	0.9655	303	298	24679	119132.62	Infiltrated air	0.9908	361	298	24679	1540476.83
2	Gas	1.0818	635	298	98714	35986585.56	Gas	0.9745	361	298	98714	6060473.13
3	Limestone	0.7664	303	298	99749	382238.17	Steam	1.962	361	298	3091	382066.15
4	Sweetener limestone	0.7632	303	298	11735	44780.76	Raw meal	0.823	361	298	362395	18793366.07
5	Laterite	0.745	303	298	5868	21858.3	Moisture	4.195	361	298	605	159892.43
6	Returned from separator	0.8142	351	298	242000	10443165.24						
7	Moisture in Limestone	4.178	303	298	1995	41675.55						
8	Moisture in Sweetener limestone	4.178	303	298	1408	29413.12						
9	Moisture in Laterite	4.178	303	298	293	6120.77						
10	Dust	0.9981	635	298	3043	1023532.81						

Table 3.14 Entropy balance of the raw mill (Production rate of 121 tonnes per hour)

Sl no	Input	c_p (kJ/KgK)	Temp, (K)	T_o (K)	Mass, m (kg/h)	Entropy, ΔS (kJ/h K)	Output	c_p (kJ/KgK)	Temp, (K)	T_o (K)	Mass, m (kg/h)	Entropy, ΔS (kJ/h K)
1	Infiltrated air	0.9655	303	298	24679	396.46	Infiltrated air	0.9908	361	298	24679	4689.52
2	Gas	1.0818	635	298	98714	80786.31	Gas	0.9745	361	298	98714	18449.28
3	Limestone	0.7664	303	298	99749	1272.04	Steam	1.962	361	298	3091	1163.08
4	Sweetener limestone	0.7632	303	298	11735	149.02	Raw meal	0.8232	361	298	362395	57210.73
5	Laterite	0.745	303	298	5868	72.74	Moisture	4.195	361	298	605	486.74
6	Returned from separator	0.8142	351	298	242000	32254.16						
7	Moisture Limestone	4.178	303	298	1995	138.69						
8	Moisture in Sweetener limestone	4.178	303	298	1408	97.88						
9	Moisture in laterite	4.178	303	298	293	20.37						
10	Dust	0.9981	635	298	3043	2297.73						

Table 3.15 Exergy Balance of the raw mill (Production rate of 121 tonnes per hour)

Sl no	Input	Enthalpy, ΔH (kJ/h)	T (K)	T ₀ (K)	Entropy, ΔS (kJ/h)	Exergy, Ex (kJ/h)	Output	Enthalpy, ΔH (kJ/h)	T (K)	T ₀ (K)	Entropy, ΔS (kJ/h K)	Exergy, Ex (kJ/h)
1	Infiltrated air	119132.62	303	298	396.46	988.39	Infiltrated air	1540476.83	361	298	4689.52	143000.93
2	Gas	35986585.56	635	298	80786.31	11912265.59	Gas	6060473.13	361	298	18449.28	562587.7
3	Lime stone	382238.17	303	298	1272.04	3171.27	Steam	382066.146	361	298	1163.08	35466.82
4	Sweetener limestone	44780.76	303	298	149.02	371.53	Raw meal	18793366.1	361	298	57210.73	1744569.5
5	Laterite	21858.3	303	298	72.74	181.35	Moisture	159892.425	361	298	486.74	14842.65
6	Returned from separator	10443165.24	351	298	32254.16	831426.57	Exergy loss					18795387.11
7	Moisture in Limestone	41675.55	303	298	138.69	345.76						
8	Moisture in Sweetner limestone	29413.12	303	298	97.88	244.03						
9	Moisture in laterite	6120.77	303	298	20.37	50.78						
10	Dust	1023532.81	635	298	2297.73	338809.43						
11.	Exergy due to electrical work					8208000						
						21295854.71						21295854.71

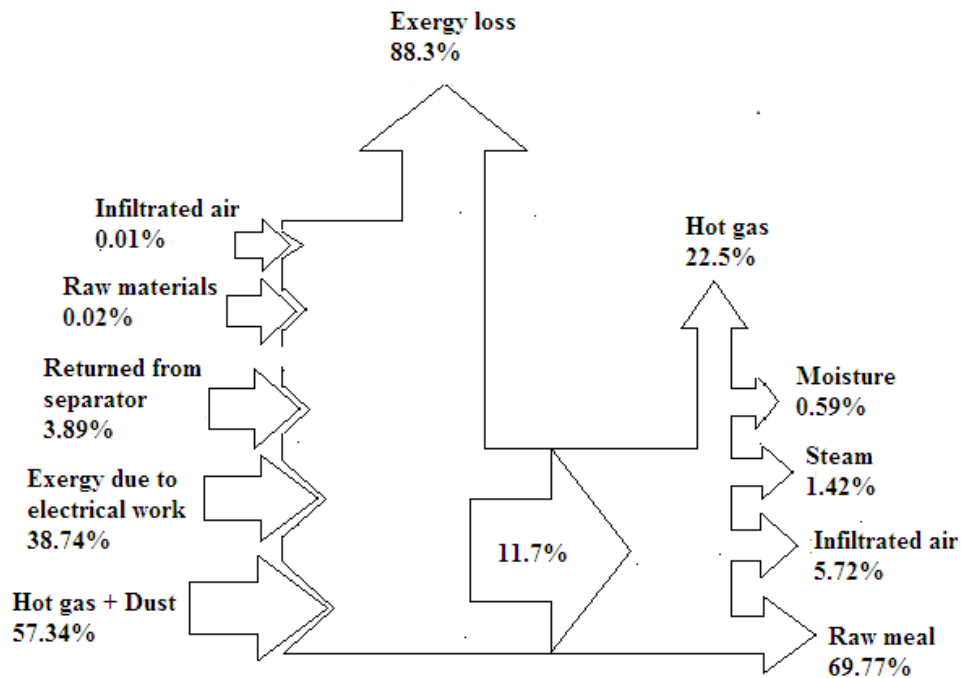


Fig.3.14 Grassmann (exergy band diagram) diagram of raw mill (Production rate of 121 tonnes per hour)

Fig.3.14 shows the results of the exergy analysis by the Grassmann diagram. The exergy efficiency was found to be 11.7%. Fig.3.14 shows the results of the analysis. The exergy loss of the system was found to be 88.3%. The results obtained for this operating condition are very close to the previous operating condition. Here the exergy of gas and dust account 57.34%, followed by electrical energy 38.4%. The returned material exergy was found to be 3.89%. The contribution of exergies of raw material and leaking air are 0.02 % and 0.01% respectively. The output exergies shows that exergy loss is responsible for 88.3 % of the all output exergies

3.8 Conclusion

The aim of this study is to determine energy and exergy utilization, heat balance, exergy balance and irreversibility for a raw mill in the cement production. Mass balance, energy and exergy utilization of the raw mill process were analysed using the actual plant operational data. The main conclusion drawn from present study may be summarized as follows.

The operation of raw mill spends a lot of energy. Gas at high temperature goes to the raw mill to reduce the humidity of the output material. So the energy losses decrease the efficiency of the raw mill. For the first operating condition (production rate of 117 tonnes per hour), the energy efficiency of the raw mill was found to be 55.94 %, while the exergy efficiency value was 11.76%. The exergy losses have been calculated about 88.24%. The total heat loss from the raw mill accounts for 44.06% of output energy. The gas, leaking air and steam account for 16.69% of output energy.

It appears that reduction in fuel and electricity consumption in a raw mill operation can be achieved by effective insulation, reducing the temperature of gases at outlet by more effective heat transfer unit and minimizing air and steam leak by effective sealing are some measures that can help reduce energy consumption.

The energy and exergy analysis were also conducted for another operating condition (production rate of 121 tonnes per hour). For this increased production rate, the energy and exergy efficiencies of the mill were found to be 55.93% and 11.7 % respectively and the values are very close to previous results. For this operating condition, in order to keep minimum moisture rate in the product (0.5%) the temperature of the

product was maintained constant (88°C) by adjusting the inlet gas temperature. So the grinding and drying room temperatures are found to be same as the previous operating condition. Therefore the raw mill efficiency was found to be constant for this operation also.

From both operating conditions, it was found that the exergy efficiency of the Raw Mill is very poor compared to the energy efficiency. This indicates that the exergy utilization in the raw mill was worse than energy utilization. That is, this process represents a big potential for increasing the exergy efficiency. So a conscious and planned effort towards building an energy management structure within the plant studied is needed to improve the exergy utilization in the raw mill.

.....❧.....

ENERGY AND EXERGY ANALYSIS OF THE KILN SYSTEM IN THE CEMENT PLANT

<i>Contents</i>	4.1 <i>Introduction</i>
	4.2 <i>Kiln System.</i>
	4.3 <i>Kiln System Analysis</i>
	4.4 <i>Results and Discussion</i>
	4.5 <i>Conclusion</i>

4.1 Introduction

The conservation, balance and management of energy are hot and emerging topic of today's discussion. In this regard, the attempts for energy balance in the industries of developing countries like India are having extreme significance. Cement industry is an energy intensive industry. Theoretically, producing one tonne of clinker requires a minimum on 1.6 GJ heat (Liu et al., 1999). The specific thermal energy consumption in cement industries in India varies from 2.95 GJ to 4 GJ/tonne of clinker. The higher specific energy consumption is due to the harder raw material and poor quality of fuel. In this study, the energy utilization efficiency for kiln system with different operating conditions was determined. Mass balance, energy and exergy utilization efficiency of the kiln system were analyzed using the actual operational data.

4.2 Kiln System

The plant uses the dry process with four stage cyclone pre-heaters and an inclined Kiln. The specification of kiln is given as follows

Length	65 m
Diameter	4.4 m
Designed capacity	1213 tonnes per day
Kiln slope	3%
Kiln speed	0.3 -2.2 RPM
Normal speed	1.2 RPM

The rotary cement kiln is a long cylindrical steel shell lined on the interior with refractory bricks. The shell slopes slightly (3%) and slowly rotates on its axis at between 0.3 - 2.2 revolutions per minute. Coal ground to fine power in the coal mill, is weighed in an electronic weight feeder and fired to the kiln through a burner pipe positioned almost concentric to the kiln at the outlet. This forms intense heat at the outlet end of kiln, imparting thermal energy for clinkerisation. The pulverised coal is injected into the kiln with the help of primary air. Secondary air is drawn first through the cooler and then through the kiln for combustion of the coal. In the cooler the air is heated by the cooling clinker, so that it may be 800-950°C before it enters the kiln, thus causing intense and rapid combustion of the coal.

Required raw meal is extracted from the storage silos, weighed in an electronic feeder and lifted to top of the preheater unit. The raw meal travels down the preheater countering the exit hot gas from kiln. In the drying zone the moisture content of material escape as water vapour. Above 600°C, calcium carbonate and magnesium carbonate in the feed starts decomposing to

form calcium oxide, magnesium oxide and carbon dioxide. The partly calcined material enters the kiln where temperature is maintained at 850°C. The feed that enters the kiln inlet gradually travel towards the outlet end due to rotation and slope of kiln. Hot gas from the kiln moves upwards, as a result the raw materials are exposed to hot gases and in its course, it gets fully calcined. The calcined material then enters to the burning zone (1450°C) of the kiln and the entire chemical reactions takes place there and clinker is formed. Fig.4.1 shows details of the kiln system.

The calcinations and reactions will take place at different zones in the kiln system to form clinker, which is a mixture of the phase components such as β -Dicalcium silicate (β - C_2S), Tri calcium aluminate(C_3A) and Tetra calcium aluminoferrite (C_4AF). The β -Dicalcium silica further reacts with more CaO at higher temperatures to form Tri calcium silicate (C_3S) in the burning zone. The main reactions in the kiln system are tabulated in Table 4.1 (Kaantee et al., 2004; Mintus et al., 2006; Mujumdar and Ranade, 2006).

Table 4.1 Chemical reactions process in kiln system

Reaction name	Reaction
Calcinations process	$CaCO_3 \rightarrow CaO + CO_2$
MgCO ₃ dissociation	$MgCO_3 \rightarrow MgO + CO_2$
β - C_2S formation	$2CaO + SiO_2 \rightarrow \beta -C_2S$
C_3S formation	$\beta -C_2S + CaO \rightarrow C_3S$
C_3A formation	$3CaO + Al_2O_3 \rightarrow C_3A$
C_4AF formation	$4CaO + Al_2O_3 + Fe_2O_2 \rightarrow C_4AF$

The clinker thus formed is dark green in colour with 30% of it in the form of nodules. Clinker leaving the kiln at around 1200 °C is quenched and cooled to around 100°C in the cooler unit and stored in the clinker stockpile.

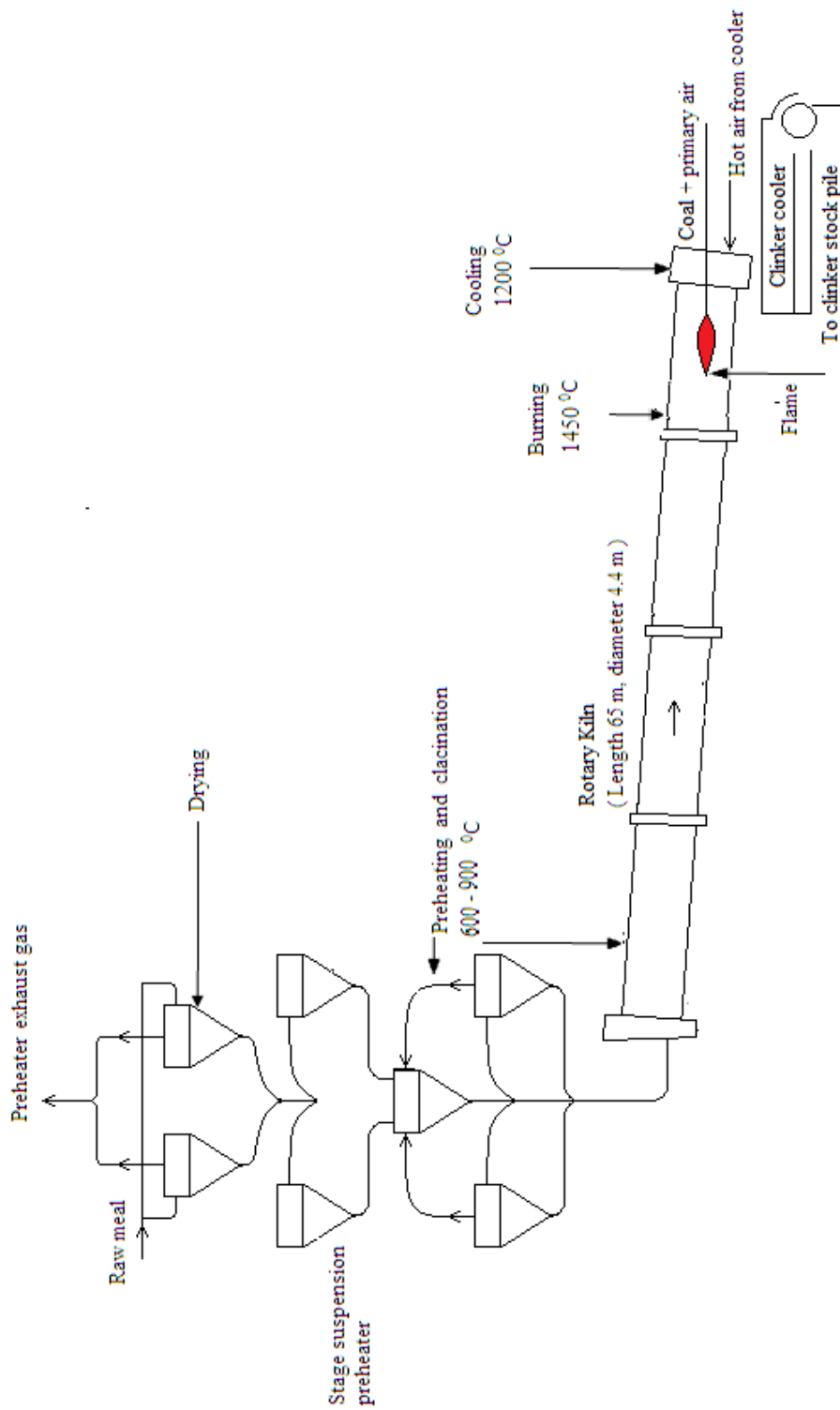


Fig. 4.1 Kiln system

4.3 Kiln System Analysis

The energy and exergy analysis of the kiln system were conducted for two operating conditions given as follows.

I. Clinker production rate of 1400 tpd

The operation data of the kiln system for the production rate of 1400 tonnes per day is given in the Table 4.2

Table 4.2 Operation data of kiln system for the production rate of 1400 tonnes per day

Ambient temperature	35 °C
Present kiln capacity	1400 TPD
Required kiln feed	87 TPH
Temperature of feed	55 °C
Raw meal /clinker factor	1.49
Coal consumption	11.08 TPH
Flow rate of preheater Exhaust gas	120666Nm ³ /hr
Preheater exhaust gas temperature	384 °C
O ₂ % Preheater exit gas	4.2%
O ₂ % Kiln inlet (junction between preheater and kiln)	1.8%
Flow rate of primary air	21508 Nm ³ /hr
Temperature of Primary air	71 °C
Flow rate of cooler inlet air	185423Nm ³ /hr
Excess air	10%
Clinker discharge temperature from cooler	95 °C
Flow rate of gas to coal mill	6157 Nm ³ /hr
Temperature of coal mill gas	330 °C
Flow rate of cooler hot air	138542Nm ³ /hr
Temperature of hot air from cooler	200°C
Temperature of secondary air	850 °C
Dust concentration in Preheater exhaust gas	36.06 g/ Nm ³
Surface temperature of kiln	300 °C
Surface temperature of preheater	80 °C
Surface temperature of cooler	82 °C

The control volume for the study includes the pre-heaters, rotary kiln and cooler. The streams into the system are the raw meal, the air into the cooler and coal fired in the kiln. The streams leaving the system are clinker out from the cooler, the exhaust gas from the preheater and hot gases from the cooler. During this operating condition (Production rate of 1400 tonnes per day) the various input and output gas volume at different locations are measured with pitot tube with manometer assembly. The kiln, preheater and cooler surface temperature were measured with radiation pyrometer. The material input and output temperature is measured by using a thermocouple. The temperatures of inlet and outlet gas are continuously measured by the online temperature probes which are installed on the system.

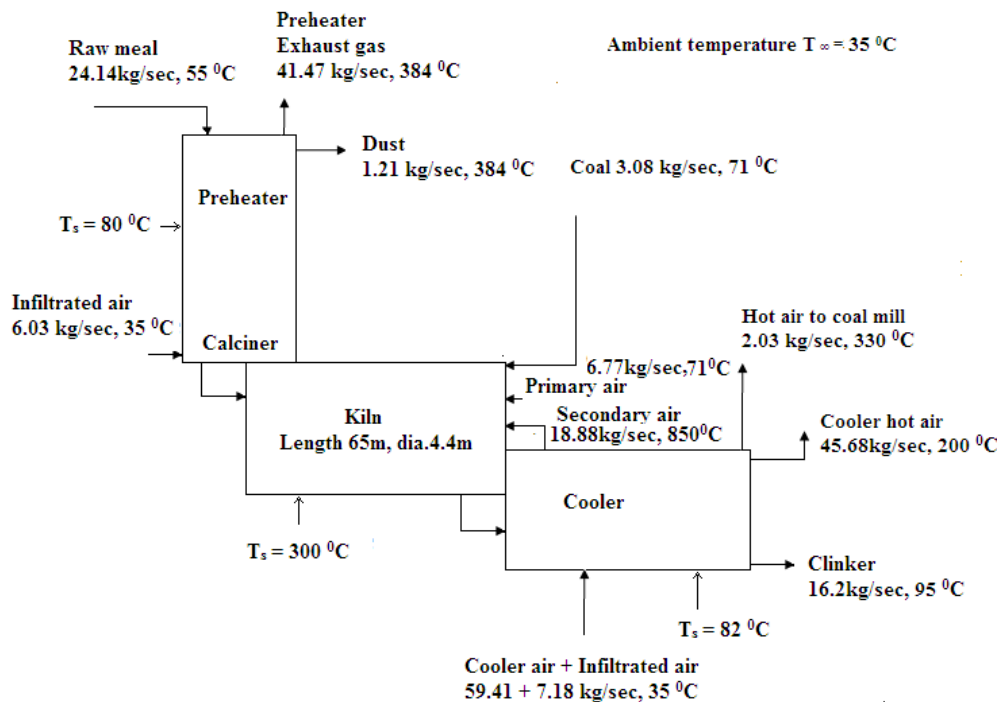


Fig.4.2 Schematic diagram of the kiln system (Production rate of 1400 tonnes per day)

The Fig. 4.2 shows the various input and output streams based on mass flow rate of the kiln system. The raw meal at the rate 24.14 kg/sec (55 °C) from the raw mill supplied to the top of the preheater and it moves down to the rotary kiln. The hot gas from kiln moves upwards as a result of which heat transfer take place between raw meal and hot gas and the gas then discharged to the surrounding (384 °C). In the kiln, raw meal subject to chemical reaction and burning, the clinker is formed and it is cooled in the clinker cooler. The clinker discharge rate from the cooler is 16.2 kg/sec at 95 °C. The pulverised coal is supplied to the kiln at the outer end with the primary air (71 °C). The secondary air (850 °C) drawn from the clinker cooler moves through the kiln and preheater. The suction is created by the preheater fan.

It was observed that, kiln inlet (junction between preheater and kiln) O₂ level was 1.8% which indicates that the kiln is operating with 10% excess air. The secondary air required for complete combustion of coal in the kiln was calculated as 18.87 kg/sec. The coal mill fan drawn air from the clinker cooler with temperature of 330°C. The temperature of cooler hot air discharged to the surrounding is about 200 °C. It was observed that the O₂ level at preheater exit is indicated to be 4.2%. Normally for optimum energy consumption, the percentage of oxygen to be maintained at preheater exit and kiln inlet are 3.5% and 1.5 % respectively. It was observed that air leakage in to the kiln is negligible. The air leakage mainly occurs across the preheater and clinker cooler. In this case the total infiltration air to the whole system was found to be 12.4%.

II Clinker production rate of 1369 tonnes per day

The operation data of the kiln system for the production rate of 1369 tonnes per day is shown in Table 4.3

Table 4.3 Operation data of kiln system for the production rate of 1369 tonnes per day

Ambient temperature	30 °C
Present kiln capacity	1369 TPD
Required kiln feed	85 TPH
Temperature of feed	55 °C
Raw meal /clinker factor	1.49
Coal consumption	10.83 TPH
Flow rate of preheater Exhaust gas	117113 Nm ³ /hr
Preheater exhaust gas temperature	395 °C
O ₂ % Preheater exhaust gas	4%
O ₂ % Kiln inlet (junction between preheater and kiln)	1.8%
Flow rate of primary air	21658 Nm ³ /hr
Temperature of Primary air	53 °C
Flow rate of cooler inlet air	137756 Nm ³ /hr
Excess air	10%
Clinker discharge temperature	150 °C
Flow rate of gas to coal mill	6405 Nm ³ /hr
Temperature of coal mill gas	340 °C
Flow rate of cooler hot air	98919 Nm ³ /hr
Temperature of hot air from cooler	220 °C
Temperature of secondary air	860 °C
Dust concentration in Preheater exhaust gas	36.28 g/ Nm ³
Surface temperature of kiln	305 °C
Surface temperature of preheater	82 °C
Surface temperature of cooler	85 °C

Fig.4.3 shows the various streams based on mass flow rate in the kiln system. The clinker discharge rate from the cooler in this operating condition is about 15.84 kg/sec at 150 °C. The required kiln feed for the

clinker production is supplied through top of the preheater about 23.6kg/sec (55⁰C). The gas streams at outlet of the system are preheater exhaust gas (395 ⁰C), cooler hot air (220 ⁰C) and coal mill gas (340 ⁰C). The gas streams at inlet of the system are primary air (53 ⁰C) and cooler air to cool the clinker. For this operating condition the pulverised coal is supplied to the kiln with the primary air at the rate of 3.01 kg/sec.

It was noted that, kiln inlet (junction between preheater and kiln) O₂ level is 1.8% which reveals that the kiln is operating with 10% excess air. The secondary air required for the complete combustion of coal in the kiln was calculated as 18.35kg/sec. The temperature of secondary air is about 860 ⁰C. It was observed that the O₂ at preheater exit and kiln inlet are indicated to be 4 % and 1.8% respectively. In this case the total infiltration air for the whole system was found to be 15 %.

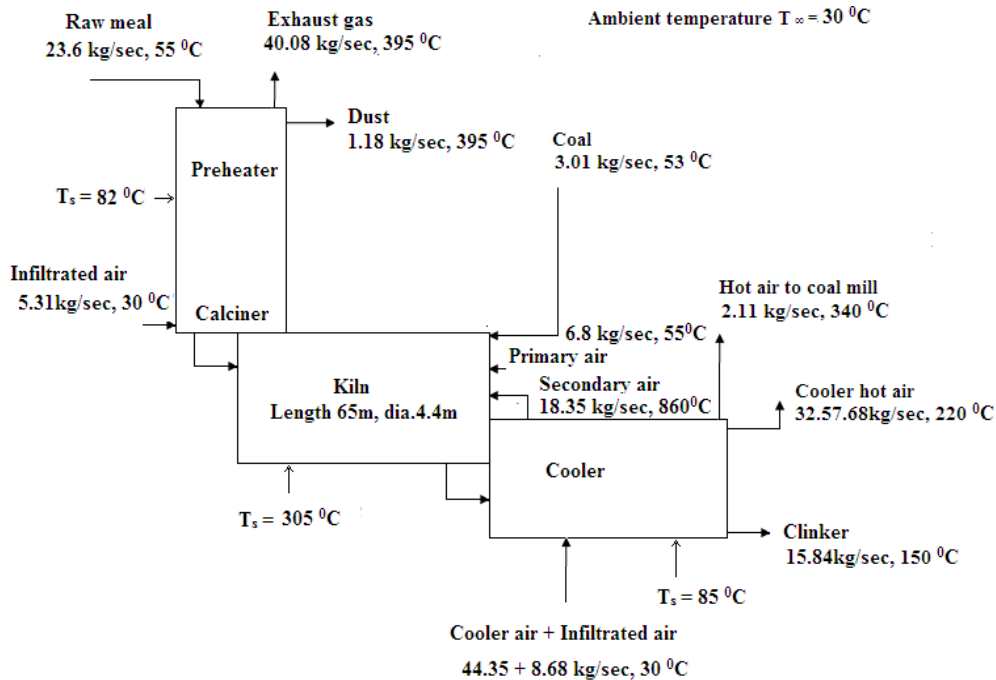


Fig. 4.3 Schematic diagram of the kiln system (Production rate of 1369 tonnes per day)

4.4 Results and Discussion

4.4.1 Mass balance of the Kiln System (Production rate of 1400 tonnes per day)

The stream data obtained from the plant is used to perform a mass balance over the system. It is usually more convenient to define mass or energy data per kg of clinker produced per unit time. The clinker production rate of in the kiln is estimated to be 16.2 kg of clinker/sec. For this production rate of various input and output components of the kiln system are estimated as follows.

Inputs

- (i) Raw meal feed = 24.14 kg/sec

$$\begin{aligned}\text{Raw meal per kg of clinker production, } (m_k)_{rm} &= \frac{24.14}{16.2} \\ &= 1.49 \text{ kg/kg-clinker}\end{aligned}$$

- (ii) Rate of coal consumption = 3.078 kg/sec

$$\begin{aligned}\text{Coal per kg of clinker production, } (m_k)_c &= \frac{3.078}{16.2} \\ &= 0.19 \text{ kg/kg-clinker}\end{aligned}$$

- (iii) Primary air mass flow rate = 6.77 kg/sec

$$\begin{aligned}\text{Primary air per kg of clinker production, } (m_k)_{pa} &= \frac{6.77}{16.2} \\ &= 0.418 \text{ kg/kg-clinker}\end{aligned}$$

- (iv) Mass flow rate of air into the cooler = 59.41 kg/sec

$$\begin{aligned}\text{Cooler air per kg of clinker production, } (m_k)_{ca} &= \frac{59.41}{16.2} \\ &= 3.667 \text{ kg/kg-clinker}\end{aligned}$$

(v) Infiltrated air mass flow rate = 13.2 kg/sec

$$\begin{aligned} \text{Infiltrated air per kg of clinker production, } (m_k)_{ia} &= \frac{13.2}{16.2} \\ &= 0.8146 \text{ kg/kg-clinker} \end{aligned}$$

Outputs

(i) Preheater exhaust gas mass flow rate = 41.47kg/sec

Preheater exhaust gas per kg of clinker production,

$$\begin{aligned} (m_k)_{eg} &= \frac{41.47}{16.2} \\ &= 2.56 \text{ kg/kg-clinker} \end{aligned}$$

(ii) Mass flow rate of dust = 1.21 kg/sec

$$\begin{aligned} \text{Dust per kg of clinker production, } (m_k)_d &= \frac{1.21}{16.2} \\ &= 0.0746 \text{ kg/kg-clinker} \end{aligned}$$

(iii) Cooler hot air mass flow rate = 45.813 kg/sec

$$\begin{aligned} \text{Cooler hot air per kg of clinker production, } (m_k)_{co} &= \frac{45.68}{16.2} \\ &= 2.82 \text{ kg/kg-clinker} \end{aligned}$$

(iv) Mass flow rate gas to coal mill = 2.025 kg/sec

$$\begin{aligned} \text{Coal mill gas per kg of clinker production } (m_k)_{cm} &= \frac{2.025}{16.2} \\ &= 0.125 \text{ kg/kg-clinker} \end{aligned}$$

(v) Clinker flow rate, m_{cli} = 16.2 kg-clinker /sec

$$\text{Clinker discharge } (m_k)_{cli} = \frac{16.2}{16.2} = 1 \text{ unit}$$

The mass balance of the kiln system is summarized in Fig.4.4. All gas streams are assumed to be ideal gases at the given temperatures.

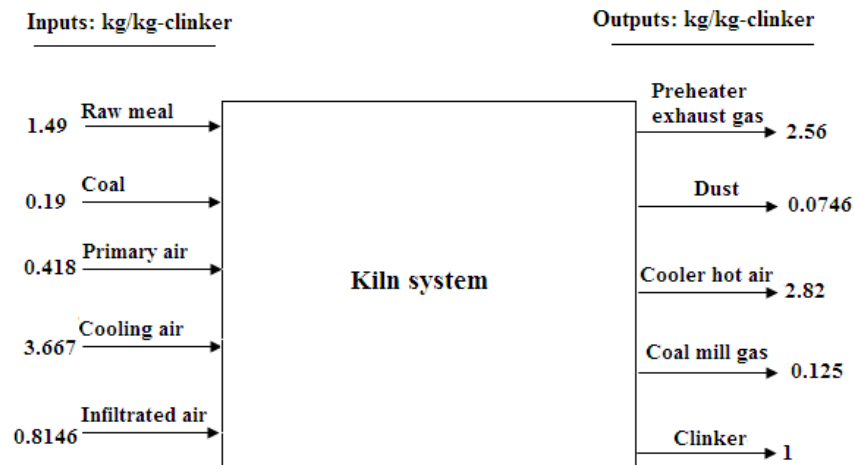


Fig. 4.4 Mass balance in the kiln system (Production rate of 1400 tonnes per day)

4.4.2 Energy balance of the Kiln System (Production rate of 1400 tonnes per day)

The following assumptions are made to analyze the kiln system.

- (a) Steady state working conditions.
- (b) The change in the ambient temperature is neglected.
- (c) Cold air leakage into the kiln is negligible.
- (d) Average kiln surface temperature does not change.

For the rotary kiln system, the energy balance equation is given as follows

$$\sum (m_k)_{in} h_{in} = \sum (m_k)_{out} h_{out} + (Q_k)_L \text{(4.1)}$$

where $(m_k)_{in}$ and $(m_k)_{out}$ are mass in and out of the kiln system.

h_{in} and h_{out} are specific enthalpy in and out of the kiln system

$(Q_k)_L =$ heat loss from the kiln surface

Based on the collected data, an energy balance is applied to the kiln system. The equations can be found in hand book (Perry, 1979). The reference enthalpy is considered to be zero at 0 °C for the calculation. The specific heat capacity (c_p) of the each input and output material for analysis has been calculated by using relation $c_p = a + b \times T + \frac{c}{T^2}$ where a, b and c are the constants for the components of material and T represents temperature in Kelvin (Perry and Green, 1984). The compositions of input and output materials are shown in Annexure A. The constants of each component of the input and output materials are taken from standard hand book (Perry and Green, 1984). The complete energy balance for the system is shown in Table 4.4

Table 4.4 Energy balance for the kiln system (Production rate of 1400 tonnes per day)

Input energy				
Sl no.		Equation	Data	Heat, Q_k (kJ/kg-clinker)
1	Coal combustion	$(m_k)_c \times H_c$	$(m_k)_c = 0.19$ kg/kg-clinker, $H_c = 20763$ kJ/kg	3945
2	Coal sensible heat	$(m_k)_c \times c_{p_c} \times T_c$	$(m_k)_c = 0.19$ kg/kg-clinker, $c_{p_c} = 0.76$ kJ/kg-K, $T_c = 71$ °C	10.25
3	Raw meal sensible heat	$(m_k)_{rm} \times c_{p_{rm}} \times T_{rm}$	$(m_k)_{rm} = 1.49$ kg/kg-clinker, $c_{p_{rm}} = 0.7919$ kJ/kg-K, $T_{rm} = 55$ °C	64.9
4	Primary air	$(m_k)_{pa} \times c_{p_{pa}} \times T_{pa}$	$(m_k)_{pa} = 0.418$ kg/kg-clinker, $c_{p_{pa}} = 0.9843$ kJ/kg-K, $T_{pa} = 71$ °C	29.21
5	Cooler air	$(m_k)_{ca} \times c_{p_{ca}} \times T_{ca}$	$(m_k)_{ca} = 3.667$ kg/kg-clinker, $c_{p_{ca}} = 0.9681$ kJ/kg-K, $T_{ca} = 35$ °C	124.25
6	Infiltrated air	$(m_k)_{ia} \times c_{p_{ia}} \times T_{ia}$	$(m_k)_{ia} = 0.815$ kg/kg-clinker, $c_{p_{ia}} = 0.9681$ kJ/kg-K, $T_{ia} = 35$ °C	27.06
Total				4201.21
Output energy				
1	Clinker formation	Calculation is shown in Annexure D	1kg	1756.24
2	Preheater exhaust gas	$(m_k)_{eg} \times c_{p_{eg}} \times T_{eg}$	$(m_k)_{eg} = 2.56$ kg/kg-clinker, $c_{p_{eg}} = 1.0878$ kJ/kg-K, $T_{eg} = 384$ °C	1069.34

3	Moisture in coal	$m_{H_2O} \times [h_{fg(71^\circ C)} + h_{(384^\circ C)} - h_{(71^\circ C)}]$	$m_{H_2O} = 0.0067 \text{ kg/kg-clinker,}$ $h_{fg(71^\circ C)} = 2334 \text{ kJ/kg,}$ $h_{(384^\circ C)} = 3248.9 \text{ kJ/kg,}$ $h_{(71^\circ C)} = 2627 \text{ kJ/kg}$	19.66
4	Hot air from cooler	$(m_k)_{co} \times c_{p_{co}} \times T_{co}$	$(m_k)_{co} = 2.82 \text{ kg/kg-clinker,}$ $c_{p_{co}} = 1.0226 \text{ kJ/kg-K,}$ $T_{air} = 200^\circ C$	576.75
5	Heat lost by dust	$(m_k)_d \times c_{p_d} \times T_d$	$(m_k)_d = 0.0746 \text{ kg/kg-clinker,}$ $c_{p_d} = 1.0093 \text{ kJ/kg-K,}$ $T_d = 384^\circ C$	28.91
6	Clinker discharge	$(m_k)_{cli} \times c_{p_{cli}} \times T_{cli}$	$(m_k)_{cli} = 1 \text{ kg/kg-clinker,}$ $c_{p_{cli}} = 0.8308 \text{ kJ/kg-K,}$ $T_{cli} = 95^\circ C$	78.93
7	Coal mill gas	$(m_k)_{cm} \times c_{p_{cm}} \times T_{cm}$	$(m_k)_{cm} = 0.125 \text{ kg/kg-clinker,}$ $c_{p_{cm}} = 1.0482 \text{ kJ/kg-K,}$ $T_{cm} = 330^\circ C$	43.24
8	Radiation from kiln surface	$\frac{\sigma \times \varepsilon \times A_{kiln} \times (T_s^4 - T_\infty^4)}{1000 \times m_{cli}}$	$\sigma = 5.67 \times 10^{-8} \text{ W/m}^2\text{K}^4,$ $A_{kiln} = 900 \text{ m}^2,$ $T_s = 573 \text{ K,}$ $T_\infty = 308 \text{ K,}$ $m_{cli} = 16.2 \text{ kg-clinker/sec}$	242.75
9	Convection heat loss from kiln surface	$\frac{h_a \times A_{kiln} \times (T_s - T_\infty)}{1000 \times m_{cli}}$	$h_a = 4.293 \text{ W/m}^2\text{ }^\circ\text{C,}$ $A_{kiln} = 900 \text{ m}^2,$ $T_s = 300^\circ\text{C, } T_\infty = 35^\circ\text{C,}$ $m_{cli} = 16.2 \text{ kg-clinker/sec,}$ $h_a = \frac{Nu k_{air}}{D_{kiln}}, \text{ Re} = 422336,$ $(V_{air} = 3 \text{ m/sec}),$ $Nu = 0.193(\text{Re}^{0.618})(Pr^{0.333}),$ (Frank, 2001) $\text{Re} = 422336, \text{ Pr} = 0.682,$ $k_{air} = 0.0371 \text{ W/m K,}$ $D_{kiln} = 4.4 \text{ m, } T_f = 177^\circ\text{C}$	63.2

10	Radiation heat loss from the pre-heater surface	$\frac{\sigma \times \varepsilon \times A_{ph} \times (T_s^4 - T_\infty^4)}{1000 \times m_{cli}}$	$\sigma = 5.67 \times 10^{-8} \text{W/m}^2\text{K}^4$, $\varepsilon = 0.78$ (oxidised surface), $A_{ph} = 250 \text{m}^2$, $T_s = 353 \text{K}$, $T_\infty = 308 \text{K}$, $m_{cli} = 16.2 \text{ kg-clinker/sec}$	4.46
11	Natural convection from the pre-heater surface	$\frac{h_a \times A_{ph} \times (T_s - T_\infty)}{1000 \times m_{cli}}$	$h_a = 1.964 \text{ W/m}^2\text{C}$, $A_{ph} = 250 \text{m}^2$, $T_s = 80^\circ\text{C}$, $T_\infty = 35^\circ\text{C}$, $m_{cli} = 16.2 \text{ kg-clinker/sec}$, $h_a = \frac{Nu k_{ph}}{L_{ph}}$, $Nu = 0.1(G_r P_r)^{0.333}$, (Frank, 2001) $T_f = 55^\circ\text{C}$, $G_r = 8.86 \times 10^{11}$, $P_r = 0.697$, $L_{ph} = 15 \text{m}$, $k_{air} = 0.02891 \text{ W/mK}$	1.35
12	Radiation heat loss from the cooler surface	$\frac{\sigma \times \varepsilon \times A_{cs} \times (T_s^4 - T_\infty^4)}{1000 \times m_{cli}}$	$\sigma = 5.67 \times 10^{-8} \text{W/m}^2\text{K}^4$, $\varepsilon = 0.78$, $A_{cs} = 81 \text{m}^2$, $T_s = 355 \text{K}$, $T_\infty = 308 \text{K}$, $m_{cli} = 16.2 \text{ kg-clinker/sec}$	1.52
13	Natural convection from the cooler surface	$\frac{h_a \times A_{cs} \times (T_s - T_\infty)}{1000 \times m_{cli}}$	$h_a = 2.06 \text{ W/m}^2\text{C}$, $A_{cs} = 81 \text{m}^2$, $T_s = 82^\circ\text{C}$, $T_\infty = 35^\circ\text{C}$, $m_{cli} = 16.2 \text{ kg-clinker/sec}$, $Nu = 0.1(G_r P_r)^{0.333}$, (Frank, 2001). $h_a = \frac{Nu \times k_{air}}{L_{cs}}$, $T_f = 55^\circ\text{C}$, $G_r = 1.984 \times 10^{11}$, $P_r = 0.696$, $L_c = 7 \text{m}$, $k_{air} = 0.02826 \text{ W/mK}$,	0.48
Total				3886.83
Unaccounted heat loss				314.38
Total				4201.21

$$\begin{aligned} \text{Efficiency} &= \frac{\text{Clinker formation energy}}{\text{total input energy}} \text{-----} (4.2) \\ &= 41.8 \% \end{aligned}$$

Fig. 4.5 shows the energy flow diagram of the kiln system. The specific thermal energy consumption of the plant was 4201.21 kJ/kg-clinker, out of which 3945 kJ/kg-clinker (93.9 %) was the combustion of coal. The other input includes sensible heat of coal 10.25kJ/kg-clinker (0.24%), sensible heat of raw meal 64.9 kJ/kg-clinker (1.55 %), and air 181.06kJ/kg-clinker (4.31 %). The kiln exhaust gas with 1069.34 kJ/kg-clinker (25.45%) and clinker cooler hot gas 576.75kJ/kg-clinker (13.73%) are discharged to the surrounding. The heat loss by convection and radiation together from the kiln surface is found to be 305.96 kJ/kg-clinker (7.28%) and that for the pre-heater and clinker cooler of the system is estimated to be 7.81 kJ/kg-clinker (0.19%). The other heat losses include clinker discharged from the cooler 78.93 kJ/kg-clinker (1.88%), gas drawn to coal mill 43.24 kJ/kg-clinker (1.03%), dust 28.91 kJ/kg-clinker(0.69%) and moisture in coal 19.66 kJ/kg-clinker (0.47%). The unaccounted heat loss was found to be 314.38 kJ/kg-clinker (7.48%). The overall efficiency of the system was found to be $\eta = 41.8\%$ and the value is close to a plant in Turkey 48.2% (Kolip, 1990).

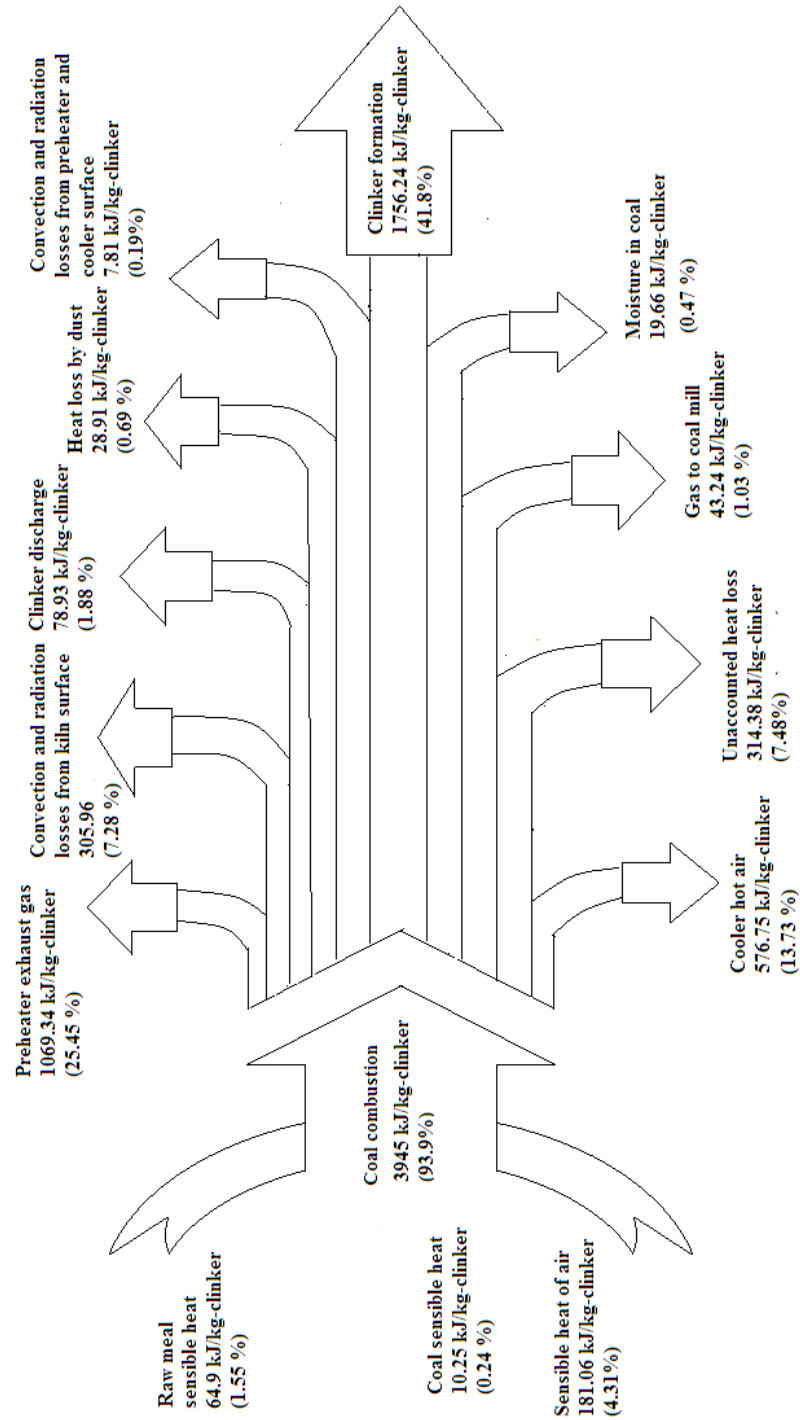
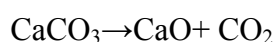
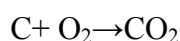


Fig.4.5 Energy flow diagram (Sankey diagram) of kiln system (Production rate of 1400 tonnes per day)

4.4.3 CO₂ emissions

For the present operating conditions the kiln was fired with coal at the rate of 11081 kg/hr. CO₂ emissions from the kiln system are mainly due to the combustion of coal and decarbonation reactions. Complete combustion of coal and decarbonation reaction is assumed. The corresponding stoichiometric of the reactions are written as follows.



Total yield of CO₂ is determined considering 1 kg-clinker, 0.19 kg of coal/kg of clinker and stoichiometric mass ratio. It is found that 0.37 kg CO₂ per kg of clinker is generated from the complete combustion of coal. The raw meal to clinker ratio at the present operating condition is 1.49 and it contains 1.176 kg of CaCO₃. Therefore it was determined that 0.52 kg of CO₂ per kg of clinker is generated during the decarbonation reaction. Hence the total emissions of CO₂ due to combustion of coal and decarbonation reaction for a clinker production rate of 1400 tonnes per day is estimated to be 1246 tonnes per day.

4.4.4 Energy conservation opportunities

One of the objectives of the energy conservation measures is to expand the use of the secondary energy as much as possible and thereby reduce the requirement for primary purchased energy. In this study, only thermal energy conservation measures are presented. Basically all output flow from the kiln system could have potential for waste heat recovery. The main sources energy conservation can be kiln and cooler exhaust gases and radiation heat from kiln. The recovered waste heat can be used for power generation, drying raw material and coal and preheating the secondary air for kiln.

4.4.5 Waste heat recovery steam generation (WHRSG) –Production rate of 1400 tonnes per day

The overall efficiency of the system can be improved by recovering some of the heat losses and the recovered heat can be used for several purposes, such as electricity generation, hot water generation etc. The waste heat recovery system can also be considered as an environment friendly system since it utilizes available wasted energy and reduces the resulting CO₂ emissions of cement production processes. It is possible to recover the major heat losses such as like kiln exhaust gas and hot air from cooler stack by using waste heat recovery steam generation (WHRSG) unit.

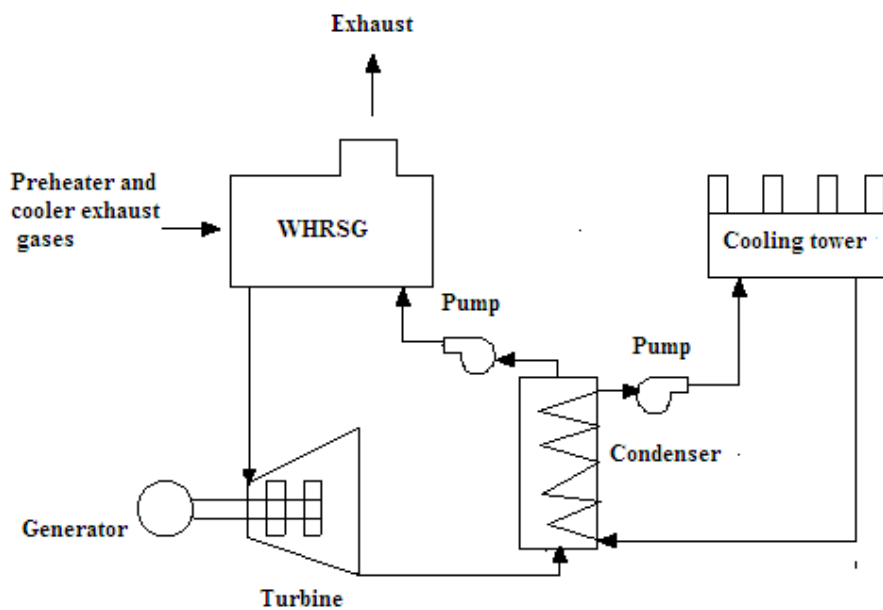


Fig. 4.6 Waste heat recovery steam generation application

The four stage pre-heaters have exhaust gases leaving at temperature 384°C. The clinker is discharged red-hot from the kiln and transferred to clinker coolers, which performs the function of cooling the clinker for downstream transport and processing and the temperature of air discharge from the cooler is 200°C. Both streams would be directed through a waste

heat recovery steam generator and available energy is transferred to water via the WHRSG. The schematic diagram of WHRSG unit is shown in Fig.4.6. The available waste energy is such that the steam would be generated. The steam would then be used to power the steam turbine driven electrical generator. The electricity generated would offset a portion of the purchased electricity, thereby reducing electrical demand.

In order to determine the size of the generator, the available energy from the gas stream must be found. Once this is determined, an approximation of the steaming rate for a specified pressure can be estimated. The steam rate and pressure will determine the size of the generator.

As the gas passes through the WHRSG, energy will be transferred and gas temperature will drop. Targeting a pressure of 8 bar at the turbine inlet, the minimum steam temperature at the WHRSG exit would be higher than corresponding saturation temperature which is roughly 170°C. After exiting the WHRSG, the energy of these streams can be recovered by using a compact heat exchanger. Hence the final temperature can be reduced as low as possible, which might be limited by the acid dew point temperature of stream. According to the final temperature of both the streams, the final enthalpies have been calculated to be $h_{co}=173.84$ kJ/kg, $h_{eg}=184.93$ kJ/kg. So the available heat energy would be

$$Q_{\text{available}} = [(m_k)_{eg}(h_{eg1}-h_{eg2}) + (m_k)_{co}(h_{co1}-h_{co2})] \times m_{cli} \text{ -----(4.2)}$$

where $(m_k)_{eg}$ is the mass of exhaust gases from the pre-heater (kg/kg-clinker), $(m_k)_{co}$ is the mass of air from the cooler (kg/kg-clinker) and m_{cli} is the mass flow rate of clinker(kg/sec)

$$Q_{\text{available}} = [2.56(417.72-184.93) + 2.82(204.52-173.84)] \times 16.2 = 8253 \text{ kW}$$

It is assuming a reasonable efficiency of 85% for the steam generator.

Then the energy that would be transferred through

$$\text{WHRSG} = 0.85 \times 8253 = 7015 \text{ kW}$$

For utilizing this available recovered heat energy, a steam turbine unit is considered with a turbine pressure of 8 bar and a condenser pressure of 10 kPa. It can be shown that the net power, which would be obtained from this turbine, is almost 1000 kW.

Then the author assumed that the useful power generated is 1000 kW, then the energy saving will be based on the 1000 kW. Assuming 8000 hours of usage per year,

$$\begin{aligned} \text{Energy saved} &= \text{power generated} \times \text{hours of usage (4.3)} \\ &= 1000\text{kW} \times 8000\text{hr/yr} = 8 \times 10^6 \text{ kWh/yr} \end{aligned}$$

The average unit price of electricity can be taken as INR 5/kWh, therefore, the cost saving would be $= 5 \times 8 \times 10^6 = \text{INR } 4 \text{ Crores/year}$.

The first cost estimate for the system is about INR 6 Crores and taking into account the operating cost, the payback period for the system is estimated as follows.

$$\begin{aligned} \text{Payback period} &= \text{implementation cost} / \text{annual cost of saving} \\ &= \frac{\text{INR } 6 \text{ Crores}}{\text{INR } 4 \text{ Crores} / \text{yr}} \\ &= 1.5 \text{ yr} = 18 \text{ months} \end{aligned}$$

For improving the performance of the waste heat recovery steam generation unit, modifying the existing cycle with flash steam system is an

excellent option. The flash steam power cycle is based on the property that a certain mass of steam can be separated from water at saturated state if the pressure is lowered. The amount of flashed steam depends on the pressure before the flash tank and the final pressure in the tank. The lower the pressure in the flashing tank the higher is the amount of steam, but on the other side, low pressure steam generates a lesser amount of power. Fig. 4.7 shows the configuration of flash steam cycle for the cement plant. In this case two heat recovery steam generators are used to recover the two waste heat sources; one for the preheater exhaust, called the suspension preheater boiler, and the other for the clinker cooler exhaust called the air quenching cooler boiler. The working fluid passed through feed pump is sent into air quenching cooler boiler and preheated initially. One part of preheated working fluid is vaporized and superheated in air quenching cooler boiler, and another part of preheated working fluid is sent to suspension preheater boiler to be vaporized and superheated. The two streams of superheated steam from air quenching cooler boiler and suspension preheater boiler are mixed and expanded through turbine to generate power. The rest of preheated working fluid is expanded in the flasher and is separated into saturated steam and saturated water. The saturated steam is then sent into turbine to generate power. The turbine exhaust is condensed in the condenser, and passes through condensing pump to be mixed with saturated water from the flasher.

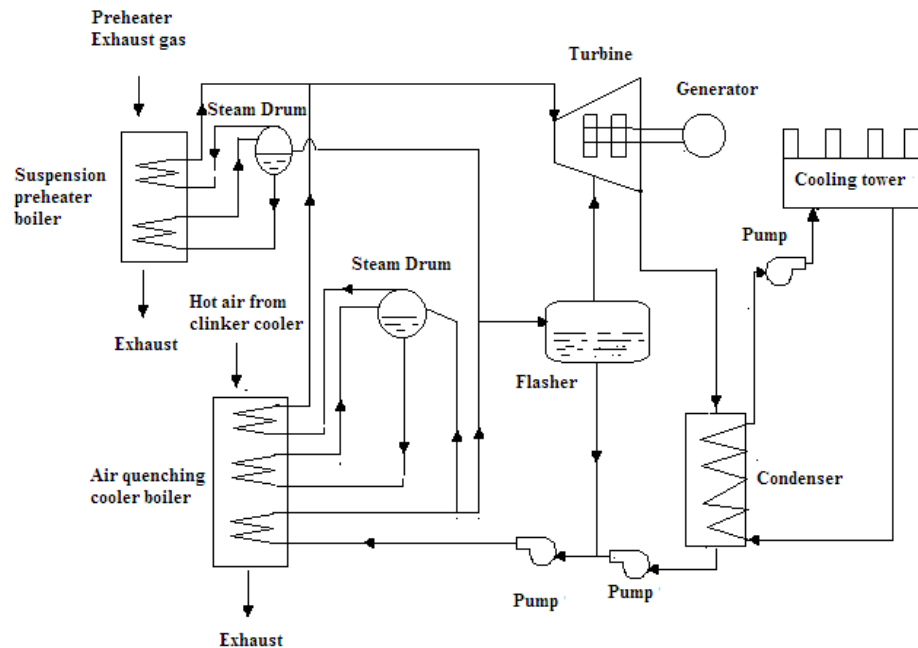


Fig.4.7 Waste heat recovery steam generation unit with steam flash cycle

4.4.6 Heat recovery from the kiln surface (Production rate of 1400 tonnes per day).

The convection and radiation heat loss from the kiln surface was found to be around 7% of the input energy. Using a secondary stationary shell on the kiln surface can significantly reduce this heat loss. For current rotary kiln, the radius is 2.2m, and for secondary shell radius of 2.6m can be considered. Since the distance between surfaces is relatively small 40cm, a realistic estimation for the temperature of secondary shell can be made. Assume the temperature of the secondary shell as 280°C (T_2). Consider the secondary shell made of steel with relatively low surface emission and thermal conductivity. The heat transfer by radiation calculated by Eq. 4.4 (Frank, 2001).

$$Q_r = \frac{A_{kiln} \times \sigma \times (T_1^4 - T_2^4)}{\left\{ (1/\varepsilon_1) + \frac{(1-\varepsilon_2)}{\varepsilon_2 \times \left(\frac{r_{kiln}}{r_{shell}} \right)} \right\}} \text{-----(4.4)}$$

where A_{kiln} is the surface area of the kiln = $2 \times \pi \times r \times L_k$

σ Stefan Boltzman constant = $5.67 \times 10^{-8} \text{ W/m}^2\text{K}^4$

T_1 is the Kiln surface temperature = 573 K

T_2 is the Shell surface temperature = 553 K.

ε_1 = emissivity for oxidized kiln surface

ε_2 = emissivity for stainless steel shell.

$Q_{ra} = 254.962 \text{ kW}$

This heat loss is to be transferred through the insulation of the secondary shell. For glass wool insulation, the thermal conductivity is taken as 0.05 W/mK. The thickness of the glass wool insulation can be determined by using the expression for resistance of the insulation. The thermal resistance of the insulation is

$$Rt_{ins} = \frac{\ln\left(\frac{r_{ins}}{r_{Shell}}\right)}{(2 \times \pi \times k_{ins} \times L_{ins})} \text{-----(4.5)}$$

where k_{ins} is the thermal conductivity of the insulation material.

r_{ins} is the outer radius of the insulated secondary shell,

r_{shell} is the outer radius of the secondary shell

L_{ins} is the length of the insulation shell

$$Rt_{ins} = \frac{\ln\left(\frac{r_{ins}}{r_{Shell}}\right)}{(2 \times \pi \times 0.05 \times 65)}$$

Assuming temperature difference of $\Delta T=250^{\circ}\text{C}$ (which means outer surface temperature of 50°C), So the radius of the insulation r_{ins} can be determined from the following relation.

$$\Delta T_{\text{ins}} = Q_{\text{ra}} \times (\text{resistance of the insulation}) \text{-----(4.6)}$$

$$250 = 254.962 \times \frac{\ln\left(\frac{r_{\text{ins}}}{2.6}\right)}{(2 \times \pi \times 0.05 \times 65)}$$

So the radius of the insulation found to be $(r_{\text{ins}}) = 2.65\text{m}$, and the thickness would be, $t = r_{\text{ins}} - r_{\text{shell}} = 2.65 - 2.4 = 0.05 \text{ m} = 50 \text{ mm}$

When the secondary shell is added to the kiln surface the convection heat loss become insignificant. Hence the total energy saving would be

$$\begin{aligned} &= (242.75\text{kJ/kg-clinker} \times 16.2\text{kg-clinker/sec}) - 254.962 = 3677.59\text{kW} \\ &\text{from the radiation and} \\ &= 63.2\text{kJ/kg-clinker} \times 16.2\text{kg-clinker/sec} = 1023.84 \text{ kW from the} \\ &\text{convection heat transfers.} \end{aligned}$$

Therefore the secondary shell would save the 4.7 MW, which is about 6.9 % of input energy. This energy saving would result the reduction in fuel consumption of the kiln system, that would reduce CO_2 emissions. The overall efficiency would be increased by approximately 3 to 4%.

4.4.7 CO_2 reduction methods in cement plants.

The following methods are also used to reduce CO_2 emissions from the cement plants:

- (i) **Use of Low carbon intensive fuels**
- (ii) **Use of Waste fuels**

- (iii) **Use of Renewable energy**
- (iv) **Use of Lower clinker to cement ratio and**
- (v) **Carbon capture and storage (CCS).**

(i) Use of Low carbon intensive fuels

It is found that lower carbon content fuels reduce CO₂ emissions from the kiln system compared to higher carbon content fuels. CO₂ emissions by fuel consumption are practically the same as the CO₂ emissions from limestone calcination. In the cement plants saving of 1 kcal reduces CO₂ emissions by about 0.325 gm (PCA, 2008).

(ii) Use of Waste fuels

Rotary kilns producing cement clinker can use waste materials as fuels. Greco et al., (2004) has found that cement kilns by and large encompass extremely elevated temperatures, high turbulence, continuously oxidizing conditions and lengthy residence times. The use of a flammable waste reduces the use of conventional fossil fuels and also the generation of CO₂ emissions. They also found that it is possible to replace more than 50% of the fuel requirements of a cement kiln with waste fuels. One of the significant sources of waste materials that can be used as fuel for cement kilns is used tires. Cement kilns totally consume used tires, with no residual waste produced.

(iii) Use of Renewable energy

In a thermal power plant using coal as fuel, power generation of one kWh results in the production of about 0.83 gm CO₂ (IPCC, 2007). CO₂ emissions due to electrical power consumption in a cement plant are dependent on the electrical power generation source and hence if

electrical power for the same is generated from other sources like hydro, wind or nuclear power, a cement plant would be contributing practically zero CO₂ emissions.

(iv) Use of Lower clinker to cement ratio

The method of reducing CO₂ emissions from the cement manufacturing industry by reducing the amount of clinker used when making finished cement is found to be better compared to the previously mentioned techniques. Blending of cement with additives to replace clinker have significant effects in the reduction of CO₂ emissions.

(v) Carbon capture and storage (CCS)

CO₂ capture and storage (CCS) is an emerging method for reducing CO₂ emissions in cement plants. There are a number of storage destinations such as saline aquifers, porous geologic formation, depleted oil and gas reservoirs and coal seams. In this method there are basically three strategies for CO₂ capture in cement plants. They are (i) Pre-combustion, (ii) Post-combustion, and (iii) Oxy-combustion

a) Precombustion

For new cement plants integrated with gasification technologies, pre-combustion CO₂ capture will be more applicable to produce Syngas (a mixture of H₂, CO, H₂O, and CO₂) from the main plant fuel. H₂ would be then fired in the cement kiln after capturing CO₂ from this Syngas. However CO₂ released by calcination of limestone will not be captured. In addition, a new generation of burner technology and cement kiln lines will be required.

b) Post-combustion

A commercially mature technology used in chemical industry for separation of CO₂ is the post combustion capture by amine scrubbing (e.g. using Monoethanolamine (MEA)). The CO₂ is stripped from ammine solution, dried, compressed and transported to storage site. Alie et al. (2005) found out that the main challenge lies in the scale up of this process and its implementation for scrubbing of CO₂ from flue gases that contain a number of contaminations potentially harmful to the operation of the scrubber unit.

Post-combustion CO₂ capture technologies exhibiting the following characteristics are extremely useful in the present cement industry: 1) technical compatibility with cement manufacturing operating conditions, 2) non-toxic, non-hazardous materials, 3) minimal impact on cement plant operations, and 4) affinity to operational experience of cement plants.

c) Oxy - firing

In this method, the combustion air is totally replaced with pure oxygen combined with recycled CO₂ rich flue gas to moderate the flame temperature. Due to high percentage of CO₂ in flue gases originating from the calcinations process, combustion in a CO₂ / O₂ atmosphere looks like one of the finest options for CO₂ reduction in the cement plant. If cement kiln could be successfully operated with a high CO₂ atmosphere and leakage could be greatly reduced, oxy-combustion of the kiln could be a reasonable option (Adia et al., 2009).

4.4.8 Exergy balance of the kiln system (Production rate of 1400 tonnes per day).

The process for which the exergy analysis performed is assumed to be the kiln system as an open system under the steady state working condition. The reference pressure and temperature for the dead state conditions are assumed to be 101 kPa and 298 K respectively. There are physical exergy in the process. The chemical reaction takes place in the preheater and rotary kiln.

The following assumptions are considered for the exergy analysis.

- a) The effect of the pressure on the input and output enthalpies are neglected.
- b) All gas steams are ideal gas mixtures.
- c) The process is at the steady-state conditions, that is no parameter changes with time.

Equations for the exergy analysis were given in the Annexure C. Table 4.5 and 4.6 shows the enthalpy and entropy balance in the kiln system. The exergy balance is shown in Fig 4.7. The detailed calculation of exergy of the input and output steams are shown in Annexure E. The exergy calculation for the clinker formation is given in Annexure D.

Table 4.5 Enthalpy balance for kiln system (Production rate of 1400 tonnes per day)

Sl no	Input	c_p (kJ/kgK)	Temp (K)	T_o (K)	Mass m_k (kg/kg clinker)	Enthalpy, ΔH_k (kJ/kg clinker)	Output	c_p (kJ/kgK)	Temp (K)	T_o (K)	Mass, m_k (kg/kg clinker)	Enthalpy ΔH_k (kJ/kg clinker)
1	Raw meal	0.7919	328	298	1.49	35.4	Preheater exhaust gas	1.0878	657	298	2.56	999.72
2	Primary air	0.9843	344	298	0.418	18.93	Dust	1.0093	657	298	0.0746	27.03
3	Cooler fan air and	0.9681	308	298	3.667	35.5	Clinker	0.8308	368	298	1	58.16
4	infiltrated air	0.9681	308	298	0.815	7.89	Cooler hot air	1.0226	473	298	2.82	504.65
5							Coal mill gas	1.0482	603	298	0.125	39.96

Table 4.6 Entropy balance for kiln system (Production rate of 1400 tones per day)

Sl no	Input	c_p (kJ/kgK)	Temp (K)	T_o (K)	Mass m_k (kg/kg clinker)	Entropy ΔS_k (kJ/kg clinker K)	Output	c_p (kJ/kg K)	Temp (K)	T_o (K)	Mass (m_k) kg/kg clinker	Entropy ΔS_k (kJ/kg clinker K)
1	Raw meal	0.7919	328	298	1.49	0.1132	Preheater exhaust gas	1.0878	657	298	2.56	2.2016
2	Primary air	0.9843	344	298	0.418	0.0591	Dust	1.0093	657	298	0.0746	0.0595
3	Cooler fan air and infiltrated air	0.9681	308	298	4.48161	0.1432	Clinker	0.8308	368	298	1	0.1753
4							Cooler exhaust gas	1.0226	473	298	2.828	1.3361
5							Coal mill gas	1.0482	603	298	0.125	0.0924

Table 4.7 Exergy balance for the kiln system (Production rate of 1400 tonnes per day)

Sl no	Input	Enthalpy, ΔH_k (kJ/kg clinker)	Temp, (K)	T_o (K)	Entropy, ΔS_k (kJ/kg clinker K)	Exergy, $(Ex)_k$ kJ/kg clinker	Output	Enthalpy, ΔH_k (kJ/kg clinker)	Temp, (K)	T_o K	Entropy, ΔS_k (kJ/kg clinker K)	Exergy, $(Ex)_k$ kJ/kg clinker
1	Raw meal	35.40	328	298	0.1132	1.67	Preheater exhaust gas	999.72	657	298	2.2016	343.65
2	Primary air	18.93	344	298	0.0591	1.33	Dust	27.03	657	298	0.0595	9.29
3	Cooler air	35.5	308	298	0.1172	0.58	Clinker	58.16	368	298	0.1753	5.92
4	Infiltrated air	7.89	308	298	0.026	0.13	Cooler hot air	504.65	473	298	1.3323	107.63
5	Coal					4089.92	Coal mill gas	39.96	603	298	0.0924	12.44
6							Chemical reaction					1152.53
7							Radiation & convection					148.06
8							Exergy lost due to irreversibility					2314.1
	Total					4093.63	Total					4093.63

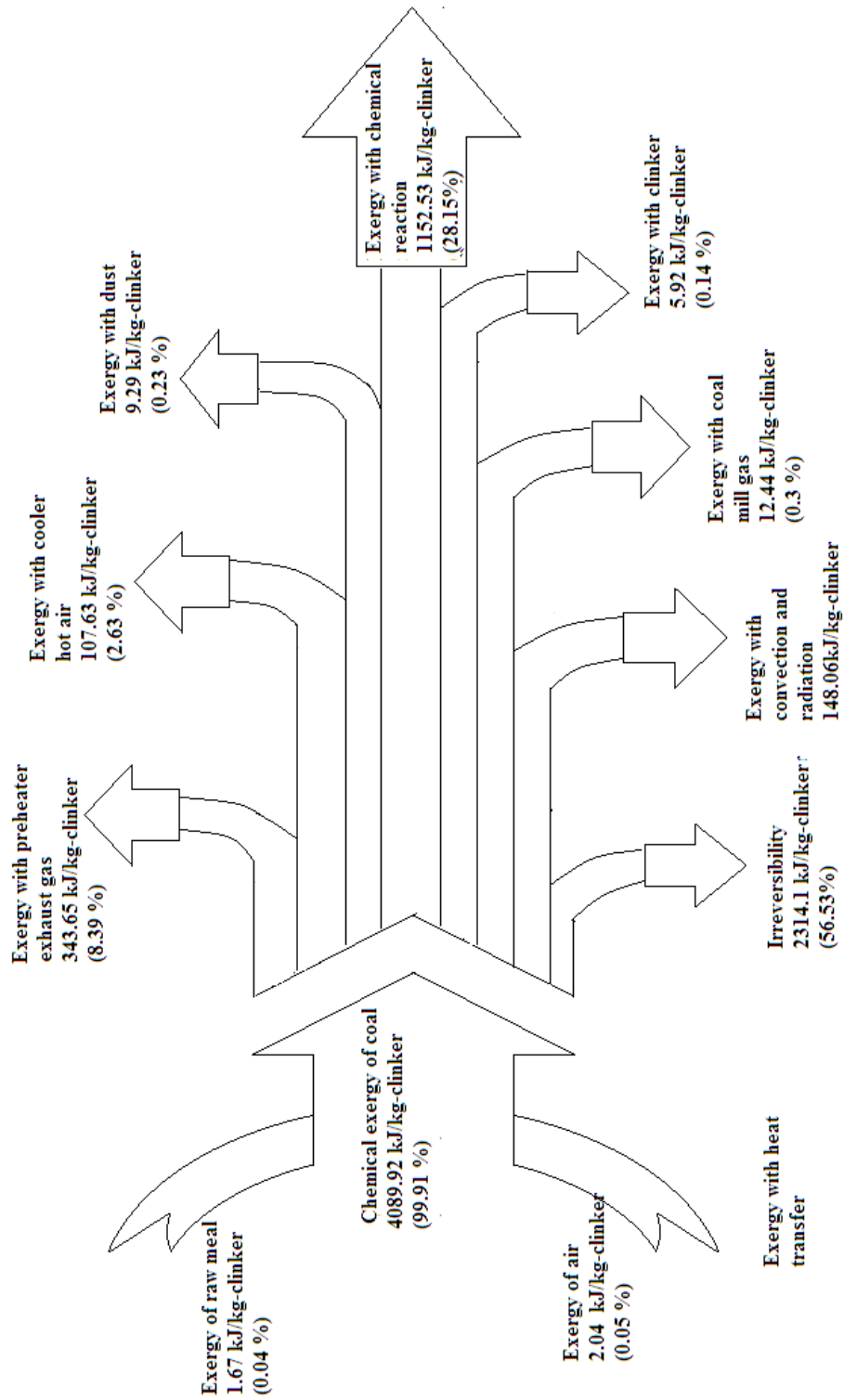


Fig.4.8 Exergy flow diagram (Sankey diagram) of the kiln system (Production rate of 1400 tonnes per day)

The exergy analysis results of the input and output components are shown in Table 4.7. It is clear from that the results exhibit good consistency between input and output exergy fluxes. The available exergy of the whole system was found to be 4093.63 kJ/kg-clinker. It is also interesting to observe from Table 4.7 that almost 99.91 % (4089.92 kJ/kg-clinker) of the input exergy is the chemical exergy of coal.

$$\begin{aligned} \text{Exergy efficiency} &= \frac{\text{Clinker formation exergy} + \text{Exergy carried by the clinker}}{\text{total input exergy}} \quad \text{----(4.7)} \\ &= 28.3 \% \end{aligned}$$

The allocation of input and output exergies of various components can be best represented by the Sankey diagram as shown in Fig. 4.8. This value represents 28.3% of the useful exergy with the remaining 71.7 % being exergy losses at the various stages of the system. The major loss is due to irreversibility in the system 56.53% (2314.1 kJ/kg-clinker). The kiln exhaust gas 343.65 kJ/kg-clinker (8.39 %) and clinker cooler hot gas 107.63 kJ/kg-clinker (2.63 %) are discharged to the surrounding. The exergy with heat losses are found to be 148.06 kJ/kg-clinker (3.62%). The coal mill gas and dust were found to be 12.44 kJ/kg-clinker (0.3%) and 9.29kJ/kg-clinker (0.23%) respectively.

4.4.9 Mass balance of the Kiln System (Production rate of 1369 tonnes per day)

In this case the clinker production rate in the kiln is estimated to be 15.84 kg of clinker/sec. For this operating condition the various input and out put components of the kiln system are estimated as follows.

Inputs

- (i) Present kiln feed (raw meal) = 23.6 kg/sec

$$\begin{aligned}\text{Raw meal per kg of clinker production, } (m_k)_{rm} &= \frac{23.6}{15.84} \\ &= 1.49 \text{ kg/kg-clinker}\end{aligned}$$

- (ii) Rate of coal consumption = 3.01 kg/sec

$$\begin{aligned}\text{Coal per kg of clinker, } (m_k)_c &= \frac{3.01}{15.84} \\ &= 0.19 \text{ kg/kg-clinker}\end{aligned}$$

- (iii) Primary air mass flow rate = 6.18 kg/sec

$$\begin{aligned}\text{Primary air per kg of clinker, } (m_k)_{pa} &= \frac{6.18}{15.84} \\ &= 0.43 \text{ kg/kg-clinker}\end{aligned}$$

- (iv) Cooler air mass flow rate, = 44.35 kg/sec

$$\begin{aligned}\text{Cooler air per kg of clinker, } (m_k)_{ca} &= \frac{44.35}{15.84} \\ &= 3.667 \text{ kg/kg-clinker}\end{aligned}$$

- (v) Infiltrated air mass flow rate = 13.99 kg/sec

$$\begin{aligned}\text{Infiltrated air per kg of clinker production, } (m_k)_{ia} &= \frac{13.99}{15.84} \\ &= 0.8835 \text{ kg/kg-clinker}\end{aligned}$$

Outputs

- (i) Preheater exhaust gas mass flow rate = 40.08kg/sec

Preheater exhaust gas per kg of clinker production,

$$(m_k)_{eg} = \frac{40.08}{15.84}$$

$$= 2.53 \text{ kg/kg-clinker}$$

- (ii) Mass flow rate of dust = 1.18 kg/sec

Dust per kg of clinker production, $(m_k)_d = \frac{1.18}{15.84}$

$$= 0.0745 \text{ kg/kg-clinker}$$

- (iii) Cooler hot air mass flow rate = 32.57 kg/sec

Cooler hot air per kg of clinker production, $(m_k)_{co} = \frac{32.57}{15.84}$

$$= 2.056 \text{ kg/kg-clinker}$$

- (iv) Mass flow rate of gas to coal mill = 2.11 kg/sec

Coal mill gas per kg of clinker production $(m_k)_{cm} = \frac{2.11}{15.84}$

$$= 0.133 \text{ kg/kg-clinker}$$

- (v) Clinker flow rate, $m_{cli} = 15.84 \text{ kg /sec}$

$$\text{Clinker discharge } (m_k)_{cli} = \frac{15.84}{15.84} = 1 \text{ unit}$$

The mass balance of the kiln system is summarized in Fig.4.9

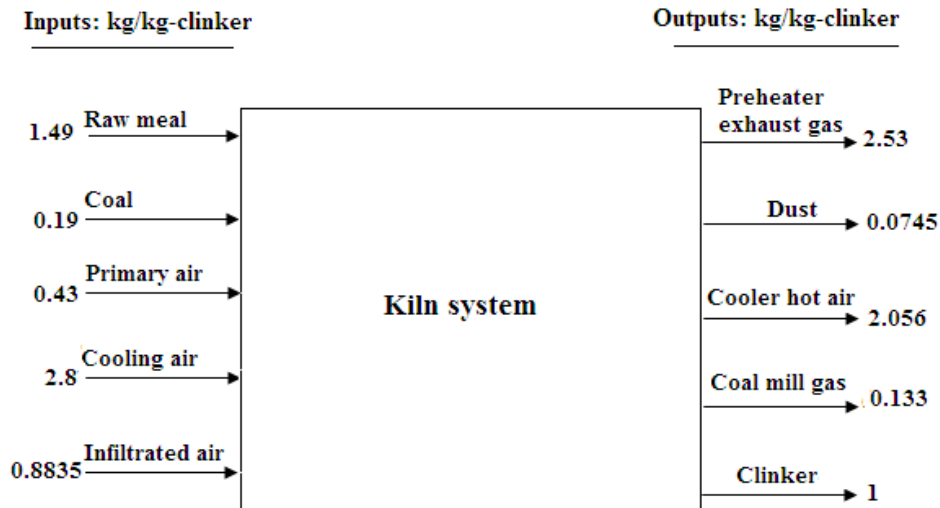


Fig. 4.9 Mass balance in the kiln system (Production rate 1369 tonnes per day)

4.4.10 Energy balance of the Kiln System (Production rate of 1369 tonnes per day)

The energy balance for the pyroprocessing unit for this the operating condition is presented in Table 4.8

Table 4.8 Energy balance for the kiln system (Production rate of 1369 tonnes per day)

Input energy				
Sl no.		Equation	Data	Heat, Q _k (kJ/kg-clinker)
1	Coal combustion	$(m_k)_c \times H_c$	$(m_k)_c = 0.19$ kg/kg-clinker, $H_c = 20763$ kJ/kg	3945
2	Coal sensible heat	$(m_k)_c \times c_{p_c} \times T_c$	$(m_k)_c = 0.19$ kg/kg-clinker, $c_{p_c} = 0.7347$ kJ/kg-K, $T_c = 53$ °C	7.4
3	Raw meal sensible heat	$(m_k)_{rm} \times c_{p_{rm}} \times T_{rm}$	$(m_k)_{rm} = 1.49$ kg/kg-clinker, $c_{p_{rm}} = 0.7919$ kJ/kg-K, $T_{rm} = 55$ °C	64.9
4	Primary air	$(m_k)_{pa} \times c_{p_{pa}} \times T_{pa}$	$(m_k)_{pa} = 0.43$ kg/kg-clinker, $c_{p_{pa}} = 0.9767$ kJ/kg-K, $T_{pa} = 53$ °C	22.26
5	Cooler air	$(m_k)_{ca} \times c_{p_{ca}} \times T_{ca}$	$(m_k)_{ca} = 2.8$ kg/kg-clinker, $c_{p_{ca}} = 0.9655$ kJ/kg-K, $T_{ca} = 30$ °C	81.1
6	Infiltrated air	$(m_k)_{ia} \times c_{p_{ia}} \times T_{ia}$	$(m_k)_{ia} = 0.8835$ kg/kg-clinker $c_{p_{ia}} = 0.9655$ kJ/kg-K, $T_{ia} = 30$ °C	25.59
Total				4146.25
Output energy				
1	Clinker formation	Calculation is shown in Annexure D	1 kg	1756.24
2	Preheater exhaust gas	$(m_k)_{eg} \times c_{p_{eg}} \times T_{eg}$	$(m_k)_{eg} = 2.53$ kg/kg-clinker, $c_{p_{eg}} = 1.0907$ kJ/kg-K, $T_{eg} = 395$ °C,	1090.03

3	Moisture in coal	$m_{H_2O} \times [h_{fg(71^\circ C)} + h_{(384^\circ C)} - h_{(71^\circ C)}]$	$m_{H_2O} = 0.0067$ kg/kg-clinker, $h_{fg(71^\circ C)} = 2375$ kJ/kg, $h_{(384^\circ C)} = 3269.5$ kJ/kg, $h_{(71^\circ C)} = 2597$ kJ/kg,	20.26
4	Hot air from cooler	$(m_k)_{co} \times c_{p_{co}} \times T_{co}$	$(m_k)_{co} = 2.056$ kg/kg-clinker, $c_{p_{co}} = 1.0271$ kJ/kg-K, $T_{co} = 220^\circ C$	464.58
5	Heat lost by dust	$(m_k)_d \times c_{p_d} \times T_d$	$(m_k)_d = 0.0745$ kg/kg-clinker, $c_{p_d} = 1.0148$ kJ/kg-K, $T_d = 395^\circ C$	29.86
6	Clinker discharge	$(m_k)_{cli} \times c_{p_{cli}} \times T_{cli}$	$(m_k)_{cli} = 1$ kg/kg-clinker, $T_{cli} = 150^\circ C$. $c_{p_{cli}} = 0.8739$ kJ/kg-K,	131.09
7	Coal mill gas	$(m_k)_{cm} \times c_{p_{cm}} \times T_{cm}$	$(m_k)_{cm} = 0.133$ kg/kg-clinker, $c_{p_{cm}} = 1.0499$ kJ/kg-K, $T_{cm} = 340^\circ C$,	47.48
8	Radiation from kiln surface	$\frac{\sigma \times \varepsilon \times A_{kiln} \times (T_s^4 - T_\infty^4)}{1000 \times m_{cli}}$	$\sigma = 5.67 \times 10^{-8}$ W/m ² K ⁴ , $A_{kiln} = 900$ m ² , $T_\infty = 303$ K, $T_s = 578$ K, $m_{cli} = 15.84$ kg-clinker/sec	259.2
9	Convection heat loss from kiln surface	$\frac{h_a \times A_{kiln} \times (T_s - T_\infty)}{1000 \times m_{cli}}$	$h_a = 4.276$ W/m ² K, $A_{kiln} = 900$ m ² , $T_s = 305^\circ C$, $T_\infty = 30^\circ C$, $m_{cli} = 15.84$ kg-clinker/sec $h_a = \frac{k_{air} \cdot Nu}{D_{kiln}}$, $Re = 408646$, $T_f = 176^\circ C$, ($V_{air} = 3$ m/sec), $Nu = 0.193(Re)^{0.618} (Pr)^{0.333}$ (Frank, 2001) $Pr = 0.681$, $D_{kiln} = 4.4$ m, $k_{air} = 0.0377$ W/mK	66.79

10	Radiation heat loss from the pre-heater surface	$\frac{\sigma \times \varepsilon \times A_{ph} \times (T_s^4 - T_\infty^4)}{1000 \times m_{cli}}$	$\sigma = 5.67 \times 10^{-8} \text{ W/m}^2\text{K}^4$, $\varepsilon = 0.78$ (oxidised surface), $A_{ph} = 250 \text{ m}^2$, $T_s = 355 \text{ K}$, $T_\infty = 303 \text{ K}$, $m_{cli} = 15.84 \text{ kg-clinker/sec}$	5.2
11	Natural convection from the pre-heater surface	$\frac{h_a \times A_{ph} \times (T_s - T_\infty)}{1000 \times m_{cli}}$	$h_a = 1.569 \text{ W/m}^2\text{C}$, $A_{ph} = 250 \text{ m}^2$, $T_s = 82 \text{ }^\circ\text{C}$, $T_\infty = 30 \text{ }^\circ\text{C}$, $m_{cli} = 15.84 \text{ kg-clinker/sec}$, $h_a = \frac{N_u L_{ph}}{k_{air}}$, $N_u = 0.1(G_r P_r)^{0.333}$, (Frank, 2001) $T_f = 57 \text{ }^\circ\text{C}$, $L_{ph} = 15 \text{ m}$ $G_r = 8.0645 \times 10^{11}$, $P_r = 0.697$, $k_{air} = 0.02878 \text{ W/mK}$	1.29
12	Radiation heat loss from the cooler surface	$\frac{\sigma \times \varepsilon \times A_{cs} \times (T_s^4 - T_\infty^4)}{1000 \times m_{cli}}$	$\sigma = 5.67 \times 10^{-8} \text{ W/m}^2\text{K}^4$, $\varepsilon = 0.78$, $A_{cs} = 81 \text{ m}^2$, $T_s = 358 \text{ K}$, $T_\infty = 303 \text{ K}$, $m_{cli} = 15.84 \text{ kg-clinker/sec}$	1.81
13	Natural convection from the cooler surface	$\frac{h_a \times A_{cs} \times (T_s - T_\infty)}{1000 \times m_{cli}}$	$h_a = 2.13 \text{ W/m}^2\text{K}$, $A_{cs} = 81 \text{ m}^2$, $T_s = 85 \text{ }^\circ\text{C}$, $T_\infty = 30 \text{ }^\circ\text{C}$, $m_{cli} = 15.84 \text{ kg-clinker/sec}$ $N_u = 0.1(G_r P_r)^{0.333}$, (Frank, 2001). $h_a = \frac{N_u L_c}{k_{air}}$, $T_f = 55 \text{ }^\circ\text{C}$, $G_r = 1.984 \times 10^{11}$, $P_r = 0.696$, $k_{air} = 0.02887 \text{ W/mK}$, $L_c = 7 \text{ m}$	0.6
Total				3874.42
Unaccounted heat loss				271.83
Total				4146.25

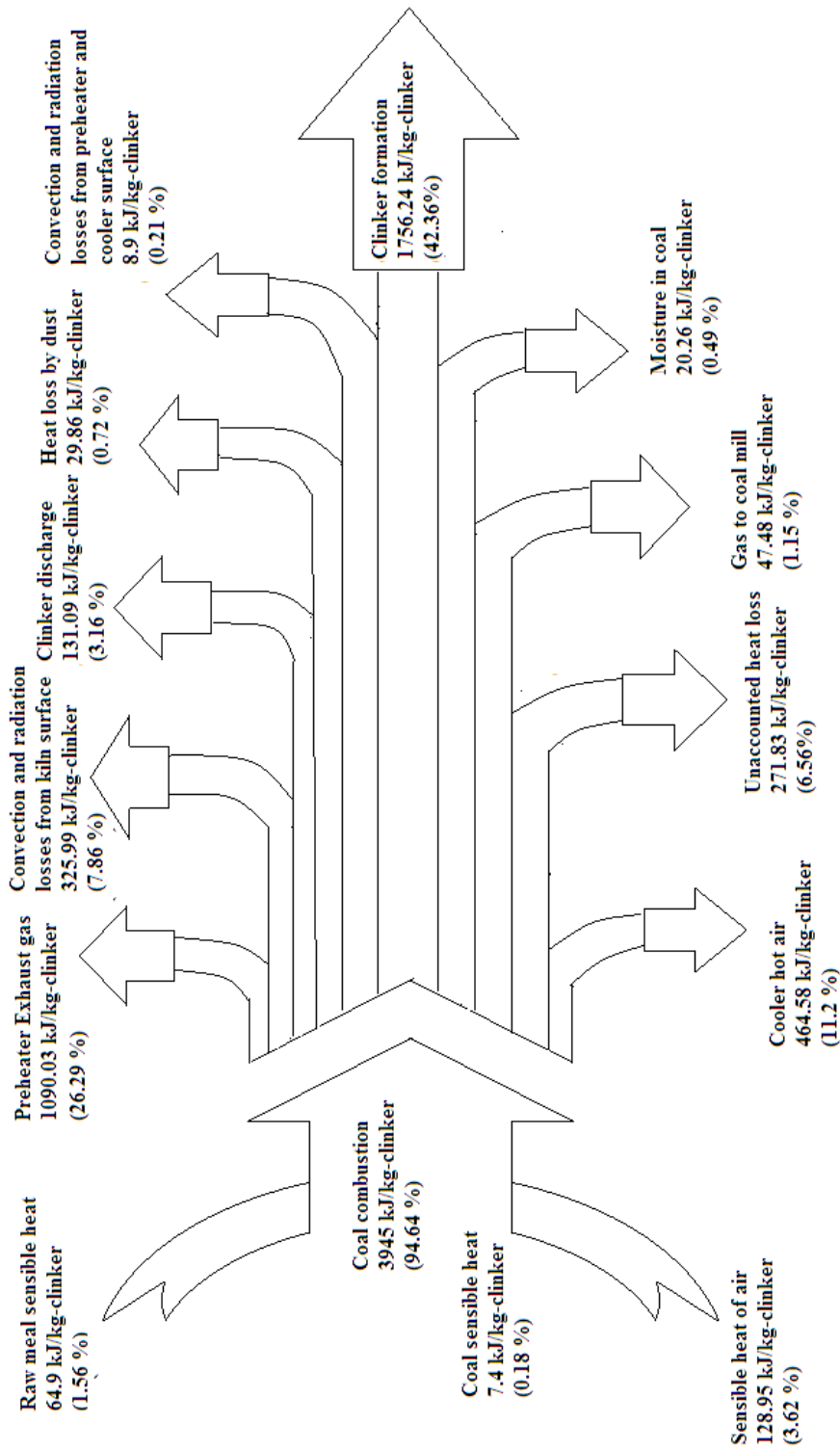


Fig.4.10 Energy flow diagram of the kiln system (Production rate of 1369 tonnes per day)

Fig.4.10 shows the Sankey diagram demonstrating magnitudes and percentages of energy flows and losses. The results shows that fuel combustion generate heat of 3945 kJ/kg-clinker (95.14%). The total sensible heats of raw meal, coal and air at the input are found to be 137.85 kJ/kg-clinker (4.86%). The first law efficiency of the system is found to be 42.36%. The major energy losses such as kiln exhaust gas, clinker cooler hot gas and radiation and convection of kin system were estimated to be 1090.03 kJ/kg-clinker (26.29%), 464.58 kJ/kg-clinker (11.2%) and 334.91 kJ/kg-clinker (8.1%) respectively. The heat energy carried by the coal mill gas was found to be 47.48 kJ/kg-clinker (1.15%). The other heat losses are clinker discharge 131.09 kJ/kg-clinker (3.16%), dust 29.89 kJ/kg-clinker (0.72%) and moisture in coal 20.26 kJ/kg-clinker (0.49%). The unaccounted heat loss was found to be 271.83 kJ/kg-clinker (6.56%). The total emissions of CO₂ due to combustion of coal and decarbonation reactions for a clinker production rate of 1369 tonnes per day is estimated to be 1218 tonnes per day.

4.4.11 Exergy balance of the kiln system (Production rate of 1369 tonnes per day)

The input and output enthalpy and entropy for this operating condition are shown in the Table 4.9 and Table 4.10 respectively. The exergy of the various streams of the clinker production process are shown in the Table 4.11.

Table 4.9 Enthalpy balance for kiln system (Production rate of 1369 tonnes per day)

Sl no	Input	c_p (kJ/kg K)	Tem p, (K)	T_o (K)	Mass, m_k (kg/kg clinker)	Enthalpy, ΔH_k (kJ/kg clinker)	Output	c_p (kJ/kg K)	Temp, (K)	T_o (K)	Mass, m_k (kg/kg clinker)	Enthalpy ΔH_k (kJ/kg clinker)
1	Raw meal	0.7919	328	298	1.49	35.4	Preheater exhaust gas	1.0907	668	298	2.53	1021.04
2	Primary air	0.9767	326	298	0.43	11.76	dust	1.0148	668	298	0.0745	27.97
3	Cooler air	0.9655	303	298	2.8	13.52	clinker	0.8739	423	298	1	109.24
4	Infiltrated air	0.9655	303	298	0.8835	4.27	Cooler hot air	1.0271	493	298	2.056	411.78
5							Coal mill gas	1.0499	613	298	0.133	43.99

Table 4.10 Entropy balance for kiln system (Production rate of 1369 tonnes per day)

Sl no	Input	c_p (kJ/kgK)	Tem P, (K)	T_o (K)	Mass, m_k (kg/kg clinker)	Entropy ΔS_k (kJ/kg clinker K)	Output	c_p (kJ/kgK)	Temp (K)	T_o (K)	Mass, (m_k) kg/kg clinker	Entropy, ΔS_k (kJ/kg clinker K)
1	Raw meal	0.7919	328	298	1.49	0.1132	Preheater exhaust gas	1.091	668	298	2.53	2.2275
2	Primary air	0.9767	326	298	0.43	0.0377	dust	1.015	668	298	0.0745	0.061
3	Cooler air	0.9655	303	298	2.8	0.045	clinker	0.8739	423	298	1	0.3061
4	Infiltrated air	0.9655	303	298	0.8835	0.0142	Cooler hot air	1.027	493	298	2.056	1.0631
5							Coal mill gas	1.0499	613	298	0.133	0.1007

Table 4.11 Exergy balance for kiln system (Production rate of 1369 tonnes per day)

Sl no	Input	Enthalpy ΔH_k (kJ/kg clinker)	Temp (K)	T_o (K)	Entropy ΔS_k (kJ/kg clinker K)	Exergy $(Ex)_k$ kJ/kg clinker	Output	Enthalpy ΔH_k (kJ/kg clinker)	Temp (K)	T_o (K)	Entropy ΔS_k (kJ/kg clinker K)	Exergy $(Ex)_k$ kJ/kg clinker
1	Raw meal	35.40	328	298	0.1132	1.67	Preheater exhaust gas	1021.04	668	298	2.2275	357.24
2	Primary air	11.76	326	298	0.0377	0.52	Dust	27.97	668	298	0.0610	9.79
3	Cooler air	13.52	303	298	0.045	0.11	Clinker	109.24	423	298	0.3061	18.02
4	Infiltrated air	4.27	303	298	0.0142	0.04	Cooler hot air	411.78	493	298	1.0631	94.99
5	Coal					4089.92	Coal mill gas	43.99	613	298	0.1007	13.97
6							Radiation & convection					159.37
7							Chemical reaction					1236.04
8							Exergy lost due to irreversibility					2202.84
	Total					4092.26	Total					4092.26

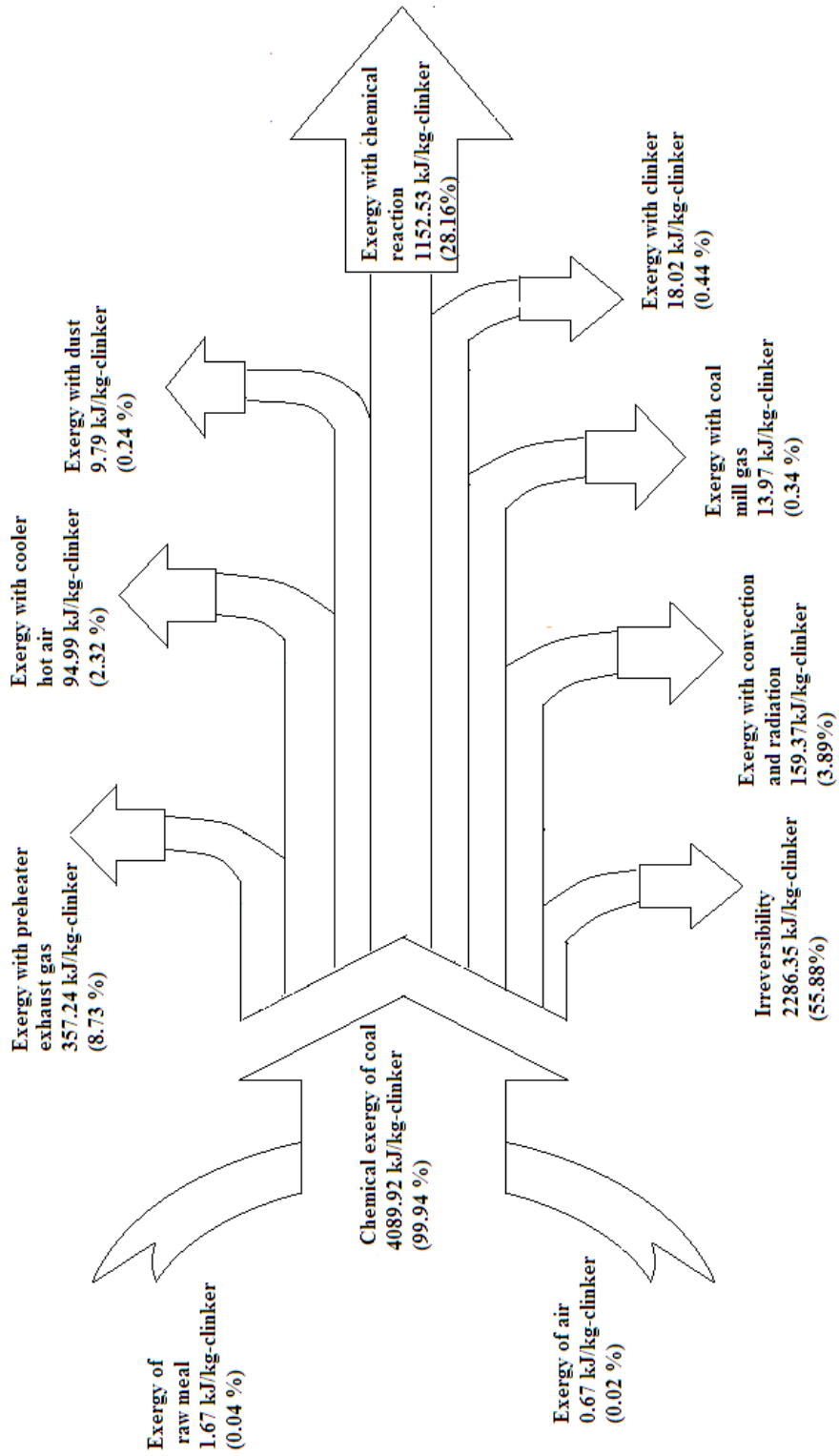


Fig.4.11 Exergy flow diagram of the kiln system (Production rate of 1369 tonnes per day)

Fig. 4.11 shows the Sankey diagram of input and output exergy of various components of the kiln system. The exergy efficiency for this operating condition was found to be 28.6%. The contribution of the major input exergy is coal and it is found to be 4089.92 (99.94%) and the remaining contains exergy of raw meal 1.67 kJ/kg-clinker (0.04%) and air 0.67 kJ/kg-clinker (0.02%). The irreversibility in the system was found to be 2286.35 kJ/kg-clinker (55.88%). The kiln exhaust gas with 357.24kJ/kg clinker (8.73%) and clinker cooler hot gas 94.99 kJ/kg-clinker (2.32%) are released to the surrounding. The exergy associated to radiation and convection heat losses are found to be 159.37 kJ/kg-clinker (3.89%). The exergy of coal mill gas and dust are found to be 13.97kJ/kg-clinker (0.35%) and 9.79 kJ/kg-clinker (0.24%) respectively.

4.5 Conclusion

Energy analysis is a powerful tool, which has been effectively used in the design and performance evaluation of energy related systems. The energy efficiency value for the kiln system for first operating condition (Production rate of 1400 tonnes per day) was found to be 41.8%. The major heat losses for the system were identified as the preheater exhaust gas and hot air discharged from the cooler. The preheater exhaust gas carries about 1069.34 kJ/kg-clinker and that of the cooler hot gas is 576.75 kJ/kg-clinker, which indicate that the total energy recovery potential from these waste gases is of the order of 39.18%. The selected retrofit steam cycle showed an energy saving potential of 7 MW from the waste heat streams. The CO₂ emission due to the combustion of coal and decarbonation reaction of raw meal in the first operating condition was found to be 1246 tonnes per day.

The heat loss by convection and radiation together from the kiln surface is about 305.96 kJ/kg-clinker (7.28%) and that for the pre-heater and clinker cooler of the system is estimated to be 7.81 kJ/kg-clinker (0.19%). For the kiln system, a secondary shell system has been proposed and designed. This system would lead to saving 6.9% of the input energy; hence the overall efficiency would be increased by approximately 3 to 4%. As for the exergy, it was determined that the exergy efficiency of the existing system is 28.3% and the irreversibility is 56.53%. Therefore it is seen that exergy analysis accounts for the operation, indicating the locations of energy degradation in the process. The main cause of irreversibility in the process is due to conversion of chemical energy of the fuel to thermal energy.

For the second operating condition (Production rate of 1369 tonnes per day) first law and second law efficiencies of the kiln system were found to be 42.36% and 28.6% respectively. The irreversibility of the system was found to be 2286.35 kJ/kg-clinker (55.87%). The values are very close to the previous operating condition. The energy loss by the preheater exhaust gas and cooler exhaust were found to be 1090.03 kJ/kg-clinker (26.29%) and 464.58kJ/kg-clinker (11.2%) respectively. As a result the total energy recovery potential from these waste gases in this operating condition was estimated to be 37.49%. Here results obtained for the energy and exergy analyses of the kiln system were almost close to the first operating condition (Production rate of 1400 tonnes per day). Therefore the average values of the energy and exergy efficiencies of the kiln system were found to be 42.08% and 28.45% respectively.

.....*OR*.....

DECOMPOSITION ANALYSIS OF CO₂ EMISSIONS CHANGES IN THE INDIAN CEMENT INDUSTRIES

Contents	5.1	<i>Introduction</i>
	5.2	<i>Decomposition Analysis</i>
	5.3	<i>Methodology</i>
	5.4	<i>Data Integration and Classification</i>
	5.5	<i>Complete Decomposition Approach</i>
	5.6	<i>Carbon dioxide emissions from the cement production process</i>
	5.7	<i>Carbon dioxide emissions from calcination (process emissions)</i>
	5.8	<i>Carbon dioxide emissions from fuel use</i>
	5.9	<i>Calculation of CO₂ emissions</i>
	5.10	<i>Results and discussion</i>
	5.11	<i>Conclusion</i>

5.1 Introduction

The growing environmental degradation observed at the local, national and global level has shifted the concern of energy analysts and policy makers towards the environmental side-effects of energy use (Torvanger, 1991). It is recognized that reducing energy use is not enough to ensure economic and social welfare. Thus, the qualitative dimension of energy use has become increasingly important. A source of major environmental concern is the global warming effect and the new question raised is how to disentangle economic growth and energy consumption from greenhouse gases emissions. As a response to the new policy needs, decomposition analysis has been extended in order to identify the factors

influencing changes in greenhouse gases emissions and in particular in carbon dioxide which is the major contributor to the greenhouse effect. India emits more than 5% of global CO₂ emissions, and emissions continue to grow. CO₂ emissions have almost tripled between 1990 and 2009. However India has the lowest CO₂ emissions per capita (1.4 tonnes of CO₂ in 2009), about one third that of the world average (IEA, 2011). The cement industry in India have dominant role in CO₂ emissions. It is the second largest emitter of CO₂ emissions (128 MT) in 2007 after iron and steel Industry (151MT) (IEA, 2011).

The objective of this study is to identify the factors influencing carbon dioxide (major contributor to greenhouse effect) emission from Indian cement industries. A total of thirteen cement industries have been selected for the study during 2001-2010. The total cement production in the selected industries increased from 55.23 MT in 2001 to 127.4 MT in 2010. It was found that due to the increases in cement production, the energy consumption of the above industries also increased significantly during the period. So the CO₂ emissions increased from 50.83 MT to 107.8 MT. The Fig 5.1 shows the total cement production and CO₂ emissions from selected cement industries in India. Following the complete decomposition model, the present study attempts to determine the contribution of the factors which influences energy related carbon dioxide emission. For analysis, the selected cement industries classified into three groups such as A, B and C according to their specific thermal energy consumption.

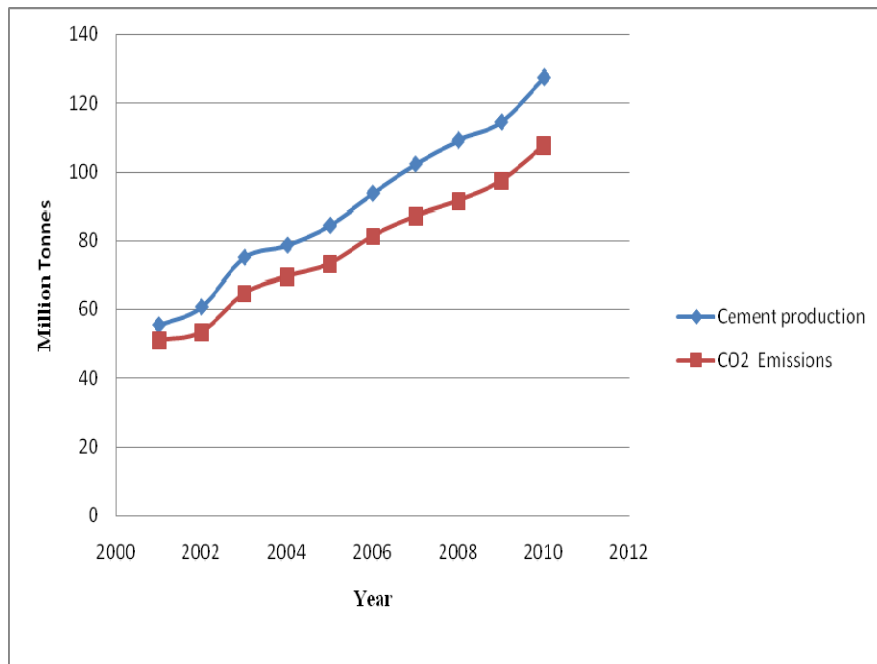


Fig 5.1 Cement production and CO₂ emissions from the selected cement industries in India

5.2 Decomposition Analysis

Decomposition analysis has been applied basically to the industrial sector which was the main driving force of economic growth and one of the major energy demand sectors. It is generally carried out on the change in energy consumption or in energy intensity over time. It is expressed in either additive form or multiplicative form. The decomposition methodologies can be extended to energy induced emissions of CO₂ and other gases.

Decomposition approaches can be broadly classified into two categories:

- a) Structural Decomposition Analysis based on input-output analysis which is capable of identifying the impact of technological changes and structural shifts in the macro-economic context on the level of energy consumption (Park, 1982; Gowdy and Miller,

1987). Despite their simplifying assumptions, input-output based techniques have a sound theoretical background and provide a thorough insight into the relationships connecting energy use and macroeconomic variables. Their main drawback is that they do not allow cross national comparisons since input-output tables of different countries are hardly comparable to each other.

- b) Index Decomposition Analysis based either on simple algebraic methods, such as those proposed by Hankinson and Rhys (1983), Sun (1998) and by Park (1992; 1993), or on indices, such as the Divisia approach (Boyd et al., 1988; Li et al., 1990) or the Laspeyres approach (Howarth et al., 1991). Although much less sophisticated than the input-output based techniques and failing to examine important macroeconomic parameters, Index Decomposition Analysis methods achieved to identify the most crucial factors that may have influenced changes in energy consumption. Furthermore, due to their simplicity, data collection and computational effort do not set any serious problems, while they enable comparisons across nations

5.3 Methodology

Divisia approach presented in many studies is known as the conventional Divisia index method (Ang, 1996). A problem associated with the conventional Divisia index decomposition technique is the existence of a residual in the results. The residual either underestimate or overestimate results and causes an estimation error. Sun (1998, 1999) used a complete decomposition method where the role of residual suppressed. The residual in the complete decomposition model is allocated by the jointly created and equally distributed rule. In the process, it refines the reliability and

accuracy of a conventional Divisia index model (Sun, 1998). In this study a complete decomposition method was used to decompose energy induced emissions of CO₂ in the selected cement industries in India. The author consider the different influencing factors for CO₂ emissions change due to the variation in the pollution effect, energy intensity, structural effect and production or activity effect as the major components.

- (a) **Pollution coefficient effect:** It is defined by the ratio of carbon dioxide emission and energy use. It evaluates fuel quality, fuel switching (fuel substitution) and the installation of abatement technologies
- (b) **Energy Intensity effect:** It is defined by the ratio of energy consumption and output. The energy intensity related to some variables energy conservation and energy-saving. The origin of disparities in energy intensity is the structure and the efficiency of the energy systems, technological choices and socio-economic behaviour.
- (c) **Structural effect:** It is measured by output of a specific group of industries and the total output. It is the measure of relative position of a particular group of industries in that sector.
- (d) **Production or activity effect:** It is measured as the output of the sector. In this analysis we are taking this as the sum of output (cement production) of the total industries being considered. It is regarded as the theoretical CO₂ emissions caused by production.

5.4 Data Integration and Classification

The data on cement production, clinker production, and fuel usage and electricity consumption are collected from the selected cement industries in India for the period 2001-2010. The cement industries

according to the average thermal energy consumption during the period has been classified into three groups ie group A (thermal energy consumption is more than 750 kcal/kg of clinker), group B (average thermal energy consumption in between 700 to 750 kcal/kg of clinker) and group C (average thermal energy consumption is less than 700 kcal/kg of clinker) as shown in the Table 5.1. Tables 5.2 to 5.5 give the details of the data collection from the selected cement industries in India.

Table 5.1 Classification of industries according to specific thermal energy consumption

Group	Average Thermal Energy Consumption kcal/kg of clinker	Company
A	More than 750	ACC Limited
		Indian Cement Limited
		Ultra Tech Cement Limited
		Malabar Cements Ltd
B	Between 700 and 750	Gujarat Ambuja Cements Ltd
		Grasim Industries Limited
		Shree Cements Limited
		J K Cement Limited
		J K Lekshmi Cement Limited
		Chettinad Cement Corporation
C	Less than 700	Prism Cement Limited
		Madras Cements Limited
		Birla Corporation Limited

Table 5.2 Cement production from the selected cement industries in India

Year	Cement Production (Million tonnes)									
	2001	2002	2003	2004	2005	2006	2007	2008	2009	2001
Gujarat Ambuja Cements Ltd	6.09	7.2	9.84	10.37	12.8	16.3	16.86	17.8	18.83	20.1
ACC Limited	10.21	11.5	13.42	14.65	16.61	18.7	19.9	20.8	21.4	21.38
Grasim Industries Limited	9.1	9.53	11.09	11.85	12.44	13.83	14.42	15.36	16.32	19.38
The Indian Cements Limited	4.84	4.24	8.45	8.48	5.49	7.26	8.42	9.23	9.11	10.43
Prism Cement Limited	1.52	1.83	1.92	2	2.11	2.16	2.69	3.06	2.22	2.56
Madras Cements Limited	2.65	3.18	3.52	3.7	3.8	4.71	5.67	5.85	6.53	8.03
Birla Corporation Limited	2.75	3.85	4.52	4.63	4.8	5.12	5.26	5.28	5.29	5.7
Shree Cements Limited	2.72	2.83	2.96	2.98	3.01	3.22	4.8	6.34	7.77	9.37
J K Cement Limited	2.81	2.96	3.32	3.42	3.51	3.64	3.76	3.77	3.79	4.28
J K Lekshmi Cement Limited	1.96	2.3	2.5	2.75	2.78	2.9	3.12	3.65	4.02	4.57
Chettinad Cement Corporation	0.77	0.93	1.68	1.91	2.21	2.36	2.68	2.905	3.14	4
Ultra Tech Cement Limited	9.82	10.25	11.73	11.79	12.11	13.33	14.64	15.07	15.87	17.64
Malabar Cements Limited	0.43	0.039	0.41	0.46	0.45	0.5	0.46	0.44	0.51	0.41

Table 5.3 Clinker production from the selected cement industries in India

Clinker Production (Million tonnes)										
Year	2001	2002	2003	2004	2005	2006	2007	2008	2009	2010
Gujarat Ambuja Cements Ltd	5.38	6.02	8.58	8.86	10.75	11.7	11.6	11.5	11.4	14.1
ACC Limited	5.1	5.3	8.7	9.4	10.5	10.7	10.9	10.8	11.4	12.3
Grasim Industries Limited	0.18	0.2	0.21	0.15	2.93	1.46	2.5	2.13	2.31	2.29
The Indian Cements Limited	4.84	4.24	4.2	4.93	5.351	5.87	6.73	7.21	6.98	8.68
Prism Cement Limited	0.85	0.92	1.29	1.43	1.59	1.62	1.68	1.72	1.74	1.8
Madras Cements Limited	3.23	3.31	3.32	3.56	3.87	3.95	4.05	4.35	4.94	6.12
Birla Corporation Limited	2.79	2.87	3.24	3.75	3.89	4.43	4.74	4.86	5.24	5.43
Shree Cements Limited	1.98	2.25	2.39	2.45	2.48	2.77	3.51	4.62	6.42	8.05
J K Cement Limited	2.7	2.96	3.53	3.87	4.23	4.65	4.78	5.34	5.78	5.96
J K Lekshmi Cement Limited	3.54	3.78	4.21	4.65	4.89	5.57	5.65	5.89	6.12	6.23
Chettinad Cement Corporation	2.89	3.38	4.45	4.69	4.75	4.89	5.23	5.31	5.46	5.87
Ultra Tech Cement Limited	10.2	10.45	11.3	12.12	12.36	12.42	13.7	14.65	15.07	15.55
Malabar Cements Limited	0.36	0.37	0.31	0.44	0.42	0.48	0.42	0.41	0.43	0.36

Table 5.4 Specific thermal energy consumption of the selected cement industries in India

Year	Specific thermal energy consumption (kcal/kg of clinker)									
	2001	2002	2003	2004	2005	2006	2007	2008	2009	2010
Gujarat Ambuja Cements Limited	730	742	729	728	715	730	742	754	755	750
ACC Limited	750	762	785	775	753	750	746.3	741.78	731.92	731
Grasim Industries Limited	705	702	694	692	689	691	756	765	7656	755
The Indian Cements Limited	753	759	760	763	773	768	753	764	772	767
Prism Cement Limited	703	693	685	680	675	670	660	655	650	642
Madras Cements Limited	700	695	690	687	685	685	521.2	611	695	776
Birla Corporation Limited	720	712	702	696	699	679	675	659	652	650
Shree Cements Limited	739	736	729	721	715	738	710	705	729	720
J K Cement Limited	735	742	720	726	710	705	695	716	712	703
J K Lekshmi Cement Limited	743	744	738	736	734	733	768	746	739	720
Chettinad Cement Corporation	730	726	720	715	702	695	690	685	687	680
Ultra Tech Cement Limited	798	809	813	820	819	765	720	725	716	709
Malabar Cements Limited	980	956	969	934	938	925	913	944	961	962

Table 5.5 Specific power consumption of the selected cement industries in India

Year	Specific Power Consumption(kWh/Tonne)									
	2001	2002	2003	2004	2005	2006	2007	2008	2009	2010
Gujarat Ambuja Cements Limited	86.2	86.3	86.2	86.1	84.4	86.6	84.6	86.3	86.4	85.9
ACC Limited	99	97	93	89	85	86.32	86	85.94	79.65	78.23
Grasim Industries Limited	83	82.51	75.47	71.17	69.87	67.04	70.03	76.32	85.94	79.65
The Indian Cements Limited	84	83.52	77.89	76.43	79.82	81.32	84.36	89.87	91.13	93.16
Prism Cement Limited	86.5	87.2	85.6	84.8	79.9	76.6	70.06	68	66	65.23
Madras Cements Limited	66.14	64.16	62.44	60.19	60.1	59.92	73.44	77.6	78.97	83.19
Birla Corporation Limited	87.23	86.32	82.23	86.23	88.16	85.9	86.3	84.2	82.13	81
Shree Cements Limited	78.25	77.32	74.18	76.32	75.17	73.5	73.9	79.4	76.7	75.3
J K Cement Limited	78.34	78.23	77.93	76.89	76.12	75.56	75.44	74.98	74.49	74.34
J K Lekshmi Cement Limited	88.29	86.51	85.8	85.2	83.28	82.09	82.91	79.31	78.32	76.42
Chettinad Cement Corporation	77.96	76.85	75.23	73.15	72.62	68.57	66.34	65.31	64.89	63.87
Ultra Tech Cement Limited	87.9	86.78	85.8	84.6	83.76	84.8	86.12	85.73	85.11	83.13
Malabar Cements Limited	118.6	113.4	107.5	99.1	98.1	90	88	89.2	87.6	89.7

5.5 Complete Decomposition Approach

The complete decomposition technique modifies the reliability and accuracy of a general decomposition model. The basic innovation of a complete decomposition technique is to decompose the residual according to the principle of jointly created and equally distributed factors which influence the estimated variables. The complete decomposition technique may be derived as follows.

Let a variable V be dependent on two factors X and Y such that $V = XY$. In a time period $[0,t]$, the change in V is

$$\begin{aligned}\Delta V &= V_t - V_0 \\ &= X_t Y_t - X_0 Y_0 \\ &= (X_t - X_0) Y_0 + (Y_t - Y_0) X_0 + (X_t - X_0)(Y_t - Y_0) \\ &= Y_0 \Delta X + X_0 \Delta Y + \Delta X \Delta Y\end{aligned}$$

Here the change in variable V is split into three parts. $Y_0 \Delta X$ denotes the contribution of change in X to the change in V , $X_0 \Delta Y$ is the contribution of change in Y to change in V ; and $\Delta X \Delta Y$ is the residual in general decomposition model. The residual depends on both the variables. In the complete decomposition model used here the residual is distributed between the independent variables by an equal weight. Thus

$$X_{\text{effect}} = Y_0 \Delta X + (\frac{1}{2}) \Delta X \Delta Y$$

$$Y_{\text{effect}} = X_0 \Delta Y + (\frac{1}{2}) \Delta X \Delta Y$$

$$\text{Therefore } \Delta V = X_{\text{effect}} + Y_{\text{effect}}$$

For a three factor model, $V = XYZ$ and contribution of the factors to the total change of variable P are as follows

$$X_{\text{effect}} = Y_0 Z_0 \Delta X + (1/2) \Delta X (Z_0 \Delta Y + Y_0 \Delta Z) + (1/3) \Delta X \Delta Y \Delta Z$$

$$Y_{\text{effect}} = X_0 Z_0 \Delta Y + (1/2) \Delta Y (Z_0 \Delta X + X_0 \Delta Z) + (1/3) \Delta X \Delta Y \Delta Z$$

$$Z_{\text{effect}} = X_0 Y_0 \Delta Z + (1/2) \Delta Z (Y_0 \Delta X + X_0 \Delta Y) + (1/3) \Delta X \Delta Y \Delta Z$$

$$\text{Therefore } \Delta V = X_{\text{effect}} + Y_{\text{effect}} + Z_{\text{effect}}$$

In general V can be situated in n -dimensional space, i.e., $V = X_1 X_2 X_3 \dots X_n$.

$\Delta V = n$ terms with order $\Delta (\Delta X_i, i=1, 2, 3, \dots, n) + \frac{n(n-1)}{2!}$ terms with two orders of $\Delta (\Delta X_i \Delta X_j, i \neq j) + \frac{n(n-1)(n-2)}{3!}$ terms with three orders of $\Delta (\Delta X_i \Delta X_j \Delta X_r, i \neq j \neq r) + \dots + \text{One term } \frac{n(n-1)(n-2) \dots 2 \times 1}{n!}$ with n order of $\Delta (\Delta X_i \Delta X_j \Delta X_r \dots \Delta X_{n-1} \Delta X_n)$.

The first n terms are the effect of each of the n factors; the other terms are interactions relative to some factors. According to the principle of 'jointly created and equally distributed', these effects of interactions have to be separated into each relative factors.

Following Sun (1999), CO_2 emissions (C) can be evaluated as the product of the pollution coefficient effect (P), energy intensity (I), structural effect (S) and activity effect (production) (A). The yearly CO_2 emissions from cement industries due to energy use can be written in the following identity form:

$$C_t = \sum_{i=1}^n \frac{C_{it}}{W_{it}} \times \frac{W_{it}}{A_{it}} \times \frac{A_{it}}{A_t} \times A_t = \sum_{i=1}^n P_{it} \times I_{it} \times S_{it} \times A_t \quad \text{-----(5.1)}$$

where n is the number of industries in the particular group; C_{it} the CO₂ emissions of particular group industry at time t; W_{it} the energy consumption of the group at time t; A_{it} is the output of the group industry at time t and A_t sum of production of all groups. P_{it}, I_{it}, S_{it}, A_t are the pollution coefficient effect, energy intensity effect, structural and activity effect of CO₂ emissions of the particular group at time t.

The change in CO₂ emission (ΔC) in a given period [0-t] is the sum of pollution coefficient effect (P_{effect}), the energy intensity effect (I_{effect}), the structural effect (S_{effect}), and the activity effect (A_{effect}) as shown in Eq. (5.2)

$$\Delta C = P_{effect} + I_{effect} + S_{effect} + A_{effect} \quad \text{-----(5.2)}$$

The calculation of each component for decomposing the change in CO₂ emissions in the above equation is as follows:

The pollution coefficient effect:

$$P_{effect} = \sum_{i=1}^n \Delta P_i I_{i0} S_{i0} A_{i0} + \left(\frac{1}{2}\right) \sum_{i=1}^n \{(\Delta P_i)\{(\Delta I_i) S_{i0} A_{i0} + I_{i0} (\Delta S_i) A_{i0} + I_{i0} S_{i0} \Delta A\} \\ + \left(\frac{1}{3}\right) \sum_{i=1}^n (\Delta P_i)\{(\Delta I_i)(\Delta S_i) A_{i0} + I_{i0} (\Delta S_i) \Delta A + (\Delta I_i) S_{i0} \Delta A\} \\ + \left(\frac{1}{4}\right) \sum_{i=1}^n (\Delta P_i)(\Delta I_i)(\Delta S_i) \Delta A.$$

The energy intensity effect:

$$\begin{aligned}
I_{effect} = & \sum_{i=1}^n P_{i0}(\Delta I_{i0})S_{i0}A_0 + (1/2) \sum_{i=1}^n (\Delta I_i)\{\Delta P_i S_{i0}A_0 + P_{i0}\Delta S_i A_0 + P_{i0}S_{i0}\Delta A\} \\
& + (1/3) \sum_{i=1}^n (\Delta I_i)\{(\Delta P_i)(\Delta S_i)A_0 + P_{i0}(\Delta S_i)\Delta A + (\Delta E_i)S_{i0}\Delta A\} \\
& + (1/4) \sum_{i=1}^n (\Delta P_i)(\Delta I_i)(\Delta S_i) \Delta A.
\end{aligned}$$

The Structural effect:

$$\begin{aligned}
S_{effect} = & \sum_{i=1}^n P_{i0}I_{i0}(\Delta S_{i0})A_0 \\
& + (1/2) \sum_{i=1}^n (\Delta S_i)\{(\Delta P_i)I_{i0}A_0 + P_{i0}(\Delta I_i)A_0 + P_{i0}I_{i0}\Delta A\} \\
& + (1/3) \sum_{i=1}^n (\Delta S_i)\{(\Delta P_i)(\Delta I_i)A_0 + P_{i0}(\Delta I_i)\Delta A + (\Delta P_i)I_{i0}\Delta A\} \\
& + (1/4) \sum_{i=1}^n (\Delta P_i)(\Delta I_i)(\Delta S_i) \Delta A.
\end{aligned}$$

The production or activity effect:

$$\begin{aligned}
A_{effect} = & \sum_{i=1}^n P_{i0}I_{i0}S_{i0}\Delta A_0 \\
& + (1/2) \sum_{i=1}^n (\Delta A)\{(\Delta P_i)I_{i0}S_{i0} + P_{i0}(\Delta I_i)S_{i0} + P_{i0}I_{i0}S_i\} \\
& + (1/3) \sum_{i=1}^n (\Delta A)\{(\Delta P_i)(\Delta I_i)S_{i0} + P_{i0}(\Delta I_i)(\Delta S_i) + (\Delta P_i)(\Delta I_i)(\Delta S_i)\} \\
& + (1/4) \sum_{i=1}^n (\Delta P_i)(\Delta I_i)(\Delta S_i) \Delta A.
\end{aligned}$$

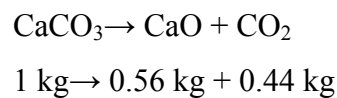
5.6 Carbon dioxide emissions from the cement production process:

Carbon dioxide emissions in cement manufacturing come directly from combustion of fossil fuels and from calcining the limestone in the raw meal. An indirect and significantly smaller source of CO₂ is from consumption of electricity assuming that the electricity is generated from

fossil fuels. Roughly half of the emitted CO₂ originates from the fuel and half originates from the conversion of the raw meal (Gautam et al., 2009).

5.7 Carbon dioxide emissions from calcination (process emissions):

Process CO₂ is formed by calcinations which can be expressed by the following equation (Gautam et al., 2009):



The share of CaO in clinker amounts to 64-67%. The remaining part consists of iron oxides and aluminium oxides. CO₂ emissions from clinker production amounts therefore at about 0.5 kg/ kg clinker (Ashenayi and Ramakumar, 1990).

5.8 Carbon dioxide emissions from fuel use:

Practically all fuel is used during the production of the clinker. The pre-process removes water from the raw meal, calcines the limestone at temperatures between 900 and 1000°C and finally clinker at about 1500°C. The amount of carbon dioxide emitted during this process is influenced by the type of fuel used (coal, fuel oil, natural gas, petroleum coke, alternative fuels) (Gautam et al., 2009).

5.9 Calculation of CO₂ emissions

The carbon dioxide emission due to fuel consumption (coal) is known as direct carbon dioxide emission while the emission due to electricity consumption is known as indirect carbon dioxide emission. Based on the available data on fuel and electricity consumption, the CO₂ emissions from

different groups of industry have been calculated based on guidelines by Intergovernmental Panel on Climate Change (IPCC, 2007).

The direct carbon dioxide emission is given by:

$$DC = F \times O \times N \times M \text{ ----- (5.3)}$$

where DC is the direct carbon dioxide emission of the fuel at time t

F is the consumption of fuel at time t

O is the carbon emission factor of the fuel

N is the fraction of carbon oxidised of the fuel

M is the molecular weight ratio of carbon dioxide to carbon (44/12)

According to IPCC (2007) guidelines, the following steps are required to calculate CO₂ emissions of fuel consumption.

- (a) Energy consumption data should be converted to terajoules (TJ) unit using standard conversion factors.
- (b) Total carbon emission [tonnes of carbon (TC)] is to be estimated by multiplying fuel consumption (tera joules) by the carbon emission factor (TC/TJ) of the corresponding fuel.
- (c) Total carbon emission is then multiplied by the fraction of carbon oxidised and the molecular weight ratio of carbon dioxide to carbon to find the total carbon dioxide emitted from fuel combustion. The molecular weight is fixed as (44/12).The carbon emission factor and the fraction of carbon oxidised are given in Table 5.6.

Table 5.6 Carbon emission factor and fraction of carbon oxidized

Sl no	Fuel	Carbon emission factor	Fraction of carbon oxidised
1	Coal	25.8	0.98
2	Soft coke	25.8	0.98
3	Natural gas	15.3	0.995
4	LPG	17.2	0.995
5	Naphtha	20.0	0.99
6	Motor gasoline	18.9	0.99
7	Aviation turbine fuel	19.5	0.99
8	Kerosene	19.6	0.99
9	High-speed oil	20.2	0.99
10	Light-speed oil	20.2	0.99
11	Fuel oil	20.2	0.99
12	Other petroleum products	20.2	0.99

Source: IPCC (2007)

The indirect carbon dioxide emission is given by:

$$IC = \frac{EC \times CE}{\eta_{td}} \text{-----(5.4)}$$

where IC is the indirect carbon dioxide emission due to electricity consumption.

EC is the electricity consumption in kWh.

CE is the CO₂ emissions per kWh electricity generation.

η_{td} is the transmission and distribution efficiency (%)

Table 5.7 Carbon dioxide emissions per kWh generation of electricity for different fuels

Fuel	(CE) grams of CO₂ / kWh
Anthracite	835
Coking coal	715
Other bituminous coal	830
Sub-bituminous coal	920
Lignite	940
Patent fuel	890
Coke oven coke	510
BKB/peat briquettes	500-1100
Gas works gas	380
Coke oven gas	390
Blast furnace gas	2100
Oxygen steel furnace gas	1900
Natural gas	370
Crude oil	610
Natural gas liquids	500
Liquefied petroleum gases	600
Kerosene	650
Gas/diesel oil	650
Fuel oil	620
Petroleum coke	970
Peat	560
Industrial waste	450-1300
Municipal waste (non-renewable)	450-2500

Source: IPCC (2007)

5.10 Results and discussion

By the application of complete decomposition analysis, the contribution of different factors to group wise energy related CO₂ emissions for the period 2001-2010 has been found out. In the analysis 2001 has been taken as the base year.

Group A

The Fig.5.2 shows the graphical representation of decomposition analysis on CO₂ emissions for group A industries. Activity (Production) effect is a dominant component affecting CO₂ emissions from group A industries. The structural share of CO₂ emissions for group A industries have shown a decreasing trend for the entire time period compared to group A and B. The energy intensity for group A industries have shown a positive rising trend till 2005 but have been decreasing from there. The Energy intensity is an important factor that controls CO₂ emissions. After 2005 the energy intensity shows a declining trend. This is the indication of energy efficiency improvement in this group of industries.

During the year 2001-02 the pollution coefficient effect is positive. But in the adjacent as well as the entire time period it is negative, leading to a reduction in CO₂ emissions. This shows that group A industries have improved their emission control methods have gone for better after treatment. The various possibilities include focusing on the development of technologies that will offer significant improvements:

- Efficiency of conversion process to reduce the amount of fuel consumed and associated CO₂ emissions.
- Fuel switching to lower carbon alternatives such as co firing with biomass.
- Carbon captures technologies.
- Development of underpinning technologies that support carbon abatement technologies.

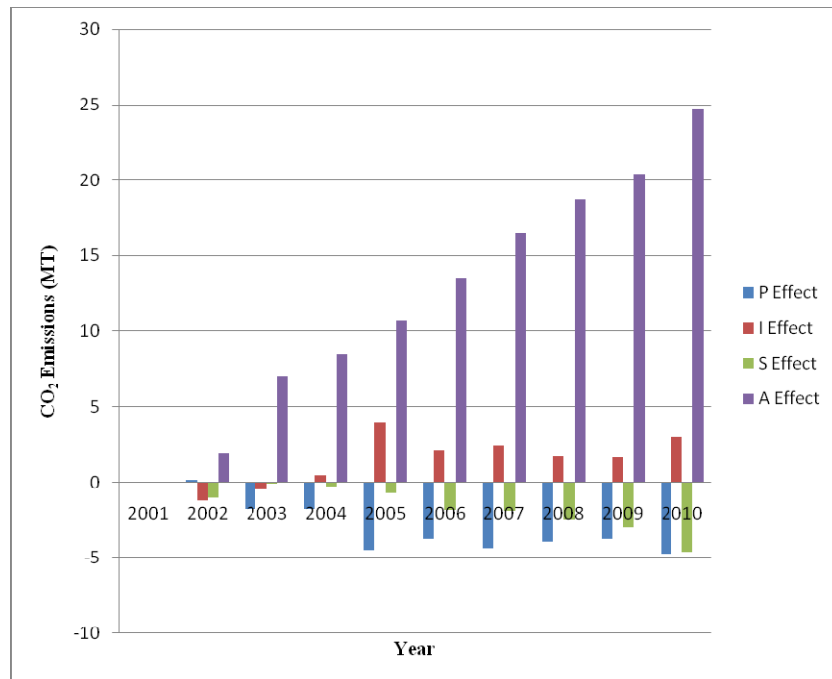


Fig. 5.2 Decompositions of CO₂ emissions changes in group A Industries

Group B

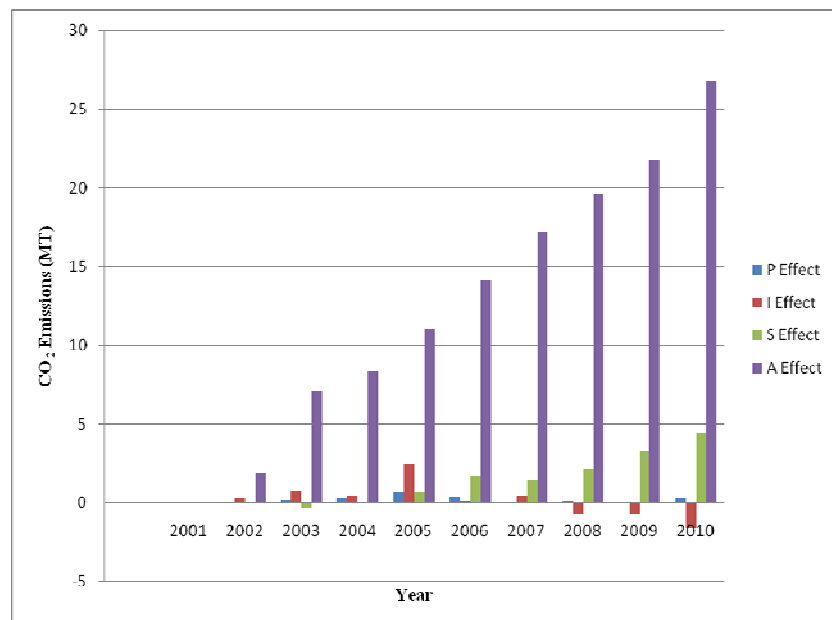


Fig. 5.3 Decompositions of CO₂ emissions changes in group B Industries

Group B industries show a slight positive trend in pollution coefficient effect. Unlike group A industries group B industries are less specific energy consuming industries but the total output is more than group A and C. Here the intensity effect is positive in the early stages i.e. from 2002 to 2006. But the intensity effect shows a negative trend from 2006 to 2010 thus contributes to the CO₂ emissions reduction. The Fig.5.3 shows the graphical representation of decomposition analysis on CO₂ emissions for group B industries. Structural effect is the dominant factor for this group industries because for the period 2001-2010 the production became more than double compared to Group A and C. Thus the productive output has shown a positive trend each year leading to a positive structural effect. The increased output represents the economic growth. Economic growth is the dominant factor affecting pollution emission from industrialisation.

Group C

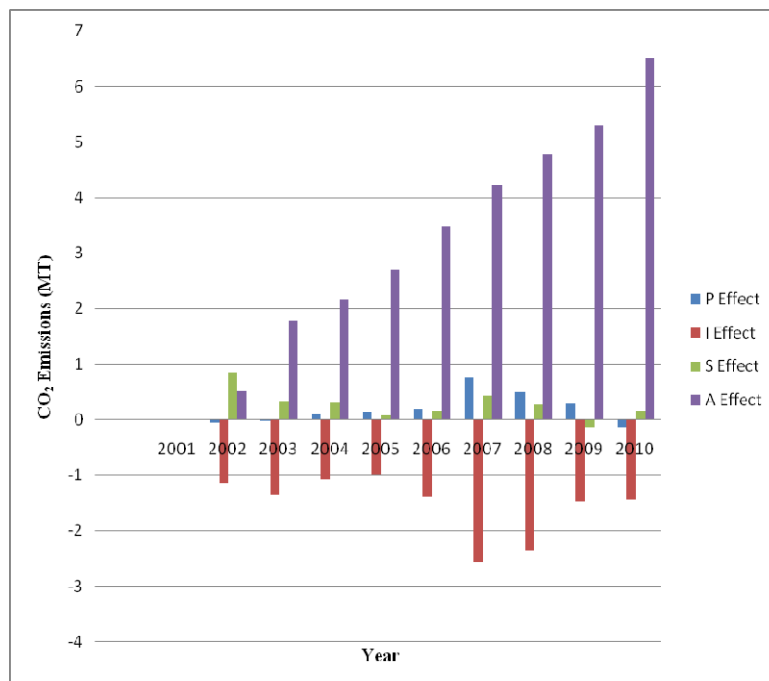


Fig. 5.4 Decompositions of CO₂ emissions changes in group C Industries

In this group C the pollution coefficient effect has shown a positive trend to increase till 2008 after which it has been consistently decreasing. The Fig.5.3 shows the graphical representation of decomposition analysis on CO₂ emissions for group C industries. As a result of continuous economic growth rate the industries have been making a steady profit. This has encouraged them to invest on pollution control measures. The intensity effect has been showing a continuous negative trend providing for reduction in CO₂ emissions. The industries in this group are relatively small units which use more energy efficient devices providing for a reduction in energy intensity. The structural effect has shown a slight positive trend. This is due to rate of increase in production in each year less than group B industries.

5.11 Conclusion

In this study, a decomposition analysis has been conducted to find the nature of factors affecting the change in energy related CO₂ emissions. The factors that lead to CO₂ emissions are pollution coefficient effect, intensity effect, structural effect and activity effect. A specific decomposition technique known as complete decomposition is used to evaluate the relative contribution of components that accounts for changes in energy induced CO₂ emissions.

The results reveal that in Indian cement industries production effect is the most important component of carbon dioxide emission. Activity (production) effect shows the economic growth of the country. Energy intensity reduces the carbon dioxide emission for all periods except for group A industries and early period of group B industries. The pollution coefficient effect has shown a decrease in carbon dioxide emission for

group A industries. This decrease in pollution coefficient effect is dependent on fuel switching or fuel cleaning technologies. The result implies that the current technological conditions and fuel pattern limits the decrease in pollution coefficient effect for group B and group C industries.

The result of decomposition analysis reveal that CO₂ emissions of Indian cement industries depends mainly on activity effect. An increase in economic growth is vital for the development of a country. The major factors that can be controlled to reduce CO₂ emissions in Indian industries are energy intensity effect and pollution coefficient effect.

.....❧.....

FORECASTING MODEL FOR CO₂ EMISSIONS

Contents	6.1 <i>Introduction</i>
	6.2 <i>Overview of Cement Industries in India</i>
	6.3 <i>History of Cement Production in India</i>
	6.4 <i>System Dynamics</i>
	6.5 <i>System Dynamic Model Based on Data Collected from the Selected Cement Industries</i>
	6.6 <i>Modified model</i>
	6.7 <i>Scenario generation</i>
	6.8 <i>Results and Discussion</i>
	6.9 <i>Conclusion</i>

6.1 Introduction

The data of cement production, clinker production and thermal and electrical energy consumption of the selected cement industries in India were collected for the period 2001 - 2010. It was found that the cement production rate increases every year and thus the related CO₂ emissions. A system dynamic model was developed in order to predict the CO₂ emissions based on data collected from the selected cement industries. Finally, the model was modified and applied to the projection of cement production and associated CO₂ emissions in India up to 2030 starting from 2010 as the base year. This modified model was run under three scenarios; such as baseline scenario, scenario-1(S1) and scenario-2 (S2). Energy

conservation policy was also incorporated in the model to estimate CO₂ emissions reduction.

6.2 Overview of Cement Industries in India

The origin of Indian cement industry can be traced back to 1914 when the first unit was set-up at Porbandar with a capacity of 10000 tonnes, thus making it a century old industry in the country. Today, cement industry comprises of 183 large cement plants and more than 360 mini cement plants. Large producers contribute to about 97% of the installed capacity, while mini plants account for the rest. Among these, 98% of the capacity is in the private sector and the rest in public sector (Ministry of Commerce & Industry, 2011). Cement industry in India has also made great progress in technological upgradation and assimilation of latest technology. Presently, about 97 per cent of the total capacity in the industry is based on modern and environment-friendly dry process technology. All new capacity to be added in the future is likely to be of dry process and even some of the existing units may also change the process to become competitive. As such, the share of cement capacity using dry process would further increase in future.

About 94% of the thermal energy requirement is met by coal in the Indian cement manufacturing and the remaining part is met by fuel oil and high speed diesel oil. Natural gas is not sufficiently available for the cement industry in India (Karwa et al., 1998). About 29% of the expense is spent on energy, 27% on raw materials, 32% on labor and 12% on depreciation in cement industry. Therefore, cement industry is characterised by energy intensive industry throughout its production stages and the calcination of its raw materials (Gielen and Taylor, 2009). The industry's average energy

consumption is estimated to be about 3 GJ/tonne of clinker thermal energy and 88 kWh/ton of cement electrical energy. The best thermal and electrical energy consumption presently achieved by the Indian cement industry is about 2.9 GJ/tonne of clinker and 67 kWh/ tonne of cement (CMA 2010) which are comparable to the best reported figures of 2.72 GJ/tonne of clinker and 65 kWh/ tonne of cement in the world best average. The comparisons of electrical and thermal specific energy consumption for the cement production of few selected countries around the world are given in the Table 6.1

Table 6.1 Electrical and thermal specific energy consumption

Country	Electrical SEC (kWh/tonne of cement)	Thermal SEC (GJ/tonne of clinker)
India	88	3.00
Spain	92	3.50
Germany	100	3.50
Japan	100	3.50
Korea	102	3.70
Brazil	110	3.70
Italy	112	3.80
China	118	4.00
Mexico	118	4.20
Canada	140	4.50
US	141	4.60
World best	65	2.72

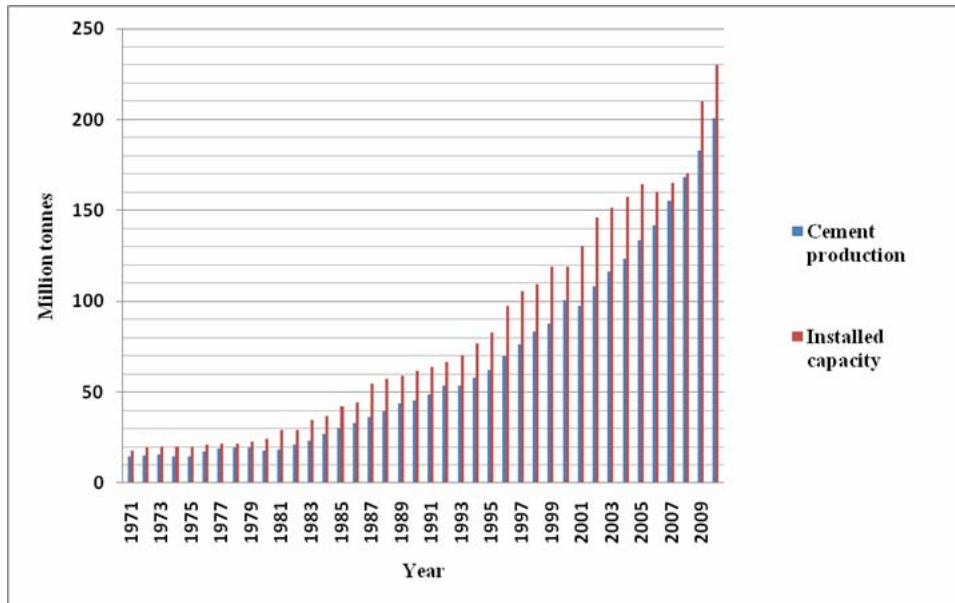
Source: Gielen and Taylor, (2009)

In the cement sector, the burning of fossil fuels (predominantly coal) during pyroprocessing and the chemical reactions (calcination) that convert limestone into clinker, results in the emission of CO₂. Hendriks et al. (1999) also stated that the global cement industry contributes to approximately 20%

of all man-made CO₂ emissions, and is consequently responsible for around 10% of man-made global warming. The cement plant releases about one tonne of CO₂ for every tonne of cement produced, half of it from the fuel it burns and the other half from the calcination process

6.3 History of Cement Production in India

World cement production for 2010 is estimated as 3294 million tonnes, increasing 9.2% compared to 2009. Around 56% of the production originates in China (CEMBUREAU, 2011). Indian cement industry is the second largest in the world with an installed capacity of 135 tonnes per annum. It accounts for nearly 6% of the world production (Cement industry, 2010). The cement industries in India are presently growing at a rapid rate, since the government of India is giving boost to various infrastructure projects, housing facilities and road networks. In 1971, India's cement production was 14.40 million tonnes (MT) and it increased to 201.16 million tonnes in 2010. In the above time period, India's annual cement consumption increased from 26 kilograms (kg) per capita to 156 kilograms (kg) per capita (CMA, 2010). In other words, India's cement output and annual cement consumption per capita increased by factors of 17 and 6 from 1971 to 2010 respectively. However India's cement consumption per capita in 2010 was quite lower than China's annual cement consumption. In 2010, china's annual cement consumption was 1380 kg per capita (Jing, 2011). Fig. 6.1 shows cement production and capacity growth of cement industries in India during the period 1971 to 2010.



Source: CMA

Fig. 6.1 Cement production and capacity in India for the period 1971-2010

6.4 System Dynamics

System dynamics is a computer-aided approach to policy analysis and design. It applies to dynamic problems arising in complex social, managerial, economic, or ecological systems literally any dynamic systems characterized by interdependence, mutual interaction, information feedback, and circular causality. The approach begins with defining problems dynamically, proceeds through mapping and modeling stages, to steps for building confidence in the model and its policy implications. Mathematically, the basic structure of a formal system dynamics computer simulation model is a system of coupled, nonlinear, first-order differential equations. The dynamics of the system are represented by $dN(t)/dt = kN(t)$, which has a solution $N(t) = N_0 e^{kt}$. Here, N_0 is the initial value of the system variable, k is a rate constant (which affects the state of the system) and t is the simulation time. For the simulations to start for the first time, initial values

of the system variables are needed. The feedback concept is the heart of the system dynamics approach. Diagrams of loops of information feedback and circular causality are tools for conceptualizing the structure of a complex system and for communicating model-based insights.

6.5 System Dynamic Model Based on Data Collected from the Selected Cement Industries

A software package “Powersim Studio 7”, available for system dynamics analysis has been used in developing the model for forecasting CO₂ emissions. The flow diagram shown in the Fig. 6.2 is useful for showing the physical and information flow in the system dynamic model for selected cement industries. The level variables are shown as rectangular boxes which represent accumulated flows to that level. A double arrow represents the physical flows, and the flow is controlled by a flow rate. A single line is for showing information flow. Source and sink of the structure are represented by a cloud. The cloud symbol indicates infinity and marks the boundary of the model.

Once the simulation is over, at the end of each step, the system variables are brought up to date for representing the results from the previous simulation step. The rate variables are represented by valves. The information from the level variables to the rate variables is transformed by third variable called auxiliary variables, represented by circles. Diamonds represents constants, which do not vary over the run period of simulation. A constant is defined by an initial value throughout the simulation.

There are three subsystems in the proposed model such as cement production, energy consumption and CO₂ emissions. The cement production is taken as level variable and production growth as the rate variables.

From the data collection, it was found the total cement production in the selected cement industries in the year 2010 was 127.4 million tonnes and this value is taken as the initial value in the forecasting model. The average production growth for the period was 9.2%. So the production rate multiplier for this model is taken as 0.092. The dynamic equation for the projection is as follows.

$$\begin{aligned} \text{Cement production} &= \text{Cement production} + dt \times (\text{Cement production rate}) \\ \text{Cement production rate} &= \text{'Production rate_multiplier'} \times \text{'Cement Production'} \\ \text{Production rate multiplier} &= \text{GRAPHSTEP} (\text{TIME}, \text{STARTTIME}, 2001 \ll \text{yr} \gg, \text{'Production growth_rate'}) \\ \text{'Production growth_rate'} &= \{9.2\} \ll \% / \text{yr} \gg \\ \text{Total CO}_2 &= \text{CO}_2\text{_clinker} + \text{'CO}_2\text{_electrical energy'} + \text{'CO}_2\text{_thermal energy'} \end{aligned}$$

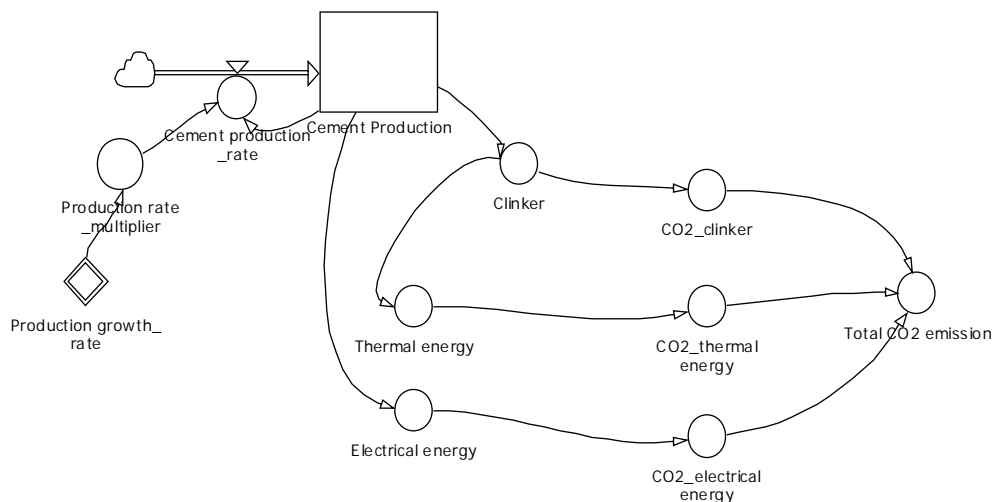


Fig. 6.2 Flow diagram of the system dynamic model

6.5.1 Model Validation

Confidence in the SD model for the system under study is established through its validation on the basis of the data utilised. Here the validation is carried out with the historical data of cement production. From the data collection, it was found that the total cement production in the selected cement industries in the year 2001 was 55.23 million tonnes. The above value is taken as the initial value for the projection with the base year 2001 and the model estimates cement production for the period 2001 to 2010 with the production rate multiplier 0.092. The dynamo equation for the actual cement production is given below.

```
Cement production      = Cement production+ dt× (Cement
                        production rate)

Cement production rate = 'Production rate _multiplier' ×
                        'Cement Production'

Production rate multiplier = GRAPHSTEP (TIME, STARTTIME,
                        2001<<yr>>, 'Production growth_ rate')

'Production growth_ rate' = 2001, {9.2} <<%/yr>>
```

The model results give good agreement with the actual values as in Table 6.5. Points representing the actual and model values of cement production showed an overall increasing trend (Fig.6.3).

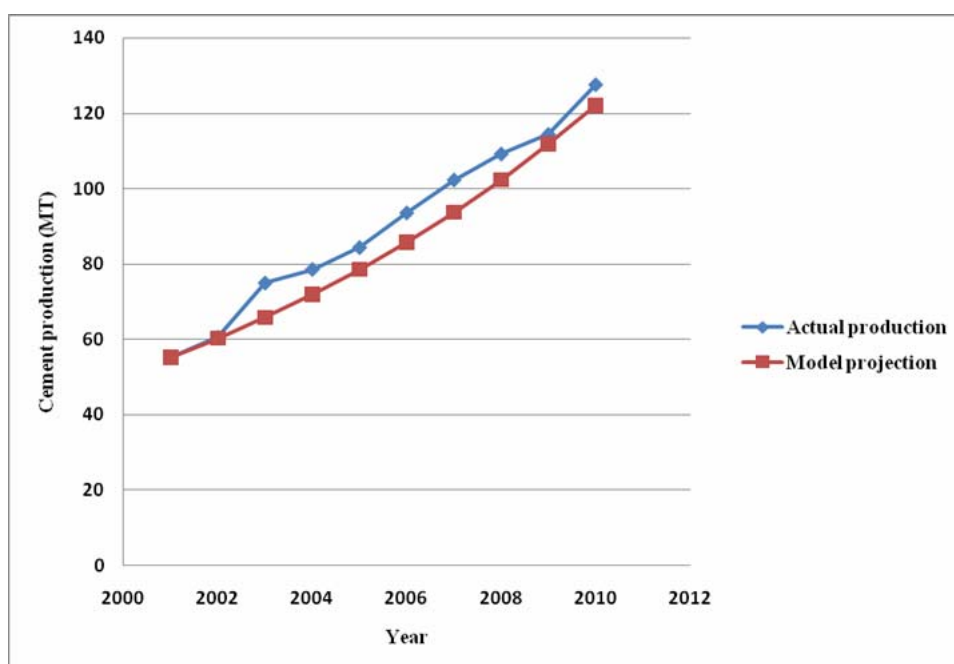


Fig. 6.3 Comparison of the quantity of cement production with model projection

Table 6.2 Comparison of the quantity of cement production with model projection

Year	Actual cement production (MT)	Model projection (MT)
2001	55.23	55.23
2002	60.6	60.31
2003	74.95	65.86
2004	78.53	71.92
2005	84.34	78.54
2006	93.53	85.76
2007	102.22	93.65
2008	109.115	102.27
2009	114.29	111.68
2010	127.44	121.95

6.5.2 Sensitivity Test

A sensitivity test basically ascertains whether or not minor shifts in the model parameters can cause shift in the behaviour of the model. Once the robustness of the model is ensured, the model can be used for policy making (Mohapatra et al., 1994). The sensitivity of the model tested by changing production growth multiplier from 0.092 to 0.101 for the year 2021(Fig 6.4). Then, the cement production increased from 740.67MT to 797.45 MT by the year 2030. Table 6.3 shows the values of sensitivity test of the model. Thus, the model is sensitive to minor shifts in the parameter ensuring its clearance of the sensitivity test.

Cement production	=	Cement production+ dt× (Cement production rate)
Cement production rate	=	'Production rate _multiplier' × 'Cement Production'
Production rate multiplier	=	GRAPHSTEP (TIME, STARTTIME,2010<<yr>>, 'Production growth_ rate')
'Production growth_ rate'	=	{9.2,9.2,9.2,9.2,9.2, 9.2,9.2,9.2,9.2,9.2,9.2, 10.1,10.1,10.1,10.1,10.1, 10.1,10.1,10.1,10.1}<<%/yr>>
Total CO ₂	=	CO ₂ _clinker+'CO ₂ _electrical energy'+'CO ₂ _thermal energy'

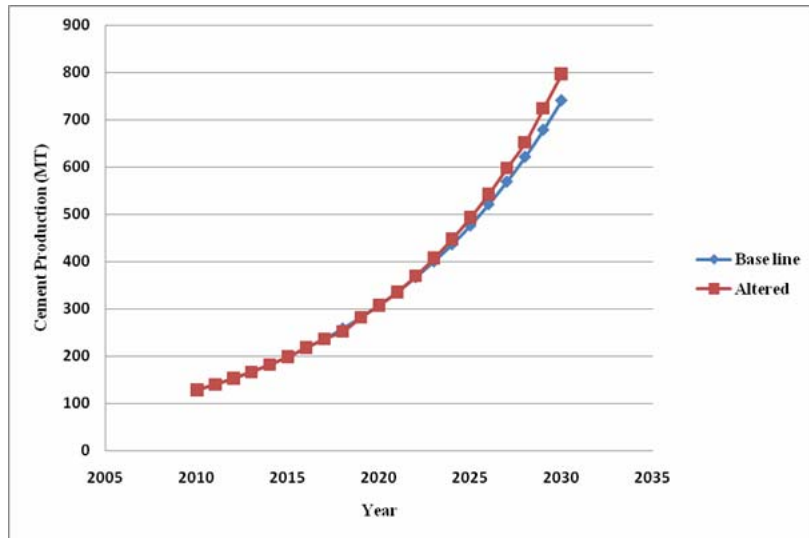


Fig. 6.4 Sensitivity of the model tested with cement production growth multiplier is changed from 0.092 to 0.101 for the year 2021 onwards

Table 6.3 Sensitivity of model tested with cement production growth multiplier is changed from 0.092 to 0.101 for the year 2021 onwards

Year	Base line cement production (MT)	Altered value of cement production (MT)
2010	127.4	127.4
2011	139.12	139.12
2012	151.92	151.92
2013	165.9	165.9
2014	181.16	181.16
2015	197.83	197.83
2016	216.9	216.9
2017	235.9	235.9
2018	257.6	257.6
2019	281.3	281.3
2020	307.18	307.18
2021	335.3	335.3
2022	366.3	369.32
2023	400	406.62
2024	436	447.69
2025	476	492.91
2026	520.87	542.69
2027	568.7	597.51
2028	621.12	651.85
2029	678.27	724.3
2030	740.67	797.45

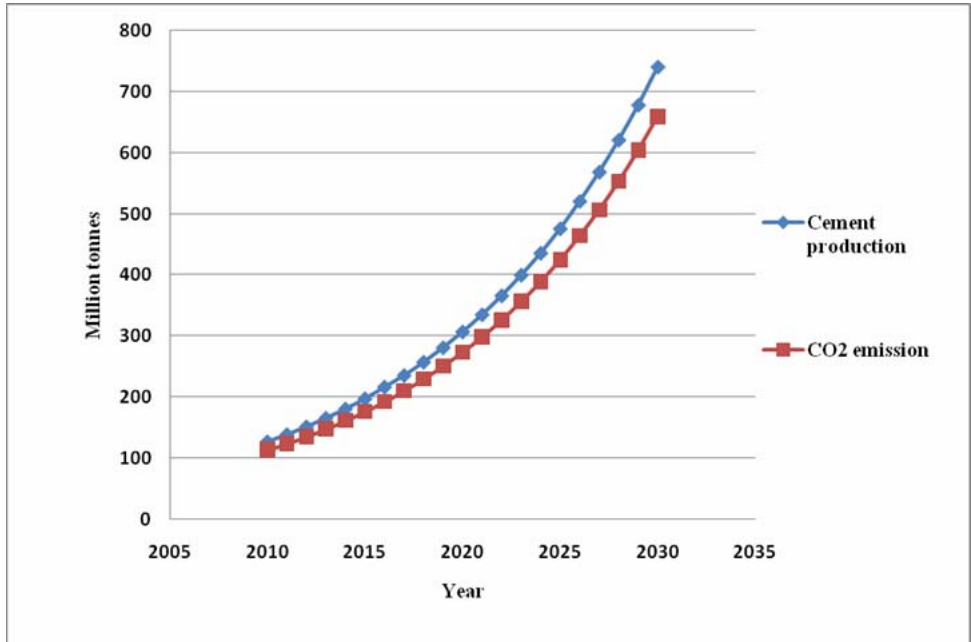


Fig. 6.5 Projections of Cement production and CO₂ emissions

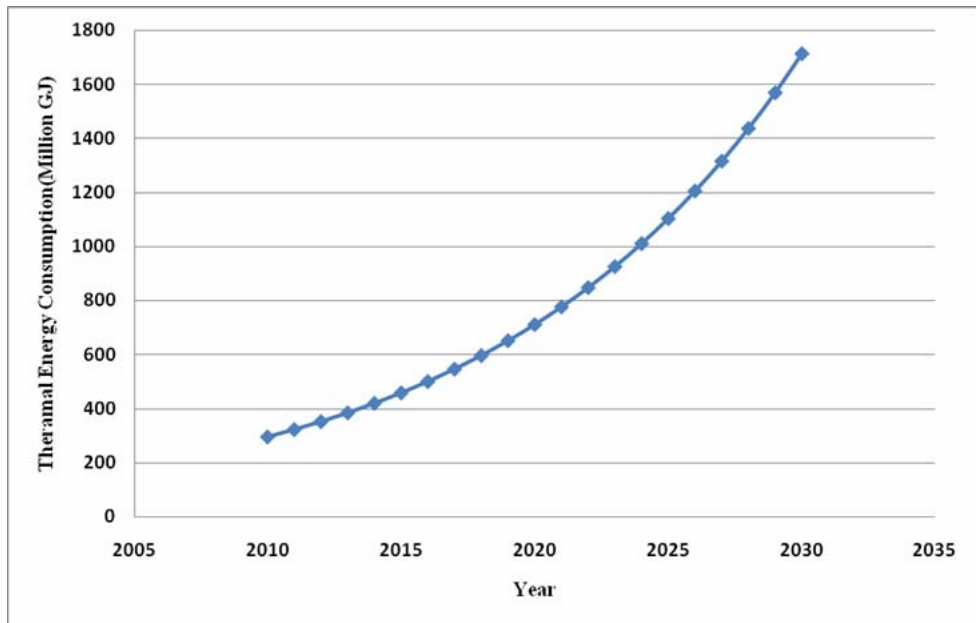


Fig. 6.6 Projection of thermal energy consumption

Table 6.4 Projection of cement production and CO₂ emissions

Year	Cement production (MT)	CO ₂ emissions (MT)
2010	127.4	113.5
2011	139.12	123.95
2012	151.92	135.35
2013	165.9	147.81
2014	181.16	161.4
2015	197.83	176.25
2016	216.9	192.42
2017	235.9	210.17
2018	257.6	229.51
2019	281.3	250.63
2020	307.18	273.68
2021	335.3	298.86
2022	366.3	326.36
2023	400	356.38
2024	436	389.17
2025	476	424.97
2026	520.87	464.07
2027	568.7	506.76
2028	621.12	553.39
2029	678.27	604.3
2030	740.67	659.89

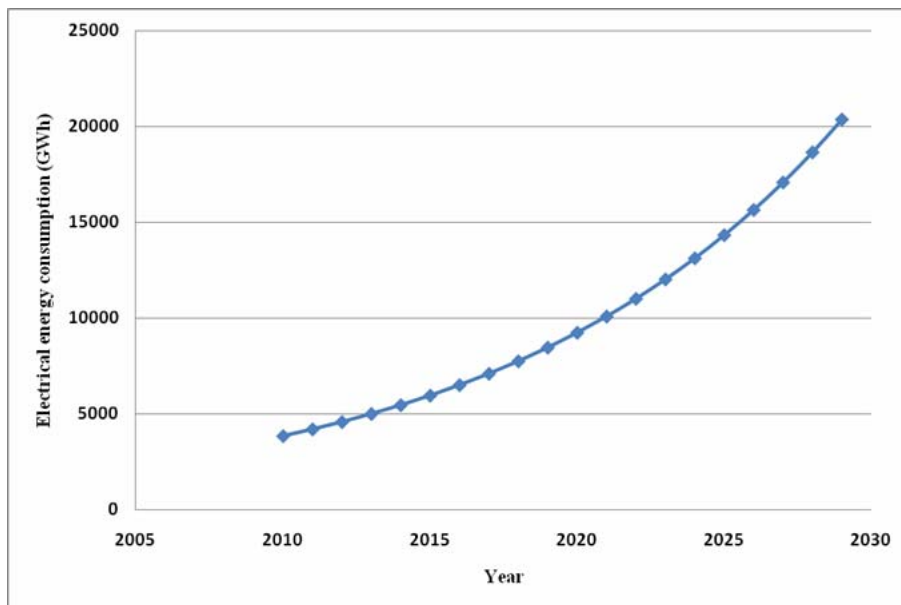


Fig. 6.7 Projection of electrical energy consumption

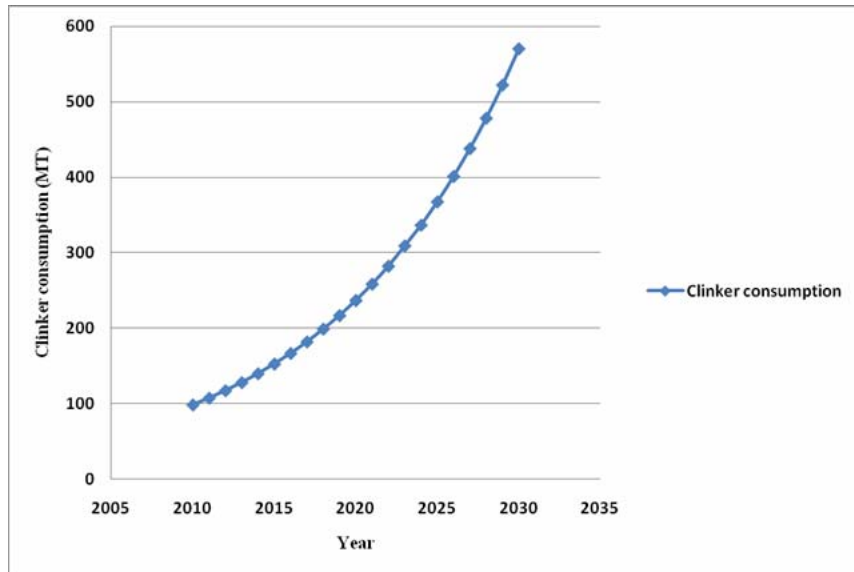


Fig. 6.8 Projection of clinker consumption

Table 6.5 Projection of thermal energy, electrical energy and clinker consumptions

Year	Thermal energy (Million GJ)	Electrical energy (GWh)	Clinker (MT)
2010	294.29	3822	98.1
2011	321.37	4173.6	107.12
2012	350.9	4555.6	116.98
2013	383.22	4976.9	127.74
2014	418.48	5434.77	139.49
2015	456.98	5934.77	152.33
2016	499.02	6480.77	166.34
2017	544.93	7077	181.64
2018	595.06	7728.08	198.64
2019	649.81	8439.07	216.6
2020	709.56	9215.46	236.53
2021	774.87	10063.28	258.29
2022	846.16	10989.11	282.05
2023	924.01	12000.2	309
2024	1009.02	13104.11	336.34
2025	1101.85	14309.11	367.28
2026	1203.22	15626.18	401.07
2027	1313.9	17063	437.97
2028	1434.9	18633.6	478.26
2029	1566.79	20347.96	522.26
2030	1710.94	22219.97	570.31

The system dynamic model is used for the projection of cement production and CO₂ emissions based on data collected from the selected cement industries. Fig.6.5 shows the projection of cement production and CO₂ emissions of the model. The cement production will grow from 127.4 million tonnes in 2010 to 740.67 million tonnes in 2030. The projection of CO₂ emissions is found to be 659.89 million tonnes. The projected values of the cement production and CO₂ emissions are shown in Table 6.4. The model predicted that by the year 2030, 1710.94 million GJ of thermal energy and 22219.97 GWh of electrical energy (Table 6.5) will be required for the cement production. The clinker requirement will be 570.31 million tonnes (Table 6.5). Figs.6.6, 6.7 and 6.8 show the projections of the thermal energy and electrical energy and clinker utilization. The results indicate that an increase in energy consumption can lead to increase in the CO₂ emissions. Cement industry provides raw materials to the essential growth sectors like construction, transportation etc. and with rapid economic growth, there has been a increase in the demand for the product. Cement industry is highly energy intensive and thus it is essential to keep a track of future energy necessities of these sectors and emission levels.

6.6 Modified model

The model is an expanded one from the previous model. This is used to forecast the cement production and corresponding CO₂ emissions from 2010 onwards to the next 21 years for total cement production in India. The proposed model is composed of three main subsystem such as cement demand and production, energy consumption and CO₂ emissions.

6.6.1 Cement demand and production

Cement demand and production are taken as level variables. The cement demand would increase with the growth of population and the gross

domestic product (GDP). Production should follow the demand and CO₂ emissions from the plants would likewise increase with more production. This requires information about population, and population is then considered as the level variables. Its variation obviously depends on the rate of population growth. The changes in population growth and cement production rate affect the rate of CO₂ emissions from the cement industry.

6.6.2 Energy consumption

The electrical energy consumption of the cement industry is estimated by considering electrical energy consumed per tonne of cement produced and thermal energy consumption is estimated by considering thermal energy consumed per tonne of clinker. Scenario considering waste heat recovery and renewable energy were also evaluated under this head.

6.6.3 CO₂ emissions

The CO₂ emissions from the cement plants are estimated as the sum of CO₂ emissions due to consumption of clinker, utilization of thermal energy and expenditure of electrical energy. Policy options are implemented while working out the scenarios for mitigation of total CO₂ emissions over a period of time.

The dynamo equation used to account the baseline scenario(BS), scenario-1 and scenario-2 in this system is

$$\text{Population} = \text{Population} + dt \times (\text{Population growth})$$

$$\text{Population growth} = \text{Conditional population growth rate multiplier} \\ \times \text{Population}$$

Conditional population growth rate multiplier =

IF ('switch A'=1, 'Population growth multiplier_BS',

IF ('switch A'=2, 'Population growth multiplier_S1',

IF ('switch A'=3, 'Population growth multiplier_S2'))

Population growth multiplier_BS = GRAPHSTEP (TIME,
START TIME, 2010, 1(1.3)<<%/yr>>)

Population growth multiplier_S1 = GRAPHSTEP (TIME,
STARTTIME, 2010, 1{ 1.31, 1.3, 1.27, 1.25, 1.23,
1.21, 1.19, 1.17, 1.15, 1.13, 1.1, 1, 0.9, 0.7, 0.5, 0.4,
0.3, 0.2, 0.1, 0}<<%/yr>>

Population growth multiplier_S2 = GRAPHSTEP (TIME,
STARTTIME, 2010, 1{ 1.31, 1.27, 1.23, 1.19, 1.15, 1.13, 1.1, 0.7, 0.
5, 0.3, 0, 0, 0, 0, 0, 0, 0, 0}<<%/y>>

Now, for the cement demand and production, the dynamo equations used in the model are:

$$\begin{aligned} \text{Cement demand} &= \text{Cement demand} + dt \times (\text{Cement demand rate}) \\ \text{Cement demand rate} &= \text{'Growth rate cement demand'} \times \text{'Cement demand'} \\ &\quad \text{Growth rate cement demand} = \text{'Conditional} \\ &\quad \text{population growth rate multiplier'} + \text{'GDP} \\ &\quad \text{increment rate'} \end{aligned}$$

Therefore,

$$\text{Cement demand} = \text{Cement demand} + dt \times \{(\text{GDP increment rate} + \text{Conditional population growth rate multiplier}) \times (\text{Cement demand rate})\}$$

$$\text{Cement production} = \text{Cement production} + dt \times (\text{Cement production rate})$$

$$\text{Cement production rate} = \text{Conditional production growth multiplier} \times \text{'Cement production'}$$

Conditional production multiplier =

IF ('Switch A'=1,'production growth multiplier BS',

IF ('Switch A'=2,'production growth multiplier based on GDP',

IF (Switch A=3, 'production growth multiplier based on GDP')))

'Production growth multiplier BS' = GRAPHSTEP (TIME,
STARTTIME, 2010, 1(8.9)
<<%yr>>

Production growth rate multiplier based on GDP =

0.142<<%/yr>>+(2.7611×'Growth rate cement demand')

$$\text{Cement exported} = \text{'Cement production' - 'Cement demand'}$$

$$\text{Total CO}_2 \text{ emissions} = (\text{'CO}_2 \text{ clinker'} + \text{'CO}_2 \text{ electrical'} + \text{'CO}_2 \text{ thermal'})$$

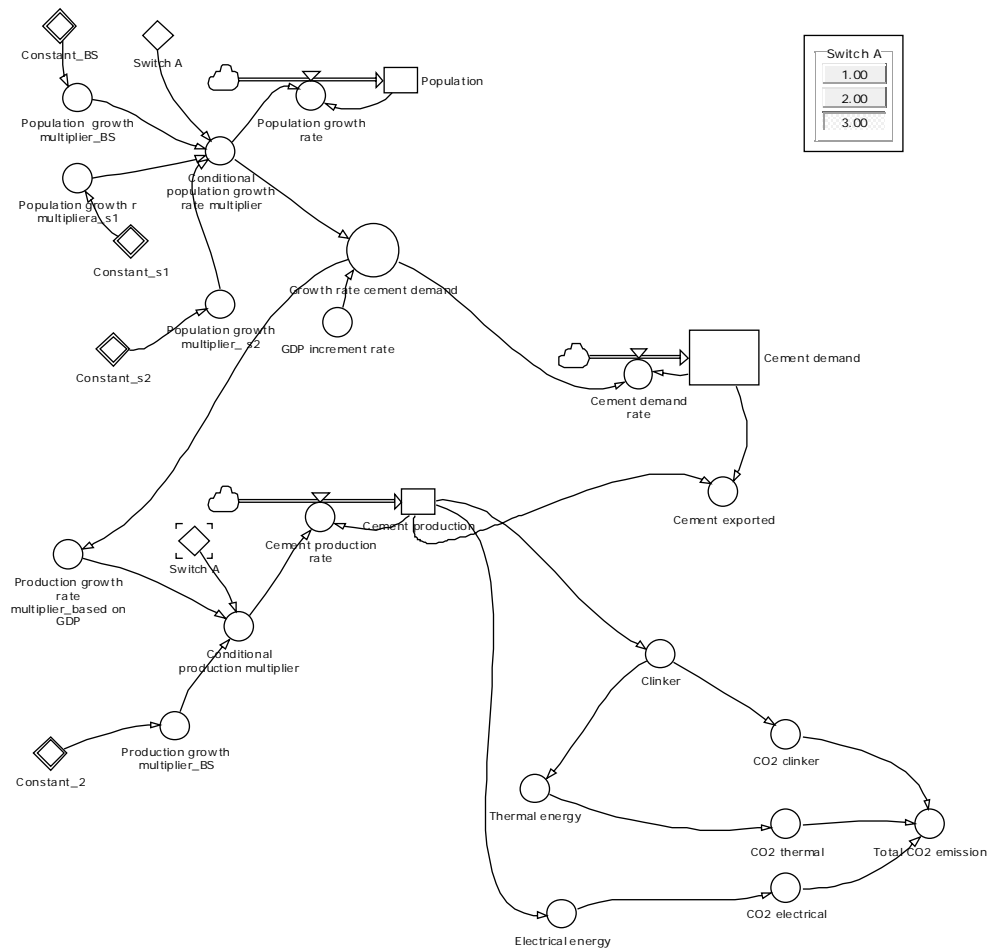


Fig.6.9 Flow diagram of the system dynamic model baseline scenario, scenario-1 (S1) and scenario- 2 (S2)

6.7 Scenario generation

Three scenarios are generated under the broad categories of baseline scenario (BS) and modified scenario 1 and 2 (S1 and S2). The model is run for a span of 21 years starting from the baseline year 2010.

6.7.1 Baseline scenario

This scenario is generated for the existing growth rate of the population in the base year 2010. The energy consumed, the amount of clinker required

and the quantity of CO₂ emitted in the process of production are estimated. In the year 2010, India's population was 1170 million and had a growth rate of 1.3%. In the eleventh five year plan, the gross domestic product (GDP) is taken as 7.3% and has stepped to 9.2% (GIO, 2007, 2011-2012). Cement production in India for the year 2010 was million tonnes and from historical data, the trend seems to increase at a rate of 8.9%. Trends of CO₂ emissions are evaluated from the consumption of clinker, thermal energy and electrical energy during the process of cement production.

6.7.2 Modified scenerios

Population growth rate are taken for the modified scenario. In the scenario-1 (S1) the growth rate of population gradually decreases and finally reaches zero by the year 2030 and in the scenario-2 (S2) a faster decline in the growth rate is analysed where zero growth rate is achieved in the year 2020 and beyond. For this scenario, a relation for the cement production growth rate and population growth rate was developed using least squares method. Data from 2001 to 2010 has been used to formulate the relation. The cement production growth rate is used as the Y variable and the growth rate cement demand (sum of population growth rate and increment rate of GDP) is the X variable in the interval of 10 years and the equation is $Y = a + bX$, where a & b are positive coefficients. The auxiliary named 'swith' is used to select the respective scenario in order test the impact of changes in CO₂ emissions.

6.7.3 Energy management scenario

The technological policy option based on energy management is evaluated for the baseline and modified scenarios. From the case study of the kiln system (Chapter 4), it was found that the waste heat streams from cooler and preheater together carries 38 % of the input heat (average of both

operating conditions). This energy could be recovered by the waste heat recovery systems. It was also found that now a days, the renewable energy plays an important role in cement plant in India. It is worth mentioning here that some of the cement plants in south India already installed wind power generators in their wind farms. Presently, they feed their output into the grid (www.cleantechindia.com/eicnew/cement.html)

For analysing energy management scenario, 38% thermal energy from the waste heat recovery systems and also 25 % of electrical energy supply to the cement plants replaced by renewable energy are taken into account. The model is run for this condition also under the BS, S1 and S2 scenarios.

6.8 Results and Discussion

The results of different scenarios of CO₂ emissions from the cement industries in India are discussed here. Trends are evaluated for a span of 21 years starting from the year 2010.

6.8.1 Baseline scenario

The rate of population growth and GDP as applicable in the year 2010 were kept constant for the base line scenario. The technology employed in making the cement was kept unaltered. Using these options India's population is projected to reach 1521.64 million by the year 2030. Fig. 6.10 shows the population growth for the baseline (BS), scenarios S1 and S2. The cement production and demand are shown in the Fig. 6.11 and Fig. 6.12 respectively. The cement production and demand projected for the year 2030 by the model is 1106 and 376.66 million tonnes respectively (Table 6.7 and 6.8). The clinker requirement will be 851.62 million tonnes (Table 6.11). The model predicted that by the year 2030, 2554.85 million GJ thermal energy and 33179.89 GWh electrical energy will be required for

making the cement (Table 6.9 and 6.10). The total CO₂ emissions are estimated to reach 985.38 million tonnes by 2030 (Table 6.12). Figs. 6.13, 6.14, 6.15 and 6.16 show the annual growth of thermal energy consumption, electrical energy utilization, clinker consumption and CO₂ emissions respectively for the baseline scenario (BS) and modified scenarios S1 and S2. The cement production projected for the year 2020 by our model is 471.49 million tonnes and this is comparable to that of Jayant et al. (2005) (485 million tonnes in 2020). So the results from the forecasting were quite satisfactory and the model represents a good foundation for future projection in this sector.

6.8.2 Modified scenario

The cement demand and production depends on the population growth and economic activity in the country. Controlling the population growth is one of the option for mitigation of CO₂ emissions. The effect of CO₂ emissions are discussed in the two modified scenario. In scenario-1 (S1) the growth rate of population is brought to zero by the year 2030 and in the scenario-2 (S2) a faster decline in the growth rate is analysed where zero growth rate is achieved by the year 2020.

Fig.6.10 shows the scenario-1 (S1) the population of India would reach 1386.36 million in the year 2030 (Table 6.6). The cement demand will then be 343.79 million tonnes (Table 6.8) a reduction of 8.7% of the base line scenario. Since the production is linked with demand, which in turn is linked with the population growth, a reduction of 15.21 % in production is projected as compared to the baseline scenario. To produce the required quantity of cement (937.68 million tonnes), the consumption of thermal energy will be 2166.03 million GJ (Table 6.9), electricity 28130.28 GWh

(Table 6.10) and clinker requirement will be 722.01 million tonnes (Table 6.11). Fig.6.13, Fig.6.14 and Fig.6.15 show the annual growth of thermal energy, electrical energy and clinker consumption. As shown in Fig. 6.16, 835.42 million tonnes of CO₂ (Table 6.12) will be emitted in the year 2030 due to the expenditure of thermal energy, electrical energy and clinker.

In the scenario-2 (S2) the population would stabilize by the year 2020 and remain constant. So further decrease in all the parameters as shown in Figs. 6.11 to 6.15. It was found that a reduction of 29.4 % (780.36 million tonne) in cement production is projected for 2030. Accordingly, the consumption of thermal energy and electrical energy will be 1802.62 million GJ (Table 6.9), 23410.68 GWh (Table 6.10) respectively. The clinker requirement will be 600.87 million tonnes (Table 6.11). A reduction of 29.44% (695.26 million tonne) in CO₂ emissions (Table 6.12) were observed compared to baseline scenario (BS).

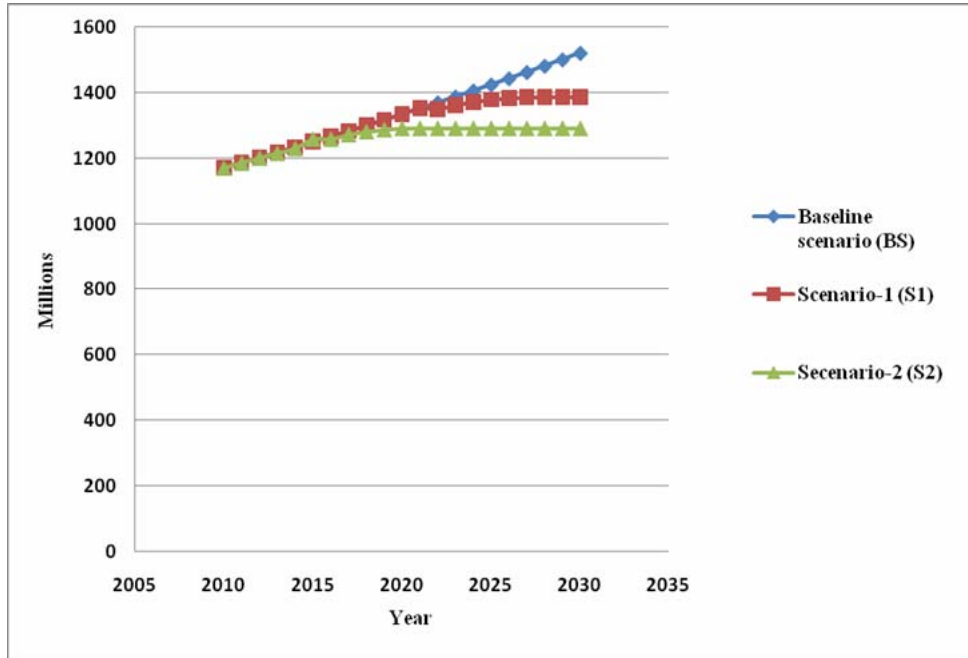


Fig. 6.10 Projections of population of India under the baseline scenario (BS), scenario-1 (S1) and scenario-2 (S2).

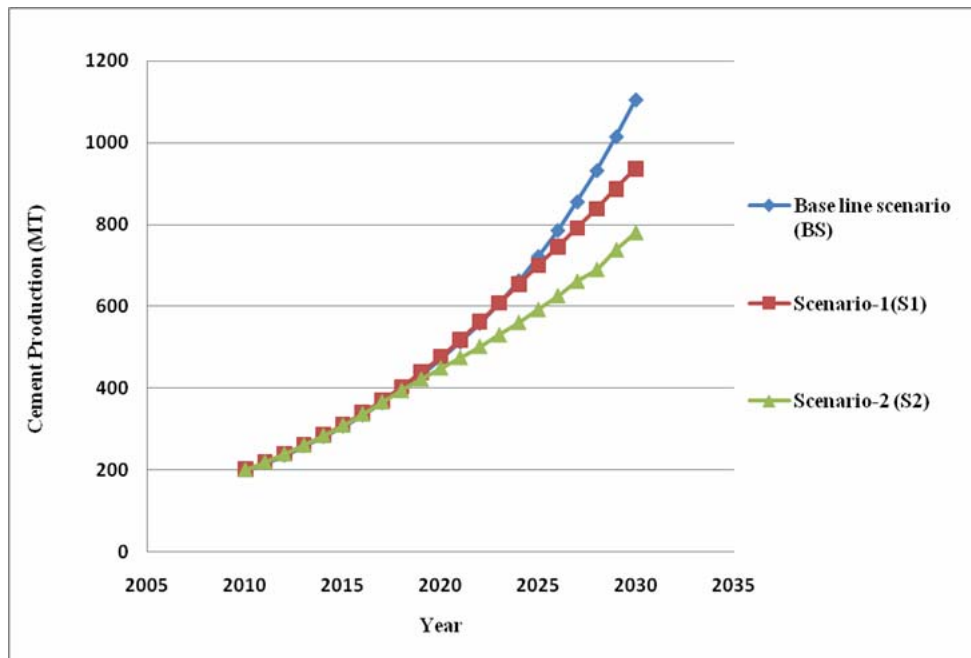


Fig. 6.11 Projections of cement production for the baseline scenario (BS), scenario-1 (S1) and scenario-2 (S2).

Table 6.6 Projection of population of India under the baseline scenario (BS), scenario-1 (S1) and scenario-(S2)

Year	Base line Scenario (BS)	Scenario-1 (S1)	Secenario-2 (S2)
2010	1170.6	1170.6	1170.6
2011	1186.05	1186.93	1185.93
2012	1201.71	1201.35	1201
2013	1217.57	1217.57	1215.77
2014	1233.64	1233.64	1230.24
2015	1249.93	1249.93	1258.45
2016	1266.43	1266.43	1258.45
2017	1283.14	1283.14	1272.29
2018	1300.08	1300.08	1281.19
2019	1317.24	1317.24	1287.6
2020	1334.63	1334.63	1291.46
2021	1352.25	1352.25	1291.46
2022	1370.1	1349.54	1291.46
2023	1388.18	1361.69	1291.46
2024	1406.5	1371.22	1291.46
2025	1425.07	1378.08	1291.46
2026	1443.88	1382.21	1291.46
2027	1462.94	1384.97	1291.46
2028	1482.25	1386.36	1291.46
2029	1501.82	1386.36	1291.46
2030	1521.64	1386.36	1291.46

Table 6.7 Projection of cement production for the baseline scenario (BS), scenario-1 (S1) and scenario-2 (S2)

Year	Baseline scenario (BS)	Scenario-1 (S1)	Scenario-2 (S2)
2010	201	201	201
2011	218.09	219.66	219.66
2012	236.62	239.98	239.8
2013	259.59	261.99	261.53
2014	282.69	285.87	284.93
2015	307.85	311.77	310.12
2016	335.25	339.85	337.36
2017	365.05	370.26	366.72
2018	397.5	403.2	394.57
2019	432.96	438.84	422.37
2020	471.49	477.39	449.79
2021	513.46	518.93	475.27
2022	559.15	562.65	502.19
2023	608.92	608.5	530.64
2024	663.11	654.73	560.69
2025	722.13	700.85	592.45
2026	786.4	746.35	626.01
2027	856.39	792.75	661.47
2028	932.61	839.84	689.94
2029	1015.6	887.41	738.52
2030	1106	937.68	780.36

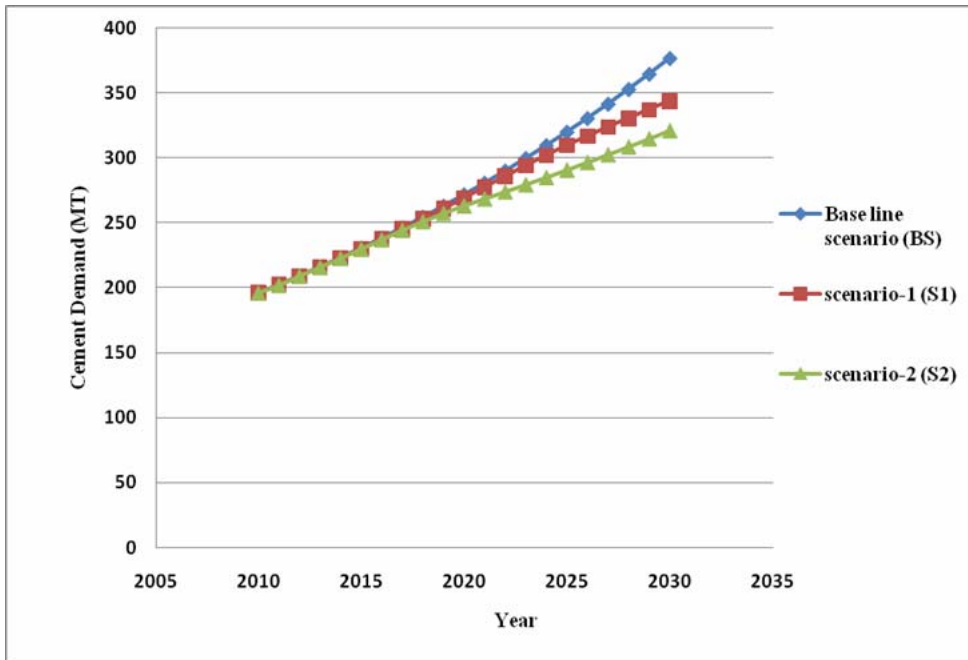


Fig. 6.12 Projections of cement demand for the baseline scenario (BS), scenario-1 (S1) and scenario-2 (S2).

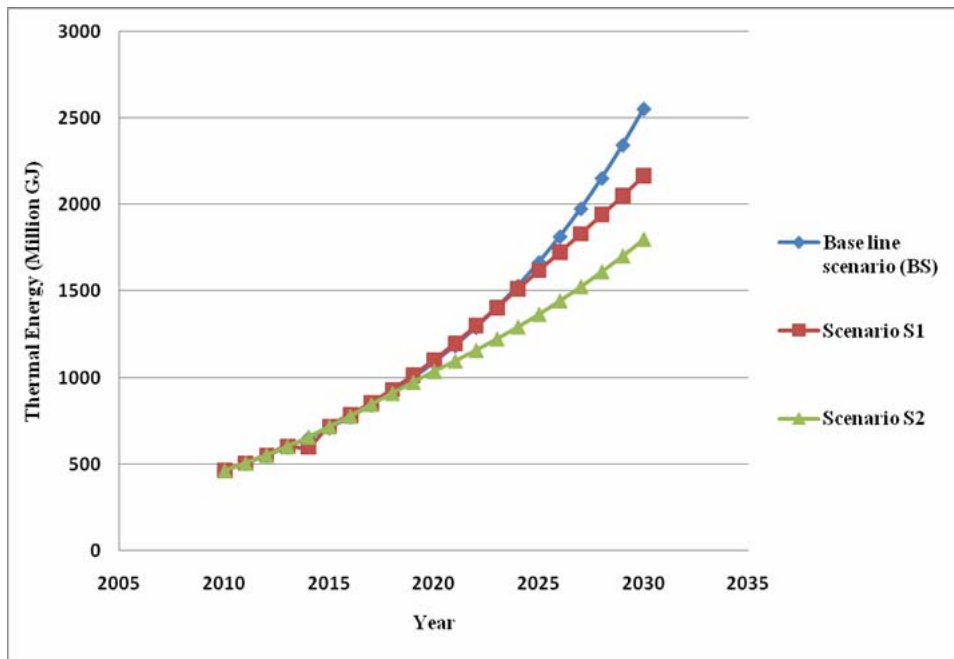


Fig. 6.13 Projections of thermal energy consumption for the baseline scenario (BS), scenario-1 (S1) and scenario-2 (S2).

Table 6.8 Projection of cement demand for the baseline scenario (BS), scenario-1 (S1) and scenario-2 (S2)

Year	Baseline scenario (BS)	scenario-1 (S1)	scenario-2 (S2)
2010	196.12	196.12	196.12
2011	202.5	202.4	202.1
2012	209.5	209.1	209.1
2013	216.18	216.1	215.86
2014	223.35	223.03	222.75
2015	230.77	230.23	229.77
2016	238.43	237.62	236.96
2017	246.35	245.2	244.3
2018	254.53	252.98	250.9
2019	262.98	260.95	257.17
2020	271.71	269.11	263.09
2021	280.73	277.46	268.35
2022	290.05	285.78	273.72
2023	299.68	294.07	279.19
2024	309.63	302.01	284.77
2025	319.91	309.56	290.47
2026	330.53	316.68	296.29
2027	341.5	323.64	302.2
2028	352.84	330.44	308.25
2029	364.55	337.05	314.41
2030	376.66	343.79	320.7

Table 6.9 Projection of thermal energy consumption for the baseline scenario (BS), scenario-1 (S1) and scenario-2 (S2)

Year	Base line scenario (BS)	Scenario-1 (S1)	Scenario-2 (S2)
2010	464.31	464.31	464.31
2011	505.6	507.4	507.4
2012	550.63	554.3	553.93
2013	599.64	605.2	604.13
2014	653.01	600.3	658.19
2015	711.13	720.1	719.37
2016	774.42	785.03	779.3
2017	843.34	855.3	847.11
2018	918.4	931.3	911.47
2019	1000.14	1013.7	975.68
2020	1089.15	1102.7	1039.03
2021	1186.08	1198.7	1097.88
2022	1291.64	1299.7	1160.66
2023	1406.6	1405.6	1225.77
2024	1531.79	1512.4	1295.2
2025	1668.12	1618.9	1368.59
2026	1816.58	1724.08	1446.08
2027	1978.25	1831.22	1527.99
2028	2154.32	1940.03	1614.45
2029	2346.05	2049.9	1705.9
2030	2554.85	2166.03	1802.62

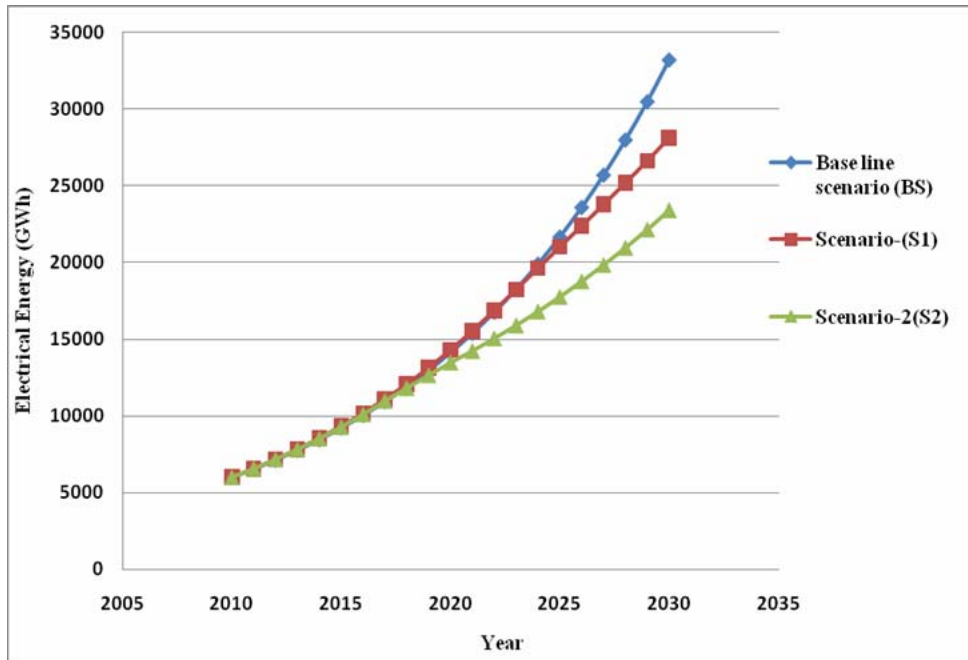


Fig. 6.14 Projections of electrical energy consumption for the baseline scenario (BS), scenario-1 (S1) and scenario-2 (S2).

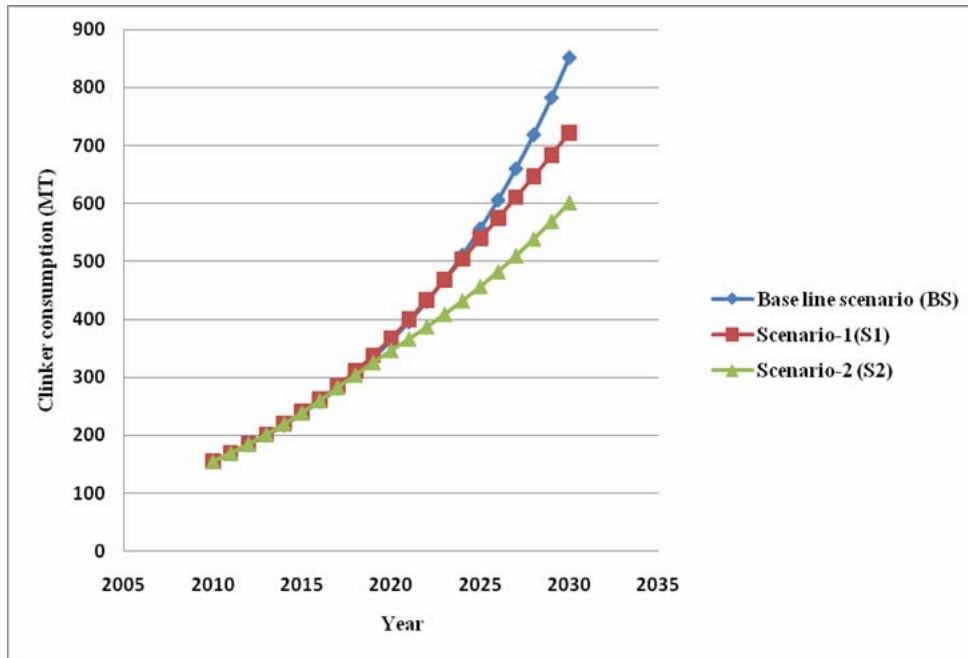


Fig. 6.15 Projections of clinker consumption for the baseline scenario (BS), scenario-1 (S1) and scenario-2 (S2)

Table 6.10 Projection of electrical energy consumption for the baseline scenario (BS), scenario-1 (S1) and scenario-2 (S2)

Year	Baseline scenario (BS)	Scenario-1 (S1)	Scenario-2 (S2)
2010	6030	6030	6030
2011	6566.6	6589.66	6589.66
2012	7151.1	7197.62	7193.98
2013	7787.55	7857.7	7845.78
2014	8480.64	8576.14	8547.78
2015	9235.42	9353.17	9303.57
2016	10057.37	10195.44	10120.82
2017	10952.4	11107.92	11001.47
2018	11927.2	12095.93	11837.25
2019	12980.7	13165.15	12671.15
2020	14144.78	14321.61	13493.83
2021	15403.66	15567.79	14258.15
2022	16774.5	16879.42	15065.76
2023	18267.53	18254.96	15919.11
2024	19898.34	19641.78	16820.81
2025	21663.84	21025.5	17773.57
2026	23591.9	22390.59	18780.3
2027	25691.61	23782.48	19844.05
2028	27978.16	25195.23	20968.06
2029	30468.22	26622.34	22155.73
2030	33179.89	28130.28	23410.68

Table 6.11 Projection of clinker consumption for the baseline scenario (BS), scenario-1 (S1) and scenario-2 (S2)

Year	Baseline scenario (BS)	Scenario-1 (S1)	Scenario-2 (S2)
2010	154.77	154.77	154.77
2011	168.54	169.13	169.13
2012	183.54	184.79	184.65
2013	199.9	201.7	201.38
2014	217.67	220.12	219.4
2015	237.64	240.66	238.79
2016	258.14	261.68	259.77
2017	281.11	285.1	282.37
2018	306.13	310.46	303.82
2019	333.38	337.91	325.23
2020	363.05	367.59	346.34
2021	395.36	399.57	365.96
2022	430.55	433.24	386.89
2023	468.87	468.51	408.59
2024	510.6	504.14	431.7
2025	556.04	539.65	456.19
2026	605.53	574.69	482.03
2027	659.42	610.42	509.33
2028	718.11	646.68	538.18
2029	782.02	683.31	568.66
2030	851.62	722.01	600.87

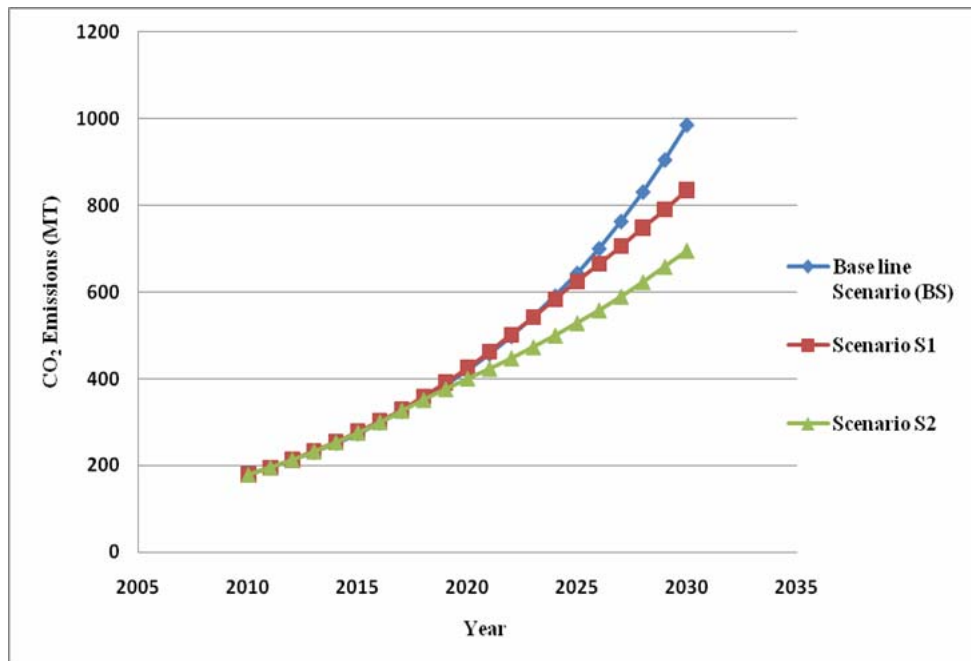


Fig. 6.16 Projections of CO₂ emissions for the baseline scenario (BS), scenario-1 (S1) and scenario-2 (S2)

CO₂ emissions from cement plants are dependent on many interrelated variables viz. population and GDP growth rate, cement demand and production, clinker consumption and energy utilised. In the baseline scenario (BS) with constant of population growth rate, an increase in trend of cement production, energy consumption and thus CO₂ emissions were observed. Compared to the baseline scenario (BS) a reduction in cement production, energy consumption and thus CO₂ emissions from the cement industries were observed in scenario-1 (S1). In this scenario population growth rate was gradually decreased to zero in the year 2030. A further reduction in cement production, energy consumption and CO₂ emissions were observed in scenario-2 (S2) in which population growth rate stabilized prior to scenario-1 (S1). Therefore, controlling the population growth is one of the option for mitigation of CO₂ emissions in Indian cement industries.

Table 6.12 Projection of CO₂ emissions for the baseline scenario (BS), scenario-1 (S1) and scenario-2 (S2)

YEAR	Baseline Scenario (BS)	Scenario-1 (S1)	Scenario-2 (S2)
2010	179.08	179.08	179.08
2011	195.02	195.7	195.7
2012	212.39	213.81	213.65
2013	231.28	233.42	233.01
2014	251.86	254.7	253.86
2015	274.28	277.77	276.3
2016	298.69	302.79	300.57
2017	325.27	329.89	326.72
2018	354.22	359.23	351.55
2019	385.74	390.98	376.31
2020	420.08	425.33	400.74
2021	457.5	462.34	423.44
2022	498.18	501.29	447.43
2023	542.5	542.14	472.77
2024	590.8	583.33	499.55
2025	643.38	624.42	527.84
2026	700.34	664.96	557.74
2027	763	706.3	589.33
2028	830.9	748.25	622.71
2029	904.85	790.64	657.99
2030	985.38	835.42	695.26

6.8.3 Energy management scenario

Fig.6.19 shows the flow diagram of the system dynamic model for cement sector under energy management scenario. In this scenario, the combined effect of 38% thermal energy recovered from waste heat streams and 25% of electrical energy supply to the cement plants is replaced by renewable energy were studied. Fig 6.17 shows the annul projection of CO₂ emissions under energy management scenario. The results show that the CO₂ emissions in 2030 declines to 915.47 million tonnes (7.1%) for base line scenario, 744.15 million tonnes (10.9 %) in Scenario-1 (S1) and 617.64 million tonnes in Scenario-2 (S2) (11.16%). Fig 6.18 shows the outcome of the energy managemet policy option for the base line scenario (BS) and scenario-1(S1) and scenario-2 (S2).

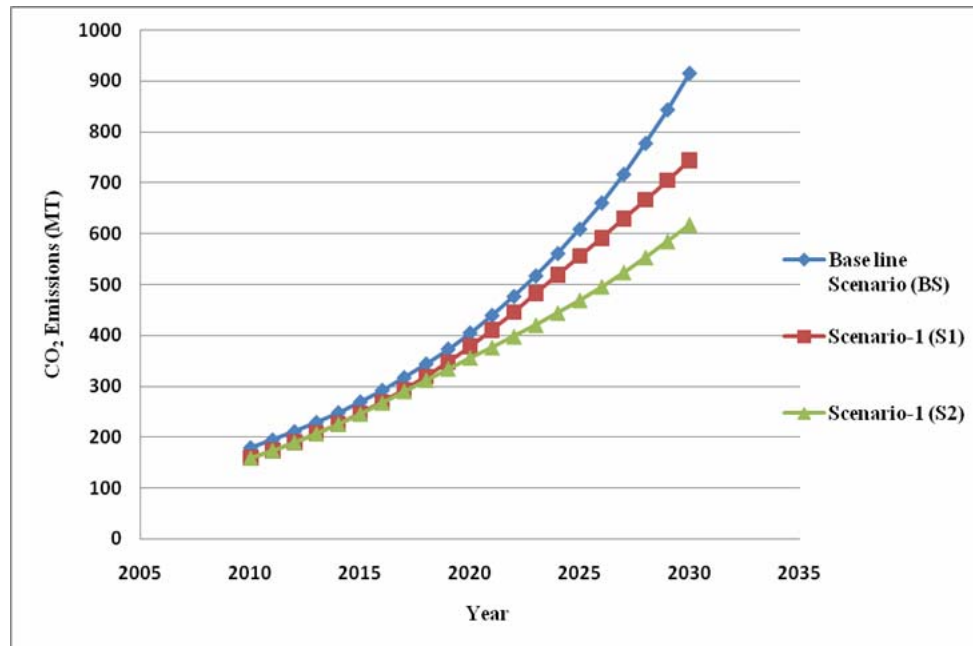


Fig. 6.17 Annual projections of CO₂ emissions from the cement industry for energy management scenario; the combined effect of 38% of thermal energy recovery from waste heat streams (WHRS) and 25% contribution of electrical energy from the renewable source of energy are taken into account

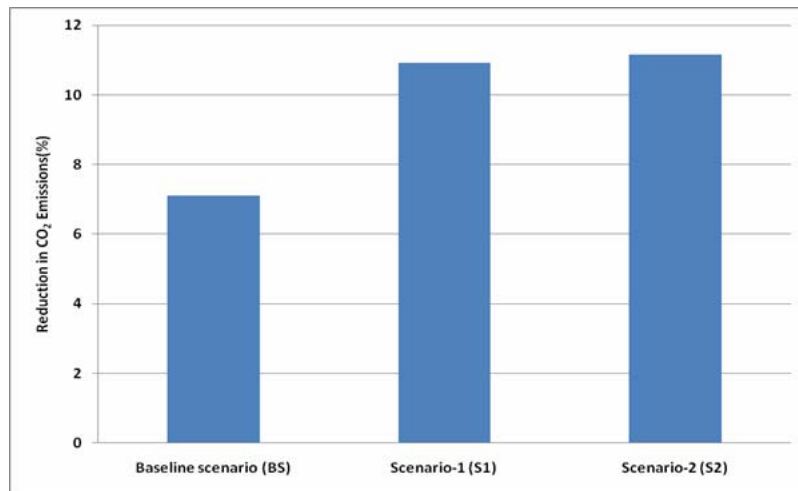


Fig. 6.18 Percent reduction in CO₂ emissions from the cement industry for energy management scenario; the combined effect of 38% of thermal energy recovery from waste heat streams(WHRS) and 25% contribution of electrical energy from the renewable source of energy are taken into account. The baseline scenario (BS), scenario-1 (S1) and scenario-2 (S2) are shown separately

In analyzing the energy management scenario, it was observed that further improvements were made in fuel and electricity savings by waste heat recovery and use of renewable energy. A drastic decline in CO₂ emissions were found in all the three scenarios. Without considering waste heat recovery and renewable energy, the baseline scenario shows that the projection of CO₂ emissions would reach 985.38 million tonnes (Table 6.12) in the year 2030. It was also observed in the combined scenario with population stabilization by the year 2020, 25% contribution from renewable energy and 38% thermal energy from waste heat streams, the CO₂ emissions would reach 617.64 million tonnes (Table 6.13) in the year 2030. From the CO₂ emissions projection, it follows that if the energy recovery and renewable energy options are adopted completely in Indian cement industry, there is a reduction possible of CO₂ emissions about 37% in the year 2030. This could be a considerable lowering of greenhouse gas load to the atmosphere.

Table 6.13 Projection of CO₂ emissions for energy management scenario

YEAR	Baseline Scenario (BS)	Scenario-1 (S1)	Scenario-2 (S2)
2010	179.08	159.09	159.09
2011	194.3	173.85	173.85
2012	210.82	189.94	189.8
2013	228.74	207.36	206.99
2014	248.14	226.26	225.52
2015	269.28	246.76	245.45
2016	292.16	268.98	267.02
2017	317	293.06	290.25
2018	343.94	319.12	312.3
2019	373.18	347.33	334.3
2020	404.9	377.84	356
2021	439.31	410.72	376.17
2022	476.66	445.33	397.48
2023	517.17	482.62	419.99
2024	561.13	519.2	443.78
2025	608.83	555.71	468.92
2026	660.58	591.73	495.48
2027	716.73	629.45	523.54
2028	777.65	666.72	553.2
2029	843.75	704.37	584.53
2030	915.47	744.15	617.64

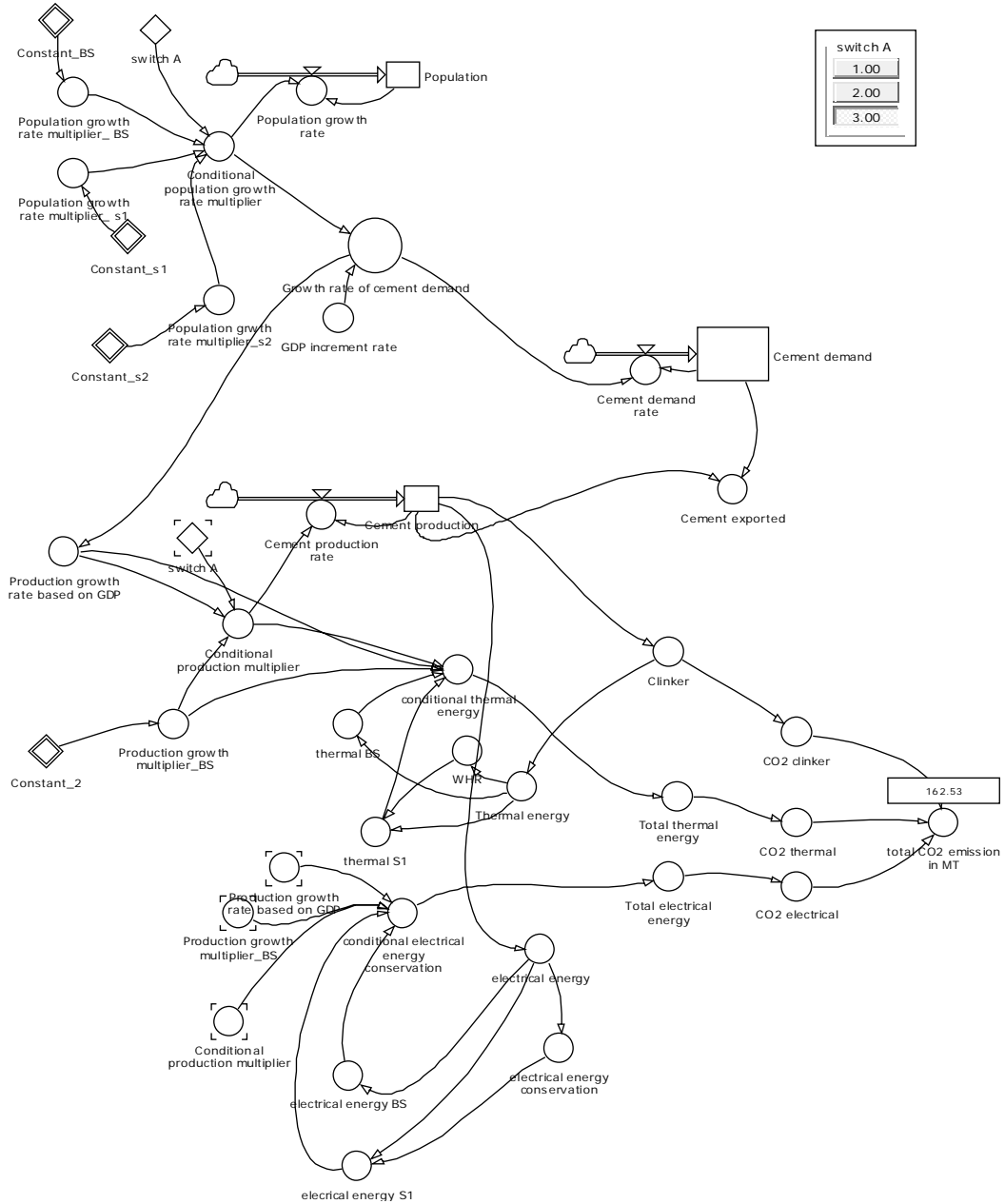


Fig.6.19 Flow diagram of the system dynamic model for cement sector under energy management scenario

6.9 Conclusion

The base model for projection of CO₂ emissions for the selected cement industries in India was developed. The base model was modified and applied to project CO₂ emissions from cement production in India for a span of 21 years with different scenario. The cement production with base line scenario is projected to contribute 985.38 million tonnes of CO₂ by the year 2030. The mitigation strategies for the reduction of CO₂ emissions from the cement production are identified and analyzed. The CO₂ emissions from cement plants are dependent on many interrelated variables viz population and GDP growth rate, cement demand and production, clinker consumption and energy utilised. The combined scenario with population stabilization by the year 2020, 25% of contribution from renewable energy sources of the cement industry and 38 % thermal energy from waste heat streams can reduce CO₂ emissions from indian cement industry approximately by 37 % in the year 2030. This could be a substantial lowering of greenhouse gas load to the environment.

.....❧.....

SUMMARY AND CONCLUSIONS

<i>Contents</i>	7.1 <i>Introduction</i>
	7.2 <i>Conclusions</i>
	7.3 <i>Scope for Future Work</i>

7.1 Introduction

The cement industry is one of the oldest and core industrial sector in India. It is a highly capital and energy intensive industry. It is also an air polluting process due to the evolution of considerable amount of CO₂. Energy consumption by the cement industry is estimated about 2% of the global primary energy consumption, and almost 5% of the total global industrial energy consumption (WEC, 1995). In cement plants, carbon dioxide is generated by three means: consumption of thermal energy due to primary use of carbon intensive fuels, consumption of electrical energy generated by thermal power stations and calcination of limestone in the clinker making process. With the above configuration, a large capacity dry process cement plant (> 3500 tonnes of clinker per day) consumes about 715 kcal/kg clinker and 80 – 90 kWh/tonne while producing ASTM Type I and Type II cement (Ordinary Portland Cement or OPC) respectively. In a cement plant with commonly used modern technology and equipment, carbon dioxide generation should be in the order of about 0.825 kg CO₂ per kg of OPC. Out of the total CO₂ emissions, the contribution from thermal energy consumption, electrical energy consumption, and process of

calcination are about 28%, 9% and 63%, respectively. Improving energy efficiency in a cement plant should be approached from several directions.

Recently, there is a growing interest in the use of both the energy analysis and exergy analysis assessments for energy utilization to save energy and thereby achieve financial savings. The exergy method of thermodynamic analysis is based upon both the first and the second laws of thermodynamics together, while the energy analysis is based upon the first law only. It is a feature of the exergy concept to allow quantitative assessment of energy degradation. In this study, the energy analysis of the typical cement plant was conducted to examine the various energy losses in the important areas like raw mill and the kiln system and proposed a waste heat recovery system to recover heat from the exhaust gas from the kiln system. The exergy analysis indicates the important areas in which energy degradation occurs in the production process.

In order to understand the natural factors which affect the change in CO₂ emissions from the cement industries in India, a decomposition analysis was conducted. The plant data from the important selected cement industries in India were collected for the period 2001 - 2010. By analysing the data it was found that CO₂ emissions from these industries increase every year due to the increase in the rate of cement production. For decomposition analysis, the selected cement industries are grouped into A, B and C according to the specific thermal energy consumption. Among the different decomposition methods, the complete decomposition approach was selected for the study, due to the inherent characteristics of equal distribution of the residual term. The natural predetermined factors selected for the decomposition model includes pollution effect, energy intensity effect, structural effect and activity effect.

A model has been developed based on system dynamic approach in order to forecast cement production and related CO₂ emissions from the ten years data of the selected cement industries in India. The credibility of the model was tested with historical data. Finally the model is modified and applied to predict cement production and CO₂ emissions in India under different scenarios up to 2030. Energy management scenario was also performed in the model to find out the reduction in CO₂ emissions.

7.2 Conclusions

The following conclusions were made based on the research work

- The energy and exergy analysis of the raw mill of the typical cement plant indicates that exergy utilisation was even worse than energy utilization. This process represents a big potential for increasing the exergy efficiency. It is clear that a conscious and planned effort is needed to improve exergy utilization in the raw mill.
- The energy analysis of the kiln emphasised the need for identifying the areas of energy saving opportunities. There are areas of serious energy losses, which lead to the drop of thermal performance of the kiln system.
- The conservation technique for improving efficiency was proposed. Waste heat recovery steam generation and secondary shell energy conservation measures were studied. Waste heat recovery steam generation unit can generate up to 7 MW of electricity.

- The secondary shell concept can save up to 6.9% of thermal energy, which is equivalent to percentage margin and energy efficiency of the unit increased by 3 to 4%.
- The above measures increase the available amount of energy or, in other words can decrease the fuel consumption considerably and thus decrease of CO₂ emissions.
- The waste heat recovery and secondary shell concept shows a relatively remarkable improvement over the existing system. It has been suggested that waste heat recovery system must also be incorporated in the design of new industries to minimize energy consumption, manufacturing cost and improve the product quality.
- The exergy analysis accounts for the operation indicating the location of energy degradation in the process. The main cause of irreversibility in the process was due to conversion of chemical energy of fuel to thermal energy in the kiln system.
- It may also be concluded that the energy and exergy analysis reported in this study will provide the investigators with knowledge about how effectively and efficiently a sector uses its energy resources.

The result of decomposition analysis reveals that CO₂ emissions of Indian cement industries depend mainly on economic activity. An increase in economic growth is vital for the development of a country. The major factors that can be controlled to reduce CO₂ emissions in Indian industries are energy intensity effect and pollution coefficient effect.

- Energy savings in the cement sector are possible by energy efficiency improvement and by increased use of blended cements, thereby reducing the demand for energy-intensive clinker. Blending cement with additives reduces the consumption of energy intensive clinker. However, saving potentials are very much determined by indigenous availability of resources commonly used to blend cement, such as blast furnace slags, fly ash, natural pozzolanes, etc. In order to reduce greenhouse gases emissions and to meet uncomprmissible objective of developments we need to concentrate on developing new energy policies. In this context, one policy in terms of reducing CO₂ emissions would be to enhance technical improvement that would enhance energy efficiency. Whenever feasible, energy conservation and reduction of output share of energy-intensive sectors are also important strategies for reducing energy intensity.

The forecasting analysis examined CO₂ emissions reduction potential in India's cement industry through analysis of different scenarios of future cement output and carbon reductions. The CO₂ emissions from cement plants are dependent on many interrelated variables viz population and GDP growth rate, cement demand and production, clinker consumption and energy utilised.

- The base model for projection of CO₂ emissions for the selected cement industries in India was developed and validated the model with hystorical data. The sensitivity analysis of the forecasting model was conducted and found satisfactory. Then the base model was modified and applied to project CO₂

emissions from cement production in India for a span of 21 years with different scenarios. .

- For the baseline scenario the model projected that the cement production in India will reach 1106.54 MT by the year 2030. The CO₂ emissions are estimated to reach 985.38 MT by the year 2030. Cement demand projected for the year 2030 is 376.66 MT and this value is comparable to that of 387 MT in 2031 (Monica and Mukherjee, 2010).
- In the scenario-1 the population would stabilize by the year 2030. The cement demand will then be 343.19 MT, a reduction of 8.7% of the base line scenario. It is found that the cement production decreased to 937.68 MT for the year 2030 and the CO₂ emissions reduced to 15.22% (835.42MT) compared to baseline scenario.
- In the scenario-2 the population would stabilize by the year 2020 and remain constant. It is found that cement production is projected to reach 780.35 MT by the year 2030 and the CO₂ emissions reduced to 29.44% (695.26MT) compared to baseline scenario.
- In the energy management scenario, the effect of 38 % thermal energy recovered from waste heat streams and 25 % of electrical energy supply to the cement plants replaced by renewable energy revealed that the CO₂ emissions in 2030 declines to 915.47 MT (7.1%) for base line scenario, 744.15 MT (10.9 %) to scenario-1 and 617.64 MT in scenario-2 (11.16%).

- The combined scenario with population stabilization by the year 2020, 25% of contribution from renewable energy sources of the cement industry and 38% thermal energy from waste heat streams can reduce CO₂ emissions from Indian cement industry to approximately 37% in the year 2030. This could be a substantial lowering of greenhouse gas load to the environment.
- The cement industry will remain one of the critical sectors for India to meet its CO₂ emissions reduction target. India's cement production will continue to grow in the near future due to its GDP growth. The control of population is one of the best option to mitigate CO₂ emissions from Indian cement industries. India's CO₂ emissions from the cement industry will rise with increased cement production, especially if there is no significant efficiency improvement in the cement production process not taken into consideration. Use of renewable energy in place of electricity is another option to reduce CO₂ emissions from Indian cement industry.
- Apart from the conventional options, CO₂ capture and storage is more efficient and technologically feasible approach to further mitigate the CO₂ emissions generated during cement manufacturing process.
- Significant energy savings and CO₂ emissions reduction potential of India's cement industry is mainly attributed to the large quantity of cement production.

7.3 Scope for Future Work

- The exergy analysis of the cement plant identifies areas in the process where irreversibility exists and allows the quantification of work that result from irreversibility. If economic environment is introduced by establishing prices for these losses at various places in the process, the researchers can concentrate on the areas that are important economically as well as thermodynamically in a single step.
- It was found that around 2/3 of the CO₂ from a cement process comes from the actual decomposition of the raw materials. Cement processes require a high temperature energy source to drive the chemical reactions to form cement clinker. This produces an excess of energy at low temperature and results in significant sensible heat within the flue gases. This excess heat could be balanced with the sensible heat required for regenerating the solvent within a potential carbon capture plant. So researchers are recommended to make a study to forecast CO₂ emissions from the cement industries in India with integrated carbon capture and compare it with the results for the option without carbon capture.

.....*SCQR*.....



References

- [1] Adem Atmaca, Mehmet Kanoglu (2012): 'Reducing energy consumption of a raw mill in cement industry', *Energy*, Vol.42, No.1, pp. 261–269.
- [2] Adia Bosoage, Ondrej Masek, John E Oakey (2009): 'CO₂ capture Technology for Cement Industry', *Energy Procedia*, Vol.1, pp. 133-140
- [3] Ahmet Kolip (2010): 'Energy and exergy analyses of a serial flow four cyclone Stages precalciner type cement plant', *Scientific Research and Essay*, Vol. 5, No.18, pp. 2702-2712.
- [4] Al-Gandoor A, Phelan P E, Villalobos R, Jaber J O (2010): 'Energy and exergy utilizations of the U.S. manufacturing sector', *Energy*, Vol.35, No.7, pp.3048–3065.
- [5] Al-Hinti, Al-Ghandoor A., Al-Naji A , Abu-Khashaneh M ,Jougeh M , Al-Hattab M (2008): 'Energy Saving Opportunities through Heat Recovery from Cement Processing Kilns: A Case Study', 3rd IASME/WSEAS Int. Conf. on Energy & Environment, University of Cambridge, UK, February 23-25, 2008.
- [6] Alie C, Backham L., Croiset E and Douglas P. L (2005): 'Simulation of CO₂ Capture Using MEA Scrubbing: A Flow sheet Decomposition Method', *Energy Conversion and Management*, Vol. 46, No. 3, pp 475-487.
- [7] Ali M.B., Saidu R.,Hossain M.S (2011): 'A Review on Emission Analysis in Cement Industries', *Renewable and Sustainable Energy Reviews Vol.15*, pp.2252 - 2261
- [8] Aljundi I. H (2009): 'Energy and Exergy Analysis of a Steam Power Plant in Jordan', *Applied Thermal Engineering*, Vol. 29, No.2-3, pp. 324-328.

References

- [9] Anand, S., Dahiya, R.P. and Vrat, P (2005): 'Investigations of methane emissions from rice cultivation in Indian context', *Environment International*, Vol.31, pp.469-482.
- [10] Ang B.W (1996): 'Decomposition of Industrial energy consumption: The energy coefficient approach', *Energy Economics*, Vol.18, pp.129-143.
- [11] Ang, B.W. and S.Y. Lee (1994): 'Decomposition of industrial energy consumption-some methodological and application issues', *Energy economics*, Vol.16, pp.83-92.
- [12] Ang, B.W (1995): 'Decomposition methodology in industrial energy demand analysis', *Energy International J.*, Vol.20 pp.1081-1095.
- [13] Architradi Priambodo, Kumar. S (2001): 'Energy Use and CO₂ emission of Indonesian Small and Medium Scale industries', *Journal of Energy Conversion Management*, Vol.42, pp.1335 – 1348.
- [14] Ashenayi, K. and Ramakumar R (1990): 'IRES-A program to design integrated renewable energy system', *Energy*, Vol. 12, pp.1143-1152.
- [15] Balkan F, Colak N, Hepbasli A (2005): 'Performance Evaluation of a Triple-effect Evaporator with Forward Feed Using Exergy Analysis', *Int J Energy Res*, Vol.29 pp.455–470
- [16] Bejan A (1996): 'Entropy generation minimization, the new thermodynamics of finite-size devices and finite-time processes', *Journal of Applied Physics*, Vol.79, pp. 1191–1218.
- [17] Bejan, A (1988): 'Advanced Engineering Thermodynamics', A Wiley – Interscience Publication, John Wiley & Sons.
- [18] Boyd, G., Hanson, D. and Sterner, T (1988): 'Decomposition of changes in energy intensity: a comparison of the Divisia index and other methods', *Energy Economics*, Vol.10, pp. 309-312.

- [19] Brian Dyson, Ni-Bin Chang (2005): 'Forecasting municipal solid waste generation in a fast growing urban region with system dynamics modelling', *Journal of Waste Management*, Vol. 25, No.7, pp. 669-679.
- [20] Bundela P.S. and Vivek Chawla (2010): 'Sustainable Development through Waste Heat Recovery', *American Journal of Environmental Sciences*, Vol.6, No.1, pp. 83-89.
- [21] Carlos de Castro, Luis Javier Miguel, Margarita Mediavilla (2008): 'World Energy-economy scenarios with system dynamics modelling', *VII annual international ASPO conference October 20-21, 2008 world trade centre, Barcelona*.
- [22] CEMBUREAU(European Cement Association) 2011. Activity Report2010. http://www.cembureau.eu/sites/default/files/Activity_Report_2010.pdf
- [23] Cement Manufacturers' Association (1964), *50 Years- The Cement Industry in India 1914 -1964*, New Delhi.
- [24] Cement Manufacturers' Association (2007, 2006, 2005), *Indian Cement Industry- At a Glance (Various Years)*, New Delhi.
- [25] Cement Manufactures' Association (2010), *Indian Cement Industry, Annual report*, New Delhi
- [26] Cement, Cement industry; 2010. Online at: <http://www.emtindia.net/process/cement/pdf/industry%20overview%20%20Cement.pdf>[accessed 10 August 2010].
- [27] Choucri N., Heye C and Lynch M (1990): 'Analyzing oil production in developing countries: a case study of Egypt', *The Energy Journal*, Vol 11, No 3, pp. 91-115.
- [28] Claudia Sheinbaum and Leticia Ozawa (1998): 'Energy Use and Emissions for Mexico's cement Industry', *Energy*, Vol. 23, No. 9, pp.725-732.
- [29] Cornelissen, R. L. (1997): 'Thermodynamics and Sustainable Development: The Use of Exergy Analysis and the Reduction of Irreversibility', PhD Thesis, University of Twente, Netherlands.

- [30] Dincer I and Rosen M. A (2009): 'Exergy Analysis of Waste Emissions,' *International Journal of Energy Research*, Vol. 23, No. 13, pp. 1153-1163.
- [31] Dincer I, Hussain M, AL-Zaharnah I (2003): 'Energy and exergy use in the industrial sector of Saudi Arabia', *Proceedings of the Institution of Mechanical Engineers Part A: Journal of Power and Energy*, Vol 217, No.5, pp.481-92.
- [32] Dincer I, Hussain MM, Al-Zaharnah I (2004): 'Energy and exergy use in public and private sector of Saudi Arabia', *Energy Policy*, Vol.32 No.141 pp.1615-24.
- [33] Dennis and Van (2009): 'Carbon Capture and Storage opportunities in the Australian Industrial Processes sector', *Energy Procedia*, Vol.1, pp.109-116.
- [34] Emad Benhelal, Gholamreza Zahedi, Haslenda Hashim (2012): 'A novel design for green and economical cement manufacturing', *Journal of Cleaner Production*, Vol.22, pp. 60-66.
- [35] Engin T, Ari V (2005): 'Energy auditing and recovery for dry type cement rotary kiln systems—a case study', *Energy Conversion Management*, Vol.46, pp.551-562.
- [36] Environment Agency (2005) Measuring environmental performance, Sector report for cement industry Environment Agency Almondsbury, Bristol www.environment-agency.gov.uk.
- [37] Fisher-Vanden, Karen, Jefferson, Gary H., Liu, Hongmei, Tao, Quan, (2003): 'What is driving China's decline in energy intensity', *Resource and Energy Economic*, Vol.26, pp.77-97.
- [38] Frank P Incropera (2001): *Fundamentals of Heat and Mass Transfer*, Fifth Edition, John Wiley and Sons, New York.
- [39] Ganapathy T, Alagumurthi N., Gakkhar R. P, Murugesan K (2009): 'Exergy Analysis of Operating Lignite Fired Thermal Power Plant,' *Journal of Engineering Science and Technology Review*, Vol. 2, No. 1, pp.123-130.

- [40] Gautam, S.P., Jain R.K., Mohapatra B.N, Joshi S.M., Gupta R.M (2009): 'Energy recovery from solid waste in cement rotary kiln and its environmental impact', *J. Solid Waste Technol. Management*, Vol.24, pp.1187-1198.
- [41] Gielen D, Taylor P (2009): 'Indicators for industrial energy efficiency in India', *Energy Technology*, Vol.85, pp.293-301.
- [42] Gowdy, J.M. and Miller, J.L (1987): 'Technological and demand change in energy use: an input-output analysis', *Environment and Planning*, Vol.19, pp.1387-1398.
- [43] Greening, L. A., W. B. Davis, L. Schipper, and M. Khrushch (1997): 'Comparison of six decomposition methods: Application of aggregate energy intensity for manufacturing in ten IECD countries', *Energy Economics*, Vol.19, pp.375-390.
- [44] Greco, Clement, Guido Picciotti, Renato Barros Greco, and Guilherme Martins Ferreira (2004): 'Fuel Selection and Use', *Innovations in Portland Cement Manufacturing*
- [45] Grossman, G.M., Krueger, A.B (1991): 'Environmental Impacts of a North American Free Trade Agreement', Papers158, Princeton, Woodrow Wilson School—Public and International Affairs.
- [46] Guangyong Yang, Hengshan Wang, Jiping Zhou, and Xinhui Liu.(2012): 'Analyzing and Predicting the Economic Growth, Energy Consumption and CO₂ Emissions in Shanghai', *Energy and Environment Research*, Vol. 2, No. 2, pp.83-91.
- [47] Hankinson, G.A. and Rhys, J.M.W. (1983): 'Electricity consumption, electricity intensity and industrial structure', *Energy Economics*, Vol.5, pp.146-152.
- [48] Hayashi, D., Krey, M (2005): 'CO₂ Emission Reduction Potential of Large-scale Energy Efficiency Measures in Heavy Industry in China, India, Brazil, Indonesia and South Africa',
<http://www.hwwi.org/uploads/tx_wilpubdb/HWWI_Research_Paper_6.pdf>.

- [49] Hendriks C A, Worrell E, Price L, Martin N, Ozawa Media I. (1999): 'Green house gases from cement production', IEA Greenhouse G R&D Programme. Report # PH 3/7. Ecofys, Utrecht, Ed. Frank Kreith, Boca Raton: CRC Press LLC.
- [50] Hepbasli, Zuhul, Oktay. (2006): 'Energy and exergy analysis of a raw mill in a cement production', *Applied thermal Engineering*, Vol.26 pp.2479-2489.
- [51] Howarth, R.B., Schipper, L., Duerr, P.A. and Strom, S. (1991): 'Manufacturing energy use in eight OECD countries: decomposing the impacts of changes in output, industry structure and energy intensity', *Energy Economics*, Vol.13, pp.135-142.
- [52] Hsiao-Tien Pao, Chung-Ming Tsai (2011): 'Modeling and forecasting the CO₂ emissions, energy consumption, and economic growth in Brazil', *Energy*, Vol.36, pp.2450-2458.
- [53] Huang, J.P (1993): 'Industrial energy use and structural change: a case study of the People's Republic of China', *Energy Economics*, Vol.15, pp.131–136.
- [54] Huntzinger D.N., Eatman T.D (2009): 'A life-cycle assessment of Portland cement manufacturing: comparing the traditional process with alternative technologies', *Journal of Cleaner Production*, Vol.17, pp 668 – 675
- [55] IEA (2011), CO₂ Emission and fuel combustion highlights, Paris 15, France. www.iea.org.
- [56] Ipek Tunc G, Serap Turut-Asik, Elif Akbostanc (2009): 'A decomposition analysis of CO₂ emissions from energy use: Turkish case', *Energy Policy*, Vol.37 No.11, pp 4689-4699.
- [57] IPCC (2007), Revised 1996 IPCC Guidelines for National Greenhouse Gas Inventories (1996 IPCC Guidelines), IPCC, Bracknell, UK.
- [58] Ishikawa K. (2005): 'Evaluation of the environmental impact from several viewpoints – a case study of Ecocement',. *Journal of Kaname Osamu Hosei University Graduate School of Engineering*, Vol.46, pp.10–17.

- [59] Jan Dejaa, Alicja Uliasz-Bochenczykb, Eugeniusz Mokrzyckib (2010): 'CO₂ emissions from Polish cement industry', *International Journal of Greenhouse Gas Control*, Vol.4, pp.583-588.
- [60] Jayant Sathaye, Lynn Price, Stephane de la Rue du Can, and David Fridley (2005) 'Assessment of Energy Use and Energy Savings Potential in Selected Industrial Sectors in India', *Energy Analysis Department Environmental Energy Technologies Division*, Ernest Orlando Lawrence Berkeley National Laboratory, Report number LBNL-57293
- [61] Jiang Jinhe (2011): 'An Evaluation and Decomposition Analysis of Carbon Emissions in China', *[J].Resources Science*, Vol.33 No.4, pp.597-604.
- [62] Jing Ke , NinaZheng, David Fridley, Lynn Price, Nan Zhou (2012): 'Potential energy savings and CO₂ emissions reduction of China's cement industry', *Energy Policy*, Vol.45, pp.739–775.
- [63] Juchen Li., Dong., X, Shangguan J., Hook M (2011): 'Forecasting the growth of China's natural gas consumption', *Energy*; Vol.36: pp.1380 - 1395.
- [64] Kaantee, U., Zevenhove, R., Backman, R., Hupa, M (2004): 'Cement manufacturing using alternative fuels and the advantages of process modeling', *Fuel Processing Technology*, Vol.85, pp.293-301.
- [65] Kabir G.,Abubakar A.I.,El-Nafaty U.A (2010): 'Energy audit and conservation opportunities for pyroprocessing unit of a typical dry process cement plant', *Energy*, Vol.35, pp.1237–1243.
- [66] Kamate S. C., Gangavati P. B (2009): 'Exergy Analysis of Cogeneration Power Plants in Sugar Industries', *Applied Thermal Engineering*, Vol. 29, No. 5-6, pp. 1187- 1194.
- [67] Karwa D V, Sathya J, Gadgil A, Mukhopadhyay M (1998): 'Energy efficiency and environmental management options in the Indian cement industry' ADB Technical Assistance Project (TA:2403-IND), ERI, Forest Knolls Calif.

- [68] Khaliq A (2009): 'Exergy Analysis of Gas Turbine Trigenation System for Combined Production of Power Heat and Refrigeration', *Refrigeration*, Vol. 32, No. 3, pp. 534-545.
- [69] Khurana S, Rangan B, Uday G (2002): 'Energy balance and cogeneration for a cement plant', *Applied Thermal Engineering*, Vol. 22, pp.485-94.
- [70] Kolip, A., Uzturk, I.T, Arikol M (1990): 'Energy and Exergy Analysis for Cement Factory', In: *Proceedings of the Workshop on Second Law of Thermodynamics*, Erciyes University and Turkish Soc. Thermal Sci. and Tech.(T.S.T.S.T), Kayyseri, Turkey.
- [71] Koroneos C, Spachos T and Moussiopoulos N (2003): 'Exergy Analysis of Renewable Energy Sources,' *Renewable Energy*, Vol. 28, No. 2, pp. 295-310.
- [72] Koroneos C., Roumbas G., Moussiopoulos N (2005): 'Exergy analysis of cement production', *International Journal of Exergy 2005 - Vol. 2, No.1, pp. 55 - 68.*
- [73] Kotas, T. J (1985): 'The Exergy Method of Thermal Plant Analysis', Butterworths: Anchor Brendon Ltd.
- [74] Kothandaraman C P, S Subramanyan (2004): Heat and Mass Transfer Data Book, Seventh Edition, New Age International Pvt. Ltd, New Delhi.
- [75] Laszlo Szaba, Ignacia Hidalgo, Juan Carlos, Antonia Soria (2006): 'CO₂ Emission Trading within European Union and Annex B countries; the Cement Industry Case', *Journal of energy*, Vol. 34, pp.72-87.
- [76] Lee, K. and W. Oh (2006): 'Analysis of CO₂ emissions in APEC countries: A time-series and a cross-sectional decomposition using the log mean Divisia method', *Energy Policy*, Vol.34, No.17 pp.2779-2787.
- [77] Li Wei, Yang Gang (2010): 'A Study on the Sustainable Development of Energy Consumption in Shanxi Province Based on System Dynamics', *[J].Resources Science*, Vol.32, No.10, pp.1871-1877.

- [78] Li Yanmei, Yang Tao (2011): 'Structural Decomposition Analysis of Decline in CO₂ Emissions Intensity in China: Input-output Analysis Based on the 1997 to 2007', *[J].Resources Science*, Vol.33, No.4, pp 605-611.
- [79] Lise, W (2006): 'Decomposition of CO₂ emissions over 1980-2003 in Turkey', *Energy Policy*, Vol.34, No.14, pp.1841- 1852.
- [80] Liu, X. Q., B. W. Ang and H. L. Ong (1992): 'The application of the Divisia index to the decomposition of changes in industrial energy consumption', *Energy J.*, Vol. 13, pp.161-177.
- [81] Liu F, Ross M, Wang S (1999): Energy efficiency of China's cement industry, *Energy* Vol. 20, No.7, pp.669 – 681.
- [82] Li, J-W., Shrestha, R.M. and Foell, W.K (1990): 'Structural change and energy use: the case of the manufacturing sector in Taiwan', *Energy Economics*, Vol.12, pp.109-115.
- [83] Luciano Charlitade Freitas, Shinji Kaneko (2011) : 'Decomposition of CO₂ emissions change from energy consumption in Brazil: Challenges and policy implications', *Energy Policy*, Vol.39, pp.1495 – 1504.
- [84] Maa C, Zhanga G.Y, Zhanga X.C, Zhoua B, Maoa T.Y (2012): 'Simulation modeling for wetland utilization and protection based on system dynamic model in a coastal city, China', *Environmental Sciences*, Vo.13, pp.202 – 213.
- [85] Madloola N.A., Saidura R., Rahimb N.A., Islama M.R., Hossianb M.S (2012): 'An exergy analysis for cement industries: An overview', *Renewable and Sustainable Energy Review*, Vol.16, pp.921 – 932.
- [86] Masanori Shukuya, Abdelaziz Hammache (2002): 'Introduction to the Concept of Exergy – for a Better Understanding of Low-Temperature-Heating and High-Temperature-Cooling Systems', VTT Research Notes 2158, Vuorimiehentie 5, Finland.

- [87] Mavratas G., Pavlidov S, Hontou V and Diakoulaki D (2000) 'Decomposition analysis of CO₂ emission from Greek Manufacturing sector', *Global Nest: the Int. J.*, Vol 2, No 1, pp 119-127.
- [88] Ministry of Commerce & Industry, Department of Industrial Policy and Promotion (2011). Report of working group on cement industry for XII five year plan http://planningcommission.nic.in/aboutus/committee/wrkgrp12/wgrep_cement.pdf.
- [89] Mintus, F., Hamel, S., Krumm, W (2006): 'Wet process rotary cement kilns: modelling and simulation', *Clean Technologies and Environmental Policy*, Vol.8, pp.112-122.
- [90] Mohanthy B and Mora J. C (1998): 'An overview of rational use of energy in industry', *Proceedings 6th Asian School on Energy*, Asian Institute of Technology, Bangkok, Thailand, 1998.
- [91] Mohapatra P K J., Mandal P, Bora M C (1994): 'Introduction of system Dynamic Modelling', Orient Logman, Hyderabad, India.
- [92] Monica Dutta, Saptarshi Mukherjee (2010): 'An outlook into energy consumption in large scale industries in India: The cases of steel, aluminium and cement', *Energy Policy*, Vol.3, pp.7286-7298.
- [93] Moran, M.J (1999): "Engineering Thermodynamics" *Mechanical Engineering Handbook*.
- [94] Morris D, Szargut J (1996): 'Standard chemical exergy of some elements and compounds on the planet earth', *Energy Conversion and Management*, Vol.2, No.8, pp.733-55.
- [95] Moya, J.A., Pardo, N., Mercier, A (2011): 'The potential for improvements in energy efficiency and CO₂ emissions in the EU27 cement industry and the relationship with the capital budgeting decision criteria', *Journal of Cleaner Production*, Vol.19, pp1207 - 1215.
- [96] Mujumdar, K.S., Ranade, V.V (2006): 'Simulation of rotary cement kilns using a one dimensional model', *Chemical Engineering Research and Design*, Vol.84, pp165-177.

- [97] Nastaran Ansari, Abbas Seifi (2012): 'A system dynamics analysis of energy consumption and corrective policies in Iranian iron and steel industry', *Energy*, Vol.43, pp. 333-343.
- [98] Nicholas B (1990): 'Understanding cement' WHD Microanalysis Consultants Ltd.<http://www.understanding-cement.com/bogue.html>
- [99] Nicola Cantore, Smeeta Fokeer (2011): 'A decomposition analysis of energy intensity for developing countries', Development Policy Statistics And Research Branch, United Nations Industrial Development Organization.
- [100] Niksiar A, Rahimi A (2009): 'Energy and exergy analysis for cocurrent gas spray cooling systems based on the results of mathematical modeling and simulation', *Energy*, Vol.34, pp.14 -21.
- [101] Oggioni G., Riccardi R., Toninelli R (2011): 'Eco-efficiency of the world cement industry: A data envelopment analysis', *Energy Policy*, Vol.39, pp.2842–2854.
- [102] Park, S. H (1992): 'Decomposition of industrial energy consumption', *Energy Economics*, Vol.13, pp.265-270.
- [103] Park, S-H (1982): 'An input-output framework for analysing energy consumption', *Energy Economics* Vol.4, pp.105-110.
- [104] Park, S-H (1992): 'Decomposition of industrial energy consumption: an alternative method', *Energy Economics*, Vol.14, pp.265-270.
- [105] Park, S-H (1993): 'A cross-country decomposition analysis of manufacturing energy consumption', *Energy*, Vol.18, No.8, pp. 843-858.
- [106] Paul S, Bhattacharya R.N (2004): 'CO₂ emission from energy use in India: a decomposition analysis', *Energy policy*, Vol.32, pp.585-593.
- [107] PCA (2008): 'Carbon Dioxide Control Technology Review', *VDZ Research Institute of the Cement Industry and PENTA Engineering Corp.*
- [108] Peray K E (1979): 'Cement manufacturers hand book', *Chemical Publishing Company Inc*, New York.

- [109] Perry R.H, Green D (1984): 'Chemical engineers handbook', McGraw-Hill, New York
- [110] Rasul M G, Widiyanto W, Mohanthy B.(2005): "Assessment of the thermal performance and energy conservation opportunities of a cement Industry in Indonesia": *Applied thermal Engineering*, Vol.25, pp.2950-2965.
- [111] Rehan R, Nehdi M (2005): 'Carbon dioxide emissions and climate change: policy implications for the cement industry', *Environmental Science & Policy*, Vol. 8 pp.105–114.
- [112] Reitler, W.M, Rudolph and Schaefer M. (1987): 'Analysis of the factors influencing energy consumption in industry: a revised method', *Energy Economics*, Vol.9, pp. 145-148.
- [113] Rodriguez, N., Alonso, M., Abanades, J.C., Grasa, G., Murillo, R (2009): 'Analysis of a process the capture the CO₂ resulting from the precalcination of the limestone feed to cement plant', *Energy Procedia*, pp.1141 -1148.
- [114] Rosemann H, Locher F.W, Jeschar R (1987): 'Fuel energy consumption and operational behaviour of rotary cement kiln with precalcining', *Zement –Kalk – Gips.*, No.10, pp.489- 498
- [115] Rosen M A, Dincer I (2004): 'Exergy as a driver achieving sustainability', *Int J Green Energy*, Vol.1, No.1, pp.1–19.
- [116] Rosen M A, Minh N, Le M N, Dincer I (2005): 'Efficiency Analysis of a Cogeneration and District Energy System', *Applied Thermal Engineering*, Vol.25,pp147–159.
- [117] Sanjib Chowdhary and Sahu K.C (1992): 'A System Dynamics Model for the Indian Oil and Gas Exploration/Exploitation Industry', *Technological Forecasting and Social change*, Vol. 42, pp. 63-83.
- [118] Shammakh M, Caruso H, Elkamel A., Croiset E., Douglas, P.L., (2008): 'Analysis and optimization of carbon dioxide emission mitigation options in the cement industry', *American Journal of Environmental Sciences*, Vol.4, No.5, pp.482-490.

- [119] Shuangzhen Wang, Xiaochun Han (2012) ‘Sustainable Cement Production with Improved Energy Efficiency and Emerging CO₂ Mitigation’, *Advances in Chemical Engineering and Science*, Vol.2, pp.123-128.
- [120] Simone Gingrich, Petra Kuskova, JuliaK.Steinberger (2011): ‘Long-term changes in CO₂ emissions in Austria and Czechoslovakia—Identifying the drivers of environmental pressures’, *Energy Policy*, Vol.39, pp.535–543.
- [121] Sogut M.Z., Oktay Z, Hepbasli A (2009): ‘Energetic and exergetic assessment of a trass mill process in a cement plant’, *Energy Conversion and Management*, Vol.50, pp.2316–2323.
- [122] Soule, M.H., Logan,J.S., Stewart,T.A (2002): ‘Trends, Challenges and Opportunities in China’s Cement Industry’,
<http://www.wbcdcement.org/pdf/battelle/china_country_analysis.pdf>.
- [123] Stefano Armenia, Fabrizio Baldoni, Diego Falsini, Emanuele Taibi (2010): ‘System Dynamics Energy Model for a Sustainable Transportation System’,<http://www.systemdynamics.org/conferences/2010/proceed/papers/P1322.pdf>.
- [124] Sudhakara Reddy B, Binay Kumar Ray(2010): ‘Decomposition of energy consumption and energy intensity in Indian manufacturing industries’, *Energy for Sustainable Development*, Vol. 14, pp.35–47.
- [125] Sun J. W (1998): ‘Changes in energy consumption and energy intensity: A complete decomposition model’, *Energy Economics*, Vol.20, pp.85-100.
- [126] Sun, J. W (1999): ‘Decomposition of aggregate CO₂ emission in the OECD: 1960-1995’, *The Energy Journal*, Vol.20, pp.147-155.
- [127] Syed Adnan, Haider Ali, Shah Bukhari and Liaqat Ali (2007): “Derivative of Energy Consumption and Energy strength in Pakistan: An application of Complete Decomposition Model”, *Research Journal Applied Sciences*, Vol. 2, No.4, pp.484-488.

- [128] Szargut J., Morris D.R, Steward F.R (1998): ‘Exergy analysis of thermal and metallurgical process’, *Hemisphere publishing corporation*.
- [129] Torres E.A., W.L.R. Gallo, (1998): ‘Exergetic evaluation of a cogeneration of a petrochemical complex, *Energy Conversion and management*’, Vol.16, No.19, pp.1845-1852.
- [130] Torvanger.A (1991): ‘Manufacturing sector carbon dioxide emissions in nine OECD countries, 1973–87, A divisia index decomposition to changes in fuel mix, emissions coefficient, industry structure, energy intensities and international structure’, *Energy Economics*, Vol.13, pp.168–186.
- [131] Utlu Z, Hepbasli A (2008) ‘Energetic and exergetic assessment of the industrial sector at varying dead (reference) state temperatures: a review with an illustrative example’, *Renewable and Sustainable Energy Reviews*, Vol.12, pp.1277–1301.
- [132] Vedat Ari (2011): ‘Energetic and exergetic assessments of a cement rotary kiln system’, *Scientific Research and Essays*, Vol. 6, No.6, pp.1428-1438.
- [133] Vladimír Hajko(2012): ‘Changes in the Energy Consumption in EU-27Countries’, *Review of economic perspectives*’, Vol.12, No.1, , pp. 3–21.
- [134] Wachsmann, U., Wood, R., Lenzen, M., Schaeffer, R (2009): ‘Structural decomposition of energy use in Brazil from 1970 to 1996’, *Applied Energy*, Vol.86, pp. 578–587.
- [135] Wang J, Dai Y, Gao L (2009): ‘Energy analyses and parametric optimizations for different cogeneration power plants in cement industry’, *Applied Energy*, Vol. 86, pp.941–48.
- [136] WEC (1995) ‘Efficient Use of Energy Utilizing High Technology: An Assessment of Energy Use in Industry and Buildings’, *World Energy Council*, London, United Kingdom.

- [137] Worrell, E., R. Smit, D. Phylipsen, K. Blok, F. van der Vleuten and J. Jansen (1995): 'International Comparison of Energy Efficiency Improvement in the Cement Industry', *Proceedings ACEEE 1995 Summer Study on Energy Efficiency in Industry* (Volume II).
- [138] Worrel E, Nathan Martin, Lynn price (2000); 'Potentials for Energy Efficiency Improvements in U S Cement Industry', *Journal of Energy*, Vol. 25, pp.1169 – 1214
- [139] Worrell, E., Price, L., Martin, N., Hendriks, C., Ozawa Meida, L (2001): 'Carbon dioxide Emissions from the Global Cement Industry', *Annual Reviews of Energy and Environment* Vol.26, No.8, pp.303–329
- [140] World Business Council for Sustainable Development (WBCSD) (2002): *Towards a Sustainable Cement Industry*, WBCSD.
- [141] Yarnal G.S., Puranik V.S (2009): 'Energy Management in Cogeneration of Sugar Industry Using System Dynamic Modelling', *Journal of Cogeneration and Distributed Generation*, Vol.24 pp.7-22.
- [142] Yeonbae Kim, Emst Warrell (2002): 'International Comparison of CO₂ emission trends in iron and steel industry', *Journal of Energy Policy*, Vol.30, pp.827-838.
- [143] Yuren Shi, Lingling Chen, Zhen Liu ,Jianmin Yan, Jian Hu (2012): 'Analysis on the Carbon Emission Reduction Potential in the Cement Industry in Terms of Technology Diffusion and Structural Adjustment: A Case Study of Chongqing', *Energy Procedia*, Vol. 16 pp.121 – 130.
- [144] Zafer Utlu, Ziya Sogut, Arif Hepbasli, Zuhul Oktay (2006): 'Energy and exergy analysis of a raw mill in a cement production', *Applied thermal Engineering*, Vol.26, pp2479-2489.
- [145] Ziya Sogut, Zuhul Oktay and Hikmet Karakoc (2010): 'Mathematical modelling of heat recovery from a rotary kiln', *Applied Thermal Engineering*, Vol.30, pp.817–825.

References

- [146] Ziya Sogut, Zuhul Oktay (2011): ‘Impact assessment of CO₂ emissions caused by exergy losses in the cement sector’ *International Journal of Exergy*, Vol. 9, No.3, pp. 280 - 296.
- [147] Ziya Sogut, Zuhul Oktay, Arif Hepbasli (2009): ‘Investigation of effect of varying dead-state temperatures on energy and exergy efficiencies of a Raw Mill process in a cement plant’, *International Journal of Exergy*, Vol. 6, No.5, pp. 655 - 670.
- [148] Ziya Sogut, Zuhul Oktay.(2009): ‘Energy and exergy analyses in a thermal process of a production line for a cement factory and applications’, *International Journal of Exergy*, Vol. 5, No.2, pp. 218 - 240.
- [149] Ziya Sougt M. (2012): ‘Research on exergy consumption and potential of total CO₂ emission in the Turkish cement sector’, *Energy Conversion and Management*, Vol. 56, pp.37–45.

.....✂.....

ANNEXURES

Annexure A

Chemical compositions of the raw materials and raw meal

Component	Limestone (wt %)	Sweetener Limestone (wt %)	Laterite (wt %)	Raw Meal (wt %)
CaO	45.9	49.28	-	44.2
SiO ₂	14	4.5	8	12.9
Al ₂ O ₃	1.6	1.5	42	3.9
Fe ₂ O ₃	0.6	2.4	30	2.36
MgO	0.6	0.2	-	0.3
SiO ₃	-	-	-	0.3

Chemical compositions clinker

Component	(wt %)
CaO	63.86
SiO ₂	22.2
Al ₂ O ₃	6.8
Fe ₂ O ₃	4.2
MgO	0.8
SiO ₃	0.65
Free lime	1.1
Ignition loss	0.39

Chemical compositions of dust

Component	(wt %)
CaO	63.5
SiO ₂	25.03
Al ₂ O ₃	6.16
Fe ₂ O ₃	4.91
MgO	0.4

Chemical compositions of exhaust gas

Component	(vol %)
CO ₂	26.03
O ₂	4.22
H ₂ O	4.84
SO ₂	0.04
N ₂	64.87

Annexure B

Energy calculation of the raw mill (Production rate of 117 tonnes per hour)

For the energy analysis the reference enthalpy is considered to be zero at 0°C for the calculation. The various input and output energy calculations given as follow.

Input Energy

1. Infiltrated air

Mass flow rate, $m_{ia} = 24114$ kg/hr

Temperature, $T_{ia} = 30^{\circ}\text{C}$

Specific heat, $c_{p_{ia}} = 0.9655$ kJ/kg K

$$\begin{aligned}\text{Infiltrated air heat energy, } Q_{ia} &= m_{ia} \times c_{p_{ia}} \times T_{ia} \\ &= 698431.2 \text{ kJ/hr}\end{aligned}$$

2. Gas

Mass flow rate, $m_g = 96458$ kg/hr

Temperature, $T_g = 30^{\circ}\text{C}$

Specific heat, $c_{p_g} = 1.0812$ kJ/kg K

$$\begin{aligned}\text{Heat energy of gas, } Q_g &= m_g \times c_{p_g} \times T_g \\ &= 37544540.26 \text{ kJ/hr}\end{aligned}$$

3. Limestone

Mass flow rate, $m_l = 96426$ kg/hr

Temperature, $T_l = 30^{\circ}\text{C}$ K

Specific heat, $c_{p_l} = 0.7664$ kJ/kg K

$$\begin{aligned}\text{Heat energy of limestone, } Q_l &= m_l \times c_{p_l} \times T_l \\ &= 2217026.59 \text{ kJ/hr}\end{aligned}$$

4. Sweetener limestone

Mass flow rate, $m_{sl} = 11344$ kg/hr

Temperature, $T_{sl} = 30^{\circ}\text{C}$

Specific heat, $c_{p_{sl}} = 0.7632$ kJ/kg K

$$\begin{aligned}\text{Heat energy of sweetener lime, } Q_{sl} &= m_{sl} \times c_{p_{sl}} \times T_{sl} \\ &= 259732.22 \text{ kJ/hr}\end{aligned}$$

5. Laterite

Mass flow rate, $m_{lt} = 5672$ kg/hr

Temperature, $T_{lt} = 30^{\circ}\text{C}$

Specific heat, $c_{p_{lt}} = 0.745$ kJ/kg K

$$\begin{aligned}\text{Heat energy of laterite, } Q_{lt} &= m_{lt} \times c_{p_{lt}} \times T_{lt} \\ &= 126769.2 \text{ kJ/hr}\end{aligned}$$

6. Material returned from separator

Mass flow rate, $m_{rs} = 234000$ kg/hr

Temperature, $T_{rs} = 78^{\circ}\text{C}$

Specific heat, $c_{p_{rs}} = 0.8142$ kJ/kg K

$$\begin{aligned}\text{Heat energy of material returned from separator, } Q_{rs} &= m_{rs} \times c_{p_{rs}} \times T_{rs} \\ &= 14860778.4 \text{ kJ/hr}\end{aligned}$$

7. Moisture in limestone

Mass flow rate, $m_{ml} = 1929$ kg/hr

Temperature, $T_{ml} = 30^{\circ}\text{C}$ K

Specific heat, $c_{p_{ml}} = 4.178$ kJ/kg K

$$\begin{aligned}\text{Heat energy of moisture in the lime stone, } Q_{ml} &= m_{ml} \times c_{p_{ml}} \times T_{ml} \\ &= 241780.86 \text{ kJ/hr}\end{aligned}$$

8. Moisture in sweetener limestone

Mass flow rate, $m_{sm} = 1361$ kg/hr

Temperature, $T_{sm} = 30^{\circ}\text{C}$

Specific heat, $c_{p_{sm}} = 4.187$ kJ/kg K

$$\begin{aligned}\text{Heat energy of moisture in the sweetener limestone, } Q_{sm} &= m_{sm} \times c_{p_{sm}} \times T_{sm} \\ &= 170587.74 \text{ kJ/hr}\end{aligned}$$

9. Moisture in laterite

Mass flow rate, $m_{lm} = 284$ kg/hr

Temperature, $T_{lm} = 30^{\circ}\text{C}$

Specific heat, $c_{p_{lm}} = 4.187$ kJ/kg K

$$\begin{aligned}\text{Heat energy of moisture in laterite, } Q_{lm} &= m_{lm} \times c_{p_{lm}} \times T_{lm} \\ &= 35596.56 \text{ kJ/hr}\end{aligned}$$

10. Dust

Mass flow rate, $m_d = 2973$ kg/hr

Temperature, $T_d = 360^{\circ}\text{C}$

Specific heat, $c_{p_d} = 0.9971$ kJ/kg K

$$\begin{aligned}\text{Heat energy of dust, } Q_d &= m_d \times c_{p_d} \times T_d \\ &= 1067138.33 \text{ kJ/hr}\end{aligned}$$

11. Heat from electrical energy, $Q_e = 2223$ kW

$$= 8002800 \text{ kJ/hr}$$

Total energy input to the raw mill,

$$\begin{aligned}Q &= Q_{ia} + Q_g + Q_l + Q_{sl} + Q_{lt} + Q_{rs} + Q_{ml} + Q_{sm} + Q_{lm} + Q_d + Q_e \\ &= 65225181.37 \text{ kJ/hr}\end{aligned}$$

Output energy

1. Infiltrated air

Mass flow rate, $m_{ia} = 24114$ kg/hr

Temperature, $T_{ia} = 88^{\circ}\text{C}$

Specific heat, $c_{p_{ia}} = 0.9908$ kJ/kg K

Heat energy of infiltrated air, $Q_{ia} = m_{ia} \times c_{p_{ia}} \times T_{ia}$ -----(A)

$$= 2102514.46\text{kJ/hr}$$

2. Gas

Mass flow rate, $m_g = 96458$ kg/hr

Temperature $T_g = 88^{\circ}\text{C}$

Specific heat, $c_{p_g} = 0.9745$ kJ/kg K

Heat energy of gas, $Q_g = m_g \times c_{p_g} \times T_g$ -----(B)

$$= 8271954.85\text{kJ/hr}$$

3. Steam

Mass flow rate, $m_{st} = 2989$ kg/hr

Temperature, $T_{st} = 88^{\circ}\text{C}$

Specific heat, $c_{p_{st}} = 1.962$ kJ/kg K

Heat energy of steam, $Q_{st} = m_{st} \times c_{p_{st}} \times T_{st}$ -----(C)

$$= 516068.78 \text{ kJ/hr}$$

4. Raw meal

Mass flow rate, $m_{rm} = 350415$ kg/hr

Temperature, $T_{rm} = 88^{\circ}\text{C}$

Specific heat, $c_{p_{rm}} = 0.8232$ kJ/kg K

Heat energy of raw meal, $Q_{rm} = m_{rm} \times c_{p_{rm}} \times T_{rm}$ -----(D)

$$= 25383247.68 \text{ kJ/hr}$$

5. Moisture

Mass flow rate, $m_m = 585$ kg/hr

Temperature, $T_m = 88^\circ\text{C}$

Specific heat, $c_{p_m} = 4.195$ kJ/kg K

Heat energy of moisture, $Q_m = m_m \times c_{p_m} \times T_m$ -----(E)

$$= 215958.6 \text{ kJ/hr}$$

Efficiency of the raw mill, $\eta = \frac{A+B+C+D+E}{\text{Total input energy}}$

$$= 55.94\%$$

7. Heat loss from raw mill

a) Drying room

Inner diameter of drying room, $D_i = 4.2$ m

Outer diameter of drying room, $D_o = 4.28$ m

Length of drying room, $L = 2.5$ m

Drying room temperature, $T_{in} = 133.07^\circ\text{C}$

Surface temperature, $T_s = 72^\circ\text{C}$

Surrounding Temperature, $T_\infty = 30^\circ\text{C}$

Outer surface heat transfer coefficient, $h_a = 5.8$ W/ $\text{W/m}^2\text{K}$

(Film temperature $T_f = 50^\circ\text{C}$

Velocity of air = 2 m/sec

Density of air $\rho = 1.06$ kg/m³

Dynamic viscosity of air $\mu = 20.1 \times 10^{-6}$ Ns/m²

Prandle number $Pr = 0.698$

Thermal conductivity of air $k = 0.02826$ W/mK

Reynold's number $Re = \frac{\rho D_o V}{\mu}$

$$= 477108$$

Diameter $D_o = 4.28$ m

Nusselt number $N_u = 0.0266 \times (Re^{0.805}) \times Pr^{0.333}$
(Frank, 2001)

Outer surface heat transfer coefficient

$$h_a = \frac{N_u k}{D_o} = 5.8 \text{ W/ W/m}^2\text{K}$$

Inner surface heat transfer coefficient, $= 6.8 \text{ W/ W/m}^2\text{K}$

(Velocity of air $V = 2.5$ m/sec

Bulk mean temperature of air $T_b = 113^\circ\text{C}$

Density of air $\rho = 0.946 \text{ kg/m}^3$

Dynamic viscosity of air $\mu = 21.87 \times 10^{-6} \text{ Ns/m}^2$

Prandtl number $Pr = 0.688$

Thermal conductivity of air $k = 0.0321 \text{ W/mK}$

$$\text{Reynold's number } Re = \frac{\rho D_o V}{\mu}$$

$$= 454184$$

Diameter $D_{in} = 4.2$ m

As per Gnielinsky correlation (Frank, 2001),

$$N_u = 0.214 \times (Re^{0.8} - 100) \times Pr^{0.4} \times \left(1 + \frac{D_o}{L}\right)^{\frac{2}{3}}$$

$$\text{Heat transfer coefficient } h_a = \frac{N_u k}{D_{in}} = 6.8 \text{ W/ W/m}^2\text{K}$$

Thermal conductivity material, $k = 52 \text{ W/m}^0\text{C}$

Emissivity of the raw mill surface, $\epsilon = 0.8$

Stefan Boltzmann constant $= 5.67 \times 10^{-8} \text{ W/m}^2\text{K}^4$

i) Heat loss with convection due to the inside temperature and the surface temperature (Q_{cv1})

$$= \pi D_{in} h_a L (T_{in} - T_s)$$

$$= 13752.05 \text{ Watts}$$

- ii) The heat loss with conduction due to the temperature difference between inner and outer surface (Q_{cd})

$$= \frac{(T_{in} - T_s)}{\frac{\ln(\frac{r_o}{r_i})}{2\pi kl}}$$

where r_{in} = inside radius of raw mill

r_o = outer radius of the raw mil.

$$= 2642371.65 \text{ Watts}$$

- iii) Heat losses with the convection from the outer surface to the environment (Q_{cv2})

$$= \pi D_o h_a L (T_s - T_\infty)$$

$$= 8184.47 \text{ Watts}$$

- iv) Heat losses with radiation occur from the outer surface to the environment (Q_{ra})

$$= \pi D_o \epsilon \sigma (T_s^4 - T_\infty^4)$$

$$= 8744.83 \text{ Watts}$$

$$\text{Drying room total heat loss} = Q_{cv1} + Q_{cd} + Q_{cv2} + Q_{ra}$$

$$= 2673053.01 \text{ Watts}$$

$$= 9622990.8 \text{ kJ/hr}$$

b) Grinding room

Inner diameter of grinding room, $D_{in} = 4.2\text{m}$

Outer diameter of grinding room, $D_o = 4.28$

Length of grinding room, $L = 10 \text{ m}$

Grinding room temperature, $T_{in} = 108.98 \text{ }^\circ\text{C}$

Surface temperature $T_s = 82 \text{ }^\circ\text{C}$

Inner surface heat transfer coefficient, $= 6.8 \text{ W/ W/m}^2\text{K}$

Outer surface heat transfer coefficient, $h_a = 5.8 \text{ W/m}^2\text{K}$

The thermal conductivity material, $k = 52 \text{ W/m}^0\text{C}$

Emissivity of the raw mill surface, $\epsilon = 0.8$

Stefan Boltzmann constant = $5.67 \times 10^{-8} \text{ W/m}^2\text{K}^4$

i) Heat losses with convection due to the inside temperatures and the surface temperature

$$= \pi D_{in} h_a L (T_{in} - T_s)$$

$$= 24301.98 \text{ Watts}$$

ii) The heat loss with conduction due to the temperature difference between inner and outer surfaces (Q_{cd})

$$= \frac{(T_{in} - T_s)}{\frac{\ln \left(\frac{r_o}{r_i} \right)}{2\pi k L}}$$

$$= 4669473.53 \text{ Watts}$$

iii) Heat losses with the convection from the outer surface to the environment (Q_{cv2})

$$= \pi D_o h_a L (T_s - T_{\infty})$$

$$= 40532.63 \text{ Watts}$$

iv) Heat losses with radiation occur from the outer surface to the environment (Q_r)

$$= \pi D_o \epsilon \sigma (T_s^4 - T_{\infty}^4)$$

$$= 45436.13 \text{ Watts}$$

Grinding room total heat loss = $Q_{cv1} + Q_{cd} + Q_{cv2} + Q_{ra}$

$$= 4779744.27 \text{ Watts}$$

$$= 17207079.36 \text{ kJ/hr}$$

Total heat loss from the raw mill (Q_{total})

= Drying room heat loss + Grinding room heat loss

$$= 26830070.19 \text{ kJ/hr}$$

Annexure C

Exergy calculation of raw mill (Production rate of 117 tonnes per hour)

For incompressible substances such as solids, both the constant pressure and constant volume specific heats are identical.

$$c_p = c_v = c$$

Internal energy change and enthalpy change values are (Bejan,1988)

$$\Delta u = \int_1^2 c(T) = c_{avg} (T_2 - T_1)$$

$$\Delta h = \Delta u + v\Delta p$$

where c_{avg} is the average specific heat, v is the specific volume and Δp is the pressure change. Pressure change in the unit is negligible so that enthalpy change is equal to internal energy change of the material. The enthalpy values of the input and output materials can be expressed in term of reference temperature (T_o).

$$\Delta h_{in} = c_{avg}(T_1 - T_o)$$

$$\Delta h_{in} = c_{avg}(T_2 - T_o)$$

where T_1 and T_2 are the input and output temperature of the materials and T_o is the reference temperature.

For incompressible substance the entropy change is

$$s_2 - s_1 = c_{avg} \ln \frac{T_2}{T_o} \text{ (Rosen et al., 2005).}$$

For ideal gases the entropy change is (Rosen et al., 2005).

$$s_2 - s_1 = c_{p,avg} \ln \frac{T_2}{T_o} - R \ln \frac{P_2}{P_o}$$

where R=Gas constant

Since the pressure of the input and output materials are equal, Δs the values for input and output materials are expressed as

$$\Delta S_{in} = c_{p_{avg}} \ln \frac{T_1}{T_0}$$

$$\Delta S_{out} = c_{p_{avg}} \ln \frac{T_2}{T_0}$$

After obtaining the entropy and enthalpy values of the input and output materials, the exergy values of the input and output materials can be calculated from

$$\Delta \psi_{in} = \Delta h_{in} - T_0 \Delta S_{in}$$

$$\Delta \psi_{out} = \Delta h_{out} - T_0 \Delta S_{out}$$

where ψ is the specific exergy

For the exergy analysis of the raw mill the reference temperature and pressure are assumed to be 298 K (T_0) and 101 kPa (dead state condition) respectively.

Input Exergy.

1. Infiltrated air

Mass flow rate, $m_{ia} = 24114$ kg/hr

Temperature, $T_{ia} = 303$ K

Specific heat, $c_{p_{ia}} = 0.9655$ kJ/kg K

$$\begin{aligned} \text{Enthalpy change, } \Delta H_{ia} &= m_{ia} \times c_{p_{ia}} \times (T_{ia} - T_0) \\ &= 116504.2 \text{ kJ/hr} \end{aligned}$$

$$\begin{aligned} \text{Entropy change, } \Delta S_{ia} &= m_{ia} \times c_{p_{ia}} \times \ln \left(\frac{T_{ia}}{T_0} \right) \\ &= 387.38 \text{ kJ/hr} \end{aligned}$$

$$\begin{aligned}\text{Exergy of infiltrated air, } Ex_{ia} &= \Delta H_{ia} - T_0 \times \Delta S_{ia} \\ &= 965.77 \text{ kJ/hr}\end{aligned}$$

2. Gas

$$\text{Mass flow rate, } m_g = 96458 \text{ kg/hr}$$

$$\text{Temperature, } T_g = 633\text{K}$$

$$\text{Specific heat, } c_{p_g} = 1.0812 \text{ kJ/kg K}$$

$$\begin{aligned}\text{Enthalpy change, } \Delta H_g &= m_g \times c_{p_g} \times (T_g - T_0) \\ &= 34937280.52 \text{ kJ/hr}\end{aligned}$$

$$\begin{aligned}\text{Entropy change, } \Delta S_g &= m_g \times c_{p_g} \times \ln\left(\frac{T_g}{T_0}\right) \\ &= 78569.97 \text{ kJ/hr}\end{aligned}$$

$$\begin{aligned}\text{Exergy of the gas, } Ex_g &= \Delta H_g - T_0 \times \Delta S_g \\ &= 11523428.22 \text{ kJ/hr}\end{aligned}$$

3. Limestone

$$\text{Mass flow rate, } m_l = 96426 \text{ kg/hr}$$

$$\text{Temperature, } T_l = 303\text{K}$$

$$\text{Specific heat, } c_{p_l} = 0.7632 \text{ kJ/kg K}$$

$$\begin{aligned}\text{Enthalpy change, } \Delta H_l &= m_l \times c_{p_l} \times (T_l - T_0) \\ &= 369504.43 \text{ kJ/hr}\end{aligned}$$

$$\begin{aligned}\text{Entropy change, } \Delta S_l &= m_l \times c_{p_l} \times \ln\left(\frac{T_l}{T_0}\right) \\ &= 1229.66 \text{ kJ/hr}\end{aligned}$$

$$\begin{aligned}\text{Exergy of the limestone, } Ex_l &= \Delta H_l - T_0 \times \Delta S_l \\ &= 3065.63 \text{ kJ/hr}\end{aligned}$$

4. Sweetener limestone

Mass flow rate, $m_{sl}=11344$ kg/hr

Temperature, $T_{sl} = 303$ K

Specific heat, $c_{p_{sl}} = 0.7632$ kJ/kg K

Enthalpy change, $\Delta H_{sl} = m_{sl} \times c_{p_{sl}} \times (T_{sl} - T_0)$

$$= 43288.7 \text{ kJ/hr}$$

Entropy change, $\Delta S_{sl} = m_{sl} \times c_{p_{sl}} \times \ln\left(\frac{T_{sl}}{T_0}\right)$

$$= 144.06 \text{ kJ/hr}$$

Exergy of the sweetener limestone, $Ex_{sl} = \Delta H_{sl} - T_0 \times \Delta S_{sl}$

$$= 359.15 \text{ kJ/hr}$$

5. Laterite

Mass flow rate, $m_{lt} = 5672$ kg/hr

Temperature, $T_{lt} = 303$ K

Specific heat, $c_{p_{lt}} = 0.745$ kJ/kg K

Enthalpy change, $\Delta H_{lt} = m_{lt} \times c_{p_{lt}} \times (T_{lt} - T_0)$

$$= 21128.2 \text{ kJ/hr}$$

Entropy change, $\Delta S_{lt} = m_{lt} \times c_{p_{lt}} \times \ln\left(\frac{T_{lt}}{T_0}\right)$

$$= 70.31 \text{ kJ/hr}$$

Exergy of the laterite, $Ex_{lt} = \Delta H_{sl} - T_0 \times \Delta S_{sl}$

$$= 175.29 \text{ kJ/hr}$$

6. Material returned from separator for recirculation.

Mass flow rate, $m_{rs} = 234000$ kg/hr

Temperature, $T_{rs} = 351$ K

Specific heat, $c_{p_{rs}} = 0.8142$ kJ/kg K

$$\begin{aligned}\text{Enthalpy change, } \Delta H_{rs} &= m_{rs} \times c_{p_{rs}} \times (T_{rs} - T_0) \\ &= 10097708.4 \text{ kJ/hr}\end{aligned}$$

$$\begin{aligned}\text{Entropy change, } \Delta S_{rs} &= m_{rs} \times c_{p_{rs}} \times \ln\left(\frac{T_{rs}}{T_0}\right) \\ &= 31187.2 \text{ kJ/hr}\end{aligned}$$

$$\begin{aligned}\text{Exergy of the material returned from separator, } Ex_{rs} &= \Delta H_{rs} - T_0 \times \Delta S_{rs} \\ &= 803923.22 \text{ kJ/hr}\end{aligned}$$

7. Moisture in the limestone

Mass flow rate, $m_{ml} = 1929$ kg/hr

Temperature, $T_{ml} = 303$ K

Specific heat, $c_{p_{ml}} = 4.178$ kJ/kg K

$$\begin{aligned}\text{Enthalpy change, } \Delta H_{ml} &= m_{ml} \times c_{p_{ml}} \times (T_{ml} - T_0) \\ &= 40296.81 \text{ kJ/hr}\end{aligned}$$

$$\begin{aligned}\text{Entropy change, } \Delta S_{ml} &= m_{ml} \times c_{p_{ml}} \times \left(\frac{T_{ml}}{T_0}\right) \\ &= 134.1 \text{ kJ/hr}\end{aligned}$$

$$\begin{aligned}\text{Exergy of moisture in the limestone, } Ex_{ml} &= \Delta H_{ml} - T_0 \times \Delta S_{ml} \\ &= 334.33 \text{ kJ/hr}\end{aligned}$$

8. Moisture in the sweetener limestone

Mass flow rate, $m_{sm} = 1361$ kg/hr

Temperature, $T_{sm} = 303$ K

Specific heat, $c_{p_{sm}} = 4.187$ kJ/kg K

$$\begin{aligned} \text{Enthalpy change, } \Delta H_{sm} &= m_{sm} \times c_{p_{sm}} \times (T_{sm} - T_0) \\ &= 28431.29 \text{ kJ/hr} \end{aligned}$$

$$\begin{aligned} \text{Entropy change, } \Delta S_{sm} &= m_{sm} \times c_{p_{sm}} \times \left(\frac{T_{sm}}{T_0} \right) \\ &= 94.62 \text{ kJ/hr} \end{aligned}$$

$$\begin{aligned} \text{Exergy of moisture in the sweetener limestone, } Ex_{sm} &= \Delta H_{sm} - T_0 \times \Delta S_{sm} \\ &= 235.88 \text{ kJ/hr} \end{aligned}$$

9. Moisture in laterite

Mass flow rate, $m_{lm} = 284$ kg/hr

Temperature, $T_{lm} = 303$ K

Specific heat, $c_{p_{lm}} = 4.187$ kJ/kg K

$$\begin{aligned} \text{Enthalpy change, } \Delta H_{lm} &= m_{lm} \times c_{p_{lm}} \times (T_{lm} - T_0) \\ &= 5932.76 \text{ kJ/hr} \end{aligned}$$

$$\begin{aligned} \text{Entropy change, } \Delta S_{lm} &= m_{lm} \times c_{p_{lm}} \times \left(\frac{T_{lm}}{T_0} \right) \\ &= 19.74 \text{ kJ/hr} \end{aligned}$$

$$\begin{aligned} \text{Exergy of moisture in the laterite, } Ex_{lm} &= \Delta H_{lm} - T_0 \times \Delta S_{lm} \\ &= 49.22 \text{ kJ/hr} \end{aligned}$$

10. Dust

Mass flow rate, $m_d = 2973$ kg/hr

Temperature, $T_d = 633$ K

Specific heat, $c_{p_d} = 0.9971$ kJ/kg K

$$\begin{aligned} \text{Enthalpy change, } \Delta H_d &= m_d \times c_{p_d} \times (T_d - T_0) \\ &= 993031.50 \text{ kJ/hr} \end{aligned}$$

$$\begin{aligned} \text{Entropy change, } \Delta S_d &= m_d \times c_{p_d} \times \left(\frac{T_d}{T_0}\right) \\ &= 2233.22 \text{ kJ/hr} \end{aligned}$$

$$\begin{aligned} \text{Exergy of the dust } Ex_d &= \Delta H_d - T_0 \times \Delta S_d \\ &= 327533.43 \text{ kJ/hr} \end{aligned}$$

11. Exergy related to electrical work $Ex_e = 8002800$ kJ/hr**Total input exergy**

$$\begin{aligned} Ex &= Ex_{ia} + Ex_g + Ex_l + Ex_{sl} + Ex_{lt} + Ex_{rs} + Ex_{ml} + Ex_{sm} + \\ &Ex_{lm} + Ex_d + Ex_e \\ &= 20662870.14 \text{ kJ/hr} \end{aligned}$$

Output exergy**1. Infiltrated air**

Mass flow rate, $m_{ia} = 24114$ kg/hr

Temperature, $T_{ia} = 361$ K

Specific heat, $c_{p_{ia}} = 0.9908$ kJ/kg K

$$\begin{aligned} \text{Enthalpy change, } \Delta H_{ia} &= m_{ia} \times c_{p_{ia}} \times (T_{ia} - T_0) \\ &= 1506268.95 \text{ kJ/hr} \end{aligned}$$

$$\begin{aligned} \text{Entropy change, } \Delta S_{ia} &= m_{ia} \times c_{p_{ia}} \times \ln\left(\frac{T_{ia}}{T_0}\right) \\ &= 4585.38 \text{ kJ/hr} \end{aligned}$$

$$\begin{aligned} \text{Exergy of the infiltrated air, } Ex_{ia} &= \Delta H_{ia} - T_0 \times \Delta S_{ia} \text{-----(A)} \\ &= 139825.45 \text{ kJ/hr} \end{aligned}$$

2. Gas

Mass flow rate $m_g = 96458$ kg/hr

Temperature, $T_g = 361$ K

Specific heat, $c_{p_g} = 0.9745$ kJ/kg K

$$\begin{aligned} \text{Enthalpy change, } \Delta H_g &= m_g \times c_{p_g} \times (T_g - T_0) \\ &= 5929794.13 \text{ kJ/hr} \end{aligned}$$

$$\begin{aligned} \text{Entropy change, } \Delta S_g &= m_g \times c_{p_g} \times \ln\left(\frac{T_g}{T_0}\right) \\ &= 18051.47 \text{ kJ/hr} \end{aligned}$$

$$\begin{aligned} \text{Exergy of the gas } Ex_g &= \Delta H_g - T_0 \times \Delta S_g \text{-----}(B) \\ &= 550456.9 \text{ kJ/hr} \end{aligned}$$

3. Steam

Mass flow rate, $m_{st} = 2989$ kg/hr

Temperature, $T_{st} = 361$ K

Specific heat, $c_{p_{st}} = 1.962$ kJ/kg K

$$\begin{aligned} \text{Enthalpy change, } \Delta H_{st} &= m_{st} \times c_{p_{st}} \times (T_{st} - T_0) \\ &= 369458.33 \text{ kJ/hr} \end{aligned}$$

$$\begin{aligned} \text{Entropy change, } \Delta S_{st} &= m_{st} \times c_{p_{st}} \times \ln\left(\frac{T_{st}}{T_0}\right) \\ &= 1124.7 \text{ kJ/hr} \end{aligned}$$

$$\begin{aligned} \text{Exergy of steam, } Ex_{st} &= \Delta H_{st} - T_0 \times \Delta S_{st} \text{-----}(C) \\ &= 34296.45 \text{ kJ/hr} \end{aligned}$$

4. Raw meal

Mass flow rate, $m_{rm} = 350415$ kg/hr

Temperature, $T_{rm} = 361$ K

Specific heat, $c_{p_{rm}} = 0.8232$ kJ/kg K

$$\begin{aligned} \text{Enthalpy change, } \Delta H_{rm} &= m_{rm} \times c_{p_{rm}} \times (T_{rm} - T_0) \\ &= 18210612.01 \text{ kJ/hr} \end{aligned}$$

$$\begin{aligned} \text{Entropy change, } \Delta S_{rm} &= m_{rm} \times c_{p_{rm}} \times \ln\left(\frac{T_{rm}}{T_0}\right) \\ &= 55436.71 \text{ kJ/hr} \end{aligned}$$

$$\begin{aligned} \text{Exergy of the raw meal, } Ex_{rm} &= \Delta H_{rm} - T_0 \times \Delta S_{rm} \text{-----(D)} \\ &= 1690473.02 \text{ kJ/hr} \end{aligned}$$

5. Moisture

Mass flow rate, $m_m = 585$ kg/hr

Temperature, $T_m = 361$ K

Specific heat, $c_{p_m} = 4.195$ kJ/kg K

$$\begin{aligned} \text{Enthalpy change, } \Delta H_m &= m_m \times c_{p_m} \times (T_m - T_0) \\ &= 154606.73 \text{ kJ/hr} \end{aligned}$$

$$\begin{aligned} \text{Entropy change, } \Delta S_m &= m_m \times c_{p_m} \times \ln\left(\frac{T_m}{T_0}\right) \\ &= 470.65 \text{ kJ/hr} \end{aligned}$$

$$\begin{aligned} \text{Exergy of the moisture, } Ex_m &= \Delta H_m - T_0 \times \Delta S_m \text{-----(E)} \\ &= 14351.99 \text{ kJ/hr} \end{aligned}$$

Exergy efficiency

$$\begin{aligned} \text{Exergy efficiency of the raw mill} &= \frac{A+B+C+D+E}{\text{Total input exergy}} \\ &= 11.76\% \end{aligned}$$

$$\text{Loss of exergy} = 88.24\%$$

Annexure D

Calculations of useful energy and exergy due to the clinker formation (1 kg of clinker) in the kiln system.

The useful heat and useful chemical exergy due to clinker formation have been calculated using the data of the enthalpies of reactions of the raw meal to form clinker (Rosemann et al., 1987) and the standard chemical exergy values of the gas and solid flows in cement kiln plant (Morris and Szargut, 1996) are shown below.

Standard chemical exergy values of the gas and solid flows in cement plant (Morris and Szargut 1996)

Species	Chemical Exergy (kJ/k mole)	Species	Chemical exergy (kJ/kmole)
Al ₂ O ₃ (s,)	200400	CaSO ₄ (s,)	8200
Al ₂ O ₃ .SiO ₂ (s)	15400	Fe ₂ O ₃ (s)	16500
CO(g)	275100	H ₂ (g)	236100
CO ₂ (g)	19870	H ₂ O(l)	900
CaCO ₃ (s)	1000	H ₂ O(g)	9490
CaCO ₃ .MgCO ₃ (s)	15100	K ₂ O (s)	413100
CaO(s)	101200	MgO(s)	66800
CaO.Al ₂ O ₃ (s)	275400	MgCO ₃ (s)	37900
2CaO.Al ₂ O ₃ (s)	460400	N ₂ (g)	690
3CaO.Al ₂ O ₃ (s)	500600	O ₂ (g)	3970
CaO.SiO ₂ (s)	23600	Na ₂ O(s)	296200
2CaO.SiO ₂ (s,)	95700	SO ₂ (g)	313400
3CaO.SiO ₂ (s)	219800	SiO ₂	1900
CaS	844600	Fe ₂ O ₃ .SiO ₂	18400
4CaO.Al ₂ O ₃ .Fe ₂ O ₃	667000		

In the investigated process the actual amount of reacting raw meal = 1.49 kg to produce 1kg of clinker. Its contents of various components, in kg, are as follows:

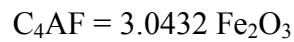
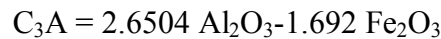
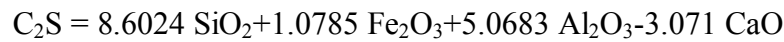
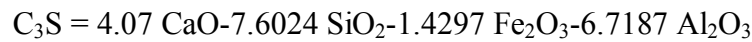
CaO	SiO ₂	Al ₂ O ₃	Fe ₂ O ₃	MgO	SiO ₃	Loss of Ignition
0.658	0.19	0.058	0.035	0.0045	0.0045	0.54

It's CaCO₃ and MgCO₃ components have been estimated as follows

CaCO₃ content = 1.176 kg

MgCO₃ content = 0.009 kg

In the burning zone of the kiln (1450°C) the chemical reactions of calcined material takes place and clinker is formed. The four clinker phases such as tricalcium silicate (C₃S), dicalcium silicate (C₂S), tricalcium aluminate (C₃A) and tetracalcium aluminoferrite (C₄AF) are calculated based on Bogue calculation (Nicholas, 1990) using the clinker analysis data of the plant.



The estimated values of the clinker phases are (in wt %) as follows:

C₂S 39 %, C₃S 36.6 %, C₃A 11.4 % and C₄AF 13%

The amounts of formed clinker phases in 1 kg of clinker are given as:

0.39 kg C₂S, 0.366 kg C₃S, 0.114 kg C₃A and 0.13 kg C₄AF

The table given below shows the detailed calculation of energy and exergy during the formation of 1 kg of clinker in the cement plant.

Reaction name	Reaction	Enthalpy of reaction $Q_k = m_k \times \Delta h_r$ (kJ/ kg of clinker)	Exergy of chemical reaction $(Ex_k) = m_k \times \psi_{ch}$ (kJ/ kg of clinker)
Calcinations process	$\text{CaCO}_3 \rightarrow \text{CaO} + \text{CO}_2$ Enthalpy $\Delta h_r = 1780$ kJ/ kg CaCO_3 Chemical exergy $\psi_{ch} = 1275.1$ kJ/ kg CaCO_3 Mass $m_k = 1.176$ kg CaCO_3 /kg-clinker	2093.28	1499.51
MgCO_3 dissociation	$\text{MgCO}_3 \rightarrow \text{MgO} + \text{CO}_2$ Enthalpy $\Delta h_r = 1395$ kJ/ kg MgCO_3 Chemical exergy $\psi_{ch} = 610$ kJ/ kg MgCO_3 Mass $m_k = 0.009$ kg MgCO_3 / kg-clinker	12.56	5.49
β - C_2S formation (Intermediate compound)	$2\text{CaO} + \text{SiO}_2 \rightarrow \beta\text{-C}_2\text{S}$ Enthalpy $\Delta h_r = -732$ kJ/ kg $\beta\text{-C}_2\text{S}$ Chemical exergy $\psi_{ch} = -735.9$ kJ/ $\beta\text{-C}_2\text{S}$ Mass $m_k = 0.5$ kg $\beta\text{-C}_2\text{S}$ / kg-clinker	-368.55	-370.51
C_3S formation	$\beta\text{-C}_2\text{S} + \text{CaO} \rightarrow \text{C}_3\text{S}$ Enthalpy $\Delta h_r = 35$ kJ/ C_3S Chemical exergy $\psi_{ch} = 33.16$ kJ/ C_3S Mass $m_k = 0.366$ kg C_3S / kg-clinker	12.95	12.27
C_3A formation	$3\text{CaO} + \text{Al}_2\text{O}_3 \rightarrow \text{C}_3\text{A}$ Enthalpy $\Delta h_r = 25$ kJ/ C_3A Chemical exergy $\psi_{ch} = 18.69$ kJ/ C_3A Mass $m_k = 0.114$ kg C_3A / kg-clinker	2.75	2.06
C_4AF formation	$4\text{CaO} + \text{Al}_2\text{O}_3 + \text{Fe}_2\text{O}_2 \rightarrow \text{C}_4\text{AF}$ Enthalpy $\Delta h_r = 25$ kJ/ C_4AF Chemical exergy $\psi_{ch} = 28.57$ kJ/ C_4AF Mass $m_k = 0.13$ kg C_4AF / kg-clinker	3.25	3.71
Total		1756.24	1152.53

Annexure E

Exergy calculation of kiln system (Production rate of 1400 tonnes per day)

For the exergy analysis the reference temperature and pressure are assumed to be $T_0 = 298$ K and 101 kPa (dead state condition) respectively.

Input Exergy
1. Raw meal.

Mass of raw meal per kg of clinker, $(m_k)_{rm} = 1.49$ kg / kg of clinker

Temperature, $T_{rm} = 328$ K

Specific heat, $c_{p_{rm}} = 0.7919$ kJ/kg-K

$$\begin{aligned} \text{Enthalpy change, } (\Delta H_k)_{rm} &= (m_k)_{rm} \times c_{p_{rm}} \times (T_{rm} - T_0) \\ &= 35.4 \text{ kJ/kg-clinker} \end{aligned}$$

$$\begin{aligned} \text{Entropy change, } (\Delta S_k)_{rm} &= (m_k)_{rm} \times c_{p_{rm}} \times \ln\left(\frac{T_{rm}}{T_0}\right) \\ &= 0.1132 \text{ kJ/kg-clinker K} \end{aligned}$$

$$\begin{aligned} \text{Exergy of raw meal, } (Ex_k)_{rm} &= (\Delta H_k)_{rm} - T_0 \times (\Delta S_k)_{rm} \\ &= 1.67 \text{ kJ/kg-clinker} \end{aligned}$$

2. Primary air

Mass of primary air per kg of clinker, $(m_k)_{pa} = 0.418$ kg/kg-clinker

Temperature, $T_{pa} = 344$ K

Specific heat, $c_{p_{pa}} = 0.9843$ kJ/kg-K

$$\begin{aligned} \text{Enthalpy change, } (\Delta H_k)_{pa} &= (m_k)_{pa} \times c_{p_{pa}} \times (T_{pa} - T_0) \\ &= 18.93 \text{ kJ/kg-clinker} \end{aligned}$$

$$\begin{aligned} \text{Entropy change, } (\Delta S_k)_{pa} &= (m_k)_{pa} \times c_{p_{pa}} \times \ln\left(\frac{T_{pa}}{T_0}\right) \\ &= 0.0591 \text{ kJ/ kg-clinker K} \end{aligned}$$

$$\begin{aligned} \text{Exergy of Primary air, } (Ex_k)_{pa} &= (\Delta H_k)_{pa} - T_0 \times (\Delta S_k)_{pa} \\ &= 1.33 \text{ kJ/kg-clinker} \end{aligned}$$

3. Cooler inlet air

Mass of cooler air per kg of clinker, $(m_k)_{ca} = 3.667$ kg/kg-clinker

Temperature, $T_{ca} = 308$ K

Specific heat, $c_{p_{ca}} = 0.9681$ kJ/kg-K

Enthalpy change, $(\Delta H_k)_{ca} = (m_k)_{ca} \times c_{p_{ca}} \times (T_{ca} - T_0)$
 35.5 kJ/kg-clinker

Entropy change, $\Delta S_{k_{ca}} = (m_k)_{ca} \times c_{p_{ca}} \times \ln\left(\frac{T_{ca}}{T_0}\right)$
 $= 0.1172$ kJ/ kg-clinker K

Exergy of cooler air, $(Ex_k)_{ca} = (\Delta H_k)_{ca} - T_0 \times (\Delta S_k)_{ca}$
 $= 0.58$ kJ/kg-clinker

4. Infiltrated air

Mass of infiltrated air per kg of clinker, $(m_k)_{ia} = 0.8146$ kg/kg-clinker

Temperature, $T_{ia} = 308$ K

Specific heat, $c_{p_{ia}} = 0.9681$ kJ/kg-K

Enthalpy change, $(\Delta H_k)_{ia} = (m_k)_{ia} \times c_{p_{ia}} \times (T_{ia} - T_0)$
 $= 7.81$ kJ/kg-clinker

Entropy change, $\Delta S_{k_{ia}} = (m_k)_{ia} \times c_{p_{ia}} \times \ln\left(\frac{T_{ia}}{T_0}\right)$
 $= 0.026$ kJ/ kg-clinker K

Exergy infiltrated air, $(Ex_k)_{ia} = (\Delta H_k)_{ia} - T_0 \times (\Delta S_k)_{ia}$
 $= 0.13$ kJ/kg-clinker

5. Chemical exergy of coal

$= [\text{Calorific value} + \text{heat of evaporation} \times (\text{percentage of Moisture})] \times \Phi$

where $\Phi = 1.0437 + 0.1882 \times (h/c) + 0.0610 \times (o/c) + 0.0404 \times (n/c)$

and c, h, o, and n are the mass fractions of Carbon, Hydrogen, Oxygen, and Nitrogen respectively (Kotas, 1985).

$$\begin{aligned} \text{Chemical Exergy of coal} &= (20763 + 2315 \times 0.035) \times 1.0722 \\ &= 21658.32 \text{ kJ/kg} \end{aligned}$$

Coal consumption in kiln = 0.183 kg/kg of clinker

$$\begin{aligned} \text{Chemical exergy of coal } (Ex_k)_c &= 21658.32 \times 0.183 \\ &= 4089.92 \text{ kJ/kg of clinker} \end{aligned}$$

Proximate analysis of coal = (Fixed carbon-43%, Ash- 25%, Volatile matter-28.5% and Moisture-3.5%) and Ultimate analysis of coal (Carbon-57.58%, Hydrogen – 3.7%, Nitrogen-1.54%, Oxygen-7.18%, Sulphur 0.5%, Mineral matter 26% and Moisture-3.5%)

6. Total input exergy of the kiln system

$$\begin{aligned} &= (Ex_k)_{rm} + (Ex_k)_{pa} + (Ex_k)_{ca} + (Ex_k)_{ia} + (Ex_k)_c \\ &= 4093.63 \text{ kJ/kg-clinker} \end{aligned}$$

Output exergy

1. Preheater Exhaust gas

Mass of the preheater exhaust gas per kg of clinker,

$$m_{k_{eg}} = 2.56 \text{ kg/kg of clinker}$$

Temperature, $T_{eg} = 657\text{K}$

Specific heat, $c_{p_{eg}} = 1.0878 \text{ kJ/kg-K}$

$$\begin{aligned} \text{Change in enthalpy, } (\Delta H_k)_{eg} &= (m_k)_{eg} \times c_{p_{eg}} \times (T_{eg} - T_0) \\ &= 999.72 \text{ kJ/kg-clinker} \end{aligned}$$

$$\begin{aligned} \text{Change in entropy, } (\Delta S_k)_{eg} &= (m_k)_{eg} \times c_{p_{eg}} \times \ln\left(\frac{T_{eg}}{T_0}\right) \\ &= 2.2016 \text{ kJ/kg-clinker K} \end{aligned}$$

$$\begin{aligned} \text{Exergy of preheater exhaust gas, } (Ex_k)_{eg} &= (\Delta H_k)_{eg} - T_0 \times (\Delta S_k)_{eg} \\ &= 343.65 \text{ kJ/kg-clinker} \end{aligned}$$

2. Dust

Mass of dust per kg of clinker, $m_{kd} = 0.0476$ kg / kg of clinker

Temperature, $T_d = 657$ K

Specific heat, $c_{pd} = 1.0093$ kJ/kg-K

$$\begin{aligned} \text{Change in enthalpy, } (\Delta H_k)_d &= (m_k)_d \times c_{pd} \times (T_d - T_0) \\ &= 27.03 \text{ kJ/kg-clinker} \end{aligned}$$

$$\begin{aligned} \text{Change in entropy, } (\Delta S_k)_d &= (m_k)_d \times c_{pd} \times \ln\left(\frac{T_d}{T_0}\right) \\ &= 0.0595 \text{ kJ/ kg-clinker K} \end{aligned}$$

$$\begin{aligned} \text{Exergy of dust, } (Ex_k)_d &= (\Delta H_k)_d - T_0 \times (\Delta S_k)_d \\ &= 9.29 \text{ kJ/kg-clinker} \end{aligned}$$

3. Clinker

Clinker discharge, $(m_k)_{cli} = 1$ kg/ kg-clinker

Temperature, $T_{cli} = 368$ K

Specific heat, $c_{p_{cli}} = 0.8308$ kJ/kg-K

$$\begin{aligned} \text{Change in enthalpy, } (\Delta H_k)_{cli} &= (m_k)_{cli} \times c_{p_{cli}} \times (T_{cli} - T_0) \\ &= 58.16 \text{ kJ/kg-clinker} \end{aligned}$$

$$\begin{aligned} \text{Change in entropy, } (\Delta S_k)_{cli} &= (m_k)_{cli} \times c_{p_{cli}} \times \ln\left(\frac{T_{cli}}{T_0}\right) \\ &= 0.1753 \text{ kJ/ kg-clinker K} \end{aligned}$$

$$\begin{aligned} \text{Exergy of clinker, } (Ex_k)_{cli} &= (\Delta H_k)_{cli} - T_0 \times (\Delta S_k)_{cli} \\ &= 5.92 \text{ kJ/kg-clinker} \end{aligned}$$

4. Cooler hot air

Mass flow of cooler hot air per kg of clinker,

$$m_{k_{co}} = 2.82 \text{ kg / kg of clinker}$$

Temperature, $T_{co} = 473K$

Specific heat, $c_{p_{co}} = 1.0226 \text{ kJ/kg-K}$

$$\begin{aligned} \text{Change in enthalpy, } (\Delta H_k)_{co} &= (m_k)_{co} \times c_{p_{co}} \times (T_{co} - T_0) \\ &= 504.65 \text{ kJ/kg-clinker} \end{aligned}$$

$$\begin{aligned} \text{Change in entropy, } (\Delta S_k)_{co} &= (m_k)_{co} \times c_{p_{co}} \times \ln\left(\frac{T_{co}}{T_0}\right) \\ &= 1.3323 \text{ kJ/ kg-clinker K} \end{aligned}$$

$$\begin{aligned} \text{Exergy of cooler hot air, } (Ex_k)_{co} &= (\Delta H_k)_{co} - T_0 \times (\Delta S_k)_{co} \\ &= 107.63 \text{ kJ/kg-clinker} \end{aligned}$$

5. Coal mill gas

Mass flow of the coal mill gas per kg of clinker,

$$m_{k_{cm}} = 0.125 \text{ kg / kg of clinker}$$

Temperature, $T_{cm} = 591 \text{ K}$

Specific heat, $c_{p_{cm}} = 1.0482 \text{ kJ/kg-K}$

$$\begin{aligned} \text{Enthalpy change, } (\Delta H_k)_{cm} &= (m_k)_{cm} \times c_{p_{cm}} \times (T_{cm} - T_0) \\ &= 39.96 \text{ kJ/kg-clinker} \end{aligned}$$

$$\text{Entropy change, } (\Delta S_k)_{cm} = (m_k)_{cm} \times c_{p_{cm}} \times \ln\left(\frac{T_{cm}}{T_0}\right)$$

$$= 0.0924 \text{ kJ/ kg-clinker K}$$

$$\text{Exergy of coal mill gas, } (Ex_k)_{cm} = (\Delta H_k)_{cm} - T_0 \times \Delta S_{k_{cm}}$$

$$= 12.44 \text{ kJ/kg-clinker}$$

Exergy efficiency of the kiln system

$$= \frac{\text{Clinker formation exergy} + \text{Exergy carried by clinker}}{\text{Total input exergy}}$$

$$= \frac{1152.53 + 5.92}{4093.63}$$

$$= 28.3\%$$

(The clinker formation exergy is calculated and given in the **Annexure D** as 1152.53 kJ/kg-clinker)

6. Exergy due to heat transfer

a) Convection radiation heat loss from kiln surface,

$$Q_k = 305.96 \text{ kJ/kg-clinker (From Table 4.4)}$$

Surface temperature of kiln, $T_s = 573\text{K}$

$$\begin{aligned} \text{Exergy} &= \left(1 - \frac{T_0}{T_s}\right) \times Q_k \\ &= 147 \text{ kJ/kg-clinker} \end{aligned}$$

b) Convection radiation heat loss from preheater surface,

$$Q_k = 5.81 \text{ kJ/kg-clinker (From Table 4.4)}$$

Surface temperature of preheater, $T_s = 353\text{K}$

$$\begin{aligned} \text{Exergy} &= \left(1 - \frac{T_0}{T_s}\right) \times Q_k \\ &= 0.9 \text{ kJ/kg-clinker} \end{aligned}$$

- c) Convection radiation heat loss from cooler surface,

$$Q_k = 2 \text{ kJ/kg-kg-clinker (From Table 4.4)}$$

Surface temperature of cooler surface, $T_s = 355\text{K}$

$$\begin{aligned} \text{Exergy} &= \left(1 - \frac{T_0}{T_s}\right) \times Q_k \\ &= 0.32 \text{ kJ/kg-clinker} \end{aligned}$$

Total exergy due to heat transfer in the kiln system = (a) + (b) + (c)

$$= 148.06 \text{ kJ/kg-clinker}$$

7. Irreversibility of the kiln system = 2314.1 kJ/kg-clinker

List of Publications

International journals

1. Ramesh.A, Madhu.G, Soloman P.A, (2012) Energy Technology Policy and Performance Analysis a Cement Industry Perspective, *European Journal of Scientific Research* ISSN 1450-216X Vol.73, Number.1 (2012), pp. 33-40.
2. Ramesh.A, Madhu.G, Deepak.B, (2012) A Decomposition Analysis of CO₂ Emission in Indian Cement Industry, *International Journal of Environmental Engineering and Management* ISSN 2231-1319 Volume 3, Number 1 (2012), pp. 23-36
3. Ramesh.A, Libin P Oommen , Madhu.G, (2012) Energy and Exergy Analysis of a 1400 TPD Kiln System of a Cement Industry, 4-6 January 2012 *Proceeding Volume of Golden Jubilee International Conference on RACE2012, International Journal of Earth Sciences and Engineering* ISSN 0974-5904 Volume Number 01 SPL January 2012, pp 541-546.

International Conference

1. Ramesh.A, Libin P Oommen , Madhu.G, (2012) Energy and Exergy Analysis of a 1400 TPD Kiln system of a Cement Industry, Golden Jubilee International Conference on Recent Advances and Challenges in Energy-2012 4th to 6th Jan 2012, Manipal Institute Technology, Manipal, Karnataka, India.
2. Ramesh.A, Abishek.P , Madhu.G, (2012) Energy and Exergy Analysis of a Raw mill of the cement Production, International Conference on Recent Innovations in Technology 10-12 Feb 2012, RIT Kottayam, Kerala.
3. Ramesh.A, Deepak.B, Madhu.G, (2012) A Decomposition Analysis on CO₂ Emission in Indian Cement Industry, International Conference on Recent Innovations in Technology 2011 10-12 Feb 2012, RIT Kottayam, Kerala
4. Ramesh.A, Madhu G, (2011) Thermal performance Analysis and Energy Conservation Opportunities in a Cement Industry, Second International Conference on Material for the Future, 23rd to 25th Feb 2011, Govt Engineering College Thrissur, Kerala

.....✍.....

Curriculum Vitae



A.RAMESH,
S/O P P Appu,
Poolanikal House,
Vyloor, Nellore (PO),
Thrissur. 680305,
Kerala

A.Ramesh, born on 31-05-1971 in Nellore, Thrissur (Dist) Kerala. He obtained B.Tech Degree in Mechanical Engineering from College of Engineering Thiruvananthapuram in 1994 with first class. He obtained M.Tech Degree in Internal Combustion Engines and Gas Turbine-Mechanical Engineering from IIT Madras in 2003. He joined as lecturer in Mechanical Engineering in Govt. Engineering College Thrissur in 1999. Presently he is working as Associate Professor in Mechanical Engineering in Govt. Engineering College, Idukki. His area of interest includes Heat transfer, Thermodynamics and Energy studies.

.....✍.....